Title
Linoleic acid and Its Oxidized Metabolites: Exposure, Bioavailability and Brain Metabolism

Author
Zhang, Zhichao

Publication Date
2021

Peer reviewed|Thesis/dissertation

Linoleic acid and Its Oxidized Metabolites: Exposure, Bioavailability and Brain Metabolism

By

ZHICHAO ZHANG
DISSERTATION

Submitted in partial satisfaction of the requirements for the degree of

DOCTOR OF PHILOSPHY

in

Food Science

in the

OFFICE OF GRADUATE STUDIES

of the

UNIVERSITY OF CALIFORNIA

DAVIS

Approved:

_____

Ameer Y. Taha, Chair

_____

Alyson E. Mitchell

_____

Carolyn M. Slupsky

Committee in Charge

2021

Acknowledgment

It has been exactly eight years since I landed in America. So many important moments, ups and downs have happened. Life has shaped me from an adolescent boy to a mature man. I am deeply grateful for my stay at UC Davis and very proud that I have finished this PhD dissertation. This will not have happened without all the enormous helps I have received.

To my parents, thank you for believing in me and giving me all the supports when I told you my wish to study abroad at 17. Dad, I hope you are proud of me in the other world. Mom, thank you for your continuous support. I love you both!

To my wife, Karla, I am so grateful that I met you in our freshman dorm. You have given me a second home. I am much honored to be your life partner and I love you.

To my PhD mentor, Ameer, you are the one who opened the door of research for me and continuously guided me through this meaningful journey. Thank you for all the efforts you put to nurture me. I learned so much from you and I am deeply grateful. I am proud to be the first Taha lab PhD graduate from the Food Science Graduate Group.

To my thesis committee member, Prof. Mitchell, thank you so much for teaching me the basics of analytical chemistry and your continuous help through my graduate study. To Prof. Sluspky, I have learned so much from my collaborations with you and am very excited to be trained under you soon.

I would also like to thank the current and previous Taha lab members, my qualifying exam committee members (Dr. G. Young, Dr. P. Lein, Dr. D. Barlie, and Dr. JLMN. de Moura Bell), my academic advisor, Dr. S. Dungan, my graduate program chair, Dr. M. Marco, collaborators, friends and my first dog, Paco.

Cheers to the end of my PhD and start of a new journey.

Abstract

Linoleic acid (LA or LNA) is an omega-6 polyunsaturated fatty acid (PUFA) abundant in Western diets. As a PUFA, LA is prone to oxidation both enzymatically and non-enzymatically. Non-enzymatic oxidation involves photo-oxidation or heat induced thermal oxidation. Enzymes involved in LA oxidation are lipoxygenase, cyclooxygenase, prostaglandin dehydrogenase, cytochrome P450 and soluble epoxide hydrolase. Both enzymatic and non-enzymatic oxidation of LA generates oxidized linoleic acid metabolites (OXLAMs), which are present in high-LA oils. OXLAMs have also been reported in the mammalian cardiovascular system, immune system, circulatory system and nervous system mainly from de novo synthesis from LA in vivo. Although exposure to OXLAMs has been widely studied in fried oil, it has not been studied in other food types. Additionally, the extent of dietary contribution of OXLAMs to health is an area still under investigation. OXLAMs are abundant especially in the developing brain and the source of it there is still unknown. Furthermore, factors that could affect developmental brain LA and OXLAM concentrations are largely unknown.

In this dissertation, I investigated the potential dietary exposure of OXLAMs in adults using processed potatoes and French fries as a model food that is commonly consumed and subjected to multiple processing steps. I also investigated exposure for infants through the consumption of human milk. Second, I used in vivo kinetics and tracers to study the absorption and incorporation of dietary OXLAMs, especially into the brain. I used tracers to determine the contribution of dietary LA to brain OXLAM levels and turnover. Finally, I assessed factors such as maternal obesity and typical medical interventions to understand their impacts on offspring LA and OXLAM metabolism.

I found that OXLAMs are the most abundant oxidized fatty acid (oxylipin) species in potatoes, French fries and human breastmilk. Interestingly, different food processing steps could alter OXLAM formation differently, not in a continuously increased oxidation trend. Dietary OXALMs can be absorbed and incorporated into adipose, liver, and heart but not the brain. Brain OXLAMs are rapidly synthesized from LA upon entering the brain. Maternal obesity interventions such as calorie restriction and use of pravastatin could cause adverse arachidonic acid and docosahexaenoic acid metabolism in the offspring prefrontal cortex without altering the metabolism of LA or OXLAMs. Continued studies on developmental brain LA and OXLAM metabolism, in vivo gastrointestinal metabolism, and bioactivities of OXLAMs in the nervous system are needed.

Table of Contents

Table of Contents

1. Introduction:

1.1 About lipids

Lipids are organic molecules that have poor water solubility. Examples include fatty acids, cholesterol, waxes, sterols, as well as fat-soluble vitamins including Vitamins A, D, E, and K. In biological systems, lipids serve as structural components of cells, co-factors in multiple enzymatic reactions, and signaling molecules.

The most abundant lipids in the food supply are fatty acids (also known as 'fats'), a hydrocarbon chain of molecules with a carboxylic terminal. Fatty acids come in different lengths and various degrees of saturation, which refers to the number of double bonds in a molecule. A saturated fatty acid (SFA), for instance, contains no double bonds (all carbon atoms in the molecule less the carboxylic terminal is saturated with hydrogen). A monounsaturated fatty acid (MUFA) has one double bond, and thus less hydrogen saturation. A polyunsaturated fatty acid (PUFA) has 2 or more double bonds and are therefore the least saturated with hydrogen. **Figure 1** (page 157 in the list of Tables and Figures Section) depicts structures of SFA, MUFA and PUFA.

Free fatty acids (FFAs) are rarely found on their own in food and biological systems. This is because they are usually bound (i.e. esterified) to glycerol, glycerophospholipid or sterol molecules to yield triacylglycerols (TAGs), phospholipids (PLs) and sterol esters (SEs), respectively. Therefore, TAGs are composed of a glycerol backbone and three fatty acids esterified to the alcohol groups on the glycerol chain. PLs consist of 2 fatty acids bound to the glycerophospholipid backbone. Sterol esters consist of one sterol bound to a fatty acid.

1.2 Essentiality and role of fatty acids

In 1929, George Oswald Burr and Mildred Burr discovered that fats were nutritionally essential for supporting optimal growth during development (Burr & Burr, 1929). The Burrs then identified linoleic acid (LA, 18:2n-6) (Burr & Burr, 1930) and alpha-linolenic acid (ALA, 18:3n-3) as the nutritionally essential PUFAs in mammals (Wesson & Burr, 1931) . This means that unlike saturated and monounsaturated fatty acids, LA and ALA cannot be synthesized de novo and must be obtained from the diet. LA is an omega-6 (n-6) fatty acid composed of two double bonds, starting on the sixth carbon from the methyl terminal of the molecule. ALA is an omega-3 (n-3) fatty acid containing 3 double bonds starting from the third carbon from the methyl terminal of the molecule.

LA and ALA are essential because they support optimal growth and development and skin barrier integrity (LA mainly). LA requirements range between 1-2% of total calories in developing children (Hansen, Haggard, Boelsche, Adam, & Wiese, 1958). ALA requirements range between 0.2-0.4% in adult humans (Bjerve, Thoresen, Mostad, & Alme, 1987; Holman & Johnson, 1981). Dietary requirements during development have not been fully established.

Biochemically, LA and ALA serve as precursors for bioactive longer-chain fatty acids through elongation, desaturation and oxidation reactions mediated by elongase, desaturase and acyl-CoA oxidase enzymes respectively. LA is a precursor to n-6 arachidonic acid (AA, 20:4 n-6). It is converted to gamma-linolenic acid (GLA,18:3 n-6) through Δ-6 desaturase, elongated to dihomo-gamma-linolenic acid (DGLA, 20:3 n-6) and desaturated to AA via Δ-5 desaturase (Howton & Mead, 1960; Mead & Howton, 1957; Mead, Steinberg, & Howton, 1953; Steinberg, Slaton, Howton, & Mead, 1956). ALA is a precursor to eicosapentaenoic acid (EPA, 20:5 n-3) and docosahexaenoic acid (DHA, 22:6n-3) which are synthesized through the same elongase and desaturase enzymes used to make AA (Klenk & Mohrhauer, 1960). DHA synthesis, however,

involves the additional oxidation of tetracosahexaenoic acid (24:6 n-3), which is an elongation-desaturation product of EPA (Metherel, Lacombe, Chouinard-Watkins, & Bazinet, 2019)

It is often thought that LA and ALA compete for desaturation elongation pathways, although studies have disputed this as the sole mechanism regulating in vivo levels of LA and ALA, and their elongation-desaturation longer-chain products. Turnover due to PUFA flux to and from liver and adipose tissues, and blood-mediated distribution to heart and other tissues, has been shown to be a more important pathway regulating in vivo PUFA concentrations (Metherel, Lacombe, Chouinard-Watkins, Hopperton, & Bazinet, 2018b).

1.3 Fatty acid oxidation

PUFAs are also substrates for non-enzymatic and enzymatic oxidation, whereby an oxygen is added to the molecule to generate an oxidized fatty acid (or oxidized PUFAs). Oxidized PUFAs are known to contribute to sensory properties of foods, e.g. flavor or rancidity (Franklin et al., 2017; Luo, Chapman, Lerno, Huang, & Mitchell, 2021). However, in vivo, they act as potent signaling molecules that regulate multiple physiological pathways by binding to their own G-protein coupled receptors (Lahvic et al., 2018).

Non-enzymatic oxidation occurs when a hydrogen next to one of the double bonds on a PUFA molecule is abstracted by a free radical or a singlet oxygen. The resulting fatty acid radical isomerizes and can either be broken down into smaller molecules (i.e. secondary volatiles) or quenched by the addition of another hydrogen (Choe & Min, 2007).

Free radical oxidation typically occurs during the thermal processing of foods (Kalogeropoulos, Salta, Chiou, & Andrikopoulos, 2007). Here, free radicals generated during thermal treatment, can abstract a hydrogen and initiate fatty acid oxidation.

Lipid oxidation can also be induced by metal ions which can abstract a hydrogen from a PUFA molecule. For instance the release of free iron during meat storage is known to oxidize PUFAs (Rhee, Ziprin, Ordonez, & Bohac, 1988).

Oxidation can be initiated by singlet oxygen molecules formed when ultraviolet light splits a naturally occurring oxygen triplet into three singlets. Singlet oxygen molecules act as nucleophiles, directly attacking the electron dense double bonds of a PUFA molecule to form a PUFA hydroperoxide. PUFA hydroperoxides are unstable, which is why they rapidly degrade to form an alcohol or ketone group. Singlet oxygen-mediated oxidation occurs when oils are stored in non-amber containers for prolonged periods of time (Choe & Min, 2007; Kato et al., 2018).

Non-enzymatic oxidation also occurs in vivo; e.g., in humans. For instance, PUFA oxidation is increased in Alzheimer's disease (AD) and cerebrovascular disease, where oxidative stress is an underlying factor. In this regard, non-enzymatic products of AA such as 8-isoprostane have been shown to be elevated in serum of elderly patients with cerebrovascular disease (Swardfager et al., 2017) and in cerebrospinal fluid of Alzheimer's disease patients (Montine, Markesbery, Morrow, & Roberts, 1998).

The enzymatic oxidation of PUFAs is mediated by lipoxygenase (LOX), cyclooxygenase (COX), prostaglandin dehydrogenase (PGH), cytochrome P450, and soluble epoxide hydrolase (sEH) enzymes to form oxidized fatty acids known as 'oxylipins' (Arnold et al., 2010; Fife, Liu, & Zeldin, 1993; Kanter, Heasley, & Brunton, 1985; S. C. Lee & Levine, 1975; Popp, Bauersachs, Hecker, Fleming, & Busse, 1996; Samuelsson, 1982) . These enzymes act in tandem to generate ketone, hydroxylated or epoxidized PUFAs.

All plants and mammals have LOX, COX, CYP450, and sEH enzymes (Anthon & Barrett, 2002; Hamberg, Sanz, & Castresana, 1999; Mowbray, Elfstrom, Ahlgren, Andersson, &

Widersten, 2006; Tijet et al., 1998). These enzymes are activated in plants during cellular injury, e.g. cuticle penetration by an insect (Gosset et al., 2009). In meats, cellular deformation associated with prolonged freezing or repeated freeze-thawing can activate these enzymes, leading to changes in sensory attributes (Rahman, Hossain, Rahman, Hashem, & Oh, 2014).

In the absence of cellular injury or deformation, thermal oxidation and light remain the main factors affecting lipid oxidation in food systems. Both processes determine shelf life stability of a food product (Kato et al., 2018), and in the case of oils, the number of times the oil can be re-used to fry foods (e.g. repeated frying of French fries) (Kalogeropoulos et al., 2007).

In vivo, most oxidation is enzymatic. As mentioned above, the enzymatic oxidation of PUFAs results in a plethora of bioactive molecules (i.e., oxylipins) involved in signaling. To date, most studies have investigated the in vivo effects of oxylipins derived from AA, EPA and DHA.

The oxidation products of AA are generally referred to as eicosanoids (20 carbon metabolites). Eicosanoids such as prostaglandins (PGs), thromboxanes, leukotrienes and epoxyeicosatrienoic acids (EETs) have been widely studied in the literature. COX-derived eicosanoids such as PGs are involved in promoting inflammation (Harizi, Juzan, Pitard, Moreau, & Gualde, 2002; Takayama et al., 2005) and pain sensitization (Ballou, Botting, Goorha, Zhang, & Vane, 2000), which is why several over-the-counter COX inhibitors such as ibuprofen are used to alleviate inflammation and pain (Orlando, Lucido, & Malkowski, 2015). COX can also convert AA to thromboxanes (TXs), which are involved in vasoconstriction (Noschka et al., 2009), whereas LOX converts it to leukotrienes involved in the immune response via neutrophils and mast cells (Feltenmark et al., 2008; Ringertz, Palmblad, Radmark, & Malmsten, 1982).

CYP-derived EETs are involved in inflammation resolution, and therefore act as in vivo antagonists to the actions of PGs (Kozak, Aronoff, Boutaud, & Kozak, 2003). They are also involved in vasodilation, which is why they have been studied as a novel target for treating hypertension (Gilroy et al., 2016; Morin, Sirois, Echave, Rizcallah, & Rousseau, 2009). EETs can be broken down by sEH into less active and potentially pro-inflammatory PUFA diols (Moghaddam, Motoba, Borhan, Pinot, & Hammock, 1996; Zeldin et al., 1993).

Omega-3 PUFAs are also substrates for enzymatic oxidation in vivo (Mukherjee, Marcheselli, Serhan, & Bazan, 2004; Serhan et al., 2000; Serhan et al., 2002). EPA and DHA can be hydroxylated via COX and LOX enzymes, or epoxidized via CYP450, to generate multiple bioactive lipid mediators involved in the resolution of inflammation. Targeting the synthesis of these pro-resolving oxylipins pharmacologically has been shown to alleviate inflammatory pain in pre-clinical animal models (Serhan et al., 2000; Serhan et al., 2002; Ulu et al., 2013). ALA-derived oxylipins have also been shown to have anti-inflammatory properties, because they inhibit COX-1 and 2 enzymes (M. Liu et al., 2013).

Similar to other PUFAs, LA can be oxidized by CYP450, LOX, COX, and sEH to form oxidized linoleic acid metabolites (OXLAMs) (Engels, Willems, & Nijkamp, 1986; W. Liu et al., 2010; Oliw, 1993; Reinaud, Delaforge, Boucher, Rocchiccioli, & Mansuy, 1989). Interestingly, several classes of these enzymes prefer LA as a substrate over AA. For example, 15-LOX was initially named because it preferentially acted on the 15^{th} carbon of AA (from the methyl terminal) which contains a double bond, but was later shown to require lower free energy to react with the 9th carbon from the methyl terminal of LA, which also contains a double bond (Soler et al., 2016). A representative OXLAM enzymatic formation pathway is shown in **Figure 2** (M. Hennebelle, R. K. Morgan, et al., 2019).

Most studies investigating the biological effects of OXLAMs have focused on peripheral tissues. For instance, in rodents, OXLAMs were shown to reduce pain thresholds via dietary LA, highlighting their role in pain regulation (Ramsden et al., 2017). Also in rodents, OXLAMs were shown to cause hepatic injury (Schuster et al., 2018b).

1.4 LA intake levels in the U.S.

The U.S. consumption of LA has increased by 3-fold since the early 1900s due to increased consumption of high-LA oils such as soybean oil and corn oil (Blasbalg, Hibbeln, Ramsden, Majchrzak, & Rawlings, 2011a). Soybean and corn oil contain ~54% and 18% LA of total fatty acids, respectively (Richardson et al., 2017). In the U.S., LA contributes 7.2% of total calories consumed per person per day (Blasbalg et al., 2011a). Notably, except for a 50% increase in ALA intake, the consumption of other omega-3 PUFAs has remained relatively stable since the 1900s (Blasbalg et al., 2011a).

There are two main drivers of increased LA consumption in the U.S. The first is linked to the expansion of soybean agriculture during the 1930s (Dutton, 1981). The second relates to studies during the 1950s showing that replacing saturated fats with high LA vegetable oils, reduces circulating cholesterol, a known risk factor for coronary artery disease (Bronte-Stewart, 1958; Keys, Anderson, & Grande, 1957). However, recent evidence from randomized control trials does not support a cardioprotective effect of replacing dietary saturated fats with high LA oils (Ramsden, 2013; Ramsden, Zamora, et al., 2016).

The increase in LA intake has increased the plasma n-6 to n-3 dietary ratio (Ramsden et al., 2012). The current recommended n-6 to n-3 dietary ratio is not well defined but has been suggested to be around 3:1 (Stanley et al., 2007; Tulk & Robinson, 2009). However, the actual ratio is approximately 11:1 or even higher, mainly due to excess LA in the diet (Flickinger, Sun,

& Empie, 2011; Molendi-Coste, Legry, & Leclercq, 2011). Multiple epidemiology studies have linked an imbalance in the n-6 to n-3 ratio to metabolic dysregulation (Delavar, Lye, Khor, Hassan, & Hanachi, 2009; Ruidavets et al., 2007).

The increase in LA intake has also been reflected in human breast milk fatty acid composition. Recent studies have shown LA accounts for 10-18% of human breast milk fatty acid composition (Yuhas, Pramuk, & Lien, 2006), which is higher than the 7% measured in breast milk during the 1940s (Hilditch & Meara, 1944) .

1.5 LA oxidation in foods and health effects

It is presumed that the use of high LA oils in food processing also results in increased OXLAM accumulation in foods, although this has not been experimentally shown. Many foods are ultra-processed, defined as "foods that are formulated mostly of cheap industrial sources of dietary energy and nutrients plus additives, using a series of processes" (Monteiro et al., 2018). These foods undergo multiple thermal processing steps involving oil oxidation during the manufacturing process.

Epidemiological studies have shown that food processing may have adverse health effects, and this may be linked to increased OXLAM intake. Increased consumption of fried foods has been linked to increased risk of cardiovascular disease, cancer, hyperlipidemia, hypertension and weight gain, as well as shorter telomere length (Bonaccio et al., 2021; Jiao, 2020; Rico-Campa et al., 2019; Santoro et al., 2014b; Veronese et al., 2017a; Z. Zhang et al., 2021; Zhuang et al., 2020). This is consistent with rodent studies showing that dietary OXLAMs may be involved in chronic illnesses such as cardiovascular disease, diabetes and other metabolic disorders by reducing pancreatic insulin production and promoting vasoconstriction (Santoro et al., 2014b; Siegfried, Aoki, Lefer, Elisseou, & Zipkin, 1990).

1.6 Bioavailability of OXLAMs

In vivo, OXLAMs are readily detectable in plasma and multiple tissues (Ramsden, Ringel, et al., 2016; Taha et al., 2018a). There are two possible mechanisms accounting for OXLAM accumulation in vivo – 1) dietary LA is absorbed and converted to OXLAMs, or 2) OXLAMs in the diet (e.g., formed during food processing) are directly absorbed and incorporated into plasma and tissues.

It is well-established that LA itself is bioavailable (Chow & Hollander, 1979a, 1979b), and that altering dietary LA levels modifies OXLAM concentrations in vivo, in both rodents and humans. In humans, lowering dietary LA from 7% to 2% energy was shown to reduce circulating OXLAM concentrations by approximately 15% (Ramsden et al., 2012). In rats, dietary LA lowering from 5% to 0.4% energy decreased plasma, brain, cervical cord, bladder and cortex OXLAM concentrations (Ramsden et al., 2012; Taha et al., 2018a). Collectively, the evidence suggests that dietary LA is an important regulator of plasma and tissue OXLAM levels.

OXLAMs can be obtained from the diet (Richardson et al., 2017). However, it is not known whether dietary OXLAMs are absorbed, and thus contribute to plasma and tissue OXLAM concentrations. This is because limited and conflicting information exists on the bioavailability of OXLAMs in vivo. For instance, some studies have shown OXLAMs are degraded in the gastrointestinal (GI) tract into secondary aldehydes upon ingestion (Kanazawa & Ashida, 1998), while others have reported that they are absorbed (Wilson, Lyall, Smyth, Fernie, & Riemersma, 2002).

A limitation of prior studies is that they used radiolabeled (^{14}C) OXLAMs provided orally, and measured radioactivity in organs and tissues. This approach is problematic because it does not inform on whether the tracer was absorbed intact, or degraded into secondary aldehydes

and ketones during absorption (Bergan & Draper, 1970; Glavind & Sylven, 1970; Kanazawa & Ashida, 1998). However, by using ^{13}C or deuterium labeled tracers coupled with sensitive mass spectrometry techniques, detailed mechanistic pathways of oral intake of OXLAMs could be elucidated. This is because mass-spectrometry techniques provide structural information on the fate of the molecule in vivo (e.g. whether it was absorbed intact or biotransformed).

1.7 The role of LA and OXLAMs in neurodevelopment

Most studies to date have focused on the effects of dietary LA or OXLAMs provided through processed foods on metabolic disorders (e.g. cardiovascular disease, diabetes and others) (Bonaccio et al., 2021; Pagliai et al., 2021; Rico-Campa et al., 2019; Z. Zhang, Jackson, Martinez, Gillespie, & Yang, 2020). A limited number of studies have investigated the effects of LA and OXLAMs on the brain. Both LA and OXLAMs have been implicated in neurodevelopment reviewed by Taha (Taha, 2020).

High maternal intake of LA during pregnancy and lactation has been linked to poor cognitive and motor performance in rodent and human infants. In rodents, elevated intake of LA during pregnancy has been associated with aggressive behavior and impaired motor development in the offspring (Raygada, Cho, & Hilakivi-Clarke, 1998). In humans, maternal plasma LA levels were positively associated with autism spectrum disorder (ASD) traits in infants (Steenweg-de Graaff et al., 2016). Further, increased maternal breast milk composition of LA has been associated with impaired motor and cognitive performance in infants (Bernard et al., 2015; Kim et al., 2017) It is not known whether lowering maternal LA intake protects against neurodevelopmental impairments.

Both LA and OXLAMs are involved in regulating neurodevelopment, although the evidence stems from in vitro and animal studies. In vitro, 13-hydroxyoctadecadienoic acid (13-

HODE) and LA have been shown to promote neuronal morphogenesis in neuron-glia co-cultures isolated from 0 to 1-day old male and female pups respectively (M. Hennebelle, R. K. Morgan, et al., 2019). Kamata et al. showed that LA induced neurite growth in rat pheochromocytoma cells (Kamata, Shiraga, Tai, Kawamoto, & Gohda, 2007)

Early in vivo studies on the effects of OXLAMs on brain development were performed in chickens and their offspring. Dam et al. reported that feeding newborn chicks a diet containing 1.5% ethyl-LA and lacking Vitamin E, resulted in 92% death from encephalomalacia, a form of neurodegeneration, within 28 days compared to a group fed 1.5% ALA without vitamin E (Dam, Nielsen, Prange, & Sondergaard, 1958). Later, Dam et al. discovered that a Vitamin E free diet containing 1.5% ethyl-AA induced encephalomalacia more abruptly than a Vitamin E free diet containing 1.5% ethyl-LA or lard. The authors concluded that the coupling of Vitamin E deficiency and auto-oxidation of omega-6 PUFAs could lead to adverse chick brain development (Dam et al., 1958; Dam & Sondergaard, 1962).

Bartov and Bornstein suggested that LA-induced encephalomalacia was likely caused by OXLAMs (Bartov & Bornstein, 1980). Offspring of chickens fed a high LA diet derived from soybean oil had a 66.7% incidence of encephalopathy compared to offspring of chickens fed a tallow-based diet low in LA. The incidence of encephalopathy was further exacerbated when the offspring chicks were placed on a Vitamin-E free diet containing 4% or 10% oxidized safflower oil, particularly in chicks hatched from chickens on the soybean oil diet (high in LA) than those from the beef tallow diet (low in LA). Supplementing with Vitamin E partially reversed these effects (Bartov & Bornstein, 1980).

Budowski et al. further investigated the effects of dietary OXLAMs on encephalomalacia. The group showed that feeding a vitamin E free diet containing 10%

thermally oxidized safflower oil methyl esters to one-day old chicks for up to 3 weeks increased the incidence of mortality by 10-fold compared to chicks fed fresh safflower oil methyl esters without vitamin E. This suggests that OXLAMs in the thermally treated oil may be the cause of increased ataxia and mortality in chicks (Budowski, Bartov, Dror, & Frankel, 1979).

To further test the potential direct effects of OXLAMs on the risk of ataxia and mortality, Budowski et al. fed young chicks a 4% lipid diet with fresh safflower oil supplemented with 0.3% crude polar lipid isolated from thermally treated oil ot sure for three days and compared the results to chicks fed the same safflower oil diet alone. The crude polar extract was analyzed and found to contain several OXLAMs including conjugated keto fatty acid esters. The authors found 70% greater incidence of ataxia and increased mortality by 20 days in chicks fed the safflower oil diet containing crude polar extract (i.e. OXLAMs) compared to chicks fed the safflower oil diet alone (Budowski et al., 1979).

Consistent with Budowski et al.'s finding, Kokatnur et al. showed that several isomers of conjuagted keto fatty acids such as 12-oxo-cos-9-octadecenoic acid, 12-oxo-octadecanoic acid, 12-oxo-trans-10-octadecenoic acid, and 12-oxo-cos-9-octadecenoic acid added to a Vitamin E free, corn oil diet significantly increased the incidence of encephalomalacia in young chicks compared to chicks fed a Vitamin E free, corn oil control diet. (Kokatnur, Okui, Kummerow, & Scott, 1960). This further confirms a direct role of early exposure to OXLAMs on brain atrophy.

1.8 Blood brain barrier penetrance of LA and OXLAMs

LA is known to cross the blood brain barrier (BBB), but it is not known whether OXLAMs cross. The chicken studies showing a direct effect of OXLAMs on encephalomalacia, suggest that OXLAMs enter the brain, although it is not known whether this assumption is true

for mammals. In 0-1 day-old rat pups, OXLAMs were shown to constitute around 51% of detected oxylipins in the brain; in adults rats this value was shown to be in the range of 7-9% (Ferdouse, Leng, Winter, & Aukema, 2019; Hennebelle et al., 2020). These observations point to one or more pathways that regulate brain OXLAM concentrations, particularly during development. They also support the notion that OXLAMs play a role in neurodevelopment.

There are two plausible mechanisms that could explain how OXLAMs accumulate in the brain. One possibility is that LA entering the brain is rapidly converted into OXLAMs. A second possibility is that dietary OXLAMs directly enter the brain.

LA is not abundant in the brain, and constitutes 1-2% of total fatty acids in both young and adult rats (M. Hennebelle, R. K. Morgan, et al., 2019). However, it is known to cross the blood brain barrier through passive diffusion, at a comparable rate as other fatty acids such as AA and DHA (Chen, Green, Orr, & Bazinet, 2008). One study showed that the majority of LA entering the brain (59%) is rapidly beta-oxidized. A smaller portion (9%) is incorporated into brain phospholipids, the main lipid species in the brain (J. C. DeMar et al., 2006). Although this may explain the low abundance of LA compared to other fatty acids, it is not known whether a portion of the LA entering the brain is converted into OXLAMs.

As discussed in Section 1.6., it is not known whether dietary OXLAMs are absorbed in the gut, and whether they incorporate into tissues, including the brain. Thus, a deeper understanding on the bioavailability and metabolism of OXLAMs in vivo is needed to understand how they regulate brain development and function.

1.9 Unknowns this thesis aims to address

There are several scientific gaps and questions that this thesis aims to address.

First, the specific processing conditions that lead to the formation of OXLAMs in foods are not known. It has always been assumed that food processing increases OXLAM concentrations in foods. To my knowledge, this assumption has not been thoroughly tested. Also, studies that investigated the effects of processing on OXLAM formation used prolonged heating conditions (days to weeks) that do no mimic real-world processing scenarios (Maszewska et al., 2018; Richardson et al., 2017). It is difficult to estimate the extent of dietary exposure to OXLAMs without knowing how different real-world processing conditions affect their formation or potential degradation.

Another unknown is the extent of OXLAM distribution in maternal breastmilk, the primary source of nutrition for most infants. Most mothers consume processed foods during pregnancy and lactation (Jardi et al., 2019). OXLAMs in the diet may accumulate in breast milk as evidenced by a recent study showing the presence of OXLAMs in breast milk (J. Wu, S. Gouveia-Figueira, M. Domellof, A. M. Zivkovic, & M. L. Nording, 2016). However, the distribution of OXLAMs within various milk lipid fractions is not known. This is because prior studies measured unesterified (free) OXLAMs in breast milk. A recent study showed that over 95% of OXLAMs in bovine milk are esterified, and thus serve as a source of free OXLAMs which are bioactive (Teixeira, Dias, Vieira, Leite Nobrega de Moura Bell, & Taha, 2021). It is not known whether the same phenomenon occurs in human breast milk.

A third unknown is whether dietary OXLAMs are absorbed and incorporate into peripheral and brain tissues. If so, dietary OXLAMs may play a more critical role in regulating circulating and tissue OXLAM concentrations than dietary LA, which has been shown to promote the synthesis of OXLAMs in plasma and tissues (Ramsden et al., 2012; Schuster et al., 2018b; Taha et al., 2018a).

Although dietary LA is known to regulate brain OXLAM concentrations, the extent of conversion of brain LA into OXLAMs is not known. Knowing this is critical to understanding the relative contribution of dietary LA versus dietary OXLAMs, to brain OXLAM concentrations. In other words, which of these two pathways is the primary contributor to brain OXLAM levels?

Lastly, while studies reported on the effects of maternal LA intake on infant neurodevelopment, no study has established whether this is due to changes in LA or OXLAM metabolism in the brain of the offspring. That is, if maternal dietary factors that affect maternal LA metabolism change, will that have a long-lasting impact on offspring brain LA and OXLAM metabolism? Because LA and OXLAMs regulate neuronal morphogenesis (Hennebelle et al., 2020), it is important to know whether their metabolism in the developing brain can be altered by the maternal diet.

1.10 Thesis hypothesis and objectives

The overall hypothesis of my thesis is that diet is an important source of exposure to OXLAMs, which can be absorbed and contribute to brain OXLAM accumulation during adulthood and development. My overall objective is to measure exposure to OXLAMs from processed foods and breast milk, determine how these OXLAMs get to the brain, and understand their regulation in the brain by the maternal diet.

To test the hypothesis, the following specific aims and specific hypotheses are proposed:

Aim 1 (Chapter 2): assess the effects of food processing on OXLAM formation using potatoes as a model food. Potatoes were chosen because they are a frequently consumed

food by the general population, including pregnant and lactating women (Bao, Tobias, Hu, Chavarro, & Zhang, 2016).

Hypothesis: *Thermal processing will increase the formation of OXLAMs.*

Aim 2 (Chapter 3): Determine exposure to OXLAMs from human breastmilk.

Hypothesis: *Similar to bovine milk, the majority of OXLAMs will be found in esterified lipid pools, i.e. esterified lipids are the main source of exposure to OXLAMs during development.*

Aim 3 (Chapter 4): Determine the absorption and incorporation of labeled OXLAMs in rats.

Hypothesis: *Labeled 13-hydroxyoctadecadieonic acid (13-HODE), an OXLAM abundant in the diet will be absorbed and incorporated into tissues, including the brain.*

Aim 4 (Chapter 5): Determine the contribution of labeled LA to brain OXLAM synthesis in rats.

Hypothesis: *LA entering the brain will be rapidly converted to OXLAMs, thus contributing to endogenous OXLAM concentrations.*

Aim 5 (Chapter 6): Understand the impact of maternal regulation of LA metabolism by dietary calorie restriction or statins on offspring brain OXLAM metabolism in a non-human primate model.

Hypothesis: *Dysregulation of maternal LA metabolism by calorie restriction or statins will have long-lasting impact on offspring brain OXLAM concentrations, through epigenetic mechanisms.*

Chapters 2, 3 and 4 have been published in Journal of *ACS Food Science & Technology*, *Lipids*, and *BBA Molecular and Cell Biology of Lipids*. Chapters 5 and 6 are drafted manuscripts which will be submitted for publication.

Chapter 2 (Aim 1): Effects of Potato Processing and Frying on Oxylipin Concentrations

Zhichao Zhang[1], Marie Hennebelle[1,+], Shiva Emami[1] and Ameer Y. Taha*[1]

[1]Department of Food Science and Technology, College of Agriculture and Environmental Sciences, University of California, Davis, CA, USA

[+] Present address: Laboratory of Food Chemistry, Wageningen University and Research, Wageningen, The Netherlands

*Corresponding author:

Dr. Ameer Y. Taha

Department of Food Science and Technology, College of Agriculture and Environmental Sciences, University of California Davis, One Shields Avenue, Davis, CA, USA 95616

Phone: (+1) 530-752-7096; Email: ataha@ucdavis.edu

Zhang, Z., Hennebelle, M., Emami, S., & Taha, A. Y. (2021). Effects of Potato processing and frying On Oxylipin Concentrations. *ACS Food Science & Technology*.

https://doi.org/10.1021/acsfoodscitech.1c00139

Abstract:

Potatoes undergo multiple processing steps including blanching and par-frying to form frozen French fries, which are typically fried in oil subjected to multiple frying cycles. The present study aimed to comprehensively measure the effects of potato processing (i.e., blanching, par-frying, deep frying and repeated frying cycles) on the concentration of primary oxidized fatty acids known as oxylipins in potatoes and the oil used to fry them. Compared to raw peeled potatoes, blanching decreased linoleic acid (LA)-derived epoxides and diols and increased α-linolenic acid (ALA)-derived hydroxides by in potatoes. Par frying and one cycle of deep frying reduced several hydroxylated and ketone metabolites of LA or ALA in raw potatoes. Repeated frying increased several LA- and ALA-derived oxylipins in oil but decreased them in potato French fries. It is concluded that distinct oxylipin profiles are observed when potatoes are subjected to different processing conditions.

Key words:

French fries, blanching, par-frying, soybean oil, lipid oxidation

1. Introduction

In the US, approximately 49.4 pounds of frozen potatoes are consumer per person per year (~1 pound/week), mostly in the form of French fries (USDA, 2016) On average, this level of intake contributes to ~ 1.5 percent of daily calories (Storey & Anderson, 2013). Epidemiological studies have linked the frequent consumption of fried potatoes to increased risk of type 2 diabetes, cardiovascular disease and hypertension (Borgi, Rimm, Willett, & Forman, 2016; Muraki et al., 2016), as well as increased all-cause mortality (Veronese et al., 2017b). This risk has been linked to bioactive metabolites derived from the oxidation of polyunsaturated fatty acids (PUFAs), known as oxylipins (Santoro et al., 2014a; Siegfried et al., 1990).

Ingested oxylipins are bioavailable in both humans and rats with absorption efficiencies ranging between 4.5% to 38.7% in humans and 14.8% in rats depending on the type of oxylipin (e.g. hydroperoxide, hydroxy or dihydroxy fatty acid) (Bergan & Draper, 1970; Penumetcha, Khan, & Parthasarathy, 2000; Wilson et al., 2002). A recent study in rats showed the deuterated 13-hydroxyoctadecadienoic acid (13-HODE), an oxylipin found in high abundance in oils and bovine milk (Dias et al., 2020; Richardson et al., 2017), is absorbed and incorporated into tissues (Z. Zhang et al., 2021). Ingested oxylipins from thermally oxidized corn oil have recently been shown to alter cerebrum and cerebellum fatty acid composition and to induce liver mitochondrial dysfunction in mice (Ramsden et al., 2018b; Schuster et al., 2018a), suggesting *in vivo* bioactivity.

The processing of French fries involves multiple processing steps which include washing, peeling, cutting, blanching, par-frying, freezing and deep fat frying (Lindhauer, Haase, & Putz, 2003). Blanching is applied to inactivate enzymes and preserve potatoes by boiling peeled and cut potatoes in water at 75 °C (167°F) for 10 mins or from 60.0 to 82.2°C (140 to 180°F) for 15

mins (Ngobese, Workneh, & Siwela, 2017; Nonaka, Sayre, & Weaver, 1977). Par-frying involves frying the blanched potatoes for a short period of time (1 min) at 160.0°C, 171.1°C or 185.0°C to achieve ideal crispness for final deep frying (Nonaka et al., 1977). The par-fried potatoes are then frozen, packaged and distributed to consumer outlets including restaurants (Keijbets, 2001), where they undergo deep frying in plant oils such as soybean, canola, corn, sunflower, and other mixed oils high in oleic acid (18:1 n-9), linoleic acid (LA, 18:2 n-6) or α-linolenic acid (ALA, 18:3 n-3).

In the US, soybean oil is the most widely used oil by fast food restaurants (Jahren & Schubert, 2010). Soybean oil contains approximately 55% LA and 9% ALA, which are precursors to oxylipins (Marmesat, Velasco, & Dobarganes, 2008; Richardson et al., 2017). Thus, processing or frying at high temperatures could induce the thermal oxidation of PUFAs in oil (Cuesta, Sanchezmuniz, Garridopolonio, Lopezvarela, & Arroyo, 1993), consistent with studies showing increased concentrations of total polar lipids, oxidized triglycerides, LA-derived epoxides and oleic acid derived ketones in French fries subjected to multiple frying cycles in sunflower oil at 175°C (Kalogeropoulos et al., 2007; Ramsden et al., 2017).

The potatoes themselves also contain fat, amounting to 40-50 mg fatty acids /100 g fresh weight. LA and ALA make up the majority of these fatty acids in potatoes, ranging between 51.3-51.9% for LA and 13.4-22.3% for ALA depending on the variety (Galliard, 1973). LA and ALA in potatoes can also serve as substrates for lipid oxidation via lipoxygenase enzymes which are activated upon peeling and cutting the potato (Galliard, 1973; Saubeau et al., 2013).

Lipid oxidation in French fries has generally been assessed using qualitative assays that measure total polar compounds, free fatty acid content or peroxide value (Flores-Alvarez Mdel, Molina-Hernandez, Hernandez-Raya, & Sosa-Morales, 2012; Ramsden et al., 2017). One study

involving gas-chromatography/mass-spectrometry reported an increase in LA-derived epoxides and oleic acid-derived ketones in both the oil and French fries after 8 frying cycles (Kalogeropoulos et al., 2007). Data on the effects of frying as well as other pre-processing conditions (e.g., blanching) on other oxidized fatty acid species (e.g., hydroxylated fatty acids), remains lacking to our knowledge. This is important to know in view of the reported risks associated with chronic consumption of fried potatoes (Borgi et al., 2016; Muraki et al., 2016).

The goal of this study was to determine the effects of blanching, par-frying and repeated frying cycles on oxylipin concentrations in potatoes, and in the oil used to fry the potatoes. Since potatoes and the soybean oil used to fry them are enriched with LA and ALA, we quantified oxylipin products of these two fatty acids with ultra-high pressure liquid chromatography coupled to tandem mass-spectrometry (UPLC-MS/MS) (Richardson et al., 2017). We hypothesized that processing and repeated frying would increase oxylipin concentrations in potatoes, and in the oil used to fry them.

2. Materials and Methods

2.1 *Study One: Effects of blanching, par frying and deep frying*

Raw potatoes were purchased from a local grocery store (Davis, CA, USA) the day before the experiment and kept at room temperature overnight. Potatoes were washed in water, peeled and cut into 0.7 cm x 0.7 cm x 8 cm rectangular prisms. A portion (~ 20 g) of the potato prisms was frozen at -80°C (baseline sample). The remaining portion (334.2 g) was submerged in cold faucet water in a steel pot for approximately 5 to 6 minutes and subsequently blanched in hot water for 15 minutes. The water containing the potatoes was continuously heated throughout

the 15 minutes on a stove. The recorded initial temperature of the hot water was 74.8°C (166.7°F); the recorded temperature at 15 minutes was 62.3°C (144.2°F).

After blanching, the water was drained and the potatoes (294.4 g) were par fried in 2130 mL Crisco soybean oil (Orrville, OH, USA) at 185.9°C (366.7°F) for 3 mins using a Presto Deep Fryer (Model 05460, Eau Claire, WI, USA). The final oil temperature after par-frying was 130°C (266 °F). Par-fried potatoes were placed on paper sorbent to remove excess oil, cooled on dry ice for 10 mins and transferred to a -80°C freezer until the fries were completely frozen for at least one hour. A portion (311.8 g) of the frozen fries were fried in fresh 2130 mL oil in the same fryer for 10 mins at 190.6°C (375°F) to make deep fried potatoes. The sample size was 5 technical replicates per treatment (i.e., from the same processed batch). This is justified because batch processing introduces some heterogeneity on the samples due to uneven thermal distribution during heating (Wu, Karayiannis, & Tassou, 2013). A schematic representation of the process is described in **Figure 3**.

Raw, blanched, par fried, and deep-fried potatoes were all frozen and mashed into powders with a pestle and mortar pre-cooled on dry ice for oxylipin analysis (described below).

2.2 Study Two: Effects of repeated frying

Crisco soybean oil (Orrville, OH, USA) and Oregon & Idaho Shoestrings frozen French fries (Pittsburgh, PA, USA) were purchased from a local grocery store in Davis, CA. Frozen French fries were kept in a -80°C freezer and oils were kept in a dark closet at room temperature until the frying experiment.

Five to six sticks of frozen French fries were crushed with a pestle and mortar on dry ice and approximately 50 mg of powder were weighed for oxylipin extraction. This, along with a 10

µL aliquot of the pre-heated oil 190.6°C (375°F) served as baseline samples (i.e., time=0) for oxylipin measurements.

Soybean oil (2130 mL) was transferred to a Presto Deep Fryer (Model 05460, Eau Claire, WI, USA) heated to 190.6°C (375°F). After pre-heating to around 190.6°C (375°F), oil from the middle of the fryer was transferred into 2 mL amber vials (Phenomenex, Torrance, CA, USA, Catalogue #AR0-3911-13) using a glass Pasteur pipette (Fisher Scientific, Hampton, NH, USA, Cat # 13-678-20A). Approximately 313 g of frozen French fries were added to a steel mesh which was placed in the fryer containing the oil for 10 mins. The mesh was occasionally shaken (2 to 3 times) using the handle to ensure even distribution of the oil. After 10 mins, the fried oil was sampled as described above and French fries were taken out of the fryer. The oil sample was cooled at room temperature for 10 mins, capped under nitrogen, and transferred to a -80°C freezer. French fries were shaken for 30 seconds to drain the oil and allowed to cool on a foiled metal baking pan at room temperature for 5 mins. They were then transferred to Ziploc bags and cooled for at least one hour at -80°C. After 1 hour, the cooled fries were crushed into powder with a pestle and mortar pre-cooled on dry ice and stored in -80°C in Ziploc bags until they were analyzed.

The 10-min frying cycle was repeated with a fresh batch of frozen French fries using the same oil, two more times. Oil and French fries were sampled at each cycle using the same process described above. Initial and final temperatures of each frying cycle were recorded using a thermometer (temperature range of 363°F to 378°F).

The overall 30-min frying experiment was carried out over a 3-day period, twice on the first two days and once on the third day, resulting in a total of 5 independent oil French fries samples per time-point (0, 10, 20 and 30 mins). Between each 30-min frying cycle, the fryer was

thoroughly washed with soap and hot water and dried with napkins. The pestle and mortar were wiped twice with methanol (Fisher Scientific, Hampton, NH, USA, Cat # A454-4), once with chloroform (Fisher Scientific, Cat #C607-4), and once with acetone (Fisher Scientific, Cat # A18-P4) between crushing each sample. A schematic representation of the process is depicted in **Figure 4**.

2.3 Oxylipin extraction

Total (i.e., free and esterified) oxylipins were extracted from oil and processed potatoes by solid phase extraction (SPE) as previously described (Richardson et al., 2017).

For oil samples, 10 µL of oil were transferred to 2 mL microcentrifuge tubes (USA Scientific, Orlando, FL, USA, Cat # 1620-2700) and spiked with 10 µL of antioxidant solution mixture and 10 µL of 2 µM surrogate standard mixture containing d11–11(12)-EpETrE (Cayman Chemical, Ann Arbor, MI, USA, Cat # 10006413), d11-14,15-DiHETrE (Cayman Chemical, Cat # 1008040), d4-6-keto-PGF1α (Cayman Chemical, Cat # 315210), d4-9-HODE (Cayman Chemical, Cat # 338410), d4-LTB4 (Cayman Chemical, Cat # 320110), d4-PGE2 (Cayman Chemical, Cat # 314010), d4-TXB2 (Cayman Chemical, Cat # 319030), d6-20-HETE (Cayman Chemical, Cat # 390030) and d8-5-HETE (Cayman Chemical, Cat # 334230) in LC-MS grade methanol (Fisher Scientific, Cat # A456). The antioxidant solution was mixed by dissolving 0.2 mg/mL butylated hydroxytoluene (BHT, Sigma-Aldrich, St. Louis, MO, USA, Cat # W218405-SAMPLE-K), triphenylphosphine (TPP, Sigma-Aldrich, Cat # 3T84), and ethylenediaminetetraacetic acid (EDTA, Sigma-Aldrich, Cat # EDS-100G) in methanol/water (50/50, v/v), vortexed and filtered with a 0.45 µm Millipore filter (Millpore, Bedford, MA, USA,

Cat # SLHVM25NS) and a B-D 1 cc syringe (Becton Dickinson& Co, Rutherford, NJ, USA, Cat # 309628). One hundred and ninety µL of extraction solvent containing 0.1% acetic acid (Sigma-Aldrich, Cat # 695092) and 0.1% BHT in methanol was added to each sample. Samples were hydrolyzed as described below.

Approximately 50 mg of powdered raw (peeled), blanched, par fried or deep fried potatoes (French fries) were spiked with the 10 µL antioxidant solution mixture, 200 µL of extraction solvent and 10 µL surrogate mixture in 2 mL micro centrifuge tubes. Samples were spiked in this particular order because in preliminary experiments we found that spiking the surrogate standard prior to adding the French fries to the tube resulted in no discernable surrogate standard peak on the LC-MS/MS, likely due to irreversible adsorption of the standard to the fries or the centrifuge tubes. Adding the standard after adding the extraction solvent ensured that this did not occur and that the standard remained in the extraction solvent.

Samples were cooled in a -80°C freezer for one hour. After cooling, the samples were homogenized using a bead homogenizer (Bullet Blender Storm, Next Advance, Troy, NY, USA, Cat #BBY24M) for one minute and placed back in the -80°C freezer for 30 min. The chilled samples were centrifuged for 10 min at 15,871 *g at 0°C on a 5430r Eppendorf micro-centrifuge (Eppendorf, Hauppauge, NY, USA). The supernatant was transferred to new 2 mL micro centrifuge tubes.

Oil and potato extracts (in extraction solvent) were mixed with 200 µl of 0.25M sodium carbonate (Sigma-Aldrich, Cat # 791768-500G) solution (in methanol/ ultrapure water, 50/50 v/v) to hydrolyze esterified oxylipins. Samples were heated at 60°C for 30 mins on a heat block. Twenty-five µL of acetic acid were added after the samples were cooled for a few minutes at room temperature and the pH was verified in one representative sample to be between 4 and 6

using litmus paper. Ultrapure water (1575 µL) was then added, and the samples were subjected to solid phase extraction (SPE).

SPE columns (60mg Oasis HLB, Waters, Milford, MA, USA, Cat # WAT094226) were first washed with one column volume of ethyl acetate (Fisher Scientific, Cat # E196-4) and two column volumes of methanol and conditioned with two column volumes of SPE buffer (0.1% acetic acid and 5% methanol in ultrapure water). Samples were loaded onto the SPE columns, washed with two column volumes of SPE buffer and dried under 14 psi vacuum for 20 mins. Oxylipins were eluted with 0.5 mL methanol and 1.5 mL ethyl acetate. The eluent from each sample was dried under nitrogen, reconstituted in 100 µL LC-MS grade methanol, vortexed, centrifuged at 0°C at 15,871 x g for 2 mins, and the supernatant was transferred and centrifuged again at 15,871*g at 0°C for 20 mins in centrifugal filter units (Ultrafree-MC VV Centrifugal filters, Burlington, MA, USA, Cat # UFC30VV00).

2.4 UPLC-MS/MS analysis

A total of 72 oxylipins were analyzed using an Agilent 1290 Infinity UHPLC system connected to an Agilent 6460 triple-quadrupole tandem mass spectrometer (Agilent, Palo Alto, CA, USA) with electron spray ionization in the negative mode and optimized dynamic Multiple Reaction Monitoring (dMRM) conditions listed in **Supplementary Table 1**. Oxylipins were separated using an Agilent Eclipse Plus C18 column (2.1 x 150 mm, 1.8 µm Agilent Corporation, Cat # 959759-902). The auto-sampler and column were kept at 4°C and 45°C, respectively. Mobile phase A contained 0.1% acetic acid in ultrapure water and mobile phase B contained LC-MS grade 80/15 acetonitrile (Fisher Scientific, Cat # A9561)/methanol (v/v) with 0.1% acetic acid. The flow gradient was: mobile phase A started at 65%, decreased to 60% at 3

mins, 54% at 4 mins, 40% at 10 mins, 30% at 20 mins, 15% at 24 mins and 1% at 24.6 mins followed by a hold to 26 mins. Mobile phase A was then increased to 65% at 26.10 mins and held constant to 27.30 mins. The flow rate initially was 0.3 mL/min from 0-3 mins, 0.25 mL/min from 3 to 24.5 mins, 0.35 mL/min from 24.6 to 27 mins, and 0.30 mL/min at 27.30 mins.

Because the surrogate d4-PGE2 degraded during the hydrolysis, quantification of LA-derived trihydroxylated metabolites (9,10,13-TriHOME and 9,12,13-TriHOME) paired to this surrogate was not possible. Other metabolites that use the d4-PGE2 standard for quantification include PGB2, PGD1, PGD2, PGD3, PGE1, PGE2, PGE3, 15-deoxy-PGJ2 and PFG2-alpha; however, these compounds are derived from arachidonic acid which is not found in potatoes or plant oils. Thus, eight oxylipins derived from LA and two from ALA were quantified with UPLC-MS/MS in this study. These were LA-derived 9-hydroxyoctadecadienoic acid (9-HODE), 13-hydroxyoctadecadienoic acid (13-HODE), 9-oxo-octadecadienoic acid (9-oxo-ODE), 13-oxo-octadecadienoic acid (13-oxo-ODE), 12(13)-epoxyoctadecamonoenoic acid (12(13)-EpOME), 9(10)-epoxyoctadecamonoenoic acid (9(10)-EpOME), 12,13-dihydroxyoctadecamonoenoic acid (12,13-DiHOME), 9,10-dihydroxyoctadecamonoenoic acid (9,10-DiHOME), and ALA-derived 9-hydroxyoctadecatrienoic acid (9-HOTrE) and 13-hydroxyoctadecatrienoic acid (13-HOTrE). Oxylipins were quantified using an external standard curve for each analyte to correct for the response factor, and deuterated surrogate standards to correct for losses during the extraction.

2.5 Statistical analysis

Oxylipin concentrations were expressed as mean ± standard deviation (SD). Data were analyzed on Graphpad Prism7 (GraphPad Software Inc., San Diego, CA, USA). A one-way

repeated measures analysis of variance (ANOVA) followed by Dunnett's multiple comparison test (comparing treatment to baseline samples) was applied to Study One samples and Study Two oil samples. A one-way ordinary ANOVA followed by Dunnett's multiple comparison (comparing treatment to baseline samples) was applied to Study Two French fries samples, since a separate batch of fries was used during each frying cycle.

3. Results and discussion

3.1 Effects of blanching, par-frying and deep-frying on raw potatoes

LA- and ALA-derived oxylipin concentrations of raw, blanched, par-fried and deep fried potatoes are reported in **Figure 5**. Hydroxy, ketone, epoxide and diol metabolites of LA were measured, whereas only hydroxylated metabolites of ALA were measured due to standard availability.

Overall, compared to raw potatoes, blanching increased hydroxylated fatty acids, and decreased LA-epoxides and diols, whereas par and deep frying decreased hydroxy, ketone or epoxy fatty acids in favor of increased diols. Specifically, blanching significantly decreased LA-derived 9,10-EpOME and 12,13-DiHOME by 46-85% and increased ALA-derived 9-HOTrE and 13-HOTrE concentrations by 139-159% compared to raw potatoes. Par-frying significantly decreased LA-derived 9-HODE, 13-HODE, 9-oxo-ODE, 13-oxo-ODE, 9,10-EpOME but significantly increased 9,10-DiHOME and 12,13-DiHOME concentrations compared to raw potato. Frying (one cycle for 10 mins, i.e. 'deep frying') significantly decreased LA-derived 9-HODE and ALA-derived 9-HOTrE and 13-HOTrE, but significantly increased LA-derived 9,10-DiHOME and 12,13-DiHOME concentrations compared to raw potato.

Blanching involves the application of heat (68.6°C) in water for fifteen minutes to inactivate enzymes, including lipoxygenases (Rosahl, 1996). However, residual lipoxygenase activity (<2.5%) was reported after blanching potatoes (Anthon & Barrett, 2002), which could explain the specific and significant increase in ALA-derived mono-hydroxylated compounds. However, LA-derived epoxides and diols were reduced after blanching, likely due to heat-induced degradation in the presence of water. It is hypothesized that these compounds are less stable in water compared to hydroxylated compounds, and that they degrade into aldehydes and ketones not captured in the present experiments (Raghavamenon et al., 2009).

Unlike blanching, par-frying and one cycle of deep frying (185.9 and 190.6°C) reduced hydroxy and ketone fatty acid metabolites of LA or ALA and increased fatty acid diols of LA compared to raw potatoes (**Figure 5**). Fatty acid epoxides were decreased or did not change by par-frying and deep frying, respectively. The parallel increase in LA-derived diols, however, suggests chemical transformation of fatty epoxides into diols during par and deep frying. It is important to note that the changes observed during par or deep frying were opposite to those observed during blanching. In particular, fatty acid diols increased during frying but decreased during blanching. This could be attributed to the use of water during the blanching process, which could catalyze the breakdown of diols into secondary volatile compounds. In the absence of excess water during par or deep frying, these diols accumulate in oil and degrade less rapidly into secondary compounds. This remains to be confirmed in future experiments.

3.2 Effect of repeated frying cycles on oxylipin levels in fried oil and French fries

In this study, blanched and par-fried frozen potatoes (i.e., French fries) were subjected to 3 frying cycles in soybean oil. The oil was not changed, whereas 3 different batches of fries

were heated for 10 minutes, one after the other. Oxylipins were measured in both oil and French Fries at baseline and after each frying cycle.

The oil data are presented in **Figure 6**. As shown, repeated frying significantly increased LA- and ALA- derived hydroxy metabolites, and LA-derived ketones and epoxides without changing LA diols in oil. Compared to baseline, LA-derived 9-HODE, 13-HODE, 9-oxo-ODE, 9,10-EpOME, 12,13-EpOME significantly increased by 78-350% and ALA-derived 13-HOTrE significantly increased by 346% after 3 cycles of frying. No significant changes were observed after repeated frying for 12,13-DiHOME, 9,10-DiHOME, and 9-HOTrE (**Figure 6**). 13-HODE was the most abundant oxylipin after 3 cycles of repeated frying both in oil and French fries; its concentration was 13477.7 nM and 10051.6 pmol/g respectively. The increase in oil oxylipin concentrations upon repeated frying is in general agreement with previous studies which showed that heating sunflower oil (rich in LA) at 180°C for 15 hours, increased LA-derived EpOMEs by 5 to 10 hours of heating (Velasco, Marmesat, Bordeaux, Marquez-Ruiz, & Dobarganes, 2004).

Three different batches of French fries were fried in the same oil used to fry the prior batch, for a duration of 10 minutes per cycle, and compared to baseline (i.e. French fries not subjected to frying). Compared to baseline, LA-epoxides decreased and LA-diols and ALA-derived 9-HOTrE increased with repeated frying cycles (**Figure 7**). Specifically, concentrations of LA-derived 13-oxo-ODE, 9,10- DiHOME, 12,13- DiHOME and ALA-derived 9-HOTrE significantly increased by 210%, 503%, 60% and 83% respectively after the 3rd frying cycle compared to baseline. Significant reductions in LA-derived epoxides (EpOMEs) were observed after 1st and 2nd cycles (non-significant reductions seen in the 3rd cycle), consistent with a study by Kalogeropoulos et al. which showed reduced 9,10- EpOME

and 12, 13-EpOME in French Fries after one frying cycle in sunflower oil and soybean shortening oil heated at 338°F for 8-9 min (Kalogeropoulos et al., 2007). This may be due to the rapid conversion of epoxides to diols at high temperatures (S. N. Gan & Hamid, 1997). The significant increase in 9,10-DiHOME and 12,13-DiHOME after the 1st and 3rd frying cycles supports this possibility.

None of the increases in oil were consistently reflected in the French Fries, particularly when the fries were subjected to oil that had been used to fry the French fries multiple times. For instance, hydroxylated and epoxidized oxylipins of LA or ALA increased with frying cycles in oil, but were unaltered (for hydroxylated compounds) or reduced (for epoxidized compounds) in fries. Differences in oxylipin changes in oil versus French fries may be explained by the greater water content of fries relative to oil, which may play a role in lipid oxidation(S. N. Gan & Hamid, 1997). Additionally, we did not consider the mass and heat transfer effect between French fries and fried oil during repeated frying. One study reported that 20% of oil migrated into tortilla chips during deep frying, suggesting limited migration of oil into the chips (Moreira, Sun, & Chen, 1997). A similar scenario may have occurred for French fries, thus limiting the rapid transfer of oil or thermal energy to inner pockets of the fries.

In the current study, LA-derived epoxide concentrations in oil (2983-8575nM) were within the range reported by Kalogeropoulos et al. (6901-15683nM) after one frying cycle using soybean shortening oil (Kalogeropoulos et al., 2007). Measured 9,10 EpOME and 12,13-EpOME concentrations in French fries (3713-9063 pmol/g, 3rd cycle) were consistent with another study which reported values in French fries subjected to 8 frying cycles (5734-8432 pmol/g) (Kalogeropoulos et al., 2007), thus confirming the validity of our analytical

methods. We are not aware of other studies that quantified hydroxy, dihydroxy, and keto forms of oxylipins in French fries.

A limitation of the present study is that the hydrolysis of oil and potato / French fries oxylipins was performed using sodium carbonate. Recently, we reported that sodium hydroxide is a better hydrolysis base than sodium carbonate when applied to fish and soybean oil and to bovine milk (Emami, Zhang, & Taha, 2020; Ramsden et al., 2020; Shen et al., 2021; Teixeira et al., 2021). We did not know this at the time the current samples were analyzed. It is likely, therefore, that our absolute oxylipin values in oil and French fries are underestimated, although differences between the groups are not likely to be impacted by the use of sodium hydroxide because the same base hydrolysis conditions were used across all groups.

Table 1 summarizes oxylipin changes observed under the various processing conditions tested in the present study. As shown, compared to raw potatoes, blanching decreased LA-derived epoxides and diols and increased ALA-derived hydroxylated products. Par-frying decreased hydroxy, ketone and epoxy fatty acids but increased LA-diols. Deep frying also decreased hydroxy fatty acids and increased diols. Frying different batches of French fries in the same oil subjected to repeated frying cycles decreased LA-epoxides and increased LA-diols (compared to non-fried French fries). LA-ketones and ALA-hydroxides also increased by the third frying cycle. In contrast, repeated frying increased almost all oxylipins in oil (i.e. LA-hydroxy, ketone, epoxide and ALA hydroxyl fatty acids) without altering LA-diols. Thus, in potatoes different processing conditions unanimously decrease fatty acid epoxides and increase diols, whereas in oil, repeated frying increases epoxides without altering diols.

In conclusion, blanching, par-frying and deep-frying caused distinct changes in oxylipins in potatoes and French fries, and in the oil used to fry the French fries. Contrary to current knowledge and expectations which assume that heat increases fatty acid oxidation products, the current study showed that some oxylipins increased and other others decreased with heat application. Water, mass transfer or thermal exchanges between the potatoes and the surrounding medium (whether water or oil) appear to play a role in modifying oxylipin composition (e.g., during blanching or frying). Future studies are needed to elucidate the mechanisms involved, and to better understand how different processing conditions modify human exposures to oxylipins and potential risks associated with their consumption (Borgi et al., 2016; Muraki et al., 2016; Veronese et al., 2017b).

Acknowledgment

None.

Funding

This project was supported by the Center for Advanced Processing and Packaging Studies (CAPPS Award # 735818-0) and USDA National Institute of Food and Agriculture, Hatch/Taha (project #1008787) to A.Y.T., and the UC Davis Provost's Undergraduate Fellowship to Z.Z. (2017-2018).

Author Contributions

ZZ, MH and AYT designed the study. ZZ and SE conducted the frying experiments. ZZ performed the oxylipin extractions. MH and ZZ performed the oxylipin analysis. ZZ did the statistical analysis. ZZ and AYT wrote the manuscript. All authors reviewed the manuscript.

Conflict of Interest

Authors declare no conflict of interest.

Chapter 3 (Aim 2): Distribution of free and esterified oxylipins in cream, cell, and skim fractions of human milk

Junai Gan[a‡], Zhichao Zhang[a‡], Karina Kurudimov[a], J. Bruce German[a,b], Ameer Y. Taha[a,*]

[a] Department of Food Science and Technology, College of Agriculture and Environmental Sciences, University of California, Davis, CA, USA

[b] Foods for Health Institute, University of California, Davis, CA, USA

[‡] J. Gan and Z. Zhang are co-first authors who contributed equally to this work.

[*] Correspondence to: Dr. Ameer Y. Taha, Department of Food Science and Technology, University of California, Davis, CA 95616, USA. E-mail address: ataha@ucdavis.edu.

Gan, J., Zhang, Z., Kurudimov, K., German, J. B., & Taha, A. Y. (2020). Distribution of free AND Esterified Oxylipins in Cream, cell, and skim fractions of human milk. *Lipids*, *55*(6), 661–670. https://doi.org/10.1002/lipd.12268

Abstract

Human milk contains oxylipins involved in infant development. Although oxylipins have been identified in whole or skim milk, their localization within human milk cream, cell and skim fractions is not known. This study aimed to determine the distribution of free and esterified oxylipins in cream, cell, and skim fractions of human milk. Out of 72 oxylipins probed by mass-spectrometry, 42, 29, and 41 oxylipins (free or bound) were detected in cream, cell, and skim fractions, respectively. Over 90% of free and bound oxylipins were derived from linoleic acid in all milk fractions. Other oxylipins were derived from n-6 arachidonic acid and dihomo-gamma-linolenic acid, and n-3 alpha-linolenic acid, eicosapentaenoic acid and docosahexaenoic acid. Free oxylipins were more abundant in skim milk compared to cream and cell pellet, whereas esterified oxylipins were most abundant in milk cream and cell pellets. The heterogenous distribution of oxylipins in different fractions of human milk may regulate the guided release of these bioactive signaling molecules within infants.

Keywords: Human milk, fractions, Oxylipins, Lipid mediators, LC-MS/MS, lipidomics

Running Title: Free and esterified oxylipins in milk fractions

1. Introduction

Human milk provides nutritional, immunological, and neurodevelopmental benefits for newborn infants (Harding, Cormack, Alexander, Alsweiler, & Bloomfield, 2017). An interest in human milk bioactive lipid mediators has emerged since oxidized metabolites of polyunsaturated fatty acids (PUFA), known as oxylipins, have been detected in human breast milk (Michael A. Pitino et al., 2019; D. T. Robinson et al., 2017; Weiss et al., 2013; J. F. Wu, S. Gouveia-Figueira, M. Domellof, A. M. Zivkovic, & M. L. Nording, 2016). Oxylipins have been shown to regulate infant development and immunity. Using mouse models with a self-limited inflammatory challenge, Arnardottir *et al.* (Arnardottir, Orr, Dalli, & Serhan, 2016) demonstrated that injected human milk oxylipins derived from docosahexaenoic acid (DHA, 22:6n-3) accelerated the resolution of acute inflammation. Using an untargeted lipidomics approach, Alexandre-Gouabau *et al.* (Alexandre-Gouabau et al., 2018) showed that human milk oxylipins derived from dihomo-γ-linolenic acid correlated with growth rate in preterm infants. None of these studies quantified oxylipin bioavailability from breast milk. However, they point to multiple regulatory roles of breast milk oxylipins in infant development.

Lipids in human milk are highly structured and organized in a three-dimensional space. The major lipid components in milk are triglycerides assembled inside a trilayer phospholipid membrane, forming milk fat globules, which are separated from somatic cells and emulsified within the aqueous phase (Brans, Schroen, van der Sman, & Boom, 2004; Singh & Gallier, 2017). The emulsion structure or spatial arrangement of milk lipids affects their lipolysis and disintegration (Bourlieu et al., 2015; J. Gan, Siegel, & German, 2019). During infant digestion, milk fat globules undergo structural and chemical changes. Three fatty acyl chains are esterified to each glycerol backbone, but only the fatty acids on the outer (sn-1 and sn-3) positions of

triglycerides are preferentially released (Bourlieu et al., 2014; Salentinig, Phan, Hawley, & Boyd, 2015).

Previous studies have measured and detected free (i.e. unbound) oxylipins in whole or skim milk (Alexandre-Gouabau et al., 2018; Arnardottir et al., 2016; Michael A. Pitino et al., 2019; D. T. Robinson et al., 2017; Weiss et al., 2013; J. F. Wu et al., 2016). However, evidence from rodent and human studies suggests that in tissues or plasma, the majority of oxylipins are bound (i.e. esterified) (Ramsden, Ringel, et al., 2016; Shearer & Newman, 2008; Taha et al., 2018b) and that the esterified pool regulates the supply and turnover (i.e. release and re-esterification) of free oxylipins (Otoki et al., 2020). Free oxylipins are more bioactive than esterified oxylipins (Lahvic et al., 2018; Obinata, Hattori, Nakane, Tatei, & Izumi, 2005), consistent with studies showing that they act as signaling molecules (Marie Hennebelle et al., 2019) understanding their localization and proportional distribution relative to esterified pools in human milk would inform on how milk serves as a signaling system in infants.

In the present study, we used a targeted mass spectrometry approach to determine the distribution of free and esterified oxylipins in cream, cell, and skim fractions of human milk. Human milk collected from healthy lactating mothers was pooled, fractionated, and subjected to free and esterified oxylipin analysis by ultra-high performance liquid chromatography coupled to tandem mass spectrometry (UPLC-MS/MS). We hypothesized that similar to the reported dominance of esterified oxylipins in mammalian blood and tissues, esterified oxylipins will be more abundant compared to free oxylipins in each milk fraction. Our analysis demonstrated that in cream and cell pellet, the majority of oxylipins were bound (74.9 to 76.9%), whereas in skim milk, the majority (59.9%) were unbound.

2. Material and methods

2.1. Human milk collection

The study protocol was approved by the Institutional Review Board at the University of California Davis (Protocol # 1049118). Informed consent was obtained from all participants. Mature milk was obtained as previously described (J. Gan, Zheng, et al., 2019) from five healthy lactating women who had delivered term infants (born after 37 weeks of gestation) at four to ten weeks of lactation. Subject information is shown in **Supplementary Table S2**. Briefly, fore and hind milk were fully expressed from one breast by hand or breast pump, and gently mixed. At least 20 ml of the milk was collected into a sterile container, transported to the laboratory on ice, and stored at -80 °C.

2.2. Compositional analysis of human milk

Pooled human milk was diluted 5-fold with Milli-Q water. Samples were warmed to 38 °C in a water bath and vortexed for 20 seconds to ensure homogeneity prior to measurement with Delta LactoScope FTIR Advanced Mid-Infrared Spectroscopy (Advanced Instruments, Norwood, MA, USA), calibrated for human milk total fat, protein, and lactose (Smilowitz, Gho, Mirmiran, German, & Underwood, 2014).

2.3. Human milk fractionation

Three aliquots (2 ml each) of pooled human milk were centrifuged at 15 000 x g on Eppendorf 5424R centrifuge for 15 min at 0 °C. After collecting the top cream layer containing milk fat globules, the remaining sample was centrifuged again at 15 000 x g for 2 min at 0 °C.

Then, 1.5 ml of skim milk was collected from the aqueous layer. The remaining cream and skim milk was discarded, and 1 ml of Dulbecco's phosphate-buffered saline (DPBS, Gibco, Grand Island, NY, USA, Cat # 14190-144) was added to each tube. After samples were centrifuged at 15 000 x g for 2 min at 0 °C, liquid was discarded. DPBS was added, each sample was centrifuged for 2 min, and the liquid was discarded again to wash off the remaining cream and skim milk from the pellet. Pellets containing somatic cells of milk were collected.

2.4. Free oxylipin extraction

To extract free oxylipins from cream and cell pellets, 200 µl of extraction solvent containing 0.1% acetic acid (Sigma-Aldrich St. Louis, MO, USA, Cat # 695092) and 0.1% butylated hydroxytoluene (BHT, Sigma-Aldrich, St. Louis, MO, USA, Cat # W218405-SAMPLE-K) in methanol (Fisher Scientific, Hampton, NH, USA, Cat # A454-4), 10 µl of antioxidant mixture and 10 µl of surrogate, and 1133.3 µl of Milli-Q water were added to approximately 50 mg cream and 8 mg pellets. The antioxidant mixture was 0.2 mg/ml BHT, ethylenediaminetetraacetic acid (EDTA, Sigma-Aldrich, St. Louis, MO, USA, Cat # EDS-100G) and triphenylphosphine (TPP, Sigma-Aldrich, St. Louis, MO, USA, Cat # 3T84409) in methanol/water (50:50, v/v) filtered through 0.45 µm Millipore filter (Millpore, Bedford, MA, USA, Cat # SLHVM25NS). The surrogate contained 2 µM d11-11(12)-EpETrE (Cayman Chemical, Ann Arbor, MI, USA; Cat # 10006413), d11-14,15-DiHETrE (Cayman Chemical, Cat # 1008040), d4-6-keto-PGF1α (Cayman Chemical, Cat # 315210), d4-9-HODE (Cayman Chemical, Cat # 338410), d4-LTB4 (Cayman Chemical, Cat # 320110), d4-PGE2 (Cayman Chemical, Cat # 314010), d4-TXB2 (Cayman Chemical, Cat # 319030), d6-20-HETE (Cayman Chemical, Cat # 390030) and d8-5-HETE (Cayman Chemical, Cat # 334230). Samples were

vortexed for 2 min, centrifuged at 15 000 x g for 2 min at 0 °C, and the supernatant was removed and vortexed again for 10 min before solid phase extraction (SPE) with Oasis HLB columns (60mg, Waters, Milford, MA, USA, Cat # WAT094226).

For the skim milk fraction, 1500 µl of extraction solvent, 10 µl of antioxidant, and 10 µl of surrogate were added to 1.5 ml of skim milk. Samples were vortexed and centrifuged to precipitate proteins. Then, 2200 µl of supernatant was collected, and 7 ml Milli-Q water was added to adjust the methanol content to 15% before Oasis HLB column extraction as described below (Section 2.6).

2.5. Neutral lipid (NL) and phospholipid (PL) oxylipin extraction

Total lipids were extracted from cream and pellet fractions by adding 2 ml chloroform (Fisher Scientific, Hampton, NH, USA, Cat # C607-4), 1 ml methanol, and 0.75 ml 0.9% KCl (Fisher Scientific, Hampton, NH, USA, Cat # P217-500) to approximately 50 mg cream or 9.4 mg pellets. The samples were vortexed and centrifuged at 458 x g on Beckman Coulter Allegra 6 centrifuge (Indianapolis, IN, USA). The bottom chloroform layer was transferred to new test-tubes, and an additional 2 ml chloroform was added to the initial samples, which were vortexed and centrifuged at 458 x g. The second chloroform extract was pooled with the first. Samples were evaporated under nitrogen and reconstituted in 1.5 ml chloroform/2-propanol (2:1, v/v) (Fisher Scientific, Hampton, NH, USA, Cat # A464-1) for pellets and in 6 ml of chloroform/2-propanol (2:1, v/v) for cream samples. To extract lipids from the skim milk fraction, 2 ml chloroform, 1 ml methanol were added to 0.75 ml skim milk, vortexed and centrifuged as described above. Dried skim milk samples were reconstituted in 1.5 ml chloroform/2-propanol.

Silica columns (Sep-Pak Silica 1 cc Vac Cartridge, 100 mg Sorbent, Waters, Milford, MA, USA, Cat # WAT023595) were used to separate esterified oxylipins. The columns were pre-washed with 1.5 ml methanol and conditioned with 1.5 ml chloroform/2-propanol. Then, 0.2 ml cream in chloroform/2-propanol, 1.5 ml pellets in chloroform/2-propanol and 1.5 ml skim milk in chloroform/2-propanol were loaded onto the silica columns and eluate was collected. Next, 1.5 ml chloroform/2-propanol was added to each column and combined with the first collection. This combined collection contained neutral lipids. Samples were dried under nitrogen, reconstituted into 200 µl extraction solvent, 10 µl antioxidant solution and 10 µl surrogate, and subjected to hydrolysis as described below.

Relatively polar compounds including free oxylipins and phospholipid-bound oxylipins were washed from the silica column with 1.5 ml 95% methanol. After collecting the eluate, 400 µl Milli-Q water was added to adjust the methanol content to 75%. Sep-Pak tC18 columns (1 cc Vac Cartridge, 100 mg Sorbent, Waters, Milford, MA, USA, Cat # WAT036820), pre-washed with 1.5 ml methanol and equilibrated with 1.5 ml 75% methanol, were used to separate phospholipid-bound oxylipins from free oxylipins. The extracts containing oxylipins and phospholipids (in 75% methanol) were loaded to tC18 column and 1.5 ml 75% methanol was added to wash the column. Then, 2 ml of methanol was added to the tC18 column to elute phospholipid-bound oxylipins.

The extracted NL- and PL- bound oxylipins were dried under nitrogen and reconstituted into 200 µl extraction solvent, 10 µl antioxidant solution and 10 µl surrogate, and hydrolyzed at 60 °C for 30 minutes with 200 µl 0.25 M sodium carbonate (Sigma-Aldrich, St. Louis, MO, USA, Cat # 791768-500G) in methanol/water (50:50, v/v). After hydrolysis, the samples were cooled at room temperature for five minutes. Then, 25 µl acetic acid was added and the pH was

verified to be between 4-6 with litmus paper in a representative sample from each fraction. Milli-Q water (1575 µl) was added, and samples were vortexed.

2.6. Oasis HLB solid phase purification of free and hydrolyzed oxylipins

Free oxylipins extracted from each milk fraction or generated during the hydrolysis of NL- and PL-bound oxylipins were purified with Oasis HLB (60 mg) columns. The columns were cleaned with one column volume of ethyl acetate (Fisher Scientific, Hampton, NH, USA, Cat # E196-4), and two column volumes of methanol, and conditioned with two column volumes of SPE buffer (0.1% acetic acid, 5% methanol in Milli-Q water). Samples were loaded, washed with two column volumes of SPE buffer and dried under vacuum for 20 min. Oxylipins were eluted with 0.5 ml methanol followed by 1.5 ml ethyl acetate. The eluate was dried under nitrogen, reconstituted in 100 µl LC-MS grade methanol (Fisher Scientific, Hampton, NH, USA, Cat # A456), vortexed and centrifuged on Eppendorf 5424R centrifuge at 15 000 x g for 2 min at 0 °C. Samples were transferred to centrifugal filter units (Ultrafree-MC VV Centrifugal filters, Burlington, MA, USA, Cat # UFC30VV00), centrifuged at 15 000 x g for 20 min at 0 °C and analyzed with UPLC-MS/MS as described below.

2.7. UPLC-MS/MS analysis

A total of 72 oxylipins (**Supplementary Table S1**) were analyzed using an Agilent 1290 Infinity UHPLC system coupled to an Agilent 6460 triple-quadrupole tandem mass spectrometer (Agilent, Santa Clara, CA, USA) with electron spray ionization in the negative mode and optimized dynamic Multiple Reaction Monitoring (dMRM) conditions as detailed previously (Marie Hennebelle et al., 2019). Oxylipins were separated using a Zorbax Eclipse Plus C18

column (2.1 x 150 mm, 1.8 μm, Agilent, Santa Clara, CA, USA, Cat # 959759-902). The auto-sampler and column were kept at 4 °C and 45 °C, respectively. Mobile phase A was 0.1% acetic acid in Milli-Q water. Mobile phase B contained 0.1% acetic acid in acetonitrile/methanol (80:15, v/v). The flow gradient was: mobile phase A started at 65%, decreased to 60% at 3 min, 54% at 4 min, 40% at 10 min, 30% at 20 min, 15% at 24 min and 1% at 24.6 min followed by a hold to 26 min. Mobile phase A was then increased to 65% at 26.10 min and held constant to 27.30 min. The flow rate was 0.30 ml/min from 0 to 3 min, 0.25 ml/min from 3 to 24.5 min, 0.35 ml/min from 24.6 to 27 min, and 0.30 ml/min at 27.30 min.

2.8. Data and statistical analysis

Peaks were manually integrated using Agilent MassHunter Quantitative Analysis B.08.00. The signal-to-noise (S/N) ratio was determined by peak height, and peaks were filtered at S/N > 3. Analyte amounts per sample were determined after correcting for the response factor of sample peak areas with an external standard curve and adjusting for extraction losses with deuterated surrogate standards. Deuterated standard recoveries were calculated by dividing the peak area of the surrogate in the sample extract (post-SPE) by the average surrogate peak area in seven pure standard mixtures and multiplying by 100. The analyte amount was normalized to the wet weight of cream and pellets or to the volume of skim milk. To compare oxylipin concentrations among NL-bound, PL-bound, and free pools in each milk fraction, one-way analysis of variance (ANOVA) followed by Newman-Keuls test was applied per milk fraction if oxylipins were present in all three pools (PL, NL and free). An unpaired t-test was used for oxylipins detected in two out of the three fractions. Data were analyzed using R v3.5.1 (https://www.R-project.org).

3. Results

The mass percent of components in the pooled human milk is presented in **Table 2**. As shown, the pooled milk contained 4.9% fat, 0.9% protein, and 7.1% lactose, consistent with previous data (Jenness, 1979).

The surrogate recovery is presented in **Supplementary Table S3**. As expected, the surrogate recovery of d4-PGE2 following base hydrolysis was zero due to degradation. The surrogate recoveries across samples ranged from 28.5- 307.9%, 85.8 to 206.2% and 61.2 to 166.4% in free, NL and PL pools derived from the three milk fractions. The high recovery of d4-TXB2 (307.9%) in cream free fraction is likely due to ion enhancement, which reflects the presence of molecules in the matrix that elute and fragment in a similar manner as d4-TXB2. Notably, however, d4-TXB2 is used as surrogate for TXB2 only, which was not detected in any of the milk lipid fractions assayed in this study.

Esterified and free oxylipin concentrations in milk cream, cell pellet, and skim milk are shown in Table 2, 3 and 4, respectively. Concentration data were expressed as mean ± standard deviation (SD) in pmol/mg of cream or pellet, or in pmol/ml of skim milk.

Out of 72 oxylipins targeted by dMRM on UPLC-MS/MS (**Supplementary Table S1**), 42, 29, and 41 free or bound oxylipins were detected in cream, cell, and skim fractions, respectively (Tables 2–4). The identified oxylipins were derived from alpha-linolenic acid (ALA, 18:3n-3), arachidonic acid (ARA, 20:4n-6), docosahexaenoic acid (DHA, 22:6n-3), eicosapentaenoic acid (EPA, 20:5n-3), dihomo-gamma-linolenic acid (DGLA, 20:3n-6), and linoleic acid (LNA, 18:2n-6).

In cream and pellet, PUFA-derived oxylipins were significantly higher in NL by approximately 8-11 times and two times than in PL and free pools, respectively **(Tables 3 and**

4). Additionally, few oxylipins were significantly higher by 2-9 times in the free pool compared to PL in cream and pellet **(Tables 3 and 4)**.

In skim fraction, PUFA-derived epoxides were significantly higher by 2-4 times in NL and in some cases, PL, compared to the free pool (**Table 5**). Other oxylipins (particularly hydroxylated compounds) were significantly higher by approximately 5% to 31 times in the free fraction, compared to NL and/or when detected, PL.

To better visualize the distribution of oxylipins in human milk, the sum of oxylipins in each fraction from each PUFA precursor was calculated and plotted **(Fig. 8)**. As shown, NL-bound oxylipins constituted the majority of oxylipins in cream and cell pellet, followed by free and PL-bound oxylipins. Free oxylipins were the main species found in skim milk, followed by NL- and PL- bound oxylipins. In cream there were 90.0 pmol/mg oxylipins in NL, 33.5 pmol/mg in the free pool, and 9.0 pmol/mg in PL. In cell pellet, there were 89.0 pmol/mg oxylipins in NL, 29.0 pmol/mg unbound oxylipins and 7.1 pmol/mg oxylipins in PL. In skim milk, oxylipin concentrations were 653.8 pmol/ml, 425.2 pmol/ml and 40.5 pmol/m in free, NL and PL pools, respectively.

The most abundant oxylipins in all milk fractions were derived from LNA. They ranged from 84.8% to 98.8% of NL-bound, PL-bound and free oxylipins in each milk fraction (Fig. 8b). ARA-derived oxylipins were the second most abundant in milk fractions ranging from 0.7% to 10.8%. NL-bound, PL-bound and free EPA metabolites ranged between 0% to 2.8% in milk fractions. ALA metabolites ranged from 0 to 1.3%. DHA metabolites ranged from 0.1% to 4.4%. DGLA metabolites were found only in the free pool of cream making up 0.05% and in the NL-bound pool of skim milk making up 0.02%.

4. Discussion

This study documented that the majority of oxylipins in human milk cream and cell pellet are bound to NL. PUFA-derived epoxides in skim fraction were mostly unbound (free), whereas other oxylipin species were bound to NL or in some cases, PL. The findings highlight the presence of a turnover pathway guiding oxylipin esterification and release within the mammary gland and portioning into each milk fraction. Our data suggest that this pathway favors esterification in NL of cream, pellet, and to some extent, skim fractions.

Oxidized LNA metabolites were the dominant oxylipin species (>85%) in all milk fractions. The high abundance of LNA-species is in general agreement with prior studies in whole or skim milk. LNA-derived oxylipins were highly abundant in whole milk pooled from seventeen human donor milk samples (Michael A. Pitino et al., 2019) and in skim milk from a mother at seven months of lactation (J. F. Wu et al., 2016). The high concentration of LNA-derived oxylipins is possibly due to a 3-fold increase in LNA in modern industrialized diets compared to pre-industrial times, and the propensity of human milk to accumulate dietary LNA (Blasbalg et al., 2011a; Whelan, 2008). Consistent with the increase in dietary LNA intake, the composition of LNA in breast milk from US women has increased from 6–7% to 15–16% of total fatty acids between 1945 and 1995 (Ailhaud & Guesnet, 2004). A study published in 2006 showed that LNA composition of mature human breast milk was 15% of total fatty acids (Yuhas et al., 2006).

Little is known about the role of variations in breast milk LNA or its oxidized metabolites on infant development. A recent study found that LNA-derived 13-hydroxyoctadecadienoic acid increased axonal outgrowth in female and male rat pups, respectively (Marie Hennebelle et al., 2019). LNA-derived oxylipins accounted for 50% of detected oxylipins in the brains of 1-day-

old pups, although it is not known whether excess LNA in breast milk would further increase these levels during lactation (Marie Hennebelle et al., 2019).

Concentrations of free oxylipins were higher compared to NL-bound oxylipins in skim milk, while NL-bound oxylipins were more concentrated than free oxylipins in milk cream and cell pellets (Fig. 1a). In rats, the esterified oxylipin pool has been proposed to serve as a reservoir for the release of free oxylipins, the bioactive form that influences cellular functions (Otoki et al., 2020; Shearer & Newman, 2008; Taha et al., 2018b). Thus, human milk can be viewed as a dynamic signal delivery system containing esterified and free bioactive lipids. Recent studies revealed that bioactive peptides that are encrypted in human milk proteins can be released by proteolytic enzymes upon pH activation during infant digestion (J. Gan, Robinson, et al., 2019; J. Gan, Zheng, et al., 2019). A similar, enzyme-based release mechanism for the controlled delivery of bioactive compounds within the gut of infants may exist for human milk lipids, though this remains to be demonstrated *in vivo*.

In many cases, concentrations of PL-bound oxylipins were lower than concentrations of NL-bound and free oxylipins in milk cream, cell pellet, and skim fractions. This is consistent with the fact that milk is high in NL in the form of triacylglycerols (Wei et al., 2019; T. Yuan et al., 2019), which could provide the necessary backbone for oxylipin esterification.

Lipid digestion within infants is facilitated by gastric lipase, bile salt-stimulated lipase, and pancreatic lipase-related protein 2 in both the milk and infant (Lindquist & Hernell, 2010). Enzyme accessibility and hydrolysis kinetics are mediated by the structure of milk (Bourlieu et al., 2015). It is proposed that the esterification and localization of oxylipins in human milk is a key factor that controls the release of bioactive oxylipins during feeding and during digestion. Further assessment of the dynamics of oxylipin distribution in human milk in response to

changes in infant digestion would elucidate the health implications of lipid signaling systems in infants. Additionally, the physiological relevance of bound and unbound milk oxylipins in infants remains to be examined.

5. Conclusions

Targeted UPLC-MS/MS analysis revealed the presence of PUFA-derived oxylipins in free and esterified lipids of human milk cream, cell pellets and skim fractions. NL-bound oxylipins were more concentrated than unesterified oxylipin in milk cream and cell pellets. NL-bound epoxides were also more concentrated in skim fraction, whereas other oxylipins were mostly in the free fraction. Oxylipins were least abundant in PL. Over 84.8% of free and esterified oxylipins were derived from LNA in all milk fractions. Other oxylipins were derived from ARA, ALA, DHA, EPA, and DGLA. The heterogeneous distribution of oxylipins in different fractions of human milk offers a potential mechanism for regulating the targeted release of bioactive signaling molecules within infants.

Acknowledgements

The authors appreciate all the women who generously donated milk to this research. We would like to acknowledge Bianca Teixeira for assisting in oxylipin extractions and Shiva Emami for helping with result calculations. This work was supported by the United States National Institutes of Health [grant numbers AT007079, AT008759]; the UC Davis Jastro-Shields Research Scholarship to J.G.; and the USDA National Institute of Food and Agriculture, Hatch/Taha [project number 1008787].

Author Contributions

J.G., Z.Z., J.B.G. and A.Y.T. conceived the study. J.G. collected the human milk samples. K.K. conducted compositional analysis of human milk. J.G. and Z.Z. performed human milk fractionation, oxylipin extraction, UPLC-MS/MS analysis and data analysis. J.G. and Z.Z. drafted the manuscript with input from A.Y.T. and J.B.G. All authors reviewed and approved the manuscript.

Conflicts of interest

The authors declare no conflicts of interest.

Chapter 4 (Aim 3): Linoleic acid-derived 13-hydroxyoctadecadienoic acid is absorbed and incorporated into rat tissues

Zhichao Zhang[1], Shiva Emami[1], Marie Hennebelle[1,+], Rhianna K Morgan[2], Larry A. Lerno[3], Carolyn M. Slupsky[1,4], Pamela J. Lein[2] and Ameer Y. Taha[1*]

[1]Department of Food Science and Technology, College of Agriculture and Environmental Sciences, University of California, Davis, CA, USA;

[2]Department of Molecular Biosciences, School of Veterinary Medicine, University of California, Davis, CA, USA;

[3]Food Safety and Measurement Facility, University of California, Davis, CA, USA;

[4]Department of Nutrition, College of Agriculture and Environmental Sciences, University of California, Davis, CA, USA

[*]Corresponding author:

Dr. Ameer Y. Taha

Department of Food Science and Technology, College of Agriculture and Environmental Sciences, University of California Davis, One Shields Avenue, RMI North (3162), Davis, CA, USA 95616

Email: ataha@ucdavis.edu

Phone: (+1) 530-752-7096

[+]Current address: Laboratory of Food Chemistry, Wageningen University and Research, Wageningen, Netherlands

Zhang, Z., Emami, S., Hennebelle, M., Morgan, R. K., Lerno, L. A., Slupsky, C. M., Lein, P. J., & Taha, A. Y. (2021). Linoleic acid-derived 13-hydroxyoctadecadienoic acid is absorbed and incorporated into rat tissues. *Biochimica Et Biophysica Acta (BBA) - Molecular and Cell Biology of Lipids*, *1866*(3), 158870. https://doi.org/10.1016/j.bbalip.2020.158870

Abbreviations: COX, cyclooxygenase; CYP450, cytochrome p450; ARA, arachidonic acid; PGE, prostaglandin; EPA, eicosapentaenoic acid; UE, unesterified ; ES, esterified; LNA, linoleic acid; LOX, lipoxygenase; OXLAMs, oxidized linoleic acid metabolites; Prostaglandin (PG); sEH, soluble epoxide hydrolase; SPE, solid phase extraction; IV, intravenous; 13-HODE, 13-hydroxyloctadecadienoic acid; UPLC-MS/MS, ultra-high performance liquid chromatography coupled to tandem mass-spectrometry.

Abstract:

Linoleic acid (LNA)-derived 13-hydroxyoctadecadienoic acid (13-HODE) is a bioactive lipid mediator that regulates multiple signaling processes *in vivo*. 13-HODE is also produced when LNA is oxidized during food processing. However, the absorption and incorporation kinetics of dietary 13-HODE into tissues is not known. The present study measured unesterified d4-13-HODE plasma bioavailability and incorporation of into rat liver, visceral adipose, heart and brain following gavage or intravenous (IV) injection (n=3 per group). Mass spectrometry analysis revealed that d4-13-HODE was absorbed within 20 minute of gavage, and continued to incorporate into plasma esterified lipid fractions throughout the 90 minute monitoring period. Following IV injection, unesterified d4-13-HODE was rapidly eliminated from plasma with a half-life of 1 minutes, whereas the gavaged tracer incorporated into esterified lipid pools and had a half-life of 71 min. Analysis of tracer incorporation kinetics into rat tissues following IV injection or gavage revealed that the esterified tracer preferentially incorporated into liver, adipose and heart compared to unesterified d4-13-HODE. No tracer was detected in the brain. This study provides new evidence that dietary 13-HODE is absorbed and incorporated into peripheral tissues from esterified plasma pools. Understanding the chronic effects of dietary 13-HODE exposure on peripheral tissue physiology and metabolism merits future investigation.

Keywords: oxidized linoleic acid metabolites (OXLAMs); brain; heart; liver; adipose tissue; kinetics

1. Introduction:

Omega-6 linoleic acid (LNA, 18:2 n-6) is a precursor to bioactive oxidized linoleic acid metabolites (OXLAMs) generated *in vivo* via auto-oxidation, or enzymatically through lipoxygenase (LOX), cyclooxygenase (COX), cytochrome P450 (CYP) and soluble epoxide hydrolase (sEH) (Blasbalg, Hibbeln, Ramsden, Majchrzak, & Rawlings, 2011b; Engels et al., 1986; Halarnkar, Wixtrom, Silva, & Hammock, 1989; W. Liu et al., 2010; Oliw, 1993; Reinaud et al., 1989). OXLAMs have multiple biological roles including the regulation of pain threshold (Ramsden et al., 2017), inflammation (Taha et al., 2017) (Schuster et al., 2018b), apoptosis (Moghaddam et al., 1997), cardiac activity (Sugiyama, Hayakawa, Nagai, Ajioka, & Ozawa, 1987), adipocyte fatty acid uptake and thermogenesis (Lynes et al., 2017), neurotransmission (Hennebelle et al., 2017) and neuronal morphology (M. Hennebelle, R. K. Morgan, et al., 2019).

Previously, we reported that dietary LNA regulates circulating OXLAM concentrations in humans (Ramsden et al., 2012), as well as plasma and tissue levels in rodents (Ramsden et al., 2018a). Increasing dietary LNA corresponded to incremental increases in plasma and tissue OXLAM concentrations, suggesting that dietary LNA plays a key role in regulating *in vivo* OXLAM levels (Taha et al., 2018a).

OXLAMs are also present in the diet, raising the possibility that they might contribute directly to *in vivo* OXLAM concentrations. Studies reported the presence of OXLAMs in non-heated soybean, canola, corn, olive, flaxseed and algae oils (Richardson et al., 2017), and in bovine and human breast milk (Dias et al., 2020; J. A. Gan, Zhang, Kurudimov, German, & Taha, 2020; M. A. Pitino et al., 2019). Thermal treatment of oils used in food processing has been shown to markedly increase OXLAM concentrations (Kalogeropoulos et al., 2007).

The contribution of dietary OXLAMs to circulating and tissue levels is not clearly known due to conflicting studies on their bioavailability (Ramsden et al., 2018a). Bergan and Draper detected radioactivity in liver and mesenteric adipose of rats 24 hours after gavage with ^{14}C-labelled 13- hydroperoxyoctadecadienoic acid (13-HPODE); however, the chemical identity of the radioactive compounds that accumulated liver and adipose is not known (Bergan & Draper, 1970). Kanazawa et al. showed that ^{14}C-labelled 13-HPODE was converted in the stomach into LNA hydroxy and epoxyketones which further degraded to aldehydes before reaching the small intestines (Kanazawa & Ashida, 1998). Another study showed that more LNA hydroxy metabolites appeared in lymphatic tissue compared to LNA hydroperoxides following intragastric administration (Glavind & Sylven, 1970). The overall evidence suggests that OXLAMs may be absorbed, but it is not known if they remain intact once in the body.

Recently, we reported that plasma and brain OXLAM concentrations were not altered in mice fed a high OXLAM diet derived from thermally oxidized corn oil for 8 weeks (Ramsden et al., 2018a; Schuster et al., 2018b). The lack of change in plasma and tissue OXLAM concentrations following dietary OXLAM feeding could be due to 1) limited absorption, 2) conversion into other ketone or hydroxylated compounds as previously suggested (Kanazawa & Ashida, 1998), and / or 3) rapid plasma and tissue turnover following absorption and tissue incorporation.

To resolve these gaps in knowledge, rats were administered the OXLAM, d4-13-hydroxyoctadecadienoic acid (d4-13-HODE) via gavage or intravenous (IV) injection, and the kinetics of its absorption and incorporation into adipose, liver, heart and brain were evaluated following optimization of the extraction and analytical procedures with Ultra High-Performance Liquid Chromatography tandem mass spectrometry (UPLC-MS/MS). d4-13-HODE was administered in its unesterified (UE) form, to determine partitioning into UE and esterified (ES;

i.e. lipoprotein-bound) plasma pools following IV or gavage. We focused on 13-HODE, because it is the most abundant OXLAM in dietary oils, and in various tissues, including the brain (Ramsden, Ringel, et al., 2016; Richardson et al., 2017; Taha et al., 2018a). Due to prior studies showing that dietary OXLAMs do not alter blood and tissue OXLAM concentrations (Ramsden et al., 2018a; Schuster et al., 2018b), we hypothesized that d4-13-HODE would have limited bioavailability and rapid metabolism.

Contrary to the hypothesis, we found that free d4-13-HODE was absorbed following gavage, and that it incorporated into liver, heart and adipose, but not brain. Most of the IV-injected tracer remained UE in plasma post-injection, and most of the gavaged free tracer was recovered in plasma ES lipid pools. We therefore calculated tissue incorporation and turnover of the UE and ES tracer from IV-injected and gavaged rats, respectively, to determine whether tissues preferentially uptake UE versus ES d4-13-HODE. Downstream conversion into ketone- and tri-hydroxylated metabolites that serve as precursors to aldehydes was also measured with mass-spectrometry (Lundstrom et al., 2011).

2. Materials and Methods

Unesterified 13(S)-HODE-d4 (13S-hydroxy-9Z,11E-octadecadienoic-9,10,12,13-d4 acid) was purchased from Cayman Chemicals (Catalog No. 338610, Ann Arbor, Michigan, USA). HEPES buffer was from Teknova (Cat No. H1030, Hollister, CA, USA). Fatty acid free Bovine Serum Albumin (BSA) Fraction V was from MP Biochemical (Cat No. 0215240105, Solon, OH, USA), and sterile saline was from Spectrum Chemical (Cat No. S1941, New Brunswick, NJ, USA). Polypropylene Heparin-Lithium-Fluoride coated tubes were obtained from Beckman Coulter (Cat No. 6528824, Indianapolis, IN, USA).

2.1 Animal Procedures:

All procedures were performed in accordance with the guidelines of National Institutes of Health ILAR Guide for the Care and Use of Laboratory Animals and were approved by the University of California Davis Institutional Animal Care and Use Committee (protocol # 19519, 21420 and 20541).

Male Fischer CDF rats weighing 200-220 g (~11.5 weeks of age; n=8) with femoral vein vascular catheterizations were obtained from Charles River (Wilmington, MA, USA) and housed in a temperature and humidity controlled vivarium for two days. Food and water were provided *ad libitum*. The rats were maintained on the same Charles River diet (LabDiet 5L79, catalogue number: 11000112) upon arrival. The diet contained 18% crude protein, 5% crude fat, 5% crude fiber, 8% ash, 12% moisture, 0.65% sodium, and 51.35% carbohydrate.

Rats were administered vehicle or d4-13-HODE via gavage or IV injection. The vehicle contained 5mM HEPES buffer mixed with 50mg/ml fatty acid free BSA. The UE-d4-13-HODE mixture contained 5mM HEPES buffer, 50mg/ml fatty acid free BSA and 0.22 mg/ml d4-13-HODE. Both vehicle and d4-13-HODE solutions were sonicated for 15 minutes. The solutions were mixed the day of, or day prior to, the experiment. If mixed the day prior, they were stored at -80°C and thawed on ice prior to use. All solutions were kept on ice throughout the experiment and were thoroughly vortexed prior to being administered to the rats.

All rats were weighed prior to injection to determine tracer volumes. Eight rats were administered vehicle via gavage (n=1), vehicle via intravenous (IV) injection (n=1), d4-13-HODE via gavage (n=3) or d4-13-HODE via IV (n=3). The vehicle-injected rats served as negative controls ensuring the absence of tracer background during mass spectrometry analysis. The d4-13-HODE dose was 0.5 mg/kg per rat for both gavage and IV injection groups. This dose was based

on a study showing bioactivity of another omega-6 fatty acid-derived lipid mediator, prostaglandin E2 (PGE2), when provided IV at 0.5 mg/kg (Long, Morimoto, Nakamori, Yamashiro, & Murakami, 1991) .The gavage and injection volumes ranged between 0.4 to 0.5 mL.

Blood was collected via tail vain or the femoral vein catheter from each rat at baseline (time 0, before tracer injection), and at 1, 3, 5, 10, 20, 30, 45, 60 and 90 min following vehicle or tracer administration, into Beckman Coulter polypropylene Heparin-Lithium-Fluoride coated tubes. The catheters were flushed with 0.1 to 0.2ml sterile saline (0.9%) prior to and after blood collection. Following the final blood collection at 90 min, the rats were euthanized with CO_2 for approximately 2.5 min, decapitated and truncal blood collected at approximately 93-95 min. Blood was kept on ice and centrifuged at 15,871*g on an Eppendorf 5425 centrifuge (Hauppauge, NY, USA) for one minute to separate plasma. The separated plasma was transferred to new Beckman Coulter polypropylene Heparin-Lithium-Fluoride coated tubes and placed on dry ice. All tubes were stored in a -80°C freezer until further analysis.

After euthanasia, the following tissues were dissected from each animal: right and left cerebrum, cerebellum, brainstem, heart, liver, lungs, stomach, small and large intestines, cecum, right and left kidney, lung and visceral and perirenal adipose, testis, skin, and hind limb muscle. All tissues were obtained within 30 minutes after decapitation starting with the brain, and immediately flash-frozen in liquid nitrogen before being transferred to dry ice and storage at -80°C. The analysis (below) was confined to adipose, liver, heart and brain. Other tissues remain stored in our freezer.

All animal procedures were completed within two consecutive days (8 rats on day 1 and 2 rats on day 2). One IV injected vehicle, one gavgaed vehicle, two IV injected and two gavaged

tracer rats were completed on day 1; one IV injected and one gavaged tracer rats were completed on day 2.

Plasma and tissues were obtained from a separate group of Sprague-Dawley timed-pregnant female rats (Charles River Laboratories, Hollister, CA, USA), for method optimization of the 13-HODE (labeled and unlabeled) measurements. Rats were individually housed on a 12:12 h light: dark cycle at ~22 °C with food and water available ad libitum. Blood and tissue collections were made following delivery of pups. Briefly, dams were deeply anesthetized with 4% isoflurane in oxygen. Blood samples were then collected via cardiac puncture. Blood was centrifuged 12,000*g for 10 min at 4 °C to obtain serum. For tissue collection, dams were euthanized via CO_2 asphyxiation followed by cervical dislocation. Brain, heart, lung, liver, and visceral adipose tissues were collected and snap frozen in liquid nitrogen. All samples were stored at -80 °C. The method optimization was done on plasma and brain.

2.2 Method optimization:

Typically, total (i.e. UE + ES) oxylipins in plasma and tissues are measured in plasma or tissues following base hydrolysis, to liberate esterified oxylipins. However, both sodium carbonate (Na_2CO_3) and sodium hydroxide (NaOH) have been used at different concentrations and volumes to liberate esterified oxylipins (Ostermann et al., 2020; Quehenberger, Dahlberg-Wright, Jiang, Armando, & Dennis, 2018; Taha et al., 2018a). Therefore, these bases were compared at different volumes and concentrations (to test whether more is better), following extraction of total lipids with the Folch method from plasma and from brain, as a representative tissue, prior to measuring d4-13-HODE in the IV and gavaged rats.

Plasma was thawed on ice and 100 µL were transferred to 8 mL Kimble glass tubes containing 500 µL 1mM ethylenediaminetetraacetic acid (EDTA, Cat No. E5134, Sigma-Aldrich, St. Louis,

MO, USA) and 0.9% NaCl (Cat No. S7653, Sigma-Aldrich, St. Louis, MO, USA) in milliQ water. Then, 2.4 mL of 2:1 (v/v) chloroform (Cat No. C607-4, Fisher Scientific, Hampton, NH, USA): methanol (Cat No. A454-4, Fisher Scientific, Hampton, NH, USA) containing 0.002% butylated hydroxytoluene (BHT, Cat No. W218405-SAMPLE-K, Sigma-Aldrich, St. Louis, MO, USA) was added. Samples were vortexed and centrifuged at 458*g for 10 min (Beckman Coulter Allegra 6 centrifuge, Indianapolis, IN, USA). The bottom chloroform layer was transferred to new tubes. 1.6 mL chloroform was added to the Kimble tubes, and the samples were vortexed, centrifuged and the second chloroform bottom layer was combined with first and evaporated under nitrogen.

The evaporated extract was reconstituted in 200 µL methanol containing 0.1% acetic acid (Cat No. 695092, Sigma-Aldrich St. Louis, MO, .USA) and 0.1% BHT, 10 µL antioxidant (composition below), and spiked with 10 µL surrogate standard mix containing 2 µM d11–11(12)-EpETrE (Cat No. 10006413, Cayman Chemical, Ann Arbor, MI, USA), d11-14,15-DiHETrE (Cat No. 1008040, Cayman Chemical), d4-6-keto-PGF1α (Cat No. 315210, Cayman Chemical), d4-9-HODE (Cat No. 338410, Cayman Chemical), d4-LTB4 (Cat No. 320110, Cayman Chemical), d4-PGE2 (Cat No. 314010, Cayman Chemical), d4-TXB2 (Cat No. 319030, Cayman Chemical), d6-20-HETE (Cat No. 390030, Cayman Chemical) and d8-5-HETE (Cat No. 334230, Cayman Chemical). The antioxidant mix was made by mixing 0.2 mg/mL BHT, ethylenediaminetetraacetic acid (EDTA, Cat No. EDS-100G, Sigma-Aldrich, St. Louis, MO, USA) and triphenylphosphine (TPP, Cat No.3T84409 Sigma-Aldrich, St. Louis, MO, USA) in methanol/water (50/50, v/v)) and filtering the contents through 0.45 µm Millipore filter (Millpore, Bedford, MA, USA, cat No. SLHVM25NS).

The sample was hydrolyzed in 200 µL or 300 µL of 0.25M NaOH (Cat No. S5881-500G, Sigma-Aldrich, St. Louis, MO, USA), 0.4M NaOH or 0.25M Na_2CO_3 (Cat No. 791768-500G,

Sigma-Aldrich, St. Louis, MO, USA) in Methanol: MilliQ water (50/50 v/v; n=4 per base treatment). Samples were vortexed and heated at 60°C for 30 min, and cooled at room temperature for approximately 5 min. Then, 25 µL and 37.5 µL acetic acid were added to the tubes containing 200 µL and 300 µL base volumes, respectively, to bring the pH to 4-6 (verified on one sample by litmus paper). 1575 µL MilliQ water was added to samples that were hydrolyzed in 200 µL base and 1796 µL was added to samples that were hydrolyzed in 300 µL of base.

Samples were loaded onto solid phase extraction (SPE) columns (Cat No. WAT094226, 60mg Oasis HLB, Waters, Milford, MA, USA) pre-washed with one column volume of ethyl acetate (Cat No. E196-4, Fisher Scientific, Hampton, NH, USA) and two column volumes of methanol, and conditioned with two column volumes of SPE buffer (0.1% acetic acid, 5% methanol in ultrapure water). Samples were loaded onto the SPE columns, washed with two column volumes of SPE buffer and dried under vacuum for 20 min. Oxylipins were eluted with 0.5 mL methanol and 1.5 mL ethyl acetate. The eluent was dried under nitrogen, reconstituted in 50 µL LC-MS grade methanol (Cat No. A956,Fisher Scientific, Hampton, NH, USA), vortexed, centrifuged on Eppendorf 5424R centrifuge at 15,871*g (at 0°C) for 2 min. The sample was transferred to centrifugal filter units (Cat No. UFC30VV00, Ultrafree-MC VV Centrifugal filters, Burlington, MA, USA) which were centrifuged at 15,871*g (0 °C) for 20 min. Samples were analyzed with UPLC-MS/MS as described below.

For optimization of the hydrolysis method on brain, a half cerebrum weighing ~845 mg was homogenized in 0.9% NaCl containing 1mM EDTA in 2 mL centrifuge tube (Cat No. 1620-2700, USA scientific, Ocala, Florida, USA) using a bead homogenizer (Cat No. BBY24M Bullet Blender Storm, Next Advance, Troy, NY 12180, USA). The entire brain homogenate (~1.5 mL) was transferred to Kimble glass test-tubes containing 4 mL chloroform. The 2 mL centrifuge tubes

were rinsed with 2 mL of methanol containing 0.006% BHT, vortexed and transferred to the 8mL glass tubes containing chloroform (thus diluting the BHT content to 0.002%). Samples were vortexed and centrifuged at 920*g for 15 min at 0°C. The bottom layer was pipetted to a clean test-tube. Lipids were re-extracted from the original sample with an additional 4 mL chloroform. The chloroform layers were pooled, evaporated under nitrogen and reconstituted into chloroform: isopropanol (Cat No. A464-1, Fisher Scientific, Hampton, NH, USA) (v/v: 2/1).

A portion of chloroform: isopropanol corresponding to 1 mg total lipid (based on an estimated 10% lipid content per brain (Schwab, Bauer, & Zwiener, 1997)) was hydrolyzed in 200 µL 0.25M Na_2CO_3, 200 µL 0.4M NaOH or 300 µL 0.4M NaOH (n=4 per treatment) at 60°C for 30 min. The samples were cooled, acidified with acetic acid, diluted in water and purified with SPE and centrifugal filtering as described above for plasma, prior to UPLC-MS/MS analysis.

Standard recovery was determined for plasma and brain. The surrogate standard recovery was determined by dividing the peak area of surrogate in the sample post Folch extraction and hydrolysis, by the peak area of an equimolar surrogate standard mix that has not been subjected to Folch extraction and hydrolysis. Ion suppression was measured in brain extracts by pooling 15 µL from each base condition (n=4 per condition; total volume = 60 µL), transferring two 20 µL aliquots of the sample mixture to new LC-MS vials, adding 30 µL of an oxylipin standard mix to one, and 30 µL methanol to the other (total volume = 50 µL per vial). Ten µL were injected into the UPLC-MS/MS, alongside 30 µL of the oxylipin standard mix diluted to the same level with 20 µL methanol. Percent ion suppression was calculated as follows: Peak area in spiked sample / (peak area in unspiked sample + peak area in standard mix) x 100.

2.3 Extraction of plasma and tissue from gavaged and IV injected rats:

As described in the Results Section, hydrolysis with 300 µL of 0.4 M NaOH yielded the best results, so we used it to for measuring total oxylipins in plasma and tissue samples from the gavaged and IV injected rats.

For plasma, free and total oxylipins were extracted on the same day. Total oxylipins were extracted from 100 µL plasma and the remainder (3-100 µL) was used for free oxylipins.

For free oxylipins, 200 µL extraction solvent, 10 µL antioxidant mix and 10 µL of 2 µM surrogate standard mixture were added to each plasma sample. Samples were vortexed and centrifuged at 21130*g at 0°C for 15 min. The supernatant layer was transferred and MilliQ water (1113-1210 mL, depending on the plasma volume used) was added to each sample to achieve 15% methanol content. Samples were extracted with Oasis HLB columns as described above. Total oxylipins were extracted from plasma with the Folch method and hydrolyzed with 300 µL of 0.4 M NaOH and subjected to SPE as described above.

Cerebrum (right side; 672 ± 36 mg), heart (663 ± 15 mg), liver (759 ± 177 mg), visceral adipose (189 ± 113mg) and peri-renal adipose (156 ± 63mg) were extracted by the Folch method. For brain, and liver, samples were homogenized in equal volumes of 0.9% NaCl containing 1mM EDTA in 2 mL centrifuge tubes using a bead homogenizer. The homogenates were transferred to 8 mL glass tube containing 5 mL chloroform: methanol (v/v: 2/1) containing 0.002% BHT. 1 mL of chloroform/methanol was used to re-extract samples remaining in the 2 mL centrifuge tubes. The samples were vortexed, centrifuged at 920*g for 15 min at 0°C and the bottom chloroform layer transferred to a new test-tube. Lipids were re-extracted by adding chloroform (4 mL) to the sample and pooling the second extract with the first.

For heart, samples were homogenized in equal volume of 0.9% NaCl containing 1mM EDTA in 2 mL centrifuge tubes using a bead homogenizer. However, due to incomplete

homogenization, the samples were transferred to 2mL centrifuge tube containing 1 mL chloroform: methanol (v/v: 2/1) with 0.002% BHT, and further homogenized on a GenoGrinder 2010 (Spex, Metuchen, NJ) for 3 min at 1200rpm then for 13 min at 1400rpm. The mixture was transferred to 8 mL glass tube containing chloroform: methanol (v/v: 2/1) with 0.002% BHT. Another 1 mL was used to rinse the tubes.

Visceral adipose was homogenized in 1.5 mL screw cap tubes (Cat No. TUBE1R5-S, Next Advance, Troy, NY 12180, USA) containing 1 mL 0.9% NaCl and 1 mM EDTA, using the bead homogenizer. The homogenates were transferred to Kimble test-tubes containing 5 mL chloroform/methanol with BHT; 1 mL of the chloroform/methanol/BHT mix was used to rinse the centrifuge tubes and the remaining extract was pooled with other 5 mL in the Kimble tubes, for a total of 6 mL solvent. Then, 0.5 mL 0.9% NaCl containing 1 mM EDTA was added to the Kimble tubes. The samples were vortexed, centrifuged and re-extracted in 4 mL chloroform as described above for the other tissues.

For perirenal adipose tissue, the samples were also homogenized in 1.5 mL 0.9% NaCl containing 1 mM EDTA in 2 mL centrifuge tubes with a cap. However, the caps opened during homogenization for all three rats given the tracer via IV and one rat given the tracer via gavage. We attempted to recover the remaining homogenate by adding 1.5 mL of 0.9% NaCl containing 1mM EDTA, vortexing and transferring the homogenate to Kimble test-tubes containing 4 mL of chloroform/methanol with 0.002% BHT. 1 mL of the chloroform/methanol/BHT mix was used to rinse the centrifuge tube twice (total of 2 mL). The samples were vortexed, centrifuged and re-extracted in 4 mL chloroform. The extraction proceeded as described above for visceral adipose tissue. Samples that were not lost during homogenization were transferred to Kimble glass-tubes

containing chloroform/methanol/BHT; 1 mL was used to rinse the tubes twice and the extracts were pooled transferred. The samples were re-extracted with 4 mL chloroform.

For all tissues, a portion of the total lipid extract, amounting to ~3 mg lipid per tissue, was reconstituted in 200 µL extraction solvent and hydrolyzed in 300 µL 0.4 M NaOH. Acetic acid and water were added and the oxylipins extracted with SPE as described above.

2.4 UPLC-MS/MS analysis

Oxylipins (72 species) were analyzed on an Agilent 1290 Infinity UHPLC system connected to an Agilent 6460 triple-quadrupole tandem mass spectrometer (Agilent, Palo Alto, CA, USA) equipped with a Jetstream electron spray ionization source as previously detailed (M. Hennebelle, A. H. Metherel, et al., 2019; M. Hennebelle, R. K. Morgan, et al., 2019). Oxylipins were analyzed in negative ionization mode and probed using published optimized dynamic Multiple Reaction Monitoring conditions (M. Hennebelle, A. H. Metherel, et al., 2019; M. Hennebelle, R. K. Morgan, et al., 2019). The optimized transition for d4-13-HODE was 299.3-198.1, which was consistent with the literature (Z. X. Yuan et al., 2013). We also probed for labeled downstream metabolites of d4-13-HODE in tissues, specifically d3-13-oxo-ODE (296.2-198.1) and d4-9,10,13-TriHOME (333.2-172.1/171.1). The collision energy for all labelled compounds was 10 V.

Oxylipin species were separated with reverse phase liquid chromatography, using an Agilent Eclipse Plus C18 column (2.1 x 150 mm, 1.8 µm Agilent Corporation). The auto-sampler was at 4°C and the column temperature was set at 45°C. The same mobile phases and conditions published previously were used. In brief, mobile phase A had 0.1% acetic acid in ultrapure water and mobile phase B had 80/15 acetonitrile/methanol (v/v) with 0.1% acetic acid (M. Hennebelle,

A. H. Metherel, et al., 2019; M. Hennebelle, R. K. Morgan, et al., 2019). Mobile phase A was initially at 65%. It was decreased to 60% at 3 min, 52% at 4 min, 40% at 10 min, 30% at 20 min, 15% at 24 min and 0% by 24.6 min. Mobile phase B was therefore at 100% at 24.6 min and held there to 26.1 min. Mobile phase A was increased to 65% at 26.10 min and held constant to 27.30 min for the remainder of the run, which ended at 28 min. The flow rate initially was 0.3 mL/min from 0-3 min, 0.25 mL/min from 3 to 24.5 min, 0.35 mL/min from 24.6 to 27.0 mins, and 0.30 mL/min from 27.3 to 28 min.

Samples that utilized d4-PGE2 as a surrogate standard were not quantified because it degrades during hydrolysis. These include LA-derived trihydroxylated metabolites (9,10,13-TriHOME and 9,12,13-TriHOME) and prostaglandins (PGB2, PGD1, PGD2, PGD3, PGE1, PGE2, PGE3, 15-deoxy-PGJ2 and PFG2-alpha).

2.5 Kinetics

The volume of distribution (V_d) of the injected UE d4-13-HODE tracer was calculated as follows:

$V_d = D/C_{UE}$ (Eqn 1), where D is the dose of the injected tracer and C_{UE} is the peak plasma concentration of UE d4-13-HODE following injection (i.e. at 1 min).

Plasma half-life of UE d4-13-HODE was derived from the plasma curve of IV-injected rats, by taking the first derivative of plasma concentration, starting at 1 min, the time at which injected d4-13-HODE concentration reached peak values, to 5 min, when the tracer appeared to plateau between the non-detectable to 1 pmol/µL range. Thus, the rate of UE tracer elimination was determined using Equation 2 below. A similar calculation was used to determine rate of total d4-13-HODE tracer elimination, by measuring changes in total d4-13-HODE concentrations over time.

$$Rate\ of\ tracer\ elimination(R) = \frac{dC*_{UE}}{dt(1-5min)}$$ (Eqn 2)

where C* is d4-13-HODE concentration in plasma, t is time, and k* is the slope constant. Zero order and first order kinetic plots were generated to determine the plot that generated a linear relationship. As shown in **Supplement Figure 1**, plotting the natural log of C versus time resulted in a linear slope with an R^2 of 0.9749, suggesting first order kinetics. The slope of the line (i.e. the k* value) was used to calculate the half-life of the free, injected d4-13-HODE as follows:

$$Plasma\ UE\ t_{1/2} = \frac{ln2}{slope\ (k*)}$$ (Eqn 3)

The rate of ES d4-13-HODE incorporation into plasma following gavage was determined by taking the first derivative of the tracer concentration versus time plot, and re-plotting that against time. Because negligible d4-13-HODE was found in the free pool, the total amount in plasma after gavage represents the ES pool. Thus,

$$Plasma\ J_{in\ (ES)} = \frac{dC*_{total}}{dt_{0\ to\ 90\ min}}$$ (Eqn 4)

The maximum rate of incorporation, $J_{in\ (ES)}$, representing maximum velocity of incorporation was derived from the maximum point on the plot. This was then used to calculate turnover (F) of esterified d4-13-HODE as follows,

$$Plasma\ F_{ES} = \frac{Jin_{ES}}{C_{total}}$$ (Eqn 5)

Here, C_{total} is the unlabeled 13-HODE concentration when the velocity of incorporation was maximum based on Eqn 4 (i.e. at $J_{in(ES)}$)

The half-life of the esterified 13-HODE was determined as follows,

$$Plasma\ ES\ t_{1/2} = \frac{ln2}{F_{ES}}$$ (Eqn 6)

The plasma area under the curve (AUC) was determined by trapezoid integration of the plasma total and free d4-13-HODE concentration from 0 to 90 min, following IV or gavage. The incorporation coefficient of UE d4-13-HODE, k^*_{UE}, for each tissue, was calculated as follows,

$$Tissue\ k^*_{UE} = \text{Tracer tissue concentration}_{\text{Total}}/\text{AUC}_{\text{UE}} \text{ (Eqn 7)},$$

where tracer tissue concentration$_{\text{Total}}$ represents the sum of ES and UE tracer measured in each tissue, because only total d4-13-HODE was measured. The AUC_{UE} is derived from the IV-injected rats.

The incorporation rate (J_{in}) of UE d4-13-HODE into tissues was determined as follows,

$Tissue\ J_{in}(UE) = k^*_{UE} x C_{UE\ plasma}$ (Eqn 8), where C_{UE} plasma is the concentration of free, unlabeled 13-HODE in plasma at 90 min or 95 min (from sample collected after decapitation) depending on availability. For one of the rats, we used UE concentration at 30 minutes, due to insufficient plasma volume at other time-points following tracer measurements.

Turnover, representing the rate of tracer replacing endogenous 13-HODE the within tissues was calculated according the following equation,

$Tissue\ F_{total} = \frac{J_{in}UE}{C_{total}}$ (Eqn 9), where C_{total} is the total (UE + ES), unlabeled amount of 13-HODE in tissues. Half-life ($t_{1/2}$) was determined using equation 5, where ln2 is divided by tissue turnover *(F)* calculated in Eqn 9.

To determine the contribution of esterified d4-13-HODE incorporation from plasma into tissues, we integrated the following equation (Trepanier et al., 2015),

The rate of tissue incorporation is, $\frac{\text{dC*tissue}}{\text{dt}} = k^*_{UE} C^*_{\text{plasma(UE)}} + k^*_{ES} C^*_{\text{plasma(ES)}}$ (Eqn 10)

The integral yielded the equation below, where k^*_{UE} is derived from the IV-injected rats using Eqn 7 above.

$$C^*_{\text{tissue}}(T) = k^*_{UE} \int_0^T C * \text{plasma(UE)} dt + k^*_{ES} \int_0^T C * \text{plasma(ES)} dt \text{ (Eqn 11)}$$

Eqn 11 was solved for k^*_{ES}, which is the incorporation coefficient for esterified d4-13-HODE in tissues. This was calculated because we did not inject ES d4-13-HODE. Notably, a similar k^*_{ES} value can be derived from the quotient of tissue total d4-13-HODE concentration and the AUC for ES d4-13-HODE, determined by subtraction the AUC of free d4-13-HODE from the AUC of total d4-13-HODE. The incorporation rate of esterified d4-13-HODE, $J_{in}(ES)$, into tissues was then calculated as follows,

$Tissue\ J_{in}(ES) = k^*_{ES} x C_{ES\ plasma}$ (Eqn 12), where C_{ES} plasma is the amount of unlabeled, esterified 13-HODE in plasma at 90 min or 95 min from the sample collected after decapitation, depending on plasma availability. C_{ES} plasma was calculated by subtracting free 13-HODE from total 13-HODE.

2.6 Statistical analysis:

The sample size justification for 3 rats per route of administration for d4-13-HODE was based on similar studies which used a sample size of 3 to 4, to examine the metabolism of labeled oxylipins (e.g. PGE2 or LNA-hydroperoxide) in rats (Glavind & Sylven, 1970; Raz, 1972; Samuelsson, 1964). Data were analyzed on GraphPad Prism version 8.4.3 (GraphPad Software, San Diego, California USA), and expressed as mean ± standard deviation (SD). One-way analysis of variance (ANOVA) followed by Tukey's post-hoc test was used to compare across methods. An unpaired t-test was used to compare log-transformed values for labeled and unlabeled 13-HODE concentrations in tissues and plasma, UE and ES tracer kinetics, because analysis by Shapiro–Wilk's test showed that the data were not normally distributed. A $P<0.05$ was considered statistically significant.

3. Results

3.1 Base hydrolysis method

The hydrolysis efficiency of 200 and 300 µL of NaOH or Na_2CO_3, at 0.25M and 0.4M each, was tested on 100 µL rat plasma. As shown in **Supplement Table 4**, 300 µL 0.4M NaOH yielded the highest concentration of oxylipins with the lowest SDs and CVs. Surrogate recoveries (**Supplement Table 5)** were similar across the different base conditions, and did not statistically differ from each other. As expected, d4-PGE2 was lost during hydrolysis with both bases.

The hydrolysis efficiency of 200 µL of 0.25M Na_2CO_3, 200 µL of 0.4M NaOH, and 300 µL of 0.4M NaOH was tested on rat brain tissue lipid extracts. As shown in **Supplement Table 6**, 300 µL of 0.4M NaOH yielded the highest concentration of oxylipins. Surrogate recoveries were similar across the various base treatments (**Supplement Table 7).** Ion suppression was minimal for the majority of compounds across the three base treatments as shown in **Supplement Table 8**.

Based on the above findings, 300 µL of 0.4M NaOH was used on plasma and tissues (below), because it yielded the highest recovery and yield of oxylipins.

3.2 Body and organ weights

Body and organ weights did not differ significantly between the gavage and IV groups ($P>0.05$ by unpaired t-test; n=4 per group including the rats gavaged or injected with vehicle). Rats in the gavage and IV-injected groups weighed 195 ± 9 g and 178 ± 49 g, respectively. At the time of sacrifice, cerebrum weighed 0.7 ± 0.04 g and 0.7 ± 0.03 g, peri-renal adipose was 0.2 ± 0.1 g and 0.2 ± 0.1 g, visceral adipose was 0.2 ± 0.1 g and 0.2 ±0.1 g,, heart was 0.7 ± 0.02 g and 0.5 ± 0.3 g and liver was 0.9 ± 0.1 g and 0.7 ± 0.2 g in the gavaged and IV-injected rats, respectively.

3.3 Volume of distribution

The volume of distribution, derived from peak d4-13-HODE concentration (at 1 min) in IV-injected rats was 104 mL. This value is 8-fold greater than the reported blood volume of 12.7 mL for rats at this age (H. B. Lee & Blaufox, 1985), suggesting that the injected tracer likely went into tissues.

3.4 Plasma tracer incorporation after IV injection and gavage

Figures 9-A and 1-B show mean UE and total d4 13-HODE concentrations over the 90-minute monitoring period following IV and gavage administration of the tracer, respectively. There were multiple missing values for UE d4 13-HODE measured in both gavage- and IV- treated rats, due to the lack of sufficient sample volume at several time-points. Hence, data were available from 2-3 rats per time-point, except for UE d4-13-HODE at 1 min in the IV-injected group, where only one sample could be assayed. Error bars (i.e. SDs) are shown when the sample size is 2 to 3. Individual Concentration-Time plots for UE and total d4 13-HODE of each rat are presented in **Supplement Figure 2**.

No tracer was detected in plasma at any time-point in vehicle-treated rats (n=1 gavage and n=1 IV). UE and total (UE+ES) d4-13-HODE were detected in plasma of gavage- and IV- treated rats (n=3 per treatment). As shown in **Figure 9-A**, after IV tracer injection, the concentration of UE d4-13-HODE was highest at 1 min (3.17 pmol/µL), and dropped rapidly to 0.18 pmol/µL within 3 min, and to negligible levels by 40 min. Total d4-13-HODE was lower in concentration by approximately 2-fold relative to UE d4-13-HODE during the first 30 min, likely due to losses of the d4-9-HODE during SPE or degradation s during base hydrolysis, as previously reported

(Ostermann et al., 2020). The fact that the majority of the tracer was recovered in the free pool, suggests that the injected tracer did not incorporate into ES lipids. This is also supported by the observation that total d4-13-HODE elimination pattern mirrored that of the free pool (**Figure 9-A**).

In gavaged rats (**Figure 9-B**), the majority of d4-13-HODE in plasma was found in the total pool (free + esterified). It was detected there from 3 to 20 min after gavage at a low concentration of approximately 0.0059 pmol/µL. This concentration gradually increased after 20 min and reached 0.10 pmol/µL by 90 min. UE d4-13-HODE was detected at 5 min (0.0054 pmol/µL) following gavage, and remained relatively low during the 90 min sampling period (range of 0.0016-0.0093 pmol/µL). UE d4-13-HODE constituted 48.2% of the total d4-13-HODE pool at the beginning (between 0 to 10 min), and 2.0% of the total pool between 45 to 60 min, suggesting that the majority of the gavaged tracer incorporated into esterified plasma lipid pools over time.

Plasma unlabeled 13-HODE concentrations (UE and total) were relatively stable over time (**Supplement Figure 3-A&B)**, suggesting that the injected or gavaged tracer did not alter endogenous pools.

3.5 Plasma AUC after tracer IV injection and gavage

In IV-injected rats, the AUC was 16.4 ± 19.3 pmol*min/µL for free total d4-13-HODE and 11.7 ± 12.1 for total d4-13-HODE ($P>0.05$ by unpaired t-test on log-transformed values). The AUC was 0.3 ± 0.2 and 2.4 ± 1.9 pmol*min/µL for free and total d4-13-HODE, respectively, in the group that received the tracer via gavage ($P<0.05$ by unpaired t-test on log-transformed values).

3.6 Plasma kinetics after IV injection and gavage

Plasma total d4-13-HODE kinetics following IV or gavage are reported in **Table 6**. Because all free tracer was found in the total pool after IV injection, it can be assumed that total d4-13-HODE elimination kinetics represent the elimination of UE d4-13-HODE. Similarly, total d4-13-HODE plasma incorporation kinetics reflect ES d4-13-HODE kinetics in the gavage rats, since most of the tracer was found in ES fractions.

The rate constant for elimination (k) of the injected UE d4-13-HODE was higher (by 42-fold) than the rate constant (F) for incorporation into plasma following gavage. This is in agreement with the greater elimination rate (R_{max}) of the IV-injected tracer compared to incorporation rate (J_{in}) of the gavaged tracer.

The half-life of the injected UE tracer was derived from the natural log-transformed concentration-time plot shown in **Supplement Figure 1**. The half-life of total 13-HODE following IV injection was approximately 1 min (61.3 ± 9.47 s, n=3; **Table 6**). A similar half-half of 58.2 s was obtained for UE d4-13-HODE, although this was based on one rat where UE tracer was measured at 1 min (we did not have sufficient plasma left in the other 2 rats to pursue further UE measurements at this time-point). Similarities between the total and free pool half-lives further confirm that the majority of injected d4-13-HODE was in the free pool.

The half-life of the esterified tracer was determined from the first derivative plots of concentration versus time following d4-13-HODE gavage (**Supplement Figure 1)**. Rats reached maximal incorporation rates (J_{in}) within 3-90 min. The calculated mean half-life was 71.2 min (**Table 6**).

3.7 Tissue total d4-13-HODE and unlabeled 13-HODE concentrations

Total (UE and ES) d4-13-HODE and endogenous (unlabeled) 13-HODE were measured in adipose, liver, heart and brain by UPLC-MS/MS. No peaks were observed in the vehicle-treated rats in all tissues assayed (**Supplement Figure 5**). Concentrations of total (UE + ES) labeled and unlabeled 13-HODE in tissues and plasma (at time of death) of rats gavaged or injected IV with the tracer are reported in **Table 7**.

D4-13-HODE was detected and quantified in visceral adipose, heart and liver following IV and gavage tracer administration. As shown in **Table 7**, there were no significant differences in tracer concentrations in these tissues between the IV-injected versus gavage-treated rats. No tracer was detected in the brain after IV or gavage administration. D4-13-HODE was detected in perirenal adipose of IV-infused rats (chromatograms in **Supplement Figure 5-A**) but as described in the Methods, due to sample loss, tracer concentrations were not quantifiable. D4-13-HODE was not detected in perirenal adipose of rats gavaged with the tracer, likely due to sample loss during the extraction (**Supplement Figure 5A**). Raw chromatograms for the remaining tissues, per rat, are in **Supplement Figure 5 (B to E)**. At the time of death, plasma total d4-13-HODE concentration was significantly higher in gavaged rats than IV-injected rats, consistent with the continued appearance of the tracer in plasma over time following gavage.

Unlabeled 13-HODE was observed in all tissues irrespective of tracer method of administration (**Table 7**). It was seen in peri-renal adipose, but again, quantitation was not possible due to accidental loss during homogenization. In visceral adipose, heart, liver and brain, no significant differences were seen in 13-HODE concentration between IV and gavage treated rats.

Notably unlabeled 13-HODE was most abundant in visceral and perirenal adipose tissue (10-27 pmol/mg), followed by heart (~1.6 pmol/mg), liver (~1.2 pmol/mg) and brain (~0.18 pmol/mg). This hierarchy was also reflected in tracer concentrations, where d4-13-HODE was 353

times and 546 times higher in visceral adipose than in heart and liver respectively (none in brain). The variability, based on standard deviations, were higher for both unlabeled and labaled 13-HODE in metabolic tissues such as adipose and liver, compared to heart and brain.

3.8 Kinetics of d4-13-HODE

The incorporation coefficient (k_i^*), incorporation rate (J_{in}), turnover (F) and half-life ($t_{1/2}$) of UE and ES d4-13-HODE in adipose, liver and heart are reported in **Table 8**. The IV-injected rats were used to derive UE incorporation into tissues, because most of the tracer was unesterified after IV injection. The gavaged rats were used to derive ES kinetics, because most of the tracer was esterified post-gavage.

The incorporation coefficient, k_i^* in liver was significantly higher by 6-fold for ES d4-13-HODE compared to UE d4-13-HODE ($P<0.05$). It was 19- and 2-fold higher for ES d4-13-HODE in visceral adipose and heart, but this change was not statistically significant.

The incorporation rate, J_{in}, into adipose, liver and heart was also higher by 38-, 11,- and 3-fold for ES versus UE d4-13-HODE, but changes were only statistically significant for liver ($P<0.05$).

Turnover, F, was significant higher for ES than UE tracer in adipose and liver by 40- and 11-fold, respectively. ES tracer turnover was 3 times higher than UE turnover in heart, but this difference was not statistically significant.

UE tracer half-life ranged from 6 to 36 days, whereas ES half-life ranged from 0.3 to 3.6 days in adipose, liver and heart. Thus, the half-life of the ES tracer in these tissues was 5-18 times shorter than the half-life of the UE tracer. Statistical significance in tracer half-life was only seen for visceral adipose and liver.

3.9 Metabolism of d4-13-HODE into other downstream metabolites in tissues

To test whether d4-13-HODE was converted into other downstream ketones or tri-hydroxylated metabolites, we probed for d3-13-oxo-ODE and d4-9,10, 13-TriHOME in adipose (peri-renal and visceral), liver, heart and brain of IV and gavage rats. As shown in **Supplement Figure 6**, no tracer was detected during the transition times for either metabolite in any of the tissues, irrespective of the mode of administration.

4. Discussion:

This study demonstrates that LNA-derived 13-HODE is bioavailable and that it rapidly incorporates into liver, heart and adipose, but not brain. Tracer incorporation into liver, heart and adipose from ES 13-HODE was faster compared to UE 13-HODE, suggesting that peripheral tissues preferentially uptake ES over free 13-HODE.

Although free OXLAM incorporation into peripheral tissues has been previously reported (Cho & Ziboh, 1994), this is the first study to quantitatively demonstrate that ES 13-HODE preferentially incorporates into peripheral tissues. Bergan and Draper (Bergan & Draper, 1970) detected radioactivity in heart, liver and adipose but not brain after gavaging free 14C labelled LA hydroperoxides. Samuelsson et al reported that tritiated PGE2 (a metabolite of arachidonic acid, ARA), also incorporated into liver, heart, adipose, and brain after IV infusion (Samuelsson, 1964). Although these studies suggest that free oxylipins enter tissues, the use of radiolabeled tracers do not inform on whether the intact tracer or a metabolite of the tracer incorporated into tissues. Mass-spectrometry analysis performed in this study ascertained that the intact d4-13-HODE tracer incorporated into peripheral tissues from plasma.

The plasma half-life of free (UE) d4-13-HODE was >70-fold lower than that of the bound (ES) tracer (~ 1 vs 71 min). The short half-life of the free tracer is consistent with its observed high volume of distribution (104 mL), relative to the average rat blood volume of 12.7 mL (H. B. Lee & Blaufox, 1985). This means that the free tracer incorporated into tissues, as confirmed in **Table 8**. The longer plasma half-life of ES d4-13-HODE is comparable to the reported absorption half-life of esterified conjugated LNA of 20 to 32 min and reflects lipoprotein-mediated mechanisms of transport (Rodriguez-Alcala et al., 2017). In contrast, UE 13-HODE likely non-covalently associates with albumin, similar to UE fatty acids (Borgstrom & Olivecrona, 1961), which means that elimination is dependent on rapid diffusion into tissues rather than lipoprotein-mediated receptor uptake (slower process) as is the case for ES lipids. The notably high variability in ES plasma half-life (coefficient of variation (CV) of 97%) compared to that of UE d4-13-HODE (CV of 15%) is likely due to postprandial differences in free d4-13-HODE absorption, since food was provided ad libitum. There is limited information on postprandial 13-HODE response in rodents, but in non-fasted humans, a high post-prandial variability in 13-HODE (CV of 40-70%) was reported (Strassburg et al., 2014). Fasting the rats may reduce the variability in 13-HODE plasma metabolism, as reported in humans (Ostermann et al., 2018).

The incorporation coefficient, k^*, is a marker of tissue avidity towards the tracer (Rapoport & Taha, 2014; P. J. Robinson & Rapoport, 1989). In this study, k^*_{ES} was 2-19 fold higher than k^*_{UE} in visceral adipose, liver and heart, with statistical significance observed only for liver only (**Table 8**), suggesting that these tissues preferentially uptake ES over UE 13-HODE. This does not imply that these tissues solely uptake the ES tracer; in fact, they showed affinity towards both the UE and ES tracer, but affinity was greater towards the lipoprotein-bound tracer (**Table 8**).

The incorporation rate, J_{in}, is a quantitative measure of the amount of tracer that incorporates from plasma into tissues, per unit time (Modi et al., 2013). As shown in **Table 8**, both UE and ES tracers incorporated in adipose, liver and heart. However, the rate of ES 13-HODE incorporation into tissues was 3-38 fold greater than UE 13-HODE (significant for liver only). This is consistent with the significantly greater tissue affinity (k^*) towards ES than UE d4-13-HODE in liver.

Turnover, reflecting the rate at which the incorporated tracer replaces endogenous (unlabeled) 13-HODE pools lost during metabolism (Rapoport, Chang, & Spector, 2001), was 3-40 times higher in adipose, liver and heart for ES d4-13-HODE than UE d4-13-HODE. Differences were statistically significant for adipose tissue and liver, and indicate rapid turnover of ES 13-HODE within these compartments. The turnover measurements are likely underestimated because they do not account for the rate of tracer acylation/deacylation within tissue lipid compartments (Rapoport et al., 2001). Measuring labeled 13-HODE-CoA pools would provide a more complete picture of d4-13-HODE recycling within adipose, liver and heart.

We were not able to detect measurable loss into downstream products (ketone- and tri-hydroxy metabolites), although metabolism into other compounds not covered by our targeted UPLC-MS/MS platform is possible. For instance, Fang et al. has shown that 13-HODE can be metabolized into to 11-hydroxyhexadecadienoic acid, 9-hydroxytetradecadienoic acid, and 7-hydroxydodecadienoic acid, which were not measured in this study (Fang, Kaduce, & Spector, 1999). Additionally, a recent study showed that hydroxylated metabolites of docosahexaenoic acid undergo β-oxidation *ex vivo*, to form malic acid, butainetriol, and other short-chain hydroxy-fatty acids (Balas et al., 2019), raising the possibility that a similar oxidation pathway may exist for 13-HODE. Tissue release is also likely, particularly for adipose tissue, which has the highest

concentration and turnover of ES 13-HODE compared to other tissues, consistent with its physiological role as a both reservoir and supplier of oxylipins (Cayer et al., 2019; Suganuma et al., 2019).

The low tissue turnover of UE 13-HODE compared to ES 13-HODE may be due to its rapid esterification upon entering tissues, resulting in 'trapping' of the tracer by peripheral tissues. If so, then the measured rates of incorporation of free d4-13-HODE (J_{inUE}) reflect actual esterification rates *in vivo*. We did not measure unlabeled tissue concentrations of free 13-HODE in this study, a limitation which prevents us from capturing turnover within the free pool. Free oxylipin concentrations are low in tissues, and increase dramatically during euthanasia due to post-mortem ischemia (M. Hennebelle, A. H. Metherel, et al., 2019). Hence, this aspect of the study should be re-examined in rats subjected to high-energy microwave fixation (M. Hennebelle, A. H. Metherel, et al., 2019).

Compared to fatty acids, the kinetics of UE 13-HODE are similar in plasma but different in tissues. For instance, the half-life of free 13-HODE (~ 1 min) is comparable to that of ethyl LNA (39s), palmitic acid (48s) and docosahexaenoic acid (40s) in rats (Borgstrom & Olivecrona, 1961; Hungund, Zheng, & Barkai, 1995; Trepanier et al., 2015). It is also comparable to the half-life of other UE oxylipins, including ARA-derived PGE2 and PGF1α in humans (<1.5min) (Hamberg & Samuelsson, 1971) and PGF2α in horses (94.2s) and cows (29.2s) (Shrestha, Beg, Burnette, & Ginther, 2012). The opposite is observed for tissues, however, where free 13-HODE incorporates slower than free fatty acids. For instance, heart UE palmitic acid, ARA and eicosapentaenoic Acid (EPA) k^* values of 0.11, 0.36 and 0.13 µL/(mg×min), respectively, are 55-180 times higher than our measured heart d4-13-HODE k^*_{UE} of 0.002 µL/(mg×min) (**Table 8**) (Igarashi, Chang, Ma, & Rapoport, 2013; Murphy, Barcelo-Coblijn, Binas, & Glatz, 2004). Liver

UE Eicosapentaenoic Acid (EPA) k^* of 0.44 µL/(mg×min) is >1200-fold higher than d4-13-HODE k^*_{UE} value of 0.00036 µL/(mg×min) in liver (Igarashi et al., 2013). Similarly, UE EPA incorporation rate into heart (0.86 pmol/(mg×min)) and liver (3.1 pmol/(mg×min)) is orders of magnitude higher than both UE and ES d4-13-HODE incorporation rate into these tissues (Igarashi et al., 2013). Collectively, the evidence suggests that tissues incorporate free fatty acids preferentially over 13-HODE.

The half-life of ES 13-HODE (71 min), is five times less than the half-life of its esterified precursor, LNA (446 min) in plasma (Metherel, Lacombe, Chouinard-Watkins, Hopperton, & Bazinet, 2018a), and more than 50 fold smaller than the plasma half-life of esterified ARA (2.2 to 27.6 days depending on the dietary content of LNA) (Domenichiello et al., 2016), suggesting faster clearance of ES 13-HODE compared to ES fatty acids. Once in tissues, however, ES 13-HODE appears to be utilized slower than fatty acids. Based on the turnover measurements, ES d4-13-HODE half-life of 3.1 and 3.6 days in heart and liver, respectively, is greater than the reported half-life of ES EPA in heart (2.7 hours) and liver (4.6 hours) (Igarashi et al., 2013). These differences suggest that incorporated OXLAMs are likely to reside longer in tissues compared to fatty acids.

Schuster et al. reported that chronic (8 week) intake of dietary OXLAMs by mice did not increase plasma OXLAM concentrations, raising questions on their bioavailability (Schuster et al., 2018b). The present study indicates that 13-HODE (an OXLAM) is indeed bioavailable. The kinetic data suggest that although 13-HODE incorporates into plasma and tissues, it is not likely to markedly alter endogenous pools due to its relatively rapid turnover. It is possible that changes in endogenous plasma or tissue OXLAM pools may be seen after prolonged periods of intake (> 8 weeks) at relatively high doses. To provide some context on exposure levels, average LNA intake

in the US is ~16 g per person per day, whereas estimated OXLAM intake is in the order of milligrams (Blasbalg et al., 2011b; Richardson et al., 2017). Thus, despite the slower turnover of 13-HODE compared to fatty acids, dietary exposure of OXLAMs remains many orders of magnitude lower than fatty acids. Hence, prolonged exposure to 13-HODE (or OXLAMs) may be necessary to alter tissue concentrations.

D4-13-HODE was not detected in either IV or gavaged brain samples, suggesting that the tracer did not accumulate in the brain. However, this does not exclude the possibility that d4-13-HODE entered the brain, but was rapidly metabolized by the time the tissue was dissected 90 minute post tracer administration. Future studies should consider dissecting the brain while the labeled 13-HODE tracer is continuously infused to steady-state in plasma (Taha, Chang, & Chen, 2016), and following high-energy microwave fixation to avoid the effects of post-mortem ischemia (M. Hennebelle, A. H. Metherel, et al., 2019).

In conclusion, this study demonstrated that ingested 13-HODE can be absorbed and incorporated into liver, heart, and adipose, and that these tissues preferentially derive 13-HODE from the ES plasma pool. Quantifying in vivo metabolism of 13-HODE and other oxylipin lipid mediators with tracers provides opportunities to understand metabolic and dietary factors regulating their concentration and bioactivity *in vivo*.

Acknowledgements/grant Support

This work was supported by the USDA National Institute of Food and Agriculture, Hatch/Taha (project #1008787) and the Eunice Kennedy Shriver National Institute of Child Health and Human Development [grant number R21-HD095391-01A1). ZZ is a recipient of the Henry A.

Jastro Research Award and MH is a recipient of the Graduate Women in Science Nell Mondy Fellowship.

Chapter 5 (Aim 4): Linoleic acid enters rat brain and rapidly metabolizes into short-lived oxidized linoleic acid metabolites

Zhichao Zhang [1], Marie Hennebelle [1,a], Theresa L. Pederson [1,2], John W. Newman [2,3,4], and Ameer Y. Taha [1,4]

[1] Department of Food Science and Technology, College of Agriculture and Environmental Sciences, University of California, Davis, CA, USA;

[2] Obesity and Metabolism Research Unit, USDA, ARS, Western Human Nutrition Research Center, Davis, CA, USA;

[3] Department of Nutrition, College of Agriculture and Environmental Sciences, University of California, Davis, CA, USA;

[4] West Coast Metabolomics Center, University of California, Davis

[a] Current address: Laboratory of Food Chemistry, Wageningen University and Research, Bornse Weilanden 9, 6708 WG Wageningen, the Netherlands.

Abstract:

Dietary linoleic acid (LNA) is precursor to bioactive oxidized linoleic acid metabolites (OXLAMs) known to concentrate in the brain. Although plasma LNA passively diffuses across the blood brain barrier, very little LNA accumulates in the brain (<2% of total fatty acids). This study tested the hypothesis that increasing dietary LNA will increase the incorporation of plasma LNA into the brain, and conversion into OXLAMs. Male rats were fed a low (0.4% energy), moderate (5.2% energy) or high (10.4% energy) LNA diet for 15-18 weeks. ^{13}C-LNA was intravenously infused into the femoral vein and brain LNA incorporation and conversion to OXLAMs was measured. D5-alpha-linolenic acid (d5-ALA) was also co-infused to test whether changes in dietary LNA target LNA metabolism specifically or other polyunsaturated fatty acids. We observed that up to 5% of LNA entering the brain was converted to OXLAMs. Increasing dietary LNA significantly increased the incorporation coefficient, incorporation rate and turnover of ^{13}C-LNA in phospholipids without altering the rate of conversion to OXLAMs. D5-ALA conversion coefficient was significantly lower in the moderate LNA group compared to the low LNA group, although the net incorporation rate and turnover did not change. Our findings indicate that increasing dietary LNA selectively increases brain LNA metabolism (i.e. net incorporation and turnover) in phospholipids without altering conversion to OXLAMs. Further studies are needed to elucidate the turnover pathways that become upregulated when brain incorporation of LNA is increased.

1. Introduction:

Linoleic acid (LNA) is an essential polyunsaturated fatty acid (PUFA) that is currently consumed in excess relative to the minimum recommended requirements of 0.5% to 2% of daily calories in rats or human (Bourre et al., 1989; Bourre, Piciotti, Dumont, Pascal, & Durand, 1990; Hansen et al., 1958). LNA is critical for maintaining skin barrier properties and for supporting normal growth and development (Hansen et al., 1958). In the United States, LNA intake accounts for approximately 7% of daily calories, owing to the widespread use of soybean oil in food processing and cooking (Blasbalg et al., 2011a; Raatz, Conrad, & Jahns, 2018).

LNA is bioactive and involved in multiple signaling pathways in the brain. Elevated intake of LNA has been shown to exacerbate inflammatory signaling pathways in rodent brain, and to correlate with migraine frequency in humans, suggesting an important signaling role of this PUFA in the brain (Ramsden et al., 2013; Taha et al., 2017). Hennebelle et al. reported that LNA is involved in neurotransmission (Hennebelle et al., 2017), consistent with evidence of anti-epileptic effects in rats (Ekici, Gurol, & Ates, 2014).

Unlike peripheral issues, there is little LNA in the rodent brain (<2% of total fatty acids) compared to other more-abundant PUFAs such as arachidonic acid (ARA) and docosahexaenoic acid (DHA), which constitute 10-15% of total fatty acids (McNamara & Carlson, 2006). However, LNA is known to enter the brain at comparable rates to ARA and DHA (Chen et al., 2008). While the majority of ARA and DHA readily incorporate and accumulate in brain phospholipids, LNA is mostly β-oxidized (~59%) into polar metabolites. A small percentage of the LNA that enters the brain (~ 12%) is incorporated into esterified lipid pools or used for ARA synthesis (0.2%) (J. C. Demar, Jr., Ma, Chang, Bell, & Rapoport, 2005; J. C. DeMar et al., 2006).

One metabolic pathway that has been overlooked in the brain, is the conversion of LNA into oxidized linoleic acid metabolites (OXLAMs). In peripheral tissues, LNA can be converted into OXLAMs via non-enzymatic or enzymatic pathways via lipoxygenase (LOX), cyclooxygenase (COX), cytochrome P450 (CYP450), and soluble epoxide hydrolase (sEH) enzymes (Breder, Dewitt, & Kraig, 1995; Chinnici, Yao, & Pratico, 2007; Sarkar, Narayanan, & Harder, 2011; Sura, Sura, EnayetAllah, & Grant, 2008; van Leyen et al., 2006). These enzymes are also present in the brain and might contribute to the rapid utilization of LNA entering the brain from plasma.

In adult rats, OXLAMs account for 5-7% of total oxidized fatty acids (i.e. oxylipins) in the brain (Ferdouse et al., 2019; Hennebelle et al., 2020), but it is not known whether they are formed de novo from LNA or obtained directly from diets high in OXLAMs. A recent study reported that labeled 13-hydroxyoctadecadienoic acid (13-HODE), an OXLAM abundant in dietary oils, does not enter the rat brain (Z. Zhang et al., 2021), suggesting that dietary LNA and subsequent conversion to OXLAMs in the brain is the likely mechanism by which the brain derives its OXLAMs. This is corroborated by data showing that increasing dietary LNA levels, increased rat brain OXLAM concentrations (Taha et al., 2018a), while feeding mice a diet enriched with OXLAMs did not alter brain OXLAM concentrations (Ramsden et al., 2018a).

The present study investigated the fate of intravenously infused uniform ^{13}C-LNA in rat brain. Rats were fed a low, moderate or high LNA diet to test whether increasing dietary LNA 1) increases brain uptake of LNA, and 2) conversion to OXLAMs. Omega-3 d5-alpha-linolenic acid (ALA) was also co-infused to test whether dietary LNA affects the metabolism of omega-3 PUFAs, in view of the fact that both LNA and ALA share the same enzymatic pathways of desaturation/elongation and oxidation (Sanders & Rana, 1987) and therefore excess intake of

LNA may dampen the metabolism of ALA (Taha et al., 2018b). We hypothesized that increasing dietary LNA will increase brain incorporation and metabolism of LNA and reduce the metabolism of ALA.

2. Material and Method:

2.1 Animal Protocol:

All animal protocols were approved by Animal Care and Use Committee at the Eunice Kennedy Schriver National Institute of Child Health and Human Development. The protocol followed the National Institutes of Health Guide for the Care and Use of Laboratory Animals (NIH Publication No. 80-23).

Male Fischer-344 (CDF) rats aged 18-21 days old were weaned from their surrogate mothers (Charles River Laboratories, Portage, MI, USA) upon arrival at a temperature and humidity controlled animal facility, and placed on a 12-hour light/dark cycle. Rats were randomized into three dietary groups (n=8 per each group): low LNA, medium LNA and high LNA groups and fed for 15 weeks. All three isocaloric diets were manufactured by Dyets Inc. (Bethlehem, PA, USA), and contained 60% carbohydrate, 20% protein, 10% fat, and 10% vitamins and minerals. LNA accounted for 0.4%, 5.2%, and 10.5% of energy for low, moderate, and high LNA diets, respectively as detailed elsewhere (Taha et al., 2018b). ALA composition was fixed at 0.9% energy in the three diets (Taha et al., 2018b).

Between 15 to 18 weeks of age, rats from each of the three dietary groups were anesthetized with isoflurane (5% for induction and 2-3% for maintenance), and infused with 3 µmol/100 g body weight of ^{13}C uniformly labelled LNA (Cambridge Isotope Laboratories, CIL, Tewksbury, MA, USA) and deuterium labeled α-linoleic acid (d5-ALA; CIL) dissolved in 50

mg/mL fatty acid-free bovine serum albumin (BSA) in phosphate saline buffer (PBS), at a rate of 0.4-0.2 mL/h for 2 h. 200 µL of plasma were collected before infusion (baseline), and at 1, 2, 3, 5, 8, 10, 20, 30, 60, 90, and 120 min during infusion. One rat from low LNA group, which was subjected to the same surgical procedures and infused with vehicle, served as a negative control. Plasma from the negative control rat was sampled as described above. Due to animal death during surgeries, the final sample size was n=6 for the low LNA, n=5 for moderate LNA, and n=4 for high LNA groups.

All rats were sacrificed by head-focused microwave irradiation (5.5 kW; Cober Electronics Inc., Norwalk, CT, USA) for 3.4 s followed by 1.4 s. The head was decapitated on dry ice and the rest of the body was subjected to microwave-irradiation for 4.8 s. Brains were dissected, flash-frozen in liquid nitrogen and transferred to a −80 °C freezer until extraction. Liver and heart were also dissected and stored in −80 °C for future analysis

2.2 Plasma labeled and unlabeled unesterified fatty Acid analysis:

To measure tracer fatty acid concentration in plasma, 50 µL of ice-thawed plasma was spiked with 50 µL of 0.157 nmol/µL of unesterified heptadecanoic acid (17:0) as an internal standard and extracted with 3 mL of 2:1 v/v chloroform (Cat No. C607-4, Fisher Scientific, Hampton, NH, USA)/methanol (Cat No. A454-4, Fisher Scientific, Hampton, NH, USA) and 0.75 mL of 0.9% KCl. Samples were centrifuged and the lower chloroform phase transferred to a new test-tube. The remaining plasma was re-extracted with 2 mL of chloroform, centrifuged and the extracts were pooled, dried under nitrogen and reconstituted in 100 µL chloroform/methanol. The extracts were separated alongside authentic identification standards on silica thin layer chromatography (TLC) plates (Whatman, Clifton, NJ, USA) using heptane: diethylether: glacial acetic acid (60:40:3 by volume) as a solvent. The unesterified fatty acid band was scraped and

transferred to 8mL Kimble Screw Thread Culture Tubes (100 x 13mm, Thomas Scientific, Cat # 9215D32). Fatty acids were extracted from the silica using the folch method as described above for plasma, and the extracts were dried under nitrogen and derivatized with 100 µL pentafluorobenzyl bromide (Sigma-Aldrich, Cat # 101052-1G): diisopropylethylamine (Sigma-Aldrich, Cat # 387649-100ML): acetonitrile (Fischer Scientific, Cat# A9561) (v/v/v: 10/100/1000; PFB) mixture by shaking for 15 min at room temperature. The samples were reconstituted in 100 µL hexane prior to GC-MS analysis.

The same fatty acid extraction and TLC procedure was performed for samples collected at baseline to measure unlabeled free fatty acids. The scraped unesterified fatty acid bands were derivitized in 1% H_2SO_4 for 3 hours at 70 °C and analyzed by GC-flame ionization detection (FID).

2.3 Brain labeled and unlabeled fatty acid analysis:

2.3.1 Folch extraction

Total lipids were extracted from the left brain hemisphere (~500-800 mg) with the Folch method (Folch, Lees, & Sloane Stanley, 1957). Half brain samples were weighed and transferred to 50 mL Falcon tube (Thomas Scientific, Santa Clara, USA, Cat # 2594G60) containing 50 µL 1% butylated hydroxytoluene (BHT, Sigma-Aldrich, St. Louis, MO, USA, Cat # W218405-SAMPLE-K) in methanol (Fisher Scientific, Hampton, NH, USA, Cat # A454-4) and 2 mL methanol. Samples were homogenized with a Polytron, and homogenates were transferred to clean glass tubes (Thomas Scientific, Cat # 9215D32). Residual homogenates were rinsed twice with 2 mL chloroform, and once with 1.5 mL 0.1 M NaCl (Sigma-Aldrich, S7653-250G) in Deionized (DI) water. Samples were vortexed and centrifuged for 10 min at 1,700 rpm on a Beckman Coulter Allegra 6 centrifuge (Beckman Coulter, Palo Alto, CA, USA.) using a GH3.8A

rotor. The bottom chloroform layer was transferred to new clean glass tubes. The remaining extract was washed with 4 mL chloroform, vortexed and centrifuging as described above. The bottom chloroform layer was combined with the first extract, dried under nitrogen, and reconstituted into 5 mL chloroform: methanol (v/v: 2/1). All samples were kept in a -80 °C freezer until further use.

2.3.2 Hydrolysis and PFB derivatization

A portion of the Folch extraction was hydrolyzed with sodium hydroxide (NaOH) prior to PFB derivitization for labeled fatty acid analysis. 50 µL of the Folch extract was spiked with 0.05 nmol 1, 2-diheptadecanoyl-sn-glycero-3-phosphocholine (C17:0 PC from Avanti Polar Lipids, Alabaster, AL, USA, Cat #850355C) as an internal standard and dried under nitrogen. 1 mL of 10% NaOH (Sigma-Aldrich, Cat # S5881-500G) in methanol was added and the samples were heated for 1 h at 70 °C. One mL HCl (37%, Sigma-Aldrich, Cat #320331) followed by 1 mL of water and 3 mL hexane (Fisher Scientific; Cat #H303-4) were added. The samples were then vortexed and centrifuged for 5 min at 1,700 rpm on a Beckman Coulter Allegra 6 centrifuge (Beckman Coulter, Palo Alto, CA, USA.) using a GH3.8A rotor. The top hexane layer was transferred to new glass tubes. Another 3 mL of hexane was added to the remaining bottom layer. The samples were vortexed and centrifuged as described above and the top hexane layer was combined with the first hexane extract. All samples were kept at -80 °C until they were derivatized in PFB.

Hexane hydrolyzed extracts were dried under nitrogen and reconstituted in 100 µL pentafluorobenzyl bromide (Sigma-Aldrich, Cat # 101052-1G): diisopropylethylamine (Sigma-Aldrich, Cat # 387649-100ML): acetonitrile (Fischer Scientific, Cat# A9561) (v/v/v: 10/100/1000; PFB mixture). The samples were shaken for 15 min at room temperature, dried

under nitrogen, reconstituted in 900 µL hexane and vortexed. They were transferred to a new 2mL centrifuge tube containing 450 µL of water, vortexed, centrifuged for 2 min at 13,000 rpm on a 5430r Eppendorf micro-centrifuge containing a FA-45-24-11 rotor (Fisher Scientific, Pittsburgh, PA). The top hexane layer was extracted, dried under nitrogen and reconstituted in 100 µL hexane for GC-MS analysis.

2.3.3 Unlabeled fatty acid transesterification

Fatty acids in total lipids (TL) were measured in 100 µL of Folch extract spiked with 125 nmol 17:0 PC was. The spiked extract was dried under nitrogen and reconstituted in 400 µL toluene. Three mL methanol and 600 µL of 3% HCl (37M) in methanol (v/v) were added and the samples were vortexed. The 3% methanolic HCl solution was prepared freshly by diluting 37% HCl solution in methanol (8:92, v: v). The samples were heated at 90 °C for 60 min, to catalyze the transesterification of fatty acids. After cooling, 1 mL DI water and 1 mL of hexane were added. The samples were vortexed and left at room temperature for 15 min to allow phase separation. The hexane layer containing the fatty acid methyl esters (FAMEs) was transferred to a microcentrifuge tube (USA Scientific, Cat # 1620-2700) containing 450 µL deionized water and centrifuged at 13,000 rpm for 2 min at 4 °C (5430R Eppendorf micro-centrifuge with FA-45-24-11 rotor, Fisher Scientific, Waltham MA). After centrifuging, the hexane layer was transferred to a new microcentrifuge tube, evaporated under nitrogen, and reconstituted in 100 µL hexane for GC-FID analysis.

2.4 Phospholipid (PL), Triacylglycerol (TAG), Cholesteryl Ester (CE) and Free Fatty Acid (FFA) Separation

The Folch extract (from step 2.3.1) was subjected to TLC to fractionate PL, TAG, FFA and CE species in brain. TLC silica plates (Thomas Scientific, Cat # 2737B25) were washed with

chloroform: methanol (v/v: 2/1) and activated in an oven maintained at 80 °C under vacuum for at least 1 hour. 200 µL of Folch extract was spiked with 50 µL of 17:0 PC (0.38 µg/mL) and 50 µL of unesterified heptadecanoic acid (0.27 µg/mL 17:0 FFA; Nu-Chek Prep; Cat #N-17-A), dried under nitrogen and reconstituted in 100 µL of chloroform/methanol (2:1). The entire 100 µL extract was plated on pre-washed TLC plates. The test-tube were rinsed with 100 µL chloroform: methanol (v/v: 2/1) to remove remaining lipids, which were re-plated on top of the first band. The TLC plates were placed in a TLC tank containing heptane (Fisher Scientific, Cat #H350SK-4): diethyl ether (Fisher Scientific, Cat #615080010): acetic acid (v/v/v: 60/40/3). The plate was sprayed with 0.02% 2', 7'-dichlorofluoroscein (Sigma-Aldrich, Cat # D6665-5G) in methanol and the bands were revealed under UV light. PL, FFA, TAG, and CE bands were identified and scraped. Fifty µL of 0.38 µg/mL 17:0 PC (around 0.05 nmol) were added to each of the scraped CE and TG bands (standards for PL and FFA were added to the Folch extract as described above). All samples were hydrolyzed and derivatized to PFB esters for labelled fatty acid analysis by GC-MS as described in Section 2.3.2. After derivatization, PL and FFA fractions were reconstituted in 100 µL hexane whereas TG and CE fractions were reconstituted in 50 µL hexane prior GC-MS analysis.

The TLC process was repeated on a parallel set of extracts, and bands were directly trans-esterified to FAMEs as described in Section 2.3.3 for unlabeled fatty acid analysis by GC-FID.

2.5 Phospholipid class Separation

Phospholipid class separation was achieved by plating 100 µL of Folch extract on silica TLC plates pre-washed in chloroform/methanol (2:1 v/v) and dried under heat (80 °C) and vacuum for at least one hour. Phospholipids were resolved in chloroform: methanol: water: acetic acid (Sigma-Aldrich, Cat # 695092), (v/v/v/v: 60/50/4/1), yielding sphingomyelin (SM),

phosphatidylcholine (PC), phosphatidylserine (PS), phosphatidylinositol (PI) and phosphatidylethanolamine (PE). The plates were sprayed with 0.02% 2', 7'-dichlorofluoroscein and the scraped bands were visualized under UV light. 50 µL of 17:0 PC 0.38 µg/mL (around 0.05 nmol) was added to each phospholipid fraction. Phospholipids were hydrolyzed in 10% NaOH and derivatized to PFB esters as described above prior to GC-MS analysis.

The TLC was repeated, and the scraped phospholipid bands were transesterified to produce FAMEs. All samples were reconstituted into 50 µL hexane and analyzed by GC-MS analysis (see below). GC-MS was used instead of GC-FID to measure LNA, because it is a minor fatty acid in most phospholipid fractions (J. C. DeMar et al., 2006); GC-MS ensures greater sensitivity compared to GC-FID.

2.6 Brain Oxylipin Extraction:

2.6.1 Total oxylipin (esterified +free) extraction

The right brain half was weighed (around 700 mg) and spiked with 10 µL of 500 nM surrogate standard mixture containing d11-11(12)-EpETrE (Cayman Chemical, Ann Arbor, MI, USA; Cat # 10006413), d11-14,15-DiHETrE (Cayman Chemical, Cat # 1008040), d4-6-keto-PGF1α (Cayman Chemical, Cat # 315210), d4-9-HODE (Cayman Chemical, Cat # 338410), d4-LTB4 (Cayman Chemical, Cat # 320110), d4-PGE2 (Cayman Chemical, Cat # 314010), d4-TXB2 (Cayman Chemical, Cat # 319030), d6-20-HETE (Cayman Chemical, Cat # 390030) and d8-5-HETE (Cayman Chemical, Cat # 334230). To each sample, 10 µL of antioxidant mix and 800 µL extraction solvent containing 0.1% acetic acid and 0.1% BHT in methanol were added. The antioxidant mix contained 0.2 mg/ml BHT, ethylenediaminetetraacetic acid (EDTA, Sigma-Aldrich, Cat # EDS-100G) and triphenylphosphine (TPP, Sigma-Aldrich, Cat # 3T84409) in

methanol/water (50:50, v/v) and filtered through 0.45 µm Millipore filter (Millipore, Bedford, MA, USA, Cat # SLHVM25NS).

The samples were pre-cooled in a -80 °C freezer for at least 30 min, and homogenized with a bead homogenizer (Next Advance, Troy, NY 12180, USA, Cat # BBY24M Bullet Blender Storm) for 4 min at power setting 10. The homogenized samples were vortexed and centrifuged at 15,000 x g on an Eppendorf 5424R centrifuge at 0 °C for 15 min. The supernatant layer was transferred to a new tube and placed in a -80 °C freezer for at least 30 min.

Four hundred µL of brain extract was mixed with 400 µL 0.25M sodium carbonate (Sigma-Aldrich, Cat # 791768-500G) in methanol/water (50:50, v/v) and heated at 60 °C for 30 min to catalyze the hydrolysis of bound oxylipins. The samples were then cooled to room temperature for approximately five minutes, followed by the addition of 50 µL of acetic acid, and the pH was verified to be between 4 and 6 using litmus paper. Milli-Q water (3150 µl) was added, and the samples were vortexed.

Oasis HLB (60 mg) columns (Waters Corporation, Cat # WAT094226) were used to separate free oxylipin generated after base hydrolysis. The columns were cleaned with one column volume of ethyl acetate (Fisher Scientific, Cat # E196-4) followed by two column volumes of methanol, and conditioned with two column volumes of SPE buffer (0.1% acetic acid, 5% methanol in Milli-Q water). Samples were loaded onto the SPE cartridge, washed with two column volumes of SPE buffer and dried under vacuum for 20 min. Oxylipins were eluted with 0.5 mL methanol followed by 1.5 mL ethyl acetate. The samples were dried under nitrogen, reconstituted in 100 µL of cold methanol containing 100 nM of CUDA/PHAV as internal standards, and filtered on 0.2-micron filter units (Ultrafree-MC VV Centrifugal filters, Burlington, MA, USA, Cat # UFC30VV00) by centrifuging at 15 000 x g for 20 min at 0 °C.

2.6.2 Free oxylipin extraction

Free oxylipins were extracted by mixing 3600 µL Milli-Q water with 400 µL of the remaining brain supernatant, after spiking with 10 uL surrogate standard and antioxidant mix respectively. The SPE was performed as described in previous section.

2.7 GC-MS Analysis:

2.7.1 Quantification of labelled PFB fatty acid esters

Derivatized fatty acid PFB esters were quantified by GC-MS (Perkin Elmer Clarus System, Perkin Elmer, Shelton, CT, USA) against a six-point calibration curve using select ion mode monitoring in chemical ionization (CI) mode. Methane was used as the reagent gas at temperature of 300 ºC. The GC was equipped with a DB-5MS capillary column (30 m long, 0.25 mm wide with film width of 0.25 µm; Agilent Technologies, Santa Clara, CA, USA). The injector temperature was set at 240 ºC. The oven temperature started at 80 ºC, held for 2 min, increased by 20 ºC/min to 185 ºC, increased by 10 ºC/ min to 240 ºC, and held for 30 min at 240 ºC. The injection volume was 1 µL. The total run time was 42.75 min.

2.7.2 Quantification of unlabeled phospholipid fatty acids:--FAMEs

Derivatized fatty acid methyl esters from brain phospholipids (SM, PC, PS, PI and PE) were quantified by GC-MS using electron impact (EI) ionization against a six-point calibration curve. Samples were separated on a DB-225ms column (30m x 0.25mm, 0.25 µm) in a 6890-gas chromatogram interfaced with a 5973A mass selective detector (Agilent Technologies, Santa Clara, CA, USA). Calibrants and internal standards were purchased from Nu-chek Prep (Elysian, MN, USA) and Avanti Polar Lipids Inc, and derivatized as described above in the derivatization section. Data were acquired with Chemstation v E.02 and processed with Mass Hunter v. 3.2. A

detailed GC-MS method was described previously (Grapov, Adams, Pedersen, Garvey, & Newman, 2012).

2.8 UPLC-MS/MS Analysis:

Isotopically enriched oxylipins (with ^{13}C) were quantified against authentic calibration standards by electrospray ionization UPLC-MS/MS as previously described (Agrawal et al., 2017). Oxylipins were separated on a BEH column (2.1 x 150 mm, 0.17µm; Waters Incorporation) and detected on an API 6500 QTRAP (Sciex; Redwood City, CA, USA) with electrospray ionization in positive/negative mode switching and multi-reaction monitoring. Oxylipins were quantified against 7-9 -point calibration curves. Calibrants and internal standards were either synthesized [CUDA, PUHA] or purchased from Cayman Chemical (Ann Arbor, MI), Medical Isotopes (Pelham, NH), Avanti Polar Lipids Inc. (Alabaster, AL), or Larodan Fine Lipids (Malmo, Sweden). Data were processed with AB Sciex MultiQuant v. 3.1.

2.9 GC-FID analysis of plasma unlabeled fatty acids

FAMEs from plasma unesterified fatty acids and brain total lipids, PL, TAG, FFA and CE fractions were measured with GC-FID as previously described (Taha et al., 2016).

2.10 Kinetics

Tracer incorporation into various lipid pools and OXLAMs was determined after subtracting background tracer levels in the rat that was not infused with the tracer. Multiple kinetic parameters were then calculated to determine the tracer incorporation coefficient, k^*, a marker of brain affinity to the tracer (Rapoport & Taha, 2014), the incorporation rate, of each PUFA into the brain, *Jin*, (i.e. amount that incorporates per unit time), the conversion rate of ^{13}C-

LNA into ^{13}C-OXLAMs, *J* conversion, the turnover of each tracer reflecting the rate at which endogenous pools are replaced, and the brain half-life of each tracer.

^{13}C-LNA incorporation coefficient, $k^*_{i,(LNA)}$ into the different brain lipid classes (e.g., TL, PL, TAG, CE, FFA, PI, PC, PS, PE and SM), was calculated as follows:

$k^*_{i,(LNA)}=\frac{C^*brain,i(LNA)(T)}{\int_0^T C^*plasma\ (LNA)dt}$, where $C^*$the labelled LNA concentration and *t* is time (min).

The conversion coefficient, (28), representing conversion of the incorporated C13-LNA to labelled OXLAMs, *j* (^{13}C-9-HODE or 9, 12, 13-TriHOME) in the free or total oxylipin pool, *i*, was calculated as follows:

$k^*_{i,(LNA\rightarrow j)}=\frac{C^*brain,i(j)(T)}{\int_0^T C^*plasma\ (LNA)dt}$

The rate of incorporation of unlabeled unesterified LNA from plasma into lipid class, *d*, $J_{in,d(LNA)}$, and rate of conversion of the incorporated LNA *j* into labelled OXLAMs (*i)*, $J_{OXLAM,i(LNA->j)}$ (nmol*g^{-1}*min^{-1}×10^{-5}), were determined as follows:

$J_{in,d\ (LNA)} = k^*_{d,(LNA)} \times C_{plasma(LNA)}$

$J_{in,i\ (LNA\rightarrow j)} = k^*_{i,(LNA\rightarrow j)} \times C_{plasma(LNA)}$

Turnover, representing the rate at which the label replaces endogenous pools was calculated as follows:

$F_{d,\ LNA}=J_{in,i\ (LNA)}/C_{brain,\ d(\ total\ LNA)}$

The half-life, $t_{1/2}$ was derived from the turnover as follows: 0.693/ $F_{d,\ LNA}$

The dilution factor, λ , represents the net efflux of LA entering brain from plasma, was determined by dividing the ratio of labeled to unlabeled OXLAM in brain to that of plasma unesterified labeled and unlabeled LNA;

Dilution factor, $\lambda = \frac{C^*_{brain(\,free\,OXLAM)} / C_{brain(\,free\,OXLAM)}}{C^*_{plasma(LNA)} / C_{plasma(LNA)}}$

The dilution factor was then used to estimate the rate of OXLAM incorporation into various lipid pools (e.g. PLs) as follows:

$J_{OXLAM,i(LNA->j)} = J_{in,i(LNA->j)} / \lambda$

OXLAM turnover within specific lipid pools was calculated as follows:

$F_{OXLAM} = J_{in,i\ (LNA \rightarrow j)} / C_{brain,\ j(\ total,\ j)}$

The half-life, $t_{1/2}$ was estimated using this equation: $0.693 / F_{OXLAM}$

Similar kinetic equations were applied for d5-ALA, but its derived oxylipins were not detected, and conversion equations were not used.

$k^*_{i,(ALA)} = \frac{C^*brain,i(ALA)(T)}{\int_0^T C^*plasma\ (ALA)dt}$, where $C^*$the labelled ALA concentration, and t is is time (min).

The rate of incorporation of unlabeled unesterified LNA from plasma into lipid class, *d*, $J_{in,d(LNA)}$, is $J_{in,d\ (ALA)} = k^*_{d,(ALA)} \times C_{plasma(ALA)}$

Turnover and half-life were calculated as: $F_{d,\ LNA} = J_{in,i\ (LNA)} / C_{brain,\ d(\ total\ ALA)}$;

$t_{1/2} = 0.693 / F_{d,\ ALA}$

2.11 Statistical Analysis:

Normality and homogeneity were verified on all data by Shapiro-Wilk test and Brown-Forsythe test respectively. Since most of the data fulfilled both assumptions, one-way ANOVA followed by Tukey's multiple comparison test were used. Data are expressed as mean ± standard deviation (SD). Statistical analysis was performed using GraphPad Prism v. 8 (La Jolla, CA, USA)

3 Results:

Increasing dietary LNA composition increased the concentration of LNA in TL and PL, but not FFA. As shown in **Table 9**, LNA concentration in TL was significantly higher in the moderate and high LNA groups compared to the low LNA group by 2.3 and 2.7 fold, respectively ($P>0.05$). LNA concentration in the high LNA group was significantly higher compared to the moderate LNA group. PL-bound LNA concentrations followed a similar pattern to TL, except that differences between the moderate and high LNA groups were not significant.

ALA concentrations did not differ significantly between the groups, although ALA was detected in the FFA fraction of the low LNA group but not the moderate or high LNA groups (**Table 9**). ALA was not detected in the TAG and CE fractions

Labeled ^{13}C-LNA concentration in TL, PL and FFA was not significantly different between the groups (**Table 10**). However, labeled d5-ALA was significantly lower by 2-fold in PL of the high LNA dietary group compared to the low LNA dietary group (**Table 10**). It did not change in other lipid compartments (TL and FFA; **Table 10**).

Table 11 shows the kinetics of class specific PL, FFA, PL, and TL of LA and ALA entering brain. The incorporation coefficient, k^*, for ^{13}C-LNA, was significantly higher in TL and PL of rats on the high LNA diet compared to low LNA controls. These changes were reflected in PE phospholipids, but not other sub-fractions (PC, PS, PI and FFA).

The incorporation rate, *Jin*, for ^{13}C-LNA was significantly higher in rats on the high LNA diet compared to rats on the low LNA diet for all lipid fractions (TL, PL, FFA) and most phospholipid fractions (PC, PI and PE). This corresponded to a significantly higher ^{13}C-LNA, turnover within TL and PL, in the high versus low LNA group. ^{13}C-LNA half-life in PL was

significantly shorter in rats on the high (0.3 ms) and moderate LNA diet (1.0 ms) compared to rats on the low LA diet (7 ms).

The incorporation coefficient, k*, for d5-ALA was 5.3 and 2.7-fold lower in brain PL of the moderate and high LNA groups compared to the low LNA group; however statistical significance was only observed between the moderate and low LNA group (**Table 11**). No other changes in brain d5-ALA kinetics (including *Jin*, *F* and half-life) were observed between the groups.

Only two ^{13}C labelled OXLAMs - 9-HODE and 9, 12, 13-TriHOME were detected in the free and total oxylipin fractions. Their concentrations ranged from 0.019-0.667 pmol/g in the free pool and 0.016 to 0.099 pmol/g in the total oxylipin pool, and did not differ significantly between the groups (**Table 10**). The similarity in concentrations between free and total labeled OXLAMs indicates that the majority of the label was in the free from. Unlabeled 9-HODE and 9, 12, 13-TriHOME concentrations also did not differ significantly between the group and the majority were found in the free pool (~3 pmol/g to 4 pmol/g in free versus total for 9-HODE and ~0.7 pmol/g to 1.1 pmol/g in free vs total for 9, 12, 13-TriHOME; **Supplementary Table 9**). No d5-ALA metabolites were detected.

Table 11 shows the kinetics of brain OXLAM metabolism. As shown, there were no significant differences between the groups in ^{13}C-9-HODE and ^{13}C-9, 12, 13-TriHOME conversion coefficient, conversion rate, or turnover from ^{13}C-LNA. OXLAM conversion half-lives from ^{13}C-LNA were 0.1 and 0.001ms for 9-HODE and 9, 12, 13-TriHOME, respectively, and did not differ significantly between the groups.

The conversion rate of ^{13}C-LNA into ^{13}C-9-HODE and ^{13}C-9, 12, 13-TriHOME was divided by the rate of ^{13}C-LNA incorporation into the brain in TLs, to estimate net brain %

conversion of ^{13}C-LNA into labeled OXLAMs in each of the dietary groups. Approximately 4%, 0.2% and 0.06% of ^{13}C-LNA incorporated in brain was converted to ^{13}C-9-HODE in the low, moderate and high LNA dietary groups, respectively. Only 1%, 0.04% and 0.01% of ^{13}C-LNA was converted to ^{13}C-9, 12, 13-TriHOME in the low, moderate and high LNA groups, respectively. The low percent conversion into OXLAMs observed in the high LNA group is due to more LNA entering the brain, rather than less LNA being converted to OXLAMs per se. The percent conversion of ^{13}C-9-HODE to ^{13}C-9, 12, 13-TriHOME (based on the dividend of the incorporation rate of product to precursor) was 24%, 24% and 17% in the low, moderate and high LNA groups, respectively.

Figure 10 summarizes the percent of LNA that was converted into OXLAMs in the context of known pathways of brain LNA metabolism in rats on the moderate LNA diet based on this and prior studies that used a similar diet to measure brain LNA metabolism (J. C. DeMar et al., 2006). As previously reported, the majority (59%) of LNA entering the brain is β-oxidized, 9 % is incorporated into PLs, 2% is incorporated into TAGs and <1% is elongated-desaturated into arachidonic acid (ARA) (J. C. DeMar et al., 2006). Based on the current study, 0.2% and 0.04% of LNA entering the brain is converted into OXLAMs in rats on the moderate LNA and high diet. Notably, up to 5% of LNA entering the brain can be diverted towards OXLAM synthesis, particularly when dietary LNA is low.

Figures 11 to 13 show the percent distribution of labeled and unlabeled LNA and LNA within the various PL classes, respectively, across the three dietary groups (i.e. % of each PL subclass of total PLs). As shown, the majority of labeled and unlabeled LNA were found in PC (46%-70%), followed by PE (10%-49%), PS (4%-13%) ad PI (not detected to 24%). Both labeled and unlabeled ALA were observed to be more abundant in PC (28% to 72%) followed by

PE (22% to 54%), PS (1% to 22%) and PI (not detected to 7%). There were no differences in tracer or unlabeled fatty acid percent abundance between the groups. These data are in general agreement with the incorporation rates, *Jin*, presented in **Table 11**. Tracers were not detected in CE and TAG fractions and were very low in FFA fractions (around 0.0003 nmol/g for ^{13}C-LNA and 0.0002 nmol/g for d5-ALA).

Discussion:

This study demonstrated that 1) increasing dietary LNA increased the incorporation and turnover of circulating ^{13}C-LNA into brain TL, PL and PL sub fractions, and 2) that up to 5% of LNA entering the brain is converted into OXLAMs (specifically 9-HODE and its downstream metabolite, 9, 12, 13-TriHOME). Brain ALA metabolism was generally unaffected by dietary LNA, except for the 3-5-fold reduction in brain k* within PL in the moderate and high LNA groups compared to the low LNA group.

Previously, we reported that labeled d4-13-HODE does not incorporate into the brain following intravenous injection or gavage (Z. Zhang et al., 2021), which suggested that other pathways are involved in generating OXLAMs in the brain (Ferdouse et al., 2019; Taha et al., 2018a). Our study indicates that LNA conversion into OXLAMs is the main mechanism by which the brain regulates endogenous OXLAM levels.

It has been assumed that 9-HODE is the precursor to 9, 12, 13-TriHOME, although evidence of conversion in vivo has not been established. To our knowledge, this is the first study to show that 9-HODE is converted to 9, 12, 13-TriHOME in rat brain. Prior studies have shown that this conversion occurs by auto-oxidation in flour dough (Graveland, 1973). However, the rapid turnover of these OXLAMs in rat brain (order of ms) suggests that enzymatic epoxidation

of 9-HODE via cytochrome P450 and subsequent hydroxylation by soluble epoxide hydrolase is a likely mechanism, since auto-oxidation occurs at much slower rates (in the order of hours to days) (Shen et al., 2021).

Increasing dietary LNA from 0.4% to 10.4% of energy increased the incorporation rate and turnover of circulating LNA within multiple brain lipid pools, particularly PL. Concurrently, brain LNA half-life was reduced, suggesting increased brain LNA utilization with increasing dietary LNA levels. It is not known which metabolic pathways shown in **Figure 10** (J. C. DeMar et al., 2006) are upregulated due to increasing dietary LNA, since this study mainly focused on the conversion of LNA into OXLAMs, which was not different between the three dietary groups. Future studies are needed to resolve the brain metabolic pathways that are altered following excess dietary LNA intake.

Brain ^{13}C-LNA conversion and turnover into ^{13}C-9-HODE and ^{13}C-9, 12, 13-TriHOME did not change with increasing dietary LNA. Either this pathway is insensitive to brain LNA turnover, or the half-life of these OXLAMs is too short (0.1-1 ms across all diets) to see a significant difference with the current sample size (4-6 rats per group). Notably, the short half-life of OXLAMs was 300-6500 times lower than the half-life of LNA itself across the three diets (0.3 to 6.5 ms), which explains why their concentration in the brain is very low (pmol/g levels) compared to that of LNA (nmol/g levels). A longer tracer infusion period or a more sensitive technique for measuring labelled OXLAMs (e.g., with atomic mass spectrometry) could lead to less variability and more accurate half-life estimates.

Previously, we reported that increasing dietary LNA levels increased rat cerebral cortex unesterified 9-HODE and 9, 12, 13-TriHOME concentrations in the high LNA group compared to the low LNA group (Taha et al., 2018a). We did not observe these changes in the present

study (**Table 9**), likely due to differences in the brain regions analyzed (cerebral cortex in our prior study versus whole brain) and the fact that the brains were subjected to high-energy microwave fixation in this study (versus CO_2 asphyxiation in the prior study) (Taha et al., 2018a). Microwave-irradiation is known to stop postmortem changes in brain oxylipin concentrations (M. Hennebelle, A. H. Metherel, et al., 2019), which is why 9-HODE and 9, 12, 13-TriHOME concentrations in this study were 4-10 times lower than previously reported (Taha et al., 2018a). This emphasizes the need to use high-energy microwave irradiation to prevent ischemia-induced differences between the groups.

PL k^* and J_{in} for LNA was 100-10,000 times higher than conversion rates to OXLAMs, suggesting that upon entering the brain, LNA is preferentially esterified into PL than oxidized (**Table 11**). This is further supported by the thousand-fold higher LNA concentration compared to OXLAM concentrations. Although OXLAMs are not as abundant in the brain as their precursor fatty acid, some are known to be highly bioactive. For instance, 13-HODE was previously shown to increase paired pulse facilitation in rat hippocampus, and to increase axonal length in pup neuron-glia co-cultures (Hennebelle et al., 2020; Hennebelle et al., 2017).

Notably, LA in some of the PL classes was not detected due to the low sensitivity of the methods used. This prevented us from establishing kinetic parameters (e.g. turnover and half-life) in some of the PL classes. Future refinement of the analytical method is needed to measure labeled LA in specific PL fractions such as PS.

TL concentration from the moderate LNA diet group was 667 nmol/g (**Table 10**), which is comparable to the 570 nmol/g reported in rats on a similar LNA diet (J. C. DeMar, Jr., Ma, Bell, & Rapoport, 2004). Also, the half-life of LNA in PL from this study was approximately 1

ms, consistent with the 1.65 ms calculated from the kinetic parameters published by DeMar et al. (J. C. Demar, Jr. et al., 2005).

D5-ALA-derived oxylipins were not detected in brain, likely because the incorporation rate of d5-ALA was at least 10-fold less than that of ^{13}C-LNA (**Table 11**). In rats, the incorporation rate of ALA into the brain was reported to be 4-fold lower than that of LNA (Chen et al., 2008), which is consistent with this study. Less ALA incorporated into the brain could be associated with less conversion into oxylipins compared to LNA. More sensitive methods are needed to establish whether ALA is converted into downstream oxidized fatty acids upon entering the brain.

Increasing dietary LNA decreased the incorporation coefficient, k^*, of d5-ALA into PL while increasing the k^* for ^{13}C-LNA. This suggests competing pathways for the incorporation of these two PUFAs into brain PL. Previously, Ramsden et al. reported that excess dietary LNA decreased brain DHA percent composition (Ramsden et al., 2018a). This could be because LNA decreases brain ALA incorporation and elongation-desaturation into DHA (despite being a minor pathway (Igarashi et al., 2007)), or because LNA directly interferes with the incorporation of DHA into the brain as reported by Igarashi et al. (Igarashi, Kim, Chang, Ma, & Rapoport, 2012)

A surprising finding of the present study is that ^{13}C-LNA incorporation coefficient, k^*, a marker of the brain's avidity towards circulating LNA, increased in brain TL and PL (major component of TL) as dietary LNA increased, suggesting a lack of negative feedback mechanisms to downregulate brain LNA uptake when dietary (and thus circulating) LNA increase. This is opposite to what has been observed for DHA incorporation into the brain. Taha et al. reported that increasing the supply of plasma DHA to the brain by increasing dietary ALA, decreases the incorporation coefficient of DHA, reflecting negative feedback mechanisms that decrease brain

DHA incorporation and turnover as supply from plasma increases (Taha et al., 2016). The lack of such regulatory mechanisms for LNA, if true for humans, reflects the absence of evolutionary pathways that control LNA incorporation into the brain, consistent with the fact that LNA was historically not abundant in human diets (Blasbalg et al., 2011a; Simopoulos, 1999)

Quantitatively, the incorporation coefficient k^* was much higher across the three diets diet (8 to 52 folds) for LNA than for ALA in all lipid pools analyzed, suggesting higher brain affinity for LNA than ALA. k^* for LNA increased and did not change for ALA when dietary LNA levels increased from 0.4 to 10.4% energy. The higher k^* values were consistent with the greater incorporation rate and turnover of LNA relative to ALA in brain lipid pools. As a result, the half-life of LNA was 4, 19 and 75-fold shorter than that of ALA in TL of rats on the low, moderate and high LNA diets, respectively (rapid turnover means shorter half-life). It is not clear as to why the biological affinity and turnover of LNA was higher than that of ALA; however, this may explain why we did not observe measurable ALA oxidized metabolites.

In summary, this study provides new evidence that LNA entering the brain is converted into short-lived OXLAMs, and that dietary LNA regulates brain LNA incorporation and turnover, but not conversion into OXLAMs. Understanding how this pathway is altered during development and aging might provide biological insights into the mechanisms of brain OXLAM regulation.

Funding:

This study was funded by the University of California Davis Start-up funds to AYT, and the USDA National Institute of Food and Agriculture, Hatch/Taha (project #1008787, A.Y.T.). Additional support was provided by the NIA Intramural Program.

Conflict of interests:

None.

Chapter 6 (study 5): Maternal pravastatin and calorie restriction increases brain lipids and epigenetic markers of soluble epoxide hydrolase in infant rhesus macaques

Zhichao Zhang[a], Benjamin I. Laufer[b], Yu Hasegawa[a], Casey E. Hogrefe[c], Amy Ryan[cd], Nuanyi Liang[a], Shiva Emami[a], Mari S. Golub[c], Judy A. Van de Water[f], Melissa Bauman[dfg], Janine M. LaSalle[b], Catherine VandeVoort[bh], Carolyn M. Slupksy[ai], Cheryl K. Walker[bh], Ameer Y. Taha[a].

[a] Department of Food Science and Technology, University of California-Davis, Davis, CA, USA

[b] Department of Medical Microbiology and Immunology, University of California-Davis, Sacramento, CA, USA

[c] California National Primate Research Center, University of California-Davis, Davis, CA, USA

[d] Department of Psychiatry and Behavioral Sciences, University of California-Davis, Sacramento CA USA

[e] Department of Internal Medicine, University of California-Davis, Davis, CA, USA

[f] Department of Internal Medicine, University of California-Davis, Sacramento, CA, USA

[g] The UC Davis MIND Institute, University of California-Davis, Sacramento, CA, USA

[h] Department of Obstetrics and Gynecology, University of California-Davis, Sacramento, CA, USA

[i] Department of Nutrition, University of California-Davis, Davis, CA, USA

Corresponding Author:

Dr. Ameer Y. Taha, ataha@ucdavis.edu. Department of Food Science and Technology, UC Davis, One Shields Avenue, Davis, CA 95616-5270

Abstract:

Maternal obesity is prevalent in the US and has been shown to be associated with adverse offspring neurodevelopment such as Autism Spectrum Disorder (ASD). Here, we investigated the effects of two interventions (pravastatin and calorie restriction) in obese Rhesus Macaques during gestation on their male offspring brain lipid metabolism. Brain cholesterol and fatty acid concentrations in the prefrontal cortex, amygdala, hippocampus, and hypothalamus were similar in offspring from obese, lean control and two obesity intervention groups. Oxylipin and epigenetic analysis revealed a pro-inflammatory profile in offspring prefrontal cortex as evidenced by significantly increased soluble epoxide hydrolase (sEH) signature in the offspring from the two treatment groups compared to the offspring from the obese control group. DHA derived resolving oxylipin, 17-HDoHE was significantly lower in calorie restriction group compared to concentration in obese group. Increased sEH has been associated with ASD-like behavior in rodents. Our results demonstrate potential adverse lipid metabolism altered by two gestational obesity interventions.

Introduction:

Approximately half of child-bearing aged women in the US are overweight or obese (Vahratian, 2009). Maternal obesity has been associated with increased risk of autism-spectrum disorder (ASD) and cognitive impairments in the offspring (Huang et al., 2014; Krakowiak et al., 2012; Pugh et al., 2016). The underlying mechanisms linking obesity to neurodevelopmental impairments are not known.

Obesity is associated with dysregulated lipid metabolism. In addition to the characteristic hyperlipidemia observed in plasma of obese individuals, recent studies have shown that obesity alters the regulation of linoleic acid (LA), an essential polyunsaturated fatty acid (PUFA) derived from the diet. Studies have reported a significant 11-69% increase in circulating LA in obese compared to lean female human subjects (Kang et al., 2017; Moushira Zaki 2020). LA is a precursor to oxidized linoleic acid metabolites (OXLAMs) known to regulate neurodevelopment in young rat pups (Hennebelle et al., 2020). It is not known whether maternal obesity disrupts OXLAM metabolism in the offspring.

Statins and calorie restriction have been proposed as interventions to reduce hyperlipidemia associated with maternal obesity (Costantine et al., 2016; Riu, Sunarno, Lukas, Wewengkang, & Amalia, 2020).Although statins are widely prescribed for obese patients who often have hyperlipidemia to reduce blood cholesterol and triglyceride levels (Branchi et al., 1999), they are not currently recommended for obese pregnant women (Zarek & Koren, 2014). Recent studies, however, have tested their efficacy in treating preeclampsia and results have been mixed (Costantine et al., 2016; Riu et al., 2020).

Several rodent studies have reported no adverse effects or a benefit to calorie restriction during pregnancy. For instance, a moderate 15% calorie restriction was shown to achieve an

optimal pregnant body weight at gestational day 20 without impacting pregnancy outcomes (Reynolds, Ho, & Taper, 1984). A 30% calorie-restricted diet during pregnancy did not compromise offspring male rat reproductive development, while improving fertility at puberty (Rocha, Bonkowski, Masternak, Franca, & Bartke, 2012).

Both statins and calorie restriction target enzymes involved in polyunsaturated fatty acid (PUFA) metabolism. In particular, statins have been shown to increase or decrease lipoxygenase (LOX) and soluble epoxide hydrolase (sEH) enzymes involved in converting PUFAs such as LA and arachidonic acid (AA) into oxylipins (Planaguma et al., 2010; P. Zhang et al., 2016). Calorie restriction has also been shown to alter plasma LA- and AA-derived oxylipins in obese women (Grapov et al., 2020).

In the present study, we investigated the effects of gestational obesity with or without pravastatin treatment and calorie restriction on offspring brain lipid metabolism in a non-human primate model. Non-human primates exhibit similar brain metabolic changes as humans (Q. Li et al., 2017), which is why they are better suited to study and model the complex biology of humans. In view of prior research showing that statins and calorie restriction alter LOX and sEH enzymes (Grapov et al., 2020), we hypothesized that pravastatin and calorie restriction would impact offspring brain cholesterol, fatty acid and oxylipin metabolism via epigenetic mechanisms involving DNA methylation of impacted genes.

Material and methods:

Animal Protocols

Animal protocols were approved by Institutional Animal Care and Use Committee. Naturally lean or obese non-pregnant female rhesus macaques (*Macaca mulatta*) with a previous successful

pregnancy were selected for this study at the California National Primate Research Center (CNPRC). Lean macaques had a body condition score (BCS) of 2.5 or less, and obese macaques had a BCS score of 3.5 or more. A BCS of 3.5 or more corresponds to a body fat content of 32%, which is close to the 30% body fat threshold for obesity in human (Summers, Clingerman, & Yang, 2012).

The lean group served as the control (n=6), and the obese group was divided into three groups; 1) obese, no intervention (n=7), 2) obese subjected to 14% calorie restriction starting one month prior to mating (n=5) and 3) obese administered pravastatin at a daily dose of 20 mg/kg body weight beginning one month prior to mating (n=7). All obese group female subjects were naturally obese. Females were mated with lean male monkeys and only male fetus carriers were selected in this study.

Pregnancy was confirmed by ultrasound around 45 days after mating. At approximately gestational day 70, females were singly housed, and two weeks later paired with compatible dams during daytime hours. Dams were allowed to deliver naturally, but cesarean sections were performed if the pregnancy lasted more than 175 days or as recommended by veterinarians. The offspring were paired with their birth dam, but 2 offspring from the control group, 1 offspring from obese no intervention group, and 3 from lean group were moved to foster dams because the biological dam did not accept her infant. This occurred in offspring born by caesarean section.

Throughout pregnancy (lasting ~165 days) and lactation (lasting ~182 days), female dams in the lean, obese, obese and pravastatin groups were provided seven biscuits (High Protein Primate Diet Jumbo #5047; LabDiet, St. Louis, MO, USA) twice a day between 6-9 am and 1-3 pm, and two more biscuits during feeding. Females in the calorie restricted group were provided one biscuit less twice a day between 6-9 am and 1-3 pm during pregnancy and lactation. The chow biscuits

contained 25% protein, 5% fat, 6.5% fiber, 6% ash, and 35% minerals. The main source of fat was soybean oil. The diets also contained fishmeal as a source of omega-3 eicosapentaenoic acid (EPA) and docosahexenoic acid (DHA). Fresh biscuits were provided twice per day and water was available *ad libitum*. The same diets were provided throughout lactation.

The offspring were sexed using qualitative real time PCR assay probing for the presence or absence of the Y chromosome. Offspring across all groups were not weaned for the duration of the study.

At approximately 6 months of age (postnatal day 180), necropsy was done on all male offspring, starting at 9:30 am and ending at 1:30 pm. Each subject was deeply anesthetized with ketamine, and plasma and urine were collected (not analyzed in this study). The subjects were then euthanized with 120 mg/kg pentobarbital. The brain was extracted and the prefrontal cortex, hippocampus, hypothalamus, and amygdala were dissected. The brain samples were immediately frozen in liquid nitrogen and stored at -80 ℃ until analysis.

Brain fatty acid and cholesterol extraction

Each brain sample was pulverized using liquid nitrogen in a pre-chilled mortar with a pestle. Approximately 30 mg of brain powder was used for lipid extraction as described (Hasegawa et al., 2020). Briefly, 560 uL of MeOH (Fisher Scientific; Cat #A454-4) with 0.006 % butylated hydroxytoluene (BHT, Cat # W218405-SAMPLE-K, Sigma-Aldrich, St. Louis, MO, USA) and 420 uL of 1mM ethylenediaminetetraacetic acid disodium salt dihydrate (EDTA, Cat No. E5134, Sigma-Aldrich, St. Louis, MO, USA) 0.9% KCl (Fisher Scientific, cat # P217-500) in water were pre-added into a clean 8 ml Kimble glass tube (Thomas Scientific, Cat # 9215D32). The tube was capped and weighed, and ~30 mg homogenized brain samples were added, and the capped tube was weighed again. The difference between two weights was taken as the weight of the

brain sample. Additional chloroform (Fisher Scientific; Cat #C607-4) and 0.006% BHT in methanol was added. The final Folch extraction volume was 600 μL: 800 μL: 1600 μL for KCl in water, methanol and chloroform respectively. Samples were vortexed for 20 s and centrifuged for 15 min at 2000 rpm at 0 °C. The bottom layer was transferred to a new 8 mL Kimble tube and ~1400 μL chloroform: methanol (v/v: 10/1) was added, vortexed for 20 s and centrifuged for 15 min at 2000 rpm at 0 °C. The second chloroform bottom layer was combined with the previous one and dried under nitrogen. The chloroform extract containing total lipids and oxylipins was reconstituted into 1.5 mL chloroform: isopropyl alcohol (Fischer Scientific, Cat #464-1) (v/v; 2/1).

Half of 1 mL of total lipid extract was spiked with 0.0125 mg 5α-Cholestane (Sigma-Aldrich, Cat #C8003-100mg) and 0.1 mg C17:0 PC (1,2-diheptadecanoyl-sn-glycero-3-phosphocholine (Avanti Polar Lipids; Cat #850355C). Spiked extracts were dried under nitrogen. Upon drying, 400 μL toluene (Fisher Scientific; Cat #T2914) was added, followed by 3 mL methanol, and 600 μL 3% HCl (Sigma-Aldrich, St. Louis, MO, USA; Cat #320331) in methanol. The samples were vortexed and heated at 90 °C for 60 min to generate fatty acid methyl esters (FAMEs) (Ichihara & Fukubayashi, 2010). After cooling at room temperature for 4–5 min, 1 mL hexane (Fisher Scientific; Cat #H303-4) and 1 mL deionized water were added to each sample. Samples were vortexed and the phases were allowed to separate for 15 min. Nine hundred microliter of the hexane top layer containing FAMEs were transferred to microfuge tubes containing 450 μL deionized water. The tubes were vortexed and centrifuged at 15,871 *g* for 2 min. The top hexane layer was evaporated under nitrogen and reconstituted in 100 μL hexane. Samples were analyzed by gas-chromatography coupled to flame ionization detection (GC-FID) as described below.

Brain total oxylipin extraction

One third of the chloroform: isopropanol (2:1, v/v/) total lipid extract (0.5 mL) was used for total (i.e. free + esterified) oxylipin extraction. The extract was dried under nitrogen and reconstituted into 200 μL methanol containing 0.1% acetic acid (Cat No. 695092, Sigma-Aldrich St. Louis, MO, USA) and 0.1% BHT (Sigma-Aldrich, Cat #W218405-SAMPLE-K), 10 μL antioxidant (composition below), and 10 μL surrogate standard mix containing 2 μM d11–11(12)-EpETrE (Cat No. 10006413, Cayman Chemical, Ann Arbor, MI, USA), d11-14,15-DiHETrE (Cat No. 1008040, Cayman Chemical), d4-6-keto-PGF1α (Cat No. 315210, Cayman Chemical), d4-9-HODE (Cat No. 338410, Cayman Chemical), d4-LTB4 (Cat No. 320110, Cayman Chemical), d4-PGE2 (Cat No. 314010, Cayman Chemical), d4-TXB2 (Cat No. 319030, Cayman Chemical), d6-20-HETE (Cat No. 390030, Cayman Chemical) and d8-5-HETE (Cat No. 334230, Cayman Chemical) in methanol. The antioxidant mix was made by mixing 0.2 mg/mL BHT, 0.2 mg/mL EDTA (Cat No. EDS-100G, Sigma-Aldrich, St. Louis, MO, USA) and 0.2 mg/mL of triphenylphosphine (TPP, Cat No.3T84409 Sigma-Aldrich, St. Louis, MO, USA) in methanol/water (50/50, v/v)) and filtering the contents through a 0.45 μm Millipore filter (Millpore, Bedford, MA, USA, Cat #SLHVM25NS).

The sample was hydrolyzed in 300 μL of 0.4 M NaOH (Cat No. S5881-500G, Sigma-Aldrich, St. Louis, MO, USA), in methanol: MilliQ water (50/50: v/v). Samples were vortexed and heated at 60 °C for 30 min, and cooled at room temperature for approximately 5 min. Then, 37.5 μL acetic acid were added to the tubes, to bring the pH to 4–6 (verified in one sample by litmus paper) and 1796 μL was added to dilute the methanol to be ~15% by volume.

The hydrolyzed samples were loaded onto solid phase extraction (SPE) columns (Cat No. WAT094226, 60 mg Oasis HLB, Waters, Milford, MA, USA) pre-washed with one column volume of ethyl acetate (Cat No. E196-4, Fisher Scientific, Hampton, NH, USA) and two

column volumes of methanol, and conditioned with two column volumes of SPE buffer (0.1% acetic acid, 5% methanol in MilliQ water). Samples were loaded onto the SPE columns, washed with two column volumes of SPE buffer and dried under vacuum for 20 min. Oxylipins were eluted with 0.5 mL methanol and 1.5 mL ethyl acetate. The eluent was dried under nitrogen, reconstituted in 100 μL LC-MS grade methanol (Fisher Scientific, Hampton, NH, USA, Cat No. A956), vortexed and centrifuged on an Eppendorf 5424R centrifuge at 15,871*g (0 °C) for 2 min. The sample was transferred to centrifugal filter units (Cat No. UFC30VV00, Ultrafree-MC VV Centrifugal filters, Burlington, MA, USA) which were centrifuged at 15,871*g (0 °C) for 2 min. Samples were analyzed with UPLC-MS/MS as described below.

Fatty acid and cholesterol composition of the biscuits

Four random biscuits collected throughout the duration of the study were crushed using a mortar and pestle pre-cooled on dry ice. Approximately 20 mg of powdered samples were spiked with 0.15 mg of C17:0 TAG (triheptanoic, Nu-Chek Prep; Cat #T-155) and 0.0125 mg 5α-Cholestane. Samples were subjected to the same lipid extraction and transesterification protocols described for brain analysis. FAMEs were analyzed by GC-FID as described below.

GC-FID quantification of fatty acid and cholesterol

A simultaneous FAME and cholesterol GC-FID method was optimized based on previous methods (Meier, Mjos, Joensen, & Grahl-Nielsen, 2006; Z. C. Zhang, Richardson, Hennebelle, & Taha, 2017). Samples were analyzed on a Perkin Elmer Clarus 500 GC-FID system (Perkin Elmer, Shelton, CT, USA) equipped with a DB-FFAP polyethylene glycol fused capillary column (30 m × 0.25 mm inner diameter, 0.25 μm film thickness; Cat #1223232, Agilent Technologies, Santa Clara, CA, USA). The injector and detector temperature were 285 °C and 300 °C, respectively. The initial oven temperature was 80 °C. It was held at 80 °C for 2 min,

increased by 10 °C/min to 185 °C, raised to 249 °C at 6 °C/min and held at 240 °C for 44 min. The total run time was 65 min. Helium was the carrier gas and was maintained at a flow rate of 1.3 mL/min. The injection volume was 1 µL per sample. The split ratio was 10: 1. A custom-made standard mix of 29 FAME standards was used to identify each fatty acid based on retention time. Fatty acid concentrations were determined by comparing GC peak areas to the internal standard area. Cholesterol concentration was calculated based on a five-point standard curve of cholesterol and 5α-Cholestane as surrogate. The linear range of the calibration curve for cholesterol was 0.125 mg/mL to 2 mg/mL.

UPLC-MS/MS quantification of oxylipins

Samples were analyzed on an Agilent 1290 Infinity UPLC system coupled to an Agilent 6460 triple-quadrupole tandem mass spectrometer (Agilent, Palo Alto, CA, USA) equipped with a jetstream electrospray ionization source as previously detailed. Seventy-six oxylipin species and nine surrogates were analyzed in negative ionization mode and probed using published optimized dynamic Multiple Reaction Monitoring conditions (Zhang et al., 2021. In press).

Analytes were separated with reverse phase liquid chromatography, using an Agilent Eclipse Plus C18 column (2.1 × 150 mm, 1.8 µm, Agilent Corporation, Cat #959759-902). The auto-sampler temperature was set at 4 °C and the column temperature was set at 45 °C. The injection volume was 10 µL. Mobile phase A had 0.1% acetic acid in MilliQ water and mobile phase B had 80/15 (v/v) LC-MS grade acetonitrile (Fisher scientific, Cat # A9561) /LC-MS grade methanol with 0.1% acetic acid. Mobile phase A was initially set at 65%. It was gradually decreased to 15% at 15 min, held at 15% until 15.1 min, and decreased to 0% at 17 min. Mobile phase A was increased to 65% at 17.10 min and held constant to the end of the run. The flow rate

was 0.3 mL/min between 0 to 2 min, 0.25 mL/min from 2 to 17 min, 0.4 mL/min from 17 to 19 min, and 0.30 mL/min from 19 to 20 min.

Analytes that used d4-PGE2 as a surrogate standard were not quantified because it degrades during hydrolysis. These include LA-derived tri-hydroxymonodecaenoic acid metabolites (9, 10, 13-TriHOME and 9, 12, 13-TriHOME) and prostaglandins (PGB2, PGD1, PGD2, PGD3, PGE1, PGE2, PGE3, 15-deoxy-PGJ2 and PFG2-alpha).

Whole Genome Bisulfite Sequencing (WGBS):

Existing WGBS data was utilized (Laufer et al., Manuscript under preparation). Briefly, brain tissue was stored in DNA/RNA shield (Zymo Research; R1100-250). The Quick-DNA Miniprep Plus kit workflow on a Tecan instrument was performed by Zymo Research to extract DNA, which was then fragmented using a E220 focused-ultrasonicator (Covaris; 500239). The EZ DNA Methylation-Lightning Kit (Zymo Research; D5031) was utilized to bisulfite convert the DNA and libraries were prepared via the Accel-NGS Methyl-Seq DNA Library Kit (Swift Biosciences; 30096) and Methyl-Seq Combinatorial Dual Indexing Kit (Swift Biosciences; 38096) according to the manufacturer's instructions. The library pool was sequenced on an Illumina NovaSeq 6000 S4, to generate 150 bp paired end reads, at the UCSF Center for Advanced Technology (CAT) core facility. The CpG_Me alignment pipeline (https://github.com/ben-laufer/CpG_Me), which is based on Trim Galore, FastQ Screen, Bismark, Picard, and MultiQC, was utilized to align the data and generate CpG count matrices (Laufer et al., 2021; H. Li et al., 2009).

Statistical analysis

Data were expressed as mean ± standard deviation (SD). Normality and homoscedasticity of all data were evaluated using Shapiro-Wilk test and Brown-Forsythe test, respectively. If data

were neither normally distributed nor homogeneous, Kruskal–Wallis followed by Dunn' multiple comparison test was used. If data were normally distributed and had equal variances, one-way analysis of variance (ANOVA) followed by Tukey's multiple comparison test was used. One-way ANOVA Welch followed by Tukey's multiple comparison test was used for heteroskedastic but normal data. Significance was defined at $p<0.05$.

Existing DMR data was utilized (Laufer et al., Manuscript under preparation). Briefly, DMR calling was performed as previously described via DMRichR (https://github.com/ben-laufer/DMRichR), which utilizes the dmrseq and bsseq algorithms (Laufer et al., 2021). ChIPseeker was used to obtain gene symbol mappings from ensembldb (Rainer, Gatto, & Weichenberger, 2019; Yu, Wang, & He, 2015). Correlation analyses were performed via Pearson correlation and the linear model in the scatterplot was fit by robust regression.

Results:

Dietary Fatty Acid and cholesterol Composition

Dietary fatty acid and cholesterol concentrations and percent composition are presented in **Table 13**. As shown, LA was the most abundant fatty acid in the diet (30.8% of total fatty acids). This was followed by oleic acid (30.4%) and palmitic acid (20.0%). Omega-3 fatty acids including α-linolenic acid (ALA), eicosapentaenoic acid (EPA), and docosahexaenoic acid (DHA) were present in the diet at 2.1%, 0.2%, and 0.3% respectively. Arachidonic acid (AA) constituted 0.22% of total fatty acids. Cholesterol was not detected, although the diets had a trace amount of lard.

Fatty Acid and cholesterol concentrations in offspring prefrontal cortex, hippocampus, hypothalamus and amygdala

Maternal intake of pravastatin or calorie restriction did not impact offspring brain cholesterol concentration. As shown in **Supplementary Figure 7**, there were no significant differences in cholesterol concentrations across the four groups in the four brain regions analyzed. Cholesterol concentration averaged 14 mg/g across the four brain regions, consistent with the 11 mg/g cholesterol concentration in monkey brain previously reported in the literature (Dietschy & Wilson, 1968).

There were no significant differences in fatty acid concentrations across four groups in the prefrontal cortex, hippocampus, hypothalamus, and amygdala. In all four groups, DHA and AA were the most abundant PUFAs in all four brain regions and amounted to 3-4 mg/g brain tissue (**Supplemental Figure 8-11**).

Total oxylipin concentrations in offspring prefrontal cortex, hippocampus, hypothalamus, and amygdala

5(6)-EpETrE, an AA-derived oxylipin significantly decreased by 4-fold in the obese pravastatin group compared to the obese, no intervention group **(Figure 15**). Neither differed significantly from lean controls. 17-HDoHE, a DHA-derived oxylipin, was significantly reduced by 2-fold in the obese calorie restricted group compared to the obese group (**Figure 15**); again neither of the groups significantly differed from lean controls.

The diol to epoxide ratio, a marker of soluble epoxide (sEH) activity (Stefanovski, Shih, Hammock, Watanabe, & Youn, 2020), was calculated. Soluble epoxide hydrolase converts anti-inflammatory AA epoxides into pro-inflammatory diols (Node et al., 1999). As shown in **Figure**

16, the ratio of two AA species (5(6) and 8(9) epoxy to corresponding diol ratio) was 2-fold higher in the pre-frontal cortex of the obese calorie restricted group and the obese pravastatin group, relative to the obese no intervention group (**Figure 16**). There we no significant differences in other brain regions. This suggests increased sEH activity, specifically in the pre-frontal cortex of offspring born to obese dams that were calorie restricted or given pravastatin throughout pregnancy.

Epigenetic analysis

Consistent with the observed increase in AA-derived diol to epoxide ratios in prefrontal cortex, significant (empirical $p < 0.05$) differential methylation of several sEH coding genes (*EPHX1, EPHX2,* and *EPHX4)* was observed in the prefrontal cortex as well as the hypothalamus and hippocampus of infants born to the pravastatin and calorie restricted dams compared to methylation level of infants from obese and lean control dams (**Table 14**). When the DMRs were merged by genomic coordinate overlap, the DNA methylation levels of some of the regions correlated with both maternal obesity intervention and lipid levels (**Figure 17A**). The strongest correlation was between EHPX1 intron (chr1:83358175-83358588) and LA concentration in pre-frontal cortex.

Discussion:

Maternal obesity did not alter offspring brain lipid metabolism. However, gestational calorie restriction and administration of pravastatin to obese dams increased offspring lipidomic and epigenetic markers of sEH and reduced pro-resolving DHA-derived 17-HDoHE or AA-derived 5(6)-EpETrE in the pre-frontal cortex compared to offspring born to obese or lean dams. Fatty acid and cholesterol concentrations did not differ in the pre-frontal cortex or other brain

regions. These data suggest long-term effects of maternal pravastatin or calorie restriction on brain lipid metabolism in infants of obese rhesus macaques.

AA and DHA derived oxylipin concentrations were significantly affected by pravastatin and calorie restriction. Specifically, DHA-derived 17-HDoHE was lower in the obese calorie restriction group, and AA-derived 5(6)-EpETrE was lower in the pravastatin group compared to obese no intervention group. Both compounds are known to promote neuronal outgrowth and survival in neuronal cell cultures (Gleissman et al., 2010; Oguro, Inoue, Kudoh, & Imaoka, 2018), and to resolve inflammation in rodent models of inflammation (Lima-Garcia et al., 2011; Node et al., 1999; Ramon et al., 2014). 17-HDoHE in the cerebral cortex was shown to be positively associated with reference memory-related learning ability in rats (Hashimoto et al., 2015). Collectively, our findings suggest that maternal pravastatin and calorie restriction reduced offspring brain concentration of pro-resolving and neurotrophic oxylipins.

Maternal calorie restriction and pravastatin also increased sEH activity in the prefrontal cortex of 6-month offspring, findings supported by epigenetic hypo-methylation of this gene. sEH is a marker of inflammation, and its upregulation in the brain of infant macaques suggests a chronic vulnerability to inflammation. The long-term effects of maternal calorie restriction and pravastatin on sEH are likely driven by *in utero* epigenetic changes that appear to have a long-lasting impact on the brain. Increased sEH activity in the cortex of rodents has been recently reported to be associated with increased risk of ASD (Pu et al., 2020). Activation of sEH has been correlated with maternal immune response (MIA) and MIA has been widely studied as a mechanism in the development of offspring ASD (Lammert & Lukens, 2019; Lombardo et al., 2018; Ma et al., 2019). Of interest, maternal obesity has been shown to be associated with higher

risk of ASD development (Krakowiak et al., 2012). However, in our study, we did not find significant differences between the obese no intervention and lean control groups.

Differences in sEH hypomethylation were observed in other brain regions such as the hippocampus and hypothalamus, but these did not translate to discernible changes in PUFA diol to epoxide ratios (markers of sEH activity). This suggests cortical vulnerability to the maternal effects on sEH hypomethylation. During development, the prefrontal cortex has been shown to be involved in social interaction and behavior regulation, and therefore changes in prefrontal cortex lipid metabolism may possibly affect its development (Damasio, Grabowski, Frank, Galaburda, & Damasio, 1994; DeYoung et al., 2010; Kurochkin et al., 2019).

There was a strong correlation between EHPX1 intron and brain LA concentration in cortex. This is novel but cannot be biologically interpreted since EHPX1 is not known to directly act on LA. Future studies are needed to better understand the significance of this association in vivo, and to establish the biochemical pathways involved.

The lack of a significant effect of maternal pravastatin treatment on infant brain cholesterol concentration was surprising, considering that statins purportedly reduce maternal supply of cholesterol to the placenta (Costantine et al., 2016). In mammals, cholesterol is synthesized de novo in multiple organs including the brain during fetal and neonatal development (Turley, Burns, Rosenfeld, & Dietschy, 1996). Thus, the lack of impact of pravastatin on infant brain cholesterol concentrations suggests adaptive responses leading to an upregulation of brain cholesterol synthesis postpartum. This is consistent with a rat study showing that lovastatin administration from 2 to 20 days postpartum resulted in transient reductions in brain cholesterol, which were reversible by 59-60 days postpartum (Serbanescu et al., 2004).

A limitation of this study is that the sample size was small (4 to 7 offspring per group), and this may have limited our ability to detect changes between infants born to lean and obese dams. Obesity was previously shown to be associated with increased levels of plasma LA (Kang et al., 2017; Moushira Zaki 2020), and the lack of changes of LA or OXLAMs in the offspring could be attributed to the small sample size or the possibility that maternal changes in LA metabolism do not exert a long-lasting impact on offspring LA or OXLAMs. Another limitation is that pravastatin and calorie restriction were only provided to obese dams and not control lean dams. Thus, potential interactions between maternal obesity and pravastatin or calorie restriction might explain the observed changes in offspring brain lipid metabolism. Future studies should investigate these treatments in lean subjects.

In conclusion, we have found evidence of reduced pro-resolving oxylipins and increased epigenetic and lipidomic signatures of sEH enzyme in pre-frontal cortex of 6 months old infants born to obese dams that were calorie restricted or treated with pravastatin. Our findings point to long-term effects of calorie restriction and pravastatin on brain lipid metabolism and reflect increased vulnerability to inflammation and reduced potential to resolve persistent inflammation. These changes may be associated with adverse neurodevelopmental outcomes, which should be further investigated.

Sources of funding:

This research was supported by National Institutes of Health award 1R01HD084203 to CV and CW, a Canadian Institutes of Health Research (CIHR) postdoctoral fellowship [MFE-146824] and a CIHR Banting postdoctoral fellowship [BPF-162684] to BIL, and in part by support from

the USDA National Institute of Food and Agriculture Hatch Project #1008787 to A.Y.T. The CNPRC is funded through an NIH Base Grant (P51 OD011107).

Acknowledgements:

We would like to thank Dana Dagget and Jasmin Zarrabi for their technical support, and the CNPRC Animal Care and Research Services staff for their help in caring for the animals in this study.

Conflict of interest:

There are no conflicts of interest to declare.

Chapter 7 Conclusion:

This thesis demonstrated that oxidized linoleic acid metabolites (OXLAMs) in the diet are bioavailable but do not enter the brain. Linoleic acid (LA or LNA) is the primary source of OXLAMs in the brain, not diet. Specifically, we found that 1) OXLAMs are the most abundant oxylipins in the diet, 2) they enter peripheral tissues but not the brain upon absorption, 3) they are synthesized de novo in the brain from LA, and 4) that during gestational obesity, which raises circulating LA, interventions such as calorie restriction and use of pravastatin do not affect offspring brain LA or OXLAM metabolism, but reduced docosahexaenoic acid (DHA)-derived resolvins and increased arachidonic acid (AA)-derived eicosanoid metabolism by increasing soluble epoxide hydrolase (sEH) expression in pre-frontal cortex.

In Aim 1 (Chapter 2), we showed that different processing conditions such as blanching, par-frying, and repeated-frying have distinct effects on OXLAM concentrations in potatoes and the oil used to fry the potatoes. This was a surprising finding, as the bulk of prior studies found that thermal treatment increased OXLAM concentrations in oils (X. Li, Li, Wang, Cao, & Liu, 2017; Richardson et al., 2017). A limitation of these studies, however, is that the thermal conditions were extreme and did not represent real-world handling of foods or oils. We were able to overcome these limitations by using sensitive mass-spectrometry measurements of oil and potato oxylipins. Another key finding is that the amount of OXLAMs formed in oil was not reflected entirely in the potatoes with increasing frying cycles; in other words, more cycles increased OXLAMs in oil but there was a limit as to how much was absorbed by the potatoes. This suggests a mass transfer effect whereby the extent of oil oxidation does not necessarily reflect how much transfers to a food beyond a certain point. These findings could be used to optimize frying cycles in industry settings.

In Aim 2 (Chapter 3), we found that OXLAMs constituted over 90% of oxylipins, and that the majority of oxylipins were esterified to complex lipids within various milk fractions. Thus, we discovered a new source of oxylipins in human breast milk which could be important for infant brain development.

In both Aims 1 and 2, OXLAMs constituted the majority of measured oxylipins. 13-hydroxyoctadecadienoic acid (13-HODE) was the most abundant OXLAM in oil, French fries and breast milk.

In Aim 3 (Chapter 4), deuterium labeled 13-HODE was used as a surrogate to probe the in vivo metabolism of OXLAMs in rats. We found that 13-HODE is rapidly absorbed (within 20 minutes) and incorporated into adipose, liver and heart but not brain. The incorporation rate of esterified 13-HODE (the form found in foods such as milk and French fries) was higher than free 13-HODE. This means that esterified OXLAMs in foods are likely to incorporate and reside in peripheral tissues for a long period of time. Future studies should elucidate the impact of these compounds on peripheral tissue metabolism.

In Aim 4 (Chapter 5), we tested whether LA is a source of OXLAMs in the brain (since we did not see measurable labeled 13-HODE incorporation into the brain in Study 3). We found that labeled LA is rapidly converted into OXLAMs upon entering the brain. However, increasing dietary LA did not alter the conversion rate of LA into OXLAMs in the brain, although it increased the LA turnover (i.e. metabolism). Further studies are needed to understand where excess LA in the brain goes. Quantitatively, however, our measurements revealed that up to 5% of LA entering the brain was oxidized to form short-lived OXLAMs (half-life of milliseconds).

In Aim 5 (Chapter 6), we investigated whether maternal obesity, which is known to dysregulate LA metabolism, is associated with long-lasting changes in brain OXLAMs in the

offspring of non-human primates. We tested this in the context of calorie restriction and pravastatin, two treatments that are being experimentally considered for treating obesity-induced hyperlipidemia during pregnancy. Obesity with or without pravastatin and calorie restriction did not have an impact on offspring brain OXLAM concentration (compared to offspring of lean mothers). However, offspring born to obese dams treated with pravastatin or who were calorie restricted, showed reduced concentrations of DHA-derived 17-HDoHE and increased lipid and epigenetic signatures of AA-derived sEH in the pre-frontal cortex compared to offspring of lean dams. Reduced brain concentrations of pro-resolving 17-HDoHE and increased sEH biosignature reflects increased vulnerability to inflammation in the offspring of obese dams treated with pravastatin or calorie restriction. Elevated sEH in brain has been associated with autistic-like behavior in mice (Ma et al., 2019; Pu et al., 2020). Thus, future studies should investigate the behavioral effects of calorie restriction and pravastatin on potential behavioral impairments in the offspring.

There are several limitations in this thesis. First, in Aims 1 and 2, the hydrolysis (for releasing and measuring bound oxylipins) was performed with sodium carbonate. In Aim 3, it became clear that sodium hydroxide is a more effective base. This observation was recently corroborated by other studies showing that sodium hydroxide is more efficient at releasing esterified oxylipins than sodium carbonate in foods and plasma (Emami et al., 2020; Quehenberger et al., 2018; Teixeira et al., 2021). We suspect that the observed changes in OXLAMs are still valid, although absolute levels may be underestimated due to inefficient hydrolysis when using sodium carbonate.

In Aim 3, the rats were not subjected to high-energy microwave fixation to stop postmortem changes in brain OXLAM metabolism following labeled 13-HODE administration.

This could have increased the metabolism of 13-HODE (M. Hennebelle, A. H. Metherel, et al., 2019), preventing us from detecting measurable incorporation of 13-HODE into the brain. Also, because the brains were isolated 90 minutes after 13-HODE tracer injection (in Aim 3), it is possible that any 13-HODE that entered the brain might have been degraded by the time we dissected the brains (due to the short millisecond half-life of OXLAMs as established in Study 4). Future studies should dissect the brains immediately after tracer injection (versus after 90 minutes), and head-focused microwave-irradiation should be used to minimize the well-established effects of post-mortem ischemia on brain oxylipins (M. Hennebelle, A. H. Metherel, et al., 2019).

A general limitation is that due to the exploratory nature of our animal studies, the sample sizes were low and in some cases, there was lack of statistical power to fully test specific hypotheses. However, the data generated from these experiments should aide in moderately estimating statistical power in future studies.

Additional research is needed to expand the findings of this thesis and improve upon current limitations. First, sodium hydroxide should be used as the hydrolysis base moving forward. Second, the analysis of oxylipins in human breast milk throughout the lactation period would shed new light on how oxylipins/OXLAMs change over time. This may have implications on oxylipin bioavailability to the infant. It will be also important to analyze human breast milk from diverse backgrounds because the consumption of LA may vary by socioeconomic status and other demographics. Analysis of infant formula should also be conducted to compare levels to human milk. This could help better formulate the nutrient composition of infant formulas.

Although OXLAMs are bioavailable, the extent of OXLAM degradation in the gastrointestinal tract needs to be studied. It is possible that they are mostly degraded into

hexanals and malonaldehydes as previously suggested (Kanazawa & Ashida, 1998). Finally, for the maternal obesity study, altering maternal dietary LA composition could be used to test whether maternal LA exposure affects brain OXLAM metabolism in the offspring.

Overall, this thesis has provided important scientific knowledge on the oxidation and bioavailability of OXLAMs and demonstrated that the brain derives OXLAMs from circulating LA rather from direct incorporation from the diet. The work in non-human primates did not find an effect of gestational obesity on offspring OXLAM metabolism, although the data suggest that calorie restriction and pravastatin increase markers of brain inflammation in the offspring, suggesting that these potential treatments for gestational obesity may adversely affect infant brain development.

Tables and Figures:

Table 1**.** Summary of LA and ALA derived oxylipin changes in potatoes and oil during processing or repeated frying cycles. NC, No change.

	Changes are relative to raw peeled potatoes for blanching, par-frying and deep frying. Changes are relative to baseline (i.e. before frying) for repeated frying					
	From Figure 5			**From Figure 7**		
	Blanching	Par frying	Deep frying	1X frying	2X frying	3X frying
LA-hydroxy	**NC**	⇩	⇩	**NC**	**NC**	**NC**
LA-ketones	**NC**	⇩	**NC**	**NC**	**NC**	⬆
LA-epoxides	⇩	⇩	**NC**	⇩	⇩	**NC**
LA-diols	⇩	⬆	⬆	⬆	⬆	⬆

ALA-hydroxy	⬆	⇩	⇩	**NC**	**NC**	⬆
	Changes in oil relative to baseline (i.e. before frying) – <u>from Figure 6</u>					
				1X frying	2X frying	3X frying
LA-hydrox	Not applicable	Not measured	Not measured	⬆	⬆	⬆
LA-ketones	Not applicable	Not measured	Not measured	**NC**	**NC**	⬆
LA-epoxides	Not applicable	Not measured	Not measured	**NC**	⬆	⬆
LA-diols	Not applicable	Not measured	Not measured	**NC**	**NC**	**NC**
ALA-hydroxy	Not applicable	Not measured	Not measured	**NC**	⬆	⬆

Table 2. Mass percent of components in pooled human milk (%m/m; n = 2 measurements from pooled milk sample)

Measurement	Fat	Protein	Lactose	Solids
1	4.922	0.879	7.1245	13.204
2	4.924	0.908	7.1463	13.204
Mean	4.923	0.894	7.1354	13.204

Table 3. Concentrations of esterified and free oxylipins in human milk cream (mean ± sd, pmol/mg wet weight; n=3 per lipid fraction)

Precursor	Compound	Esterified NL	Esterified PL	Free	p-value[1]
LNA (18:2n-6)	9-HODE	4.43 ± 0.24[a]	0.77 ± 0.03[b]	5.56 ± 1.78[a]	0.003
	13-HODE	4.51 ± 0.42[a]	0.98 ± 0.10[b]	3.55 ± 1.18[a]	0.002
	9-oxo-ODE	6.89 ± 0.88[a]	0.53 ± 0.07[b]	5.16 ± 1.35[a]	<0.001
	13-oxo-ODE	18.20 ± 3.10[a]	1.50 ± 0.43[b]	7.39 ± 1.60[c]	<0.001
	9(10)-EpOME	13.06 ± 3.15[a]	1.37 ± 0.22[b]	2.38 ± 0.80[b]	<0.001
	12(13)-EpOME	35.60 ± 8.24[a]	3.52 ± 0.72[b]	5.70 ± 1.95[b]	<0.001
	9,10-DiHOME	0.14 ± 0.02[a]	0.05 ± 0.02[a]	0.25 ± 0.08[b]	0.008
	12,13-DiHOME	0.17 ± 0.01[a]	0.06 ± 0.02[a]	0.53 ± 0.17[b]	0.003
	9,10,13-TriHOME	NQ	NQ	0.46 ± 0.19	NA
	9,12,13-TriHOME	NQ	NQ	0.51 ± 0.22	NA
DGLA (20:3n-6)	15(S)-HETrE	ND	ND	0.02 ± 0.005	NA
ARA (20:4n-6)	5-HETE	0.24 ± 0.02	ND	0.28 ± 0.09	NS
	8-HETE	ND	ND	0.02 ± 0.01	NA
	11-HETE	0.05 ± 0.001	ND	0.03 ± 0.01*	0.019
	12-HETE	ND	ND	0.03 ± 0.01	NA
	15-HETE	0.10 ± 0.01	ND	0.04 ± 0.02*	0.011
	20-HETE	ND	ND	0.07 ± 0.02	NA
	5-oxo-ETE	ND	ND	0.19 ± 0.06	NA
	12-oxo-ETE	0.03 ± 0.05	ND	0.02 ± 0.02	NS

	15-oxo-ETE	ND	ND	0.15 ± 0.05	NA
	5(6)-EpETrE	0.28 ± 0.03[a]	0.03 ± 0.01[b]	0.12 ± 0.04[c]	<0.001
	8(9)-EpETrE	0.16 ± 0.04	ND	0.03 ± 0.01*	0.004
	11(12)-EpETrE	0.40 ± 0.01[a]	0.05 ± 0.02[b]	0.02 ± 0.01[b]	<0.001
	14(15)-EpETrE	1.25 ± 0.20[a]	0.12 ± 0.07[b]	0.04 ± 0.02[b]	<0.001
	5,6-DiHETrE	0.02 ± 0.03	ND	0.04 ± 0.01	NA
	8,9-DiHETrE	ND	ND	0.01 ± 0.003	NA
	11,12-DiHETrE	ND	ND	0.01 ± 0.003	NA
	14,15-DiHETrE	ND	ND	0.01 ± 0.002	NA
ALA (18:3n-3)	9-HOTrE	0.22 ± 0.03	ND	0.27 ± 0.08	NS
	13-HOTrE	0.22 ± 0.05	ND	0.18 ± 0.05	NS
EPA (20:5n-3)	5-HEPE	0.15 ± 0.01	ND	0.08 ± 0.03*	0.018
	8-HEPE	ND	ND	0.01 ± 0.002	NA
	12-HEPE	ND	ND	0.01 ± 0.004	NA
	15-HEPE	ND	ND	0.02 ± 0.01	NA
	14(15)-EpETE	0.19 ± 0.02	ND	0.01 ± 0.004*	<0.001
	17(18)-EpETE	2.20 ± 0.19	ND	0.17 ± 0.06*	<0.001
	14,15-DiHETE	ND	ND	0.03 ± 0.01	NA
	17,18-DiHETE	ND	ND	ND	NA
DHA (22:6n-3)	7(8)-EpDPE	0.18 ± 0.03	ND	0.01 ± 0.003	NA
	10(11)-EpDPE	0.18 ± 0.01	0.005 ± 0.01	0.03 ± 0.01	NA
	13(14)-EpDPE	0.31 ± 0.11	0.04 ± 0.04	0.02 ± 0.004	NA

16(17)-EpDPE	0.37 ± 0.09	ND	0.01 ± 0.003*	0.003
19(20)-EpDPE	0.43 ± 0.06	ND	0.01 ± 0.005*	<0.001

ND: not detected.

NQ: not quantifiable in NL and PL due to degradation of the deuterated standard (d4-PGE2) used to quantify them during hydrolysis.

[1]: p-value of ANOVA for three groups or unpaired t-test for two groups.

NS: not significant (p-value > 0.05).

NA: not available.

Alphabetical superscripts indicate significant differences between the groups by Newman-Keuls post-hoc test; asterisk (*) indicates significant differences between the groups by unpaired t-test.

Table 4. Concentrations of esterified and free oxylipins in human milk pellet (mean ± sd, pmol/mg wet weight; n=3 per lipid fraction)

Precursor	Compound	Esterified NL	Esterified PL	Free	p-value[1]
LNA (18:2n-6)	9-HODE	0.64 ± 0.20[a]	0.23 ± 0.23[b]	1.17 ± 0.11[c]	0.003
	13-HODE	0.80 ± 0.20	0.35 ± 0.36	0.78 ± 0.06	NS
	9-oxo-ODE	3.42 ± 1.18[a]	0.79 ± 0.72[b]	2.98 ± 0.35[a]	0.017
	13-oxo-ODE	9.16 ± 3.62[a]	1.85 ± 1.86[b]	3.26 ± 0.50[b]	0.020
	9(10)-EpOME	22.87 ± 11.69[a]	0.99 ± 0.89[b]	5.98 ± 1.69[b]	0.018
	12(13)-EpOME	50.67 ± 26.59[a]	2.64 ± 2.53[b]	14.17 ± 3.77[b]	0.022
	9,10-DiHOME	0.03 ± 0.02	ND	0.04 ± 0.01	NA
	12,13-DiHOME	0.04 ± 0.01	ND	0.07 ± 0.01	NA
	9,10,13-TriHOME	NQ	NQ	0.11 ± 0.02	NA
	9,12,13-TriHOME	NQ	NQ	0.12 ± 0.03	NA
DGLA (20:3n-6)	15(S)-HETrE	ND	ND	ND	NA
ARA (20:4n-6)	5-HETE	0.03 ± 0.01	0.06 ± 0.06	0.05 ± 0.01	NS
	8-HETE	ND	ND	ND	NA
	11-HETE	ND	0.02 ± 0.02	0.01 ± 0.001	NS

	12-HETE	ND	ND	ND	NA
	15-HETE	ND	ND	ND	NA
	20-HETE	ND	ND	ND	NA
	5-oxo-ETE	ND	ND	ND	NA
	12-oxo-ETE	0.01 ± 0.01	ND	ND	NS
	15-oxo-ETE	0.02 ± 0.03	ND	ND	NA
	5(6)-EpETrE	0.05 ± 0.02	0.03 ± 0.03	0.04 ± 0.01	NS
	8(9)-EpETrE	0.08 ± 0.02	ND	0.03 ± 0.01*	0.015
	11(12)-EpETrE	0.13 ± 0.06	0.04 ± 0.04	0.04 ± 0.01	NS
	14(15)-EpETrE	0.23 ± 0.12	0.10 ± 0.10	0.05 ± 0.01	NS
	5,6-DiHETrE	0.05 ± 0.03	ND	ND	NA
	8,9-DiHETrE	ND	ND	ND	NA
	11,12-DiHETrE	ND	ND	ND	NA
	14,15-DiHETrE	ND	ND	ND	NA
ALA (18:3n-3)	9-HOTrE	0.03 ± 0.01	ND	0.06 ± 0.01*	0.006
	13-HOTrE	0.03 ± 0.01	ND	0.04 ± 0.01	NS
EPA (20:5n-3)	5-HEPE	ND	ND	ND	NA
	8-HEPE	ND	ND	ND	NA
	12-HEPE	ND	ND	ND	NA
	15-HEPE	ND	ND	ND	NA
	14(15)-EpETE	0.04 ± 0.02	ND	ND	NA
	17(18)-EpETE	0.44 ± 0.27	ND	ND	NA
	14,15-DiHETE	ND	ND	ND	NA

	17,18-DiHETE	ND	ND	ND	NA
DHA (22:6n-3)	7(8)-EpDPE	0.06 ± 0.03	ND	ND	NA
	10(11)-EpDPE	0.05 ± 0.02	ND	0.01 ± 0.002	NA
	13(14)-EpDPE	0.06 ± 0.03	0.004 ± 0.01	0.01 ± 0.002	NA
	16(17)-EpDPE	0.07 ± 0.04	0.003 ± 0.01	ND	NA
	19(20)-EpDPE	0.06 ± 0.02	ND	0.01 ± 0.002*	0.032

ND: not detected.

NQ: not quantifiable in NL and PL due to degradation of the deuterated standard (d4-PGE2) used to quantify them during hydrolysis.

[1]: p-value of ANOVA for three groups or unpaired t-test for two groups.

NS: not significant (p-value > 0.05).

NA: not available.

Alphabetical superscripts indicate significant differences between the groups by Newman-Keuls post-hoc test; asterisk (*) indicates significant differences between the groups by unpaired t-test.

Table 5. Concentrations of esterified and free oxylipins in skim human milk (mean ± sd, pmol/ml; n=3 per lipid fraction)

Precursor	Compound	Esterified NL	Esterified PL	Free	p-value[1]
LNA (18:2n-6)	9-HODE	26.51 ± 1.25[a]	1.33 ± 0.08[b]	41.88 ± 1.38[c]	<0.001
	13-HODE	18.61 ± 0.16[a]	1.81 ± 0.02[b]	19.60 ± 0.73[c]	<0.001
	9-oxo-ODE	36.07 ± 1.95[a]	3.53 ± 0.20[b]	96.65 ± 8.42[c]	<0.001
	13-oxo-ODE	76.99 ± 5.61[a]	4.31 ± 0.26[b]	51.28 ± 8.31[c]	<0.001
	9(10)-EpOME	71.06 ± 3.11[a]	7.05 ± 3.75[b]	21.34 ± 2.87[c]	<0.001
	12(13)-EpOME	170.12 ± 6.52[a]	16.16 ± 9.14[b]	65.11 ± 9.40[c]	<0.001
	9,10-DiHOME	3.41 ± 0.30[a]	0.08 ± 0.02[b]	13.32 ± 0.69[c]	<0.001
	12,13-DiHOME	4.70 ± 0.48	0.07 ± 0.08	24.00 ± 1.97	NA
	9,10,13-TriHOME	NQ	NQ	149.62 ± 7.64	NA
	9,12,13-TriHOME	NQ	NQ	153.19 ± 5.37	NA

DGLA (20:3n-6)	15(S)-HETrE	0.07 ± 0.01	ND	ND	NA
ARA (20:4n-6)	5-HETE	1.00 ± 0.02[a]	0.42 ± 0.09[b]	2.33 ± 0.26[c]	<0.001
	8-HETE	0.08 ± 0.07	ND	0.33 ± 0.04	NA
	11-HETE	0.14 ± 0.02	0.11 ± 0.01	0.12 ± 0.02	NS
	12-HETE	ND	ND	0.18 ± 0.02	NA
	15-HETE	0.28 ± 0.01	0.27 ± 0.02	0.26 ± 0.06	NS
	20-HETE	ND	ND	ND	NA
	5-oxo-ETE	ND	ND	0.53 ± 0.07	NA
	12-oxo-ETE	0.27 ± 0.16[a]	0.03 ± 0.04[b]	0.02 ± 0.01[b]	0.028
	15-oxo-ETE	ND	ND	0.62 ± 0.14	NA
	5(6)-EpETrE	0.81 ± 0.06[a]	0.49 ± 0.25[b]	0.20 ± 0.04[b]	0.007
	8(9)-EpETrE	0.62 ± 0.16[a]	0.32 ± 0.06[b]	0.16 ± 0.05[b]	0.004
	11(12)-EpETrE	0.92 ± 0.11[a]	0.81 ± 0.41[a]	0.19 ± 0.04[b]	0.022
	14(15)-EpETrE	1.80 ± 0.19[a]	1.92 ± 1.06[a]	0.34 ± 0.07[b]	0.038
	5,6-DiHETrE	0.15 ± 0.04	ND	0.44 ± 0.01*	<0.001
	8,9-DiHETrE	ND	ND	0.12 ± 0.01	NA
	11,12-DiHETrE	ND	ND	0.13 ± 0.002	NA
	14,15-DiHETrE	ND	ND	0.16 ± 0.02	NA
ALA (18:3n-3)	9-HOTrE	2.25 ± 0.16	ND	4.46 ± 0.08*	<0.001
	13-HOTrE	1.49 ± 0.09	ND	2.07 ± 0.12*	0.002
EPA (20:5n-3)	5-HEPE	0.54 ± 0.02	ND	2.01 ± 0.15*	<0.001
	8-HEPE	ND	ND	0.10 ± 0.08	NA

	12-HEPE	ND	ND	ND	NA
	15-HEPE	0.33 ± 0.06	ND	0.22 ± 0.05	NS
	14(15)-EpETE	0.37 ± 0.01	ND	ND	NA
	17(18)-EpETE	4.60 ± 0.40	ND	ND	NA
	14,15-DiHETE	ND	ND	1.10 ± 0.06	NA
	17,18-DiHETE	ND	ND	1.34 ± 0.18	NA
DHA (22:6n-3)	7(8)-EpDPE	0.39 ± 0.07	0.24 ± 0.12	ND	NS
	10(11)-EpDPE	0.36 ± 0.05[a]	0.26 ± 0.14[ab]	0.12 ± 0.002[b]	0.033
	13(14)-EpDPE	0.36 ± 0.08	0.34 ± 0.19	0.16 ± 0.02	NS
	16(17)-EpDPE	0.42 ± 0.03	0.37 ± 0.17	ND	NS
	19(20)-EpDPE	0.44 ± 0.07	0.57 ± 0.32	0.09 ± 0.03	NS

ND: not detected.

NQ: not quantifiable in NL and PL due to degradation of the deuterated standard (d4-PGE2) used to quantify them during hydrolysis.

[1]: p-value of ANOVA for three groups or unpaired t-test for two groups.

NS: not significant (p-value > 0.05).

NA: not available.

Alphabetical superscripts indicate significant differences between the groups by Newman-Keuls post-hoc test; asterisk (*) indicates significant differences between the groups by unpaired t-test.

Table 6. Kinetics of d4-13-HODE in plasma total (i.e. UE + ES fractions) following IV or gavage free d4-13-HODE administration.

	IV (n=3)	Gavage (n=3)
***k* or F* (min^{-1})[a]**	0.67 ± 0.10	0.016 ± 0.010
R_{max} or J_{in}[b] ((pmol/(uL×min))	-0.34 ± 0.13	0.0028 ± 0.0018
Half-life ($t_{1/2}$, min)	1.05 ± 0.16	71.19 ± 68.95

Data are mean ± SD of n=3 per group. Data were not statistically compared because IV kinetics reflect tracer elimination and gavage kinetics reflect tracer incorporation. Data are presented as mean ± SD of n=3 rats per group. [a]*k** is the rate constant for UE 13-HODE; *F* is turnover for ES 13-HODE. [b] R_{max} is the rate of UE d4-13-HODE elimination from plasma; J_{in} is the rate of ES d4-13-HODE incorporation into plasma following gavage.

Table 7**.** Total (UE + ES) labeled and unlabeled 13-HODE concentrations (pmol/mg or pmol/uL) in visceral and perirenal adipose, liver, heart, brain and plasma (after death). UE, Unesterified; ES, Esterified.

	d4-13-HODE concentration (pmol/mg)		**13-HODE concentration (pmol/mg)**	
	IV	Gavage	IV	Gavage
Visceral adipose	0.33 ± 0.30	3.11 ± 5.00	16.49 ± 12.86	9.84 ± 5.60
Perirenal adipose	Detected but not quantified due to sample loss[1]	Not detected, likely due to sample loss[1]	Detected but not quantified due to sample loss[1]	26.86 ± 7.81
Liver	0.0036 ± 0.0029	0.0057 ± 0.0057	1.08 ± 0.38	1.22 ± 0.88
Heart	0.011 ± 0.001	0.0088 ± 0.0061	1.40 ± 0.40	1.56 ± 0.35
Brain	Not detected	Not detected	0.11 ± 0.03	0.18 ± 0.08
Plasma (after death)	0.004 ± 0.002	0.100 ± 0.073*	0.20 ±0.05	0.13±0.06

Data are mean ± SD of n=3 per group. [1]Not quantifiable because the sample tube caps opened during homogenization, resulting in sample loss (as described in the methods section). *P<0.05 by unpaired t-test on log-transformed data, comparing gavage versus IV.

Table 8. AUC (pmol×min/μL), incorporation coefficient (k*) (μL/(mg×min), incorporation rate, J_{in} ((pmol/(mg×min)), turnover, F (min^{-1}), half life, $t_{1/2}$ (min) in visceral adipose, liver, and heart in IV and gavage rats.

		IV (UE)	*Gavage (ES)*
Plasma d4-13-HODE AUC		16.4 ± 19.3	2.1 ± 1.7[1]
Visceral adipose	k*	0.047 ± 0.041	0.88 ± 1.16
Liver	k* (×10^{-4})		
Heart	k* (×10^{-4})	3.6 ± 3.8	22.9 ± 12.2[†]
		20.3 ± 21.1	42.4 ± 23.0
Visceral adipose	J_{in} (×10^{-4})	22.2 ± 17.1	846.2 ± 1250.0
Liver	J_{in} (×10^{-4})		
Heart	J_{in} (×10^{-4})	0.18 ± 0.15	1.9 ± 1.3[†]
		1.0 ± 1.0	3.2 ± 1.7
Visceral adipose	F (×10^{-4})	1.6 ± 1.5	65.1 ± 72.3[†]
Liver	F (×10^{-4})		
Heart	F (×10^{-4})	0.15 ± 0.075	1.7 ± 1.1[††]
		0.7 ± 0.6	2.2 ± 1.5

Visceral adipose	$t_{1/2}$ ($\times 10^4$)	0.9 ± 0.9 (6.2 days)	0.05 ± 0.07 (0.34 day)†
Liver	$t_{1/2}$ ($\times 10^4$)	5.5 ± 2.3 (38.3 days)	0.5 ± 0.3 (3.6 days)††
Heart	$t_{1/2}$ ($\times 10^4$)	2.1 ± 2.3 (14.7 days)	0.4 ± 0.3 (3.1 days)

Data are mean ± SD of n=3 per group. † Indicates significant differences in log-transformed values between IV and gavage groups, by unpaired t-test applied to log-transformed values.

[1] *Ester*ified d4-13-HODE AUC determined by subtracting free from total d4-13-HODE AUC in each individual rat that received the tracer via gavage.

Table 9. Concentrations (nmol/mg) of rat brain LNA and ALA (mean± SD) in PL, FFA, and TL from low, moderate and high LNA diet.

	Low LNA diet	Moderate LNA diet	High LNA diet
LNA (nmol/g)			
PL	422.54±30.15[a]	666.90±39.72[b]	879.62±46.67[c]
FFA	0.53±0.35	0.48±0.13	0.41±0.10
TL	459.42±68.03[a]	1078.25±544.04[b]	1241.52±92.24[b]
ALA (nmol/g)			
PL	250.66±114.99	164.96±89.70	202.23±96.79
FFA	0.12±0.29	n.d.	n.d.
TL	250.66±114.99	164.96±89.70	202.23±96.79

Data are mean ± SD. Sample size of low, moderate, and high LNA dietary groups was 6, 5, and 4 respectively. Data were analyzed by one-Way ANOVA followed by Tukey's post-hoc test. N.D.: not detected. TL concentrations was the same as PL concentrations for ALA. Different letters represent significant differences between the means at $p < 0.05$.

Table 10. Concentrations (nmol/g) of rat brain ^{13}C-LNA and d5-ALA (mean± SD) in PL, FFA, and TL from low, moderate, and high LNA diet.

	Low LNA diet	Moderate LNA diet	High LNA diet
^{13}C-LNA (nmol/g)			
PL	0.014±0.003	0.010±0.002	0.011±0.002
FFA	0.0003±0.0002	0.0015±0.0017	0.0003±0.0002
TL	0.026±0.009	0.037±0.021	0.036±0.005
d5-ALA (nmol/g)			
PL	0.0014±0.0005^{b}	0.0006±0.0003^{ab}	0.0008±0.0004^{b}
FFA	0.0002±0.0003	0.0011±0.0013	0.0002±0.0001
TL	0.0024±0.0019	0.0064±0.0046	0.0030±0.0009

Data are reported as mean ± SD. Sample size of low, moderate, and high LNA diet groups was 6, 5, and 4 respectively. One-Way ANOVA followed by Tukey's test was applied. Different letters represent significant differences between the means at $p < 0.05$.

Table 11. Kinetic parameters of LNA and ALA incorporation coefficient (k*,mL*g^{-1}*min^{-1}×10^{-5}), incorporation rate (J_{in}, nmol*g^{-1}*min^{-1}×10^{-5}), turnover (F, 10^{5}min^{-1}) and half-life ($t_{1/2}$, ms) in rat brain PI, PS PC, PE, PL, FFA, and TL fractions.

		Low LNA diet	Moderate LNA diet	High LNA diet
LNA				
PI	k*	0.155±0.135	0.527±0.243	0.549±0.502
	J_{in}	4.106±3.600[a]	130.735±56.216[ab]	239.317±224.829[b]
	F	n/a	n/a	n/a
	$t_{1/2}$	n/a	n/a	n/a
PS	k*	0.189±0.173	0.426±0.366	0.662±0.589
	J_{in}	5.468±5.263	116.445±114.121	263.738±261.037
	F	n/a	n/a	n/a
	$t_{1/2}$	n/a	n/a	n/a
PC	k*	1.291±1.406	1.211±0.605	2.523±1.740
	J_{in}	38.829±48.343[a]	327.487±210.319[ab]	972.063±733.717[b]
	F	n/a	n/a	n/a
	$t_{1/2}$	n/a	n/a	n/a
PE	k*	0.202±0.214[a]	0.559±0.344[ab]	0.958±0.585[b]
	J_{in}	5.641±6.508[a]	153.945±117.717[ab]	408.044±267.085[b]
	F	n/a	n/a	n/a
	$t_{1/2}$	n/a	n/a	n/a
PL	k*	1.306±0.685[a]	1.529±0.947[a]	3.513±1.009[b]
	J_{in}	36.790±26.063[a]	401.263±267.125[a]	1365.845±430.347[b]
	F	0.086±0.049[a]	0.621±0.451[a]	1.542±0.422[b]
	$t_{1/2}$	6.515±3.574[a]	0.987±0.684[b]	0.284±0.070[b]

FFA	*k**	0.038±0.032	0.168±0.128	0.090±0.046
	J_{in}	1.087±1.036[a]	41.488±31.321[b]	36.103±22.241[ab]
	F	n/a	n/a	n/a
	$t_{1/2}$	n/a	n/a	n/a
TL	*k**	2.694±1.678[a]	5.097±2.809[a]	11.648±4.603[b]
	J_{in}	76.434±54.550[a]	1288.859±585.479[a]	4603.385±2172.119[b]
	F	0.162±0.103[a]	1.316±0.657[a]	3.768±1.977[b]
	$t_{1/2}$	5.351±6.549	0.433±0.295	0.128±0.045
ALA				
PI	*k**	0.008±0.006	0.009±0.010	0.002±0.003
	J_{in}	0.20±0.15	0.34±0.41	0.08±0.11
	F	n/a	n/a	n/a
	$t_{1/2}$	n/a	n/a	n/a
PS	*k**	0.003±0.008	0.001±0.003	0.001±0.002
	J_{in}	0.10±0.24	0.05±0.10	0.02±0.04
	F	n/a	n/a	n/a
	$t_{1/2}$	n/a	n/a	n/a
PC	*k**	0.13±0.12	0.08±0.07	0.08±0.05
	J_{in}	3.75±4.30	3.03±3.18	2.48±1.72
	F	n/a	n/a	n/a
	$t_{1/2}$	n/a	n/a	n/a
PE	*k**	0.04±0.03	0.03±0.02	0.03 ±0.02
	J_{in}	1.12±0.96	1.08±0.85	1.09±0.76
	F	n/a	n/a	n/a
	$t_{1/2}$	n/a	n/a	n/a
PL	*k**	0.16±0.11[a]	0.03±0.01[b]	0.06±0.01[ab]
	J_{in}	4.11±2.92	1.06±0.37	2.10±0.39
	F	0.02±0.02	0.01±0.003	0.01±0.009
	$t_{1/2}$	56.85±63.31	64.35±25.47	40.74±19.12

FFA	k*	0.02±0.02	0.07±0.09	0.02±0.01
	J_{in}	0.59±0.75	2.29±2.50	0.52±0.36
	F	n/a	n/a	n/a
	$t_{1/2}$	n/a	n/a	n/a
TL	k*	0.23±0.17	0.33±0.15	0.30±0.16
	J_{in}	6.54±5.53	11.24±4.38	9.45±4.52
	F	0.04±0.04	0.10±0.08	0.05±0.03
	$t_{1/2}$	22.83±24.96	8.15±6.85	9.66±4.69

Data were expressed as mean± SD. Sample size of low, moderate, and high LNA diet groups was 6, 5, and 4 respectively. One-Way ANOVA followed by Tukey's test was applied. Different letters represent significant differences between the means at $p < 0.05$.

Table 12. Kinetics of LNA and ALA conversion coefficient (*k**), conversion rate (J_{OXLNAM}), turnover (*F*) and half-life ($t_{1/2}$) into free OXLAMs in rat brain.

	Low LNA diet	Moderate LNA diet	High LNA diet
9-HODE			
*K** (min*g^{-1}*mL^{-1}×10^{-5})	0.003±0.002	0.004±0.004	0.003±0.001
λ	0.084±0.128	0.513±0.574	0.829±0.805
J_{OXLNAM} (nmol*g^{-1}*min^{-1}×10^{-5})	3.238±3.201	2.165±0.639	2.728±2.422
F (×10^{5}min^{-1})	749±496	575±222	683±584
$t_{1/2}$ (ms)	0.0008±0.001	0.0009±0.001	0.001±0.001
9,12,13-TriHOME			
*K** (min*g^{-1}*mL^{-1}×10^{-5})	0.002±0.001	0.002±0.003	0.002±0.002
λ	0.159±0.222	1.226±1.796	2.592±2.708
J_{OXLNAM} (nmol*g^{-1}*min^{-1}×10^{-5})	0.784±0.655	0.518±0.126	0.477±0.298
F (×10^{7}min^{-1})	5.31±3.59	4.68±1.79	4.14±2.33

$t_{1/2}$ (ms)	0.001±0.001	0.001±0.001	0.001±0.001

Data are mean ± SD. Sample size of low, moderate, and high LNA dietary groups was 6, 5, and 4 respectively. Data were analyzed by one-Way ANOVA followed by Tukey's test was applied. No significant differences were detected at $p<0.05$.

Table 13. Concentration (mg/g) and percent composition of fatty acids in pooled monkey chow biscuits (n=4).

	Mean		SD	% composition
Tridecylic acid/Tridecanoic acid	0.17	±	0.07	0.81
Myristic Acid/Tetradecanoic Acid	0.20	±	0.04	0.96
Palmitic Acid/Hexadecanoic Acid	4.15	±	0.78	19.96
Palmitoleic Acid	0.33	±	0.06	1.57
Stearic Acid/Octadecanoic Acid	1.98	±	0.36	9.54
Oleic Acid	6.33	±	1.15	30.47
Eladic Acid	0.37	±	0.06	1.77
Linoleic Acid (LA)	6.40	±	1.18	30.79
Gamma-linolenic acid	0.05	±	0.00	0.25
Linolenic Acid (ALA)	0.43	±	0.07	2.08
Gondoic Acid/11-eicosanoic acid	0.14	±	0.03	0.68
11,14-Eicosadienoic acid	0.09	±	0.02	0.42
Arachidonic acid (AA)	0.05	±	0.01	0.22
Eicosapentaenoic acid (EPA)	0.04	±	0.02	0.20
Docosahexaenoic Acid (DHA)	0.06	±	0.01	0.29

Table 14. Male offspring DMR gene mappings to soluble epoxide hydrolase (EPHX) genes from pairwise comparisons of maternal groups in right prefrontal cortex, hippocampus, and hypothalamus at 6 months.

Analysis		***Genomic Coordinates***				***Annotation***		***Statistics***	
Brain Region	Contrast	Chr	Start	End	Width	Region	Symbol	Difference	Empirical p-value
Prefrontal Cortex	RvC	chr1	83,358,175	83,358,588	414	Intron	*EPHX1*	-12%	0.031
Hippocampus	RvC	chr1	83,358,275	83,358,954	680	Promoter	*EPHX1*	-12%	0.004
Hypothalamus	RvO	chr1	83,385,656	83,386,392	737	Exon	*EPHX1*	12%	0.045
Hypothalamus	PvC	chr1	131,968,356	131,969,182	827	Intron	*EPHX4*	10%	0.048
Prefrontal Cortex	PvC	chr1	131,969,062	131,969,256	195	Intron	*EPHX4*	14%	0.006
Prefrontal Cortex	PvO	chr1	131,969,151	131,969,224	74	Intron	*EPHX4*	14%	0.038
Prefrontal Cortex	PvO	chr1	132,020,286	132,021,576	1,291	Intron	*EPHX4*	-11%	0.018
Prefrontal Cortex	OvC	chr1	132,141,796	132,142,125	330	Exon	*EPHX4*	15%	0.012
Prefrontal Cortex	RvC	chr1	132,143,529	132,144,177	649	Intron	*EPHX4*	-12%	0.043
Prefrontal Cortex	PvC	chr1	132,143,767	132,144,177	411	Intron	*EPHX4*	-19%	0.004
Hippocampus	RvC	chr8	27,758,351	27,758,511	161	Promoter	*EPHX2*	18%	0.021
Hippocampus	RvC	chr8	27,764,935	27,765,614	680	Intron	*EPHX2*	14%	0.013
Hippocampus	RvC	chr8	27,777,548	27,778,550	1,003	Exon	*EPHX2*	-14%	0.030
Hypothalamus	RvC	chr8	27,777,734	27,778,590	857	Exon	*EPHX2*	-15%	0.037
Prefrontal Cortex	RvC	chr8	27,777,754	27,778,688	935	Exon	*EPHX2*	-15%	0.025
Prefrontal Cortex	RvC	chr8	27,786,470	27,786,975	506	Intron	*EPHX2*	15%	0.026
Hippocampus	RvO	chr8	27,789,232	27,790,169	938	Exon	*EPHX2*	12%	0.028
Prefrontal Cortex	RvC	chr8	27,799,632	27,800,093	462	Intron	*EPHX2*	-13%	0.033
Hippocampus	RvC	chr8	27,800,281	27,800,734	454	Intron	*EPHX2*	9%	0.034
Hypothalamus	PvC	chr8	27,800,943	27,802,162	1,220	Intron	*EPHX2*	7%	0.047
Hippocampus	RvC	chr19	14,826,517	14,826,694	178	Downstream	*EPHX3*	-15%	0.013
Hypothalamus	PvC	chr19	14,836,329	14,836,464	136	Promoter	*EPHX3*	11%	0.022

OvC = Obese vs. Control, RvO = Restriction vs. Obese, PvO = Pravastatin vs. Obese, RvC = Restriction vs. Control, PvC = Pravastatin vs. Control.

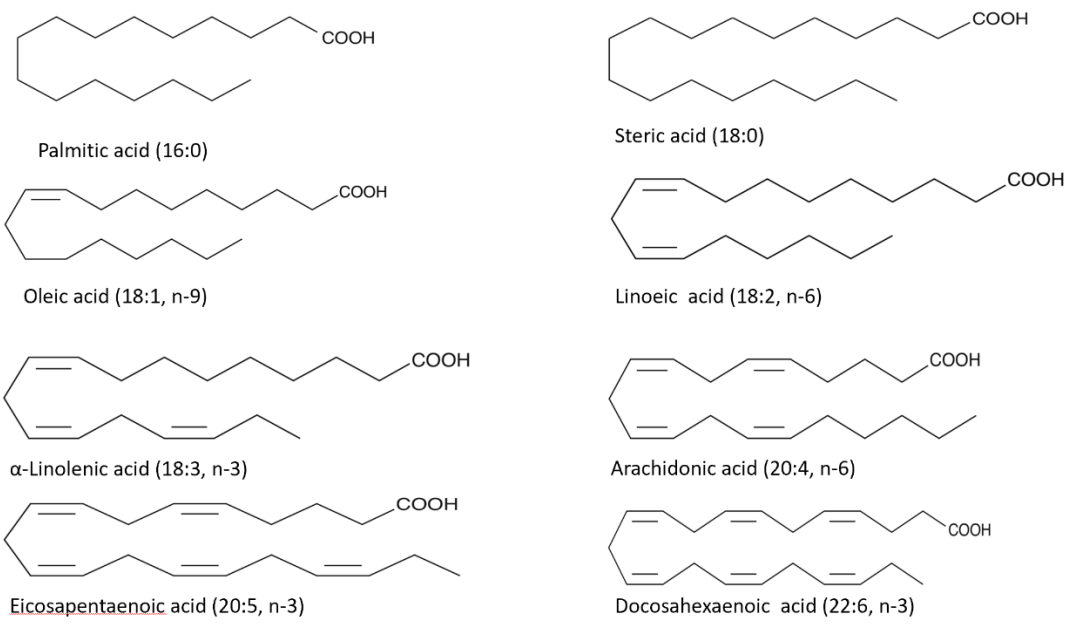

Figure 1. Examples of saturated, monounsaturated, and polyunsaturated fatty acids.

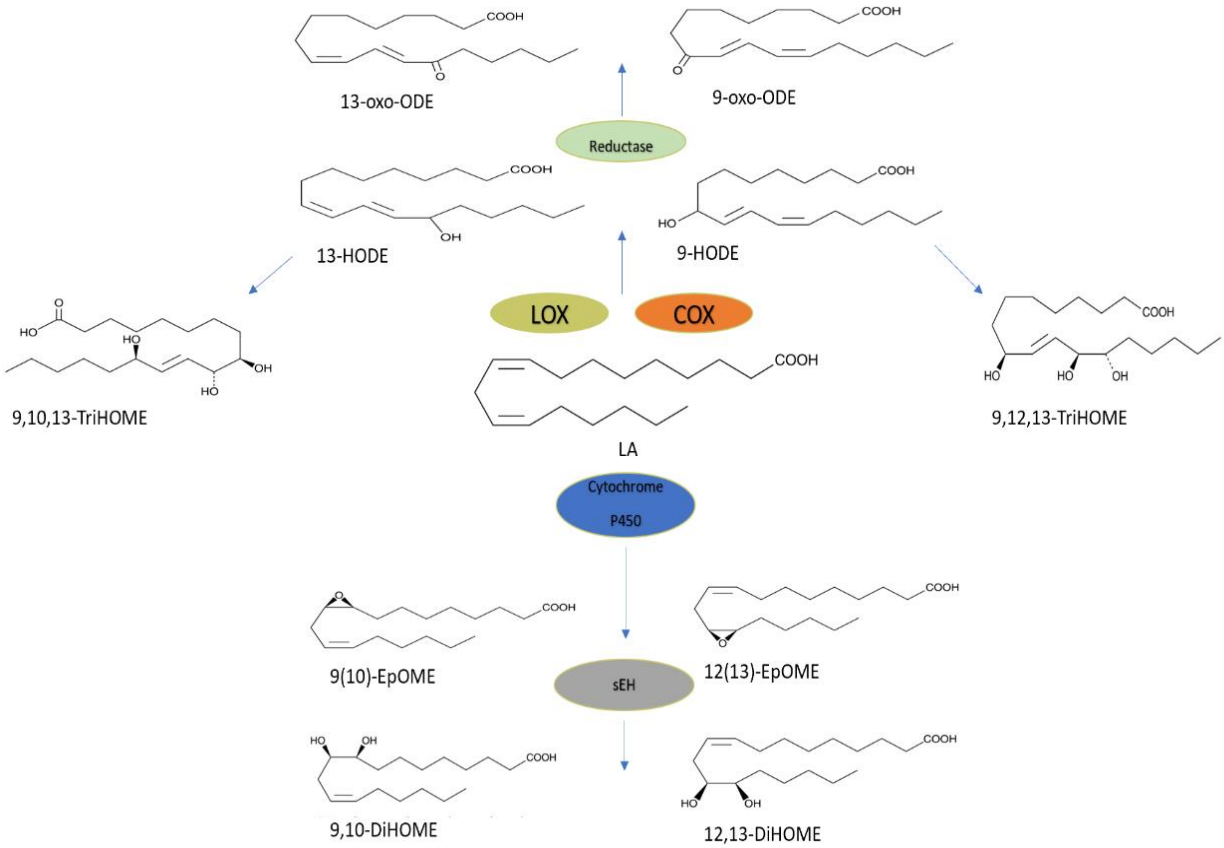

Figure 2. Enzymatic pathways of oxidized linoleic acid metabolites formation (revised from Hennebelle et al 2020).

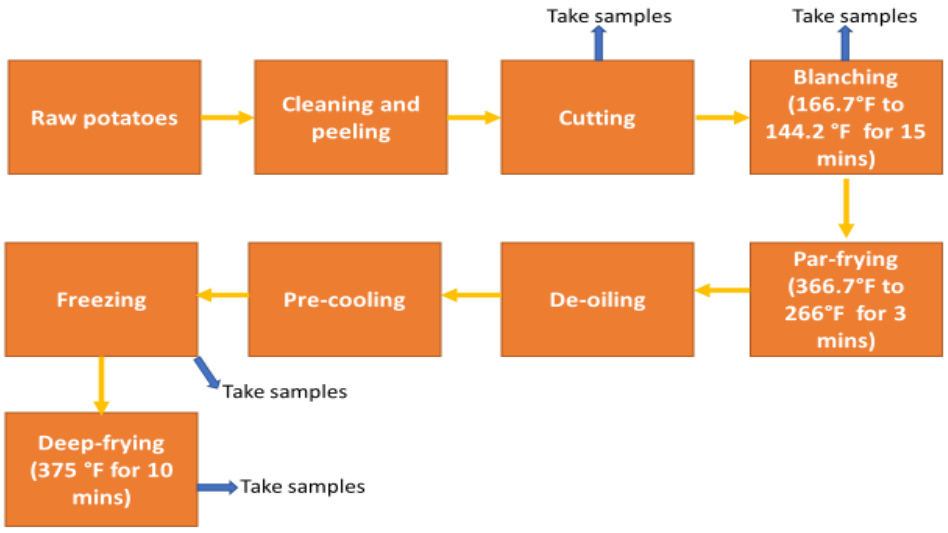

Figure 3. Schematic representation of raw potato process.

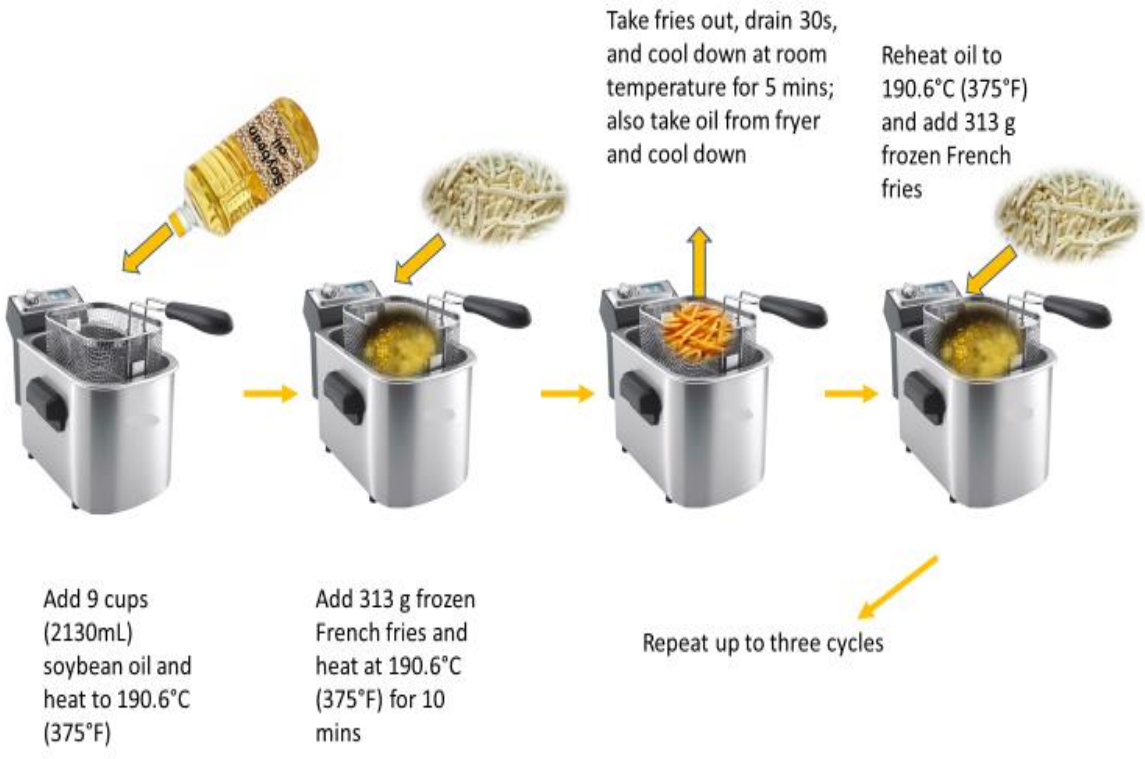

Figure 4. Schematic representation of repeated frying.

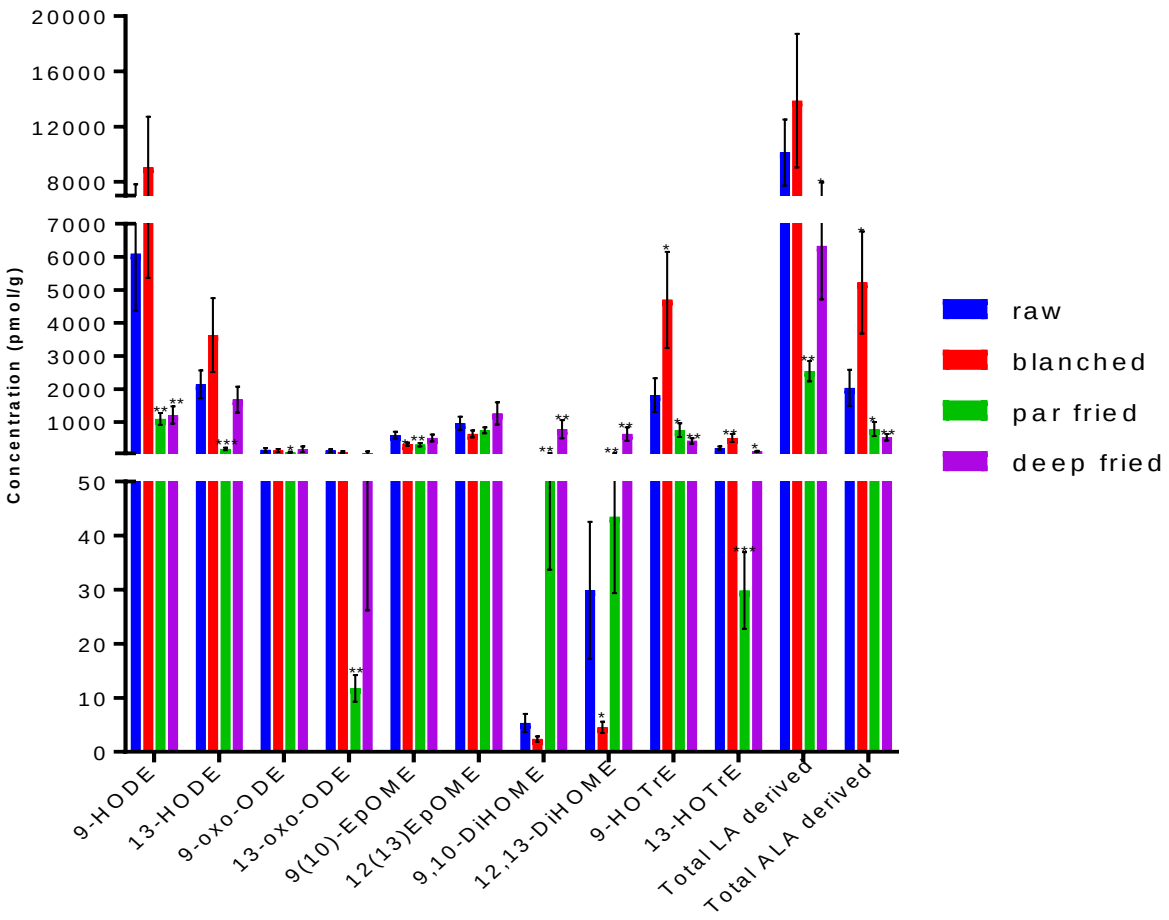

Figure 5. Concentrations (pmol/g) of LA- and ALA- derived oxylipins in peeled and sliced raw potatoes, blanched potatoes, par fried potatoes and deep fried potatoes. Concentrations are expressed as mean ± standard deviation (SD); n=5 per condition. One-way repeated measure ANOVA followed by Dunnett's multiple comparison test (compared to baseline samples) was applied. Significant differences are expressed in the figure as $p<0.05$ *, $p<0.01$ **, $p<0.001$ ***. 9-hydroxyoctadecadienoic acid: 9-HODE,13-hydroxyoctadecadienoic acid: 13-HODE, 9-oxo-octadecadienoic acid: 9-oxo-ODE, 13-oxo-octadecadienoic acid: 13-oxo-ODE, 12(13)-epoxyoctadecamonoenoic acid: 12(13)-EpOME, 9(10)-epoxyoctadecamonoenoic acid: 9(10)-EpOME, 12,13-dihydroxyoctadecamonoenoic acid: 12,13-DiHOME, 9,10-

dihydroxyoctadecamonoenoic acid: 9,10-DiHOME, 9-hydroxyoctadecatrienoic acid : 9-HOTrE, 13-hydroxyoctadecatrienoic acid: 13-HOTrE.

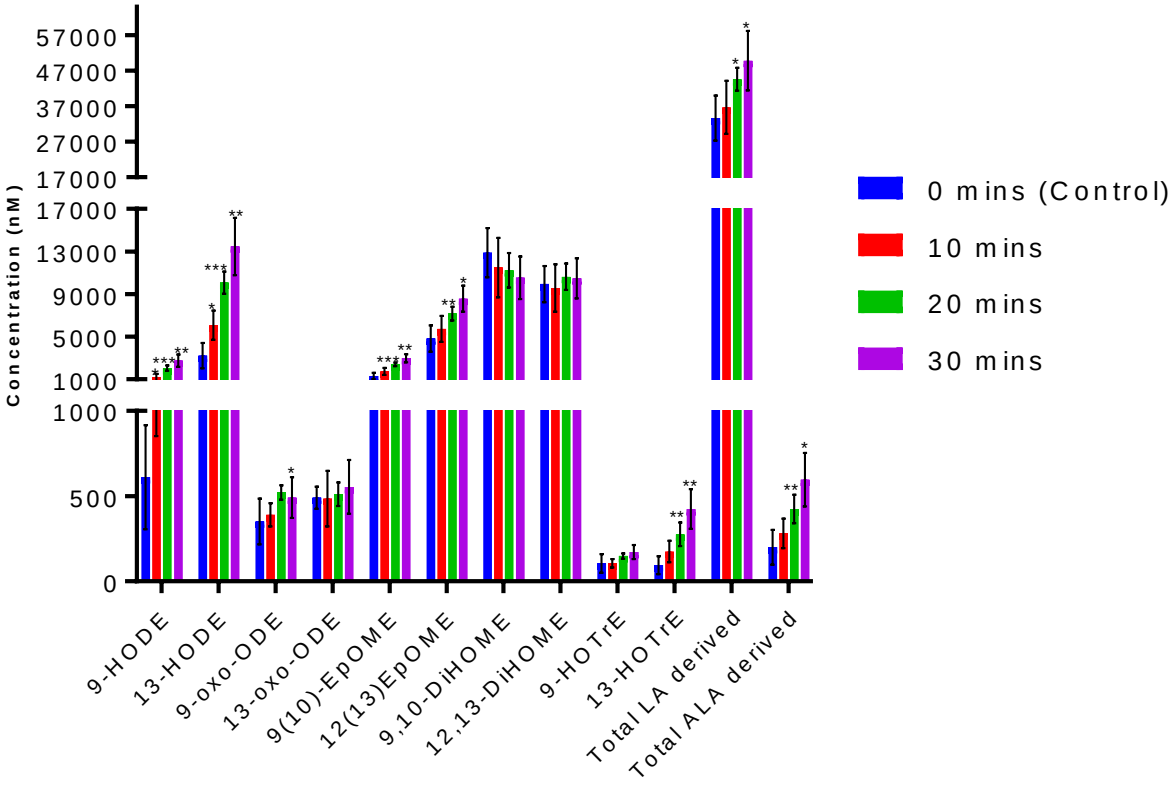

Figure 6. Concentration (nM) of LA and ALA derived oxylipins in oil subjected to repeated heat cycles, 10 minutes each. Baseline samples consisted of non-heated oil (i.e. 0 min control). Concentrations are expressed at mean ± standard deviation (SD); n=5 per time point. One-way repeated measure ANOVA followed by Dunnett's multiple comparison test (compared to baseline samples) was applied. Significant differences are expressed on the figure as $p<0.05$ *,

p<0.01 **, p<0.001 ***. 0 min is preheated oil, 10 min is 1st frying cycle, 20 min is 2nd frying cycle, and 30 min 3rd frying cycle. 9-hydroxyoctadecadienoic acid: 9-HODE,13-hydroxyoctadecadienoic acid: 13-HODE, 9-oxo-octadecadienoic acid: 9-oxo-ODE, 13-oxo-octadecadienoic acid: 13-oxo-ODE, 12(13)-epoxyoctadecamonoenoic acid: 12(13)-EpOME, 9(10)-epoxyoctadecamonoenoic acid: 9(10)-EpOME, 12,13-dihydroxyoctadecamonoenoic acid: 12,13-DiHOME, 9,10-dihydroxyoctadecamonoenoic acid: 9,10-DiHOME, 9-hydroxyoctadecatrienoic acid : 9-HOTrE, 13-hydroxyoctadecatrienoic acid: 13-HOTrE.

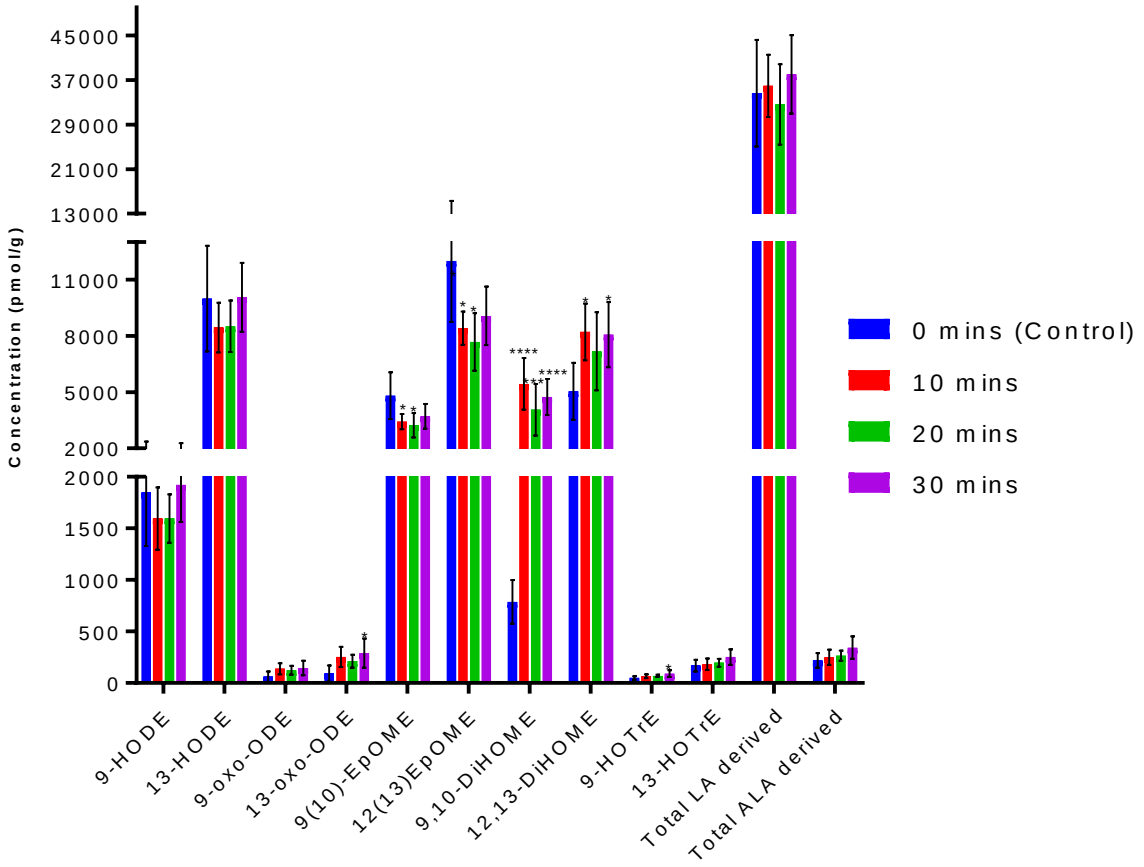

Figure 7. Concentration (pmol/g) of LA- and ALA- derived oxylipins in French fries subjected to three repeated frying cycles. Concentrations are expressed at mean ± standard

deviation (SD); n=5 per time point. Control concentrations were obtained from frozen French fries (0 min). Three batches of French fries were then fried for 10 minutes each using the same oil. Thus, 10, 20 and 30 min on the graph reflect the total heat applied to the oil used to fry the French fries. 10 min reflects the first batch that was fried for 10 min. 20 min reflects the second batch that was fried for 10 min using the same oil. 30 min reflects the third batch that was fried for 10 min using the same oil. One-way ordinary ANOVA followed by Dunnett's multiple comparison test (compared to baseline samples) was applied. Significant differences are expressed in the figure as $p<0.05$ *, $p<0.01$ **, $p<0.001$ ***, $p<0.0001$ ****. 9-hydroxyoctadecadienoic acid: 9-HODE,13-hydroxyoctadecadienoic acid: 13-HODE, 9-oxo-octadecadienoic acid: 9-oxo-ODE, 13-oxo-octadecadienoic acid: 13-oxo-ODE, 12(13)-epoxyoctadecamonoenoic acid: 12(13)-EpOME, 9(10)-epoxyoctadecamonoenoic acid: 9(10)-EpOME, 12,13-dihydroxyoctadecamonoenoic acid: 12,13-DiHOME, 9,10-dihydroxyoctadecamonoenoic acid: 9,10-DiHOME, 9-hydroxyoctadecatrienoic acid : 9-HOTrE, 13-hydroxyoctadecatrienoic acid: 13-HOTrE.

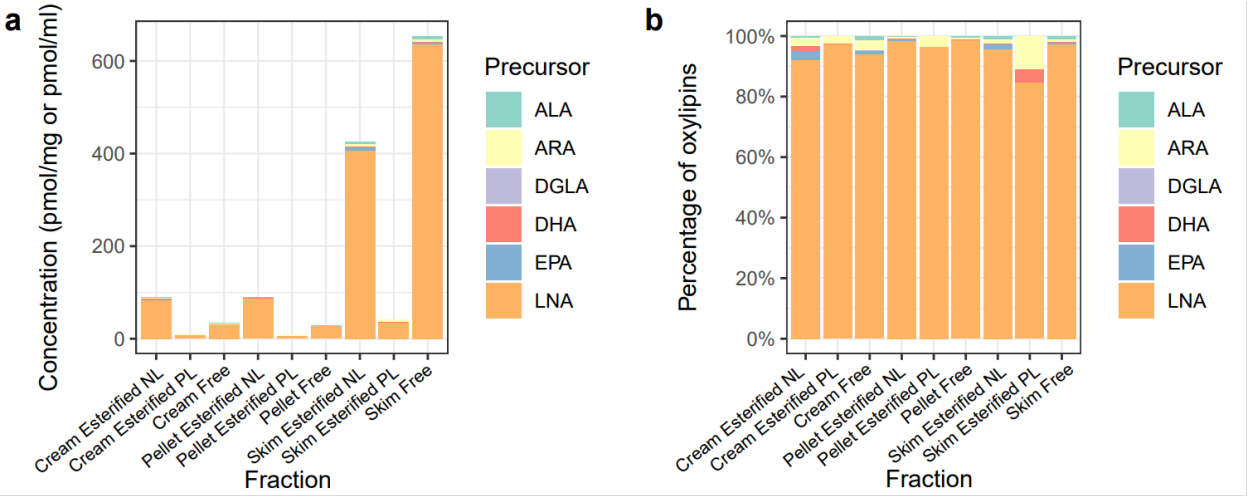

Fig. 8. Oxylipin distribution in cream, cell pellet, and skim fractions of human milk (n=3 per lipid fraction). Concentration (a) and percentage (b) of oxylipins esterified to NL, esterified to PL and in free form are presented.

(A) IV-injected rats

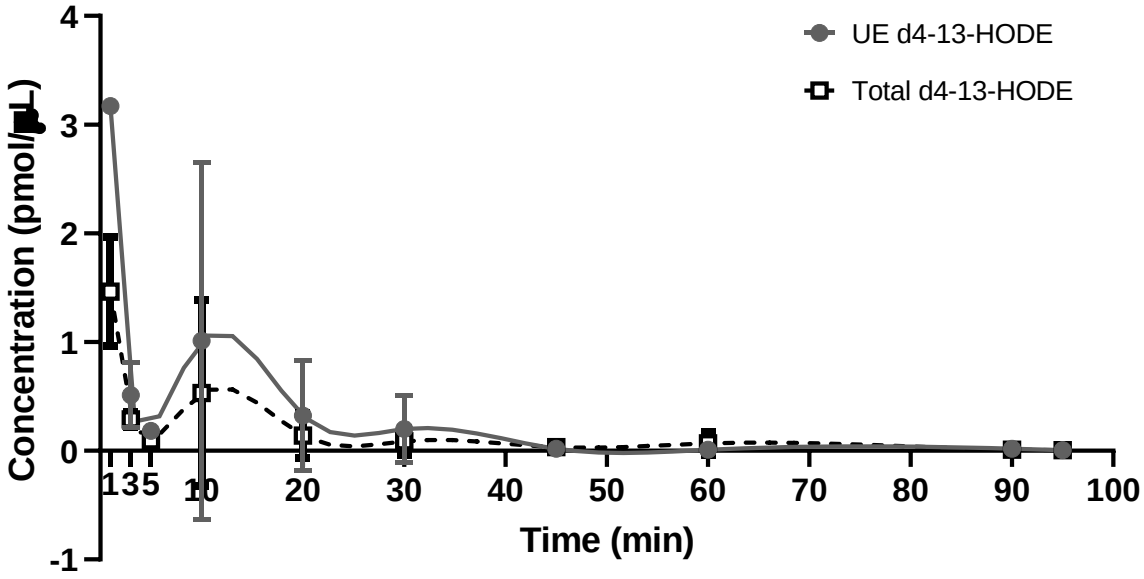

(B) Gavaged rats

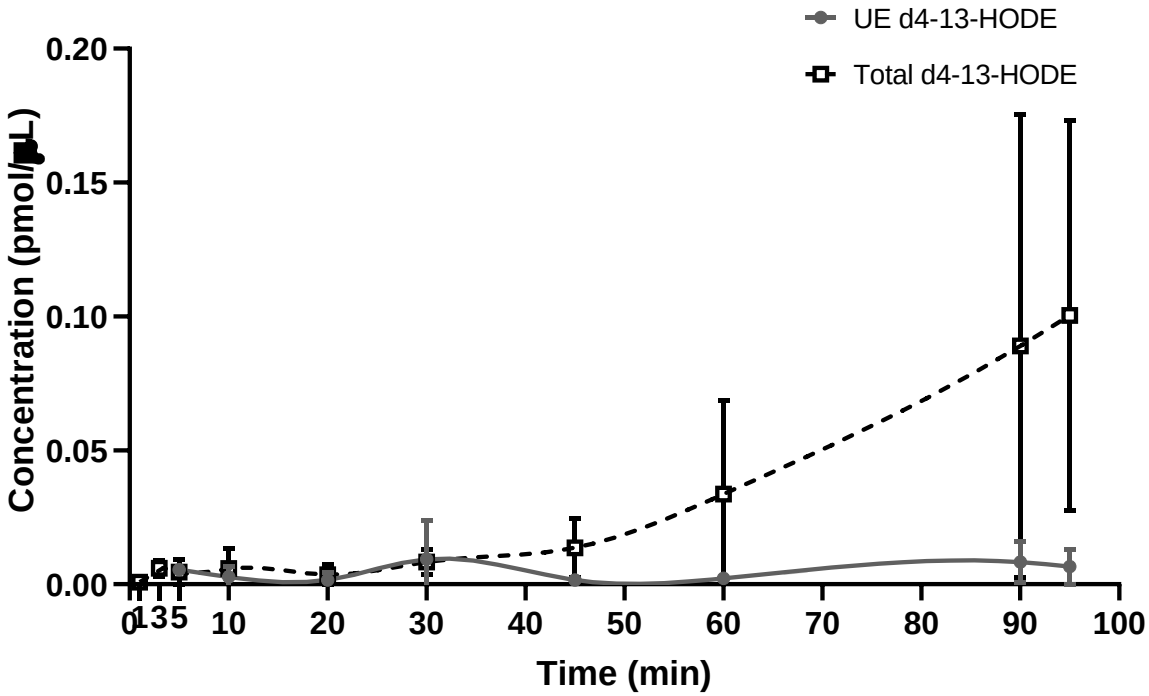

Figure 9: Concentration-Time plot of d4-13-HODE in plasma of rats injected IV (A) or gavaged (B) with the tracer. For (A), data are mean ± SD of n=3 per group for total d4-13-HODE, and n=2-3 for unesterified (UE) d4-13-HODE, except at one min where n=1. For (B), data are mean ± SD of n=3 per group for total d4-13-HODE, except at 3, 10 and 45 min when n=2. Data are 2-3 per time-point for UE d4-13-HODE, except at 1 min (n=1) and at 3 and 5 min, where we did not have sufficient plasma volume left in all 3 rats for free tracer measurements.

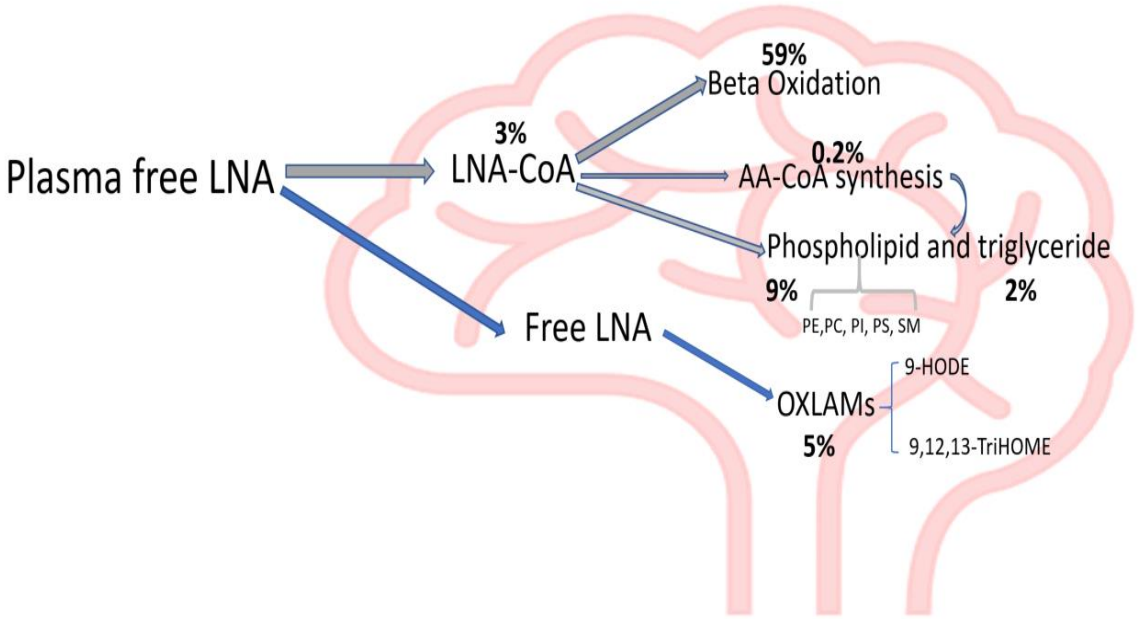

Figure 10. Schematic pathways of plasma LNA upon entering the brain.

Grey arrows indicate pathways that have been reported in the literature. Blue arrows indicate pathways found in this present study. Percent utilization of LNA from each pathway is shown.

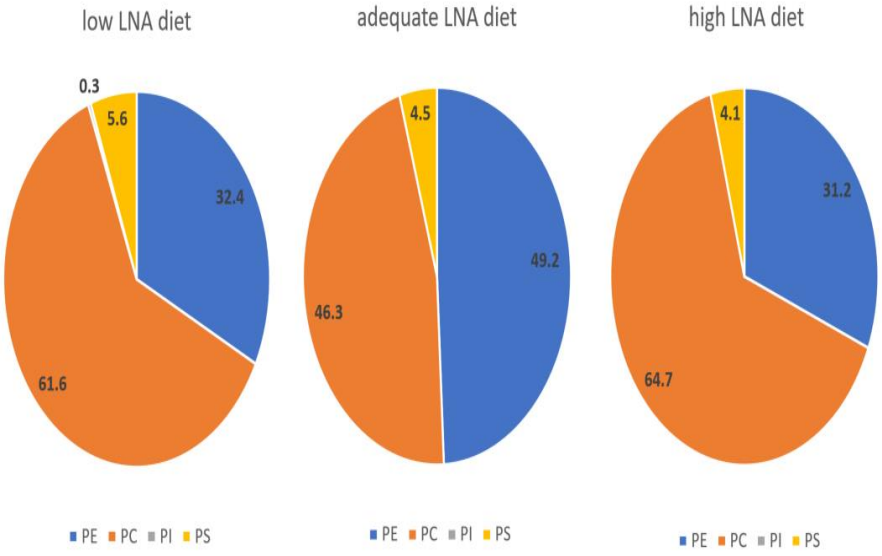

Figure 11. Distribution percentage of endogenous LA from PE, PC, PI, and PS classes in rat brain from low, moderate, and high LNA diet groups. Sample size of low, moderate, and high LNA diet groups was 6, 5, and 4 respectively. PI was not detected in moderate and high LNA groups

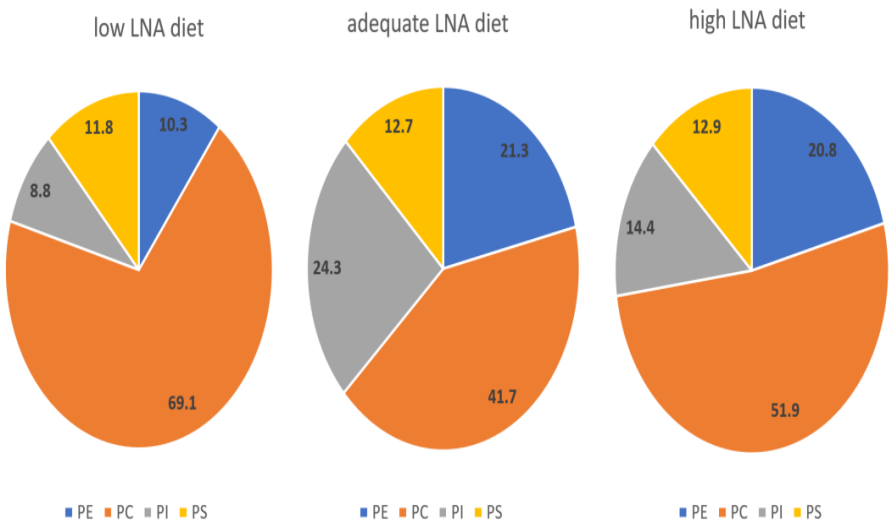

Figure 12. Distribution percentage of 13C labelled LA from PE, PC, PI, and PS classes in rat brain from low, moderate, and high LNA diet groups. Sample size of low, moderate, and high LNA diet groups was 6, 5, and 4 respectively.

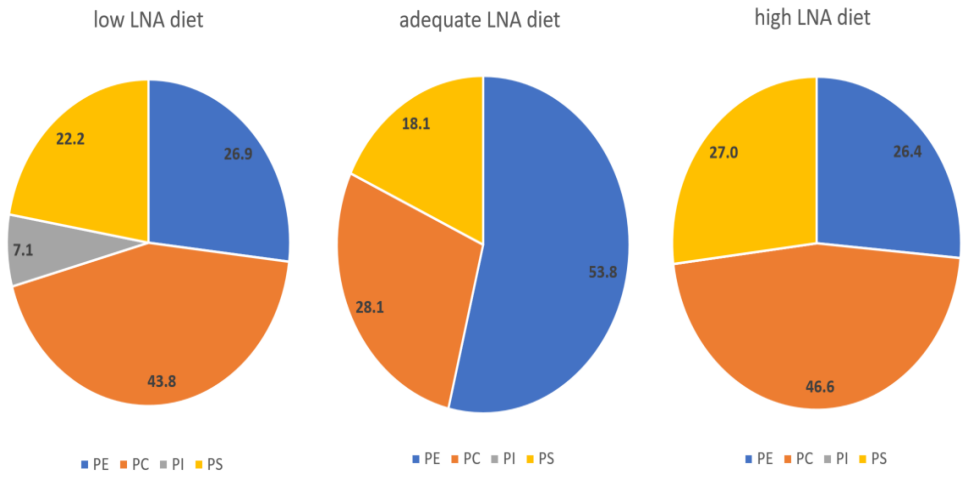

Figure 13. Distribution percentage of endogenous ALA from PE, PC, PI, and PS classes in rat brain from low, moderate, and high LNA diet groups. Sample size of low, moderate, and high

LNA diet groups was 6, 5, and 4 respectively. PI was not detected in moderate and high LNA groups.

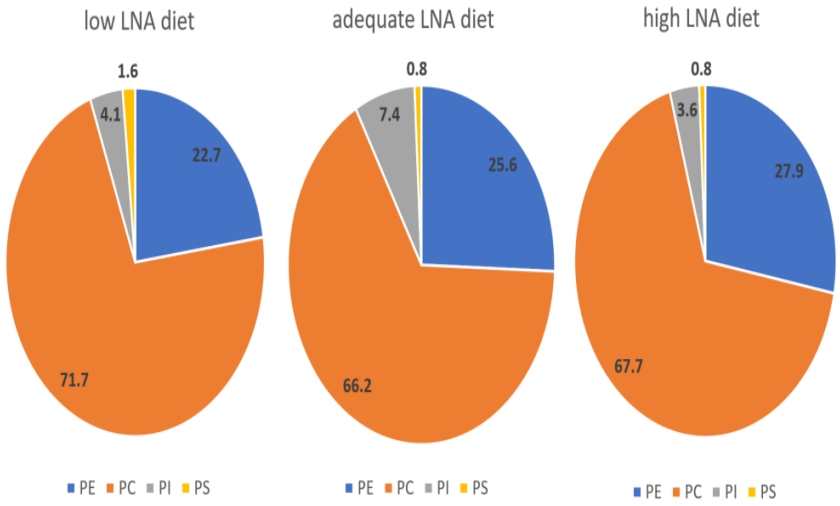

Figure 14. Distribution percentage of deuterium labelled d-ALA from PE, PC, PI, and PS classes in rat brain from low, moderate, and high LNA diet groups. Sample size of low, moderate, and high LNA diet groups was 6, 5, and 4 respectively.

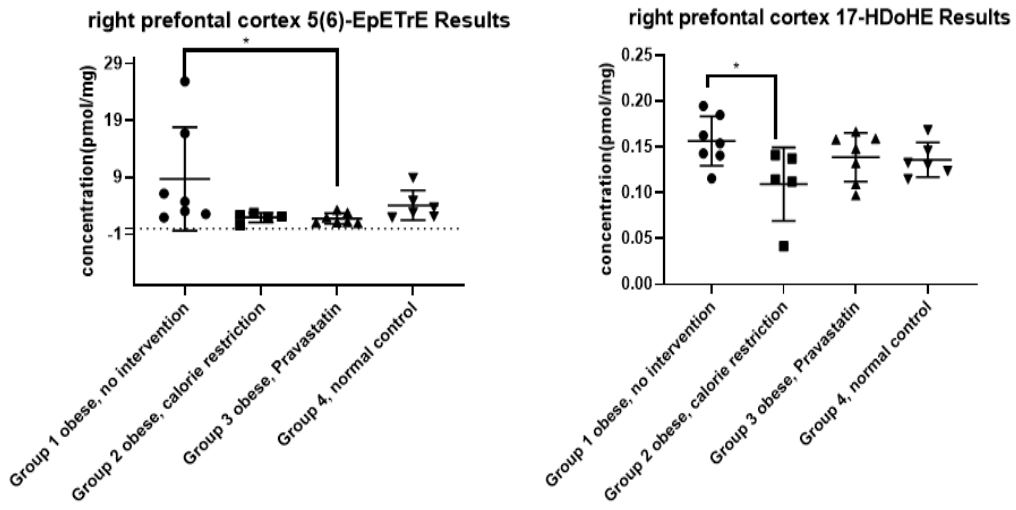

Figure 15. Significant oxylipin concentrations in male offspring right prefrontal cortex at 6 months. Data were expressed as mean ± SD. Each individual sample was expressed as a dot. Significant diffidence was expressed as * at $p<0.05$. Kruskal-Wallis one-way ANOVA followed by Dunn's multiple comparison test was applied for5(6)-EpETrE and one-way ANOVA followed by Tukey's multiple comparison was used. for 17-HDoHE data.

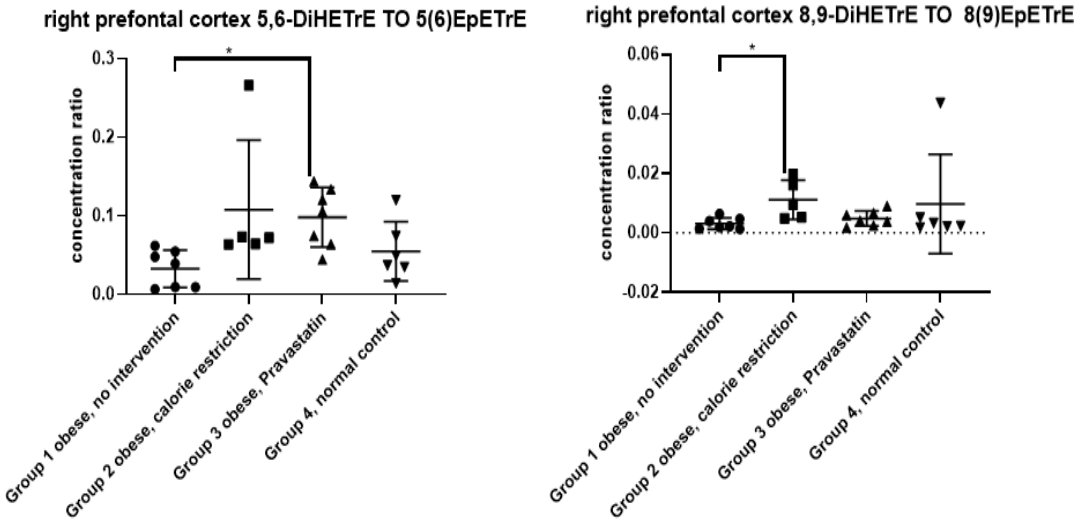

Figure 16. Significant diol to epoxy ratios in male offspring right prefrontal cortex at 6 months. Data were expressed as mean ± SD. Each individual sample was expressed as a **dot. Significant**

diffidence was expressed as * at $p<0.05$. Kruskal-Wallis one-way ANOVA followed by Dunn's multiple comparison test was applied.

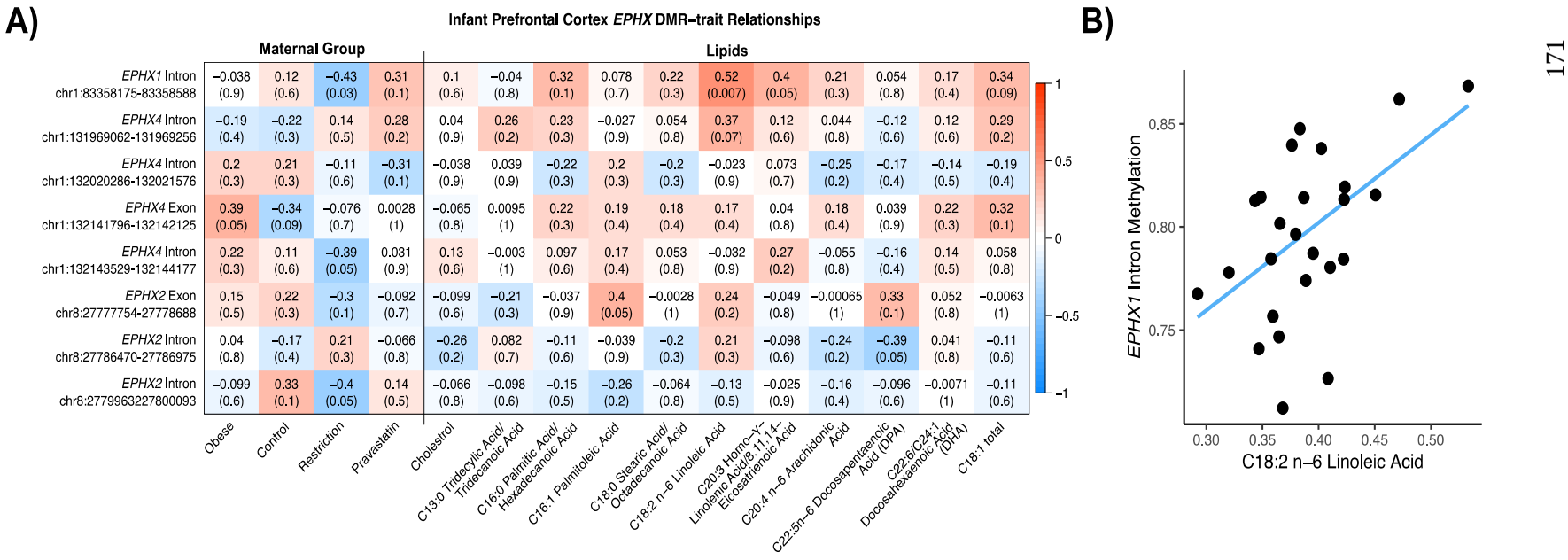
A)
Infant Prefrontal Cortex EPHX DMR–trait Relationships
Maternal Group
Lipids
EPHX1 Intron chr1:83358175-83358588
EPHX4 Intron chr1:131969062-131969256
EPHX4 Intron chr1:132020286-132021576
EPHX4 Exon chr1:132141796-132142125
EPHX4 Intron chr1:132143529-132144177
EPHX2 Exon chr8:27777754-27778688
EPHX2 Intron chr8:27786470-27786975
EPHX2 Intron chr8:2779963227800093
Obese
Control
Restriction
Pravastatin
Cholestrol
C13:0 Tridecylic Acid/ Tridecanoic Acid
C16:0 Palmitic Acid/ Hexadecanoic Acid
C16:1 Palmitoleic Acid
C18:0 Stearic Acid/ Octadecanoic Acid
C18:2 n–6 Linoleic Acid
C20:3 Homo–γ–Linolenic Acid/8,11,14–Eicosatrienoic Acid
C20:4 n–6 Arachidonic Acid
C22:5n–6 Docosapentaenoic Acid (DPA)
C22:6/C24:1 Docosahexaenoic Acid (DHA)
C18:1 total
1
0.5
0
−0.5
−1
B)
EPHX1 Intron Methylation
0.85
0.80
0.75
0.30
0.35
0.40
0.45
0.50
C18:2 n–6 Linoleic Acid

Figure 17. Correlations between the smoothed methylation levels of DMRs mapping to *EPHX* genes and lipid levels in male offspring prefrontal cortex at 6 months old. **A)** Heatmap of correlation testing results. The heatmap colors represent the correlation between the methylation values of the gene regions with the maternal group and lipid levels. Correlation values are reported with their p-values in parentheses. Overlapping DMRs were merged. **B)** Scatter plot with a line of best fit for smoothed methylation levels in the *EHPX1* intron (chr1:83358175-83358588) and linoleic acid levels

Appendix: supplemental materials

Supplementary Table 1**.** List of 72 oxylipins measured by LC-MS/MS and their abbreviations and precursor fatty acids.

	Abbreviation	Surrogate	Precursor ion *m/z*	Parent ion *m/z*	RT
Linoleic acid (LA, 18:2 n-6) metabolites:					
• 9-hydroxyoctadecadienoic acid	9-HODE	d4-9-HODE	295.2	171.1	17.42
• 13-hydroxyoctadecadienoic acid	13-HODE	d4-9-HODE	295.2	195.2	17.25
• 9-oxo-octadecadienoic acid	9-oxo-ODE	d6-20-HETE	293.2	185.1	19.25
• 13-oxo-octadecadienoic acid	13-oxo-ODE	d6-20-HETE	293.2	195.1	18.44
• 12(13)-epoxyoctadecamonoenoic acid	12(13)-EpOME	d-11-11(12)EpEtrE	295.3	195.2	21.65
• 9(10)-epoxyoctadecamonoenoic acid	9(10)-EpOME	d-11-11(12)EpEtrE	295.3	171.1	22.07
• 12,13-dihydroxyoctadecamonoenoic acid	12,13-DiHOME	d11-14,15-DiHETrE	313.2	183.2	11.95
• 9,10-dihydroxyoctadecamonoenoic acid	9,10-DiHOME	d11-14,15-DiHETrE	313.2	201.2	12.42
• 9,12,13-trihydroxyoctadecamonoenoic acid	9,12,13-TriHOME	d4-PGE2	329.2	211.1	6.1
• 9,10,13-trihydroxyoctadecamonoenoic acid	9,10,13-TriHOME	d4-PGE2	329.2	171.1	6.2
Di-homo-gamma-linoleic acid (DGLA) 20:3 n-6) metabolites:					
• 15(S)-hydroxyeicosatrienoic acid	15(S)-HETrE	d8-5-HETE	321.2	221.2	20.15
• Prostaglandin E1	PGE1	d4-PGE2	353.3	317.2	6.72
• Prostaglandin D1	PGD1	d4-PGE2	353.3	317.2	6.9
Arachidonic acid (AA, 20:4 n-6) metabolites					
• 14(15)-epoxyeicosatrienoic acid	14(15)-EpETrE	d-11-11(12)EpEtrE	319.2	219.3	22.1
• 8(9)-epoxyeicosatrienoic acid	8(9)-EpETrE	d-11-11(12)EpEtrE	319.2	167.2	23.12

• 11(12)-epoxyeicosatrienoic acid	11(12)-EpETrE	d-11-11(12)EpEtrE	319.2	167.2	23.4
• 5(6)-epoxyeicosatrienoic acid	5(6)-EpETrE	d-11-11(12)EpEtrE	319.2	191.1	23.75
• 20-hydroxyeicosatetraenoic acid	20-HETE	d6-20-HETE	319.2	275.1	15.7
• 6-trans-leukotriene B4	6-trans-LTB4	d4-LTB4	335.2	195.1	10.8
• Leukotriene B4	LTB4	d4-LTB4	335.2	195.1	11.27
• Leukotriene C4	LTC4	d4-LTB4	624.3	272.1	8.9
• Leukotriene D4	LTD4	d4-LTB4	495.3	177.1	7.3
• Leukotriene E4	LTE4	d4-LTB4	438.2	333.3	8.9
• 20-OH-Leukotriene B4	20-OH-LTB4	d4-LTB4	351.2	195.2	4.32
• 20-COOH- Leukotriene B4	20-COOH-LTB4	d4-LTB4	365.2	347.2	3.7
• Tromboxane B2	TXB2	d4-TXB2	369.2	169.1	6
• 6-keto-prostaglandin F1-α	6-keto-PGF1α	d4-PGE2	369.3	163.2	4
• Prostaglandin F2-α	PGF2α	d4-PGE2	353.2	309.2	6.25
• Prostaglandin E2	PGE2	d4-PGE2	351.2	271.3	6.5
• Prostaglandin D2	PGD2	d4-PGE2	351.2	271.3	6.9
• Prostaglandin J2	PGJ2	d4-PGE2	333.3	189.2	9.32
• Prostaglandin B2	PGB2	d4-PGE2	333.3	175.1	9.45
• 15-deoxy-Prostaglandin J2	15-deoxy-PGJ2	d4-PGE2	315.2	271.2	15.35
• 5-hydroxyeicosatetraenoic acid	5-HETE	d8-5-HETE	319.2	115.1	20.55
• 15-hydroxyeicosatetraenoic acid	15-HETE	d8-5-HETE	319.2	219.2	18.23
• 11-hydroxyeicosatetraenoic acid	11-HETE	d8-5-HETE	319.2	167.2	18.94
• 8-hydroxyeicosatetraenoic acid	8-HETE	d8-5-HETE	319.2	155.2	19.55
• 12-hydroxyeicosatetraenoic acid	12-HETE	d8-5-HETE	319.2	179.2	19.6
• 9-hydroxyeicosatetraenoic acid	9-HETE	d8-5-HETE	319.2	167.2	20.05

• 15-oxo-eicosatetraenoic acid	15-oxo-ETE	d8-5-HETE	317.2	113.1	19.3
• 12-oxo-eicosatetraenoic acid	12-oxo-ETE	d8-5-HETE	317.2	153.1	20.45
• 5-oxo-eicosatetraenoic acid	5-oxo-ETE	d8-5-HETE	317.2	273.2	22.83
• Lipoxin A4	LXA4	d4-TXB2	351.2	115.2	7.55
• 14,15-dihydroxyeicosatrienoic acid	14,15-DiHETrE	d11-14,15-DiHETrE	337.2	207.1	13.15
• 11,12-dihydroxyeicosatrienoic acid	11,12-DiHETrE	d11-14,15-DiHETrE	337.2	167.1	14.02
• 8,9-dihydroxyeicosatrienoic acid	8,9-DiHETrE	d11-14,15-DiHETrE	337.2	127.1	14.75
• 5,6-dihydroxyeicosatrienoic acid	5,6-DiHETrE	d11-14,15-DiHETrE	337.2	145.1	15.82
• 8,15-dihydroxyeicosatetraenoic acid	8,15-DiHETE	d11-14,15-DiHETrE	335.2	235.2	10.4
• 5,15-dihydroxyeicosatetraenoic acid	5,15-DiHETE	d11-14,15-DiHETrE	335.2	173.2	10.83
α-linolenic acid (α-LNA, 18:3 n-3) metabolites:					
• 9- hydroxyoctadecatrienoic acid acid	9-HOTrE	d4-9-HODE	293.2	171.2	14.42
• 13- hydroxyoctadecatrienoic acid acid	13-HOTrE	d4-9-HODE	293.2	195.1	14.83
Eicosapentaenoic acid (EPA, 20:5 n-3) metabolites:					
• 17(18)-epoxyeicosateteaenoic acid	17(18)-EpETE	d-11-11(12)EpEtrE	317.2	215.2	18.4
• 11(12)-epoxyeicosateteaenoic acid	11(12)-EpETE	d-11-11(12)EpEtrE	317.2	167.2	19.67
• 8(9)-epoxyeicosateteaenoic acid	8(9)-EpETE	d-11-11(12)EpEtrE	317.2	127.2	19.95
• 15-hydroxyeicosapentaenoic acid	15-HEPE	d8-5-HETE	317.2	219.2	15.8
• 12-hydroxyeicosapentaenoic acid	12-HEPE	d8-5-HETE	317.2	179.2	16.42
• 8-hydroxyeicosapentaenoic acid	8-HEPE	d8-5-HETE	317.2	155.2	16.17
• 5-hydroxyeicosapentaenoic	5-HEPE	d8-5-HETE	317.2	115.1	17.05

acid					
• Prostaglandin E3	PGE3	d4-PGE2	349.3	269.2	5.6
• Prostaglandin D3	PGD3	d4-PGE2	349.3	269.2	5.9
• Resolvin E1	Resolvin E1	d4-PGE2	349.3	195	4.05
• 17,18-dihydroxyeicosatetraenoic acid	17,18-DiHETE	d11-14,15-DiHETrE	335.3	247.2	11
• 14,15-dihydroxyeicosatetraenoic acid	14,15-DiHETE	d11-14,15-DiHETrE	335.3	207.2	11.57
• 14,15-epoxy Eicosatetraenoic acid	14(15)-EpETE	d-11-11(12)EpEtrE	317.2	207.2	19.42
• 5,6-dihydroxyeicosatetraenoic acid	5,6-DiHETE	d11-14,15-DiHETrE	335.2	115.2	10.85
Docosahexaenoic acid (DHA, 22:6 n-3) metabolites:					
• 19(20)-epoxydocosapentaenoic acid	19(20)-EpDPE	d-11-11(12)EpEtrE	343.2	241.2	21.7
• 16(17)-epoxydocosapentaenoic acid	16(17)-EpDPE	d-11-11(12)EpEtrE	343.2	233.2	22.62
• 13(14)-epoxydocosapentaenoic acid	13(14)-EpDPE	d-11-11(12)EpEtrE	343.2	193.2	22.8
• 10(11)-epoxydocosapentaenoic acid	10(11)-EpDPE	d-11-11(12)EpEtrE	343.2	153.2	22.97
• 7(8)-epoxydocosapentaenoic acid	7(8)-EpDPE	d-11-11(12)EpEtrE	343.2	113.1	23.35
• 17- hydroxydocosahexaenoic acid	17-HDoHE	d4-9HODE	343.2	281.2	18.62
Eicosatrienoic acid (ETA; 20:3 n-9) metabolites:					
• Leukotriene B3	LTB3	d4-LTB4	337.2	195.2	13.38

Supplemental Table 2. Subject information

Subject	Maternal age	Parity	Lactation stage
1	29	1	4 weeks
2	29	1	10 weeks
3	30	1	8 weeks
4	34	2	10 weeks
5	38	2	9 weeks

Supplemental Table 3. Surrogate recovery (mean ± SD) in esterified neutral lipid (NL), esterified phospholipid (PL) and free fraction in skim, cream and pellet of pooled human breast milk.

	Skim			Cream			Pellet		
	Esterified NL	Esterified PL	free	Esterified NL	Esterified PL	free	Esterified NL	Esterified PL	free
d-11-11(12)EpEtrE	119.33 ± 9.29	160.62 ± 23.38	49.42 ± 12.45	155.64 ± 14.01	140.42 ± 3.48	90.69 ± 28.62	123.14 ± 3.01	97.63 ± 67.03	115.55 ± 12.16
d11-14,15-DiHETrE	192.42 ± 12.18	166.43 ± 22.16	112.14 ± 13.27	206.23 ± 19.57	141.39 ± 4.26	114.69 ± 35.53	199.65 ± 19.99	99.29 ± 68.39	121.97 ± 5.70
d4-6-keto-PGF1a	88.30 ± 1.73	94.76 ± 5.79	49.80 ± 5.66	100.60 ± 0.37	98.58 ± 3.90	87.73 ± 28.74	87.60 ± 1.59	71.49 ± 45.23	87.78 ± 6.11
d4-9HODE	135.52 ± 4.21	138.79 ± 12.74	54.77 ± 1.72	149.19 ± 5.47	123.09 ± 7.62	60.17 ± 19.00	145.74 ± 5.68	89.47 ± 61.42	97.98 ± 2.80
d4-LTB4	93.59 ± 2.76	97.53 ± 4.86	65.87 ± 3.97	98.40 ± 3.55	93.94 ± 4.73	80.54 ± 23.36	93.75 ± 1.76	68.99 ± 47.47	97.11 ± 6.92
d4-PGE2	0.00 ± 0.00	0.00 ± 0.00	102.40 ± 7.92	0.00 ± 0.00	0.00 ± 0.00	200.20 ± 71.74	0.00 ± 0.00	0.00 ± 0.00	135.48 ± 11.71
d4-TXB2	85.76 ± 1.57	86.20 ± 3.89	99.22 ± 4.70	89.85 ± 3.61	91.02 ± 2.11	307.90 ± 107.22	86.62 ± 1.45	61.22 ± 41.19	124.06 ± 12.41
d6-20-HETE	144.15 ± 6.69	146.44 ± 10.20	28.45 ± 2.65	164.39 ± 8.78	144.21 ± 7.87	70.01 ± 15.13	155.90 ± 6.97	107.96 ±71.01	113.22 ± 10.98
d8-5-HETE	143.85 ± 9.39	127.49 ± 22.59	59.43 ± 5.50	157.61 ± 10.43	107.92 ± 4.57	87.44 ± 27.80	154.68 ± 5.63	79.12 ± 53.24	90.92 ± 3.48

Supplement Table 4. Effect of NaOH or Na_2CO_3 at different volumes and concentrations on rat plasma oxylipin concentrations (pmol/mL).

	300µL of 0.25M NaOH		200 µL of 0.25M NaOH		300 µL of 0.25M Na_2CO_3		200 µL of 0.25M Na_2CO_3		300 µL of 0.4M NaOH		200 µL of 0.4M NaOH	
	Mean ± SD	**CV**	**Mean ± SD**	**CV**	**Mean ± SD**	**CV**	**Mean ± SD**	**CV**	**Mean ± SD**	**CV**	**Mean ± SD**	**CV**
10(11)-EpDPE	87.6 ± 35.6^{ab}	41	91.6 ± 28.03^{ab}	31	64.3 ± 13.2^{a}	21	63.9^{a} ± 11.5^{a}	18	101.0 ± 23.7^{ab}	23	129.7 ± 44.0^{b}	34
11(12)-EpETrE	447.0 ± 155.1	35	583.3 ± 170.7	29	500.4 ± 96.4	19	455.1 ± 137.4	30	522.5 ± 106.4	20	714.9 ± 227.4	32
12(13)EpOME	4206.7 ± 915.2^{ab}	22	4811.0 ± 1450.9^{ab}	30	2610.9 ± 485.0^{a}	19	3058.3 ± 769.1^{a}	25	3815.5 ± 534.9^{ab}	14	5829.6 ± 1442.3^{b}	25
13(14)-EpDPE	143.1 ± 49.4	35	164.5 ± 54.2	33	155.9 ± 35.3	23	133.9 ± 45.7	34	163.1 ± 31.9	20	179.2 ± 67.7	38
14(15)-EpETE	26.5 ± 8.8^{ab}	33	26.2 ± 11.6^{ab}	44	15.0 ± 4.2^{a}	28	15.7 ± 5.5^{a}	35	27.1 ± 8.6^{ab}	32	36.9 ± 14.6^{b}	40
14(15)-EpETrE	1496.7 ± 397.8	27	1872.5 ± 490.7	26	1704.9 ± 248.9	15	1370.5 ± 549.7	40	1724.2 ± 362.9	21	2227.8 ± 670.8	30
16(17)-EpDPE	152.0 ± 45.9	30	189.7 ± 72.4	38	196.8 ± 37.4	19	170.5 ± 68.1	40	171.0 ± 37.5	22	187.7 ± 75.7	40
17(18)-EpETE	181.1 ± 55.6	31	257.7 ± 110.5	43	159.3 ± 32.8	21	162.0 ± 52.5	32	220.7 ± 58.3	26	326.5 ± 143.6	44
5(6)-EpETrE	552.5 ± 212.9	39	585.5 ± 143.0	24	482.3 ± 153.1	32	414.5 ± 70.7	17	567.9 ± 84.8	15	665.4 ± 220.8	33
7(8)-EpDPE	76.7 ± 27.0	35	88.3 ± 23.2	26	63.8 ± 21.9	34	61.9 ± 11.7	19	79.0 ± 14.0	18	107.0 ± 35.3	33
8(9)-EpETE	10.2 ± 6.4	63	9.0 ± 3.5	39	2.2 ± 2.7	124	4.6 ± 1.7	36	8.4 ± 3.2	39	9.3 ± 2.4	26
8(9)-EpETrE	481.9 ± 129.8^{ab}	27	515.7 ± 140.4^{ab}	27	356.4 ± 96.2^{a}	27	345.0 ± 62.9^{a}	18	500.1 ± 91.9^{ab}	18	616.9 ± 160.6^{b}	26
9(10)-EpOME	1330.2 ± 365.9^{ab}	28	1513.8 ± 651.9^{bc}	43	567.4 ± 180.2^{a}	32	786.3 ± 391.2^{ab}	50	1208.6 ± 140.5^{ab}	12	2123.1 ± 358.5^{c}	17
11,12-DiHETrE	11.7 ± 1.2^{b}	10	7.9 ± 3.9^{ab}	49	2.6 ± 0.4^{a}	16	4.6 ± 4.8^{a}	103	13.2 ± 2.8^{b}	22	13.7 ± 0.3^{b}	2
11(12)-EpETE	27.6 ± 4.4^{c}	16	13.4 ± 8.0^{ab}	60	5.2 ± 0.7^{a}	13	8.2 ± 7.5^{ab}	92	25.0 ± 1.7^{c}	7	17.5 ± 2.5^{bc}	14
12,13-DiHOME	57.1 ± 8.5^{b}	15	43.2 ± 9.9^{ab}	23	32.5 ± 7.2^{a}	22	37.7 ± 13.1^{ab}	35	43.7 ± 10.9^{ab}	25	43.6 ± 6.4^{ab}	15
14,15-DiHETrE	3.3 ± 1.1^{ab}	32	3.7 ± 1.0^{ab}	28	2.1 ± 0.4^{a}	17	3.3 ± 2.3^{ab}	72	5.4 ± 1.0^{b}	19	8.2 ± 0.3^{c}	4
19(20)-EpDPE	283.1 ± 88.6	31	257.3 ± 94.0	37	314.4 ± 37.8	12	239.5 ± 92.0	38	282.6 ± 67.0	24	267.8 ± 86.1	32
5,6-DiHETrE	95.7 ± 5.3^{b}	6	77.5 ± 35.9^{b}	46	32.4 ± 21.1^{a}	65	34.2 ± 14.8^{a}	43	79.8 ± 27.6^{b}	35	89.8 ± 11.9^{b}	13
8,9-DiHETrE	5.5 ± 0.9^{abc}	17	3.7 ± 1.8^{ab}	48	1.9 ± 0.4^{a}	23	3.2 ± 3.3^{ab}	102	6.5 ± 1.8^{bc}	27	7.4 ± 0.4^{c}	6
9,10-DiHOME	76.4 ± 10.7^{b}	14	49.1 ± 18.7^{ab}	38	21.8 ± 5.9^{a}	27	34.4 ± 24.6^{a}	72	70.5 ± 10.4^{b}	15	71.7 ± 5.3^{b}	7

13-HOTrE	29.3 ± 2.6^{de}	9	19.4 ± 5.8^{bc}	30	9.2 ± 3.1^{a}	33	13.3 ± 5.1^{ab}	39	31.6 ± 3.4^{e}	11	22.0 ± 2.7^{cd}	12
13HODE	592.4 ± 26.6^{b}	4	503.5 ± 55.5^{b}	11	221.3 ± 60.1^{a}	27	330.0 ± 129.8 ^{a}	39	613.8 ± 49.8^{b}	8	560.9 ± 74.9^{b}	13
17-HDoHE	12.8 ± 1.8^{bc}	14	9.6 ± 2.1^{ab}	22	5.8 ± 2.0^{a}	34	5.6 ± 2.5^{a}	45	16.0 ± 4.0^{c}	25	11.8 ± 2.1^{bc}	18
9-HOTrE	21.2 ± 1.4^{c}	6	13.7 ± 4.8^{b}	35	4.4 ± 1.3^{a}	30	7.5± 4.2^{ab}	55	28.0 ± 4.4^{c}	16	23.0 ± 3.6^{c}	16
9HODE	340.5 ± 20.9^{c}	6	267.8 ± 54.1^{bc}	20	128.6 ± 32.8^{a}	26	189.0 ± 78.0 ^{ab}	41	352.3 ± 26.6^{c}	8	294.5 ± 52.0^{c}	18
LXA4	2.0 ± 0.6^{c}	30	1.4 ± 1.0^{c}	71	Not detected		0.3 ± 0.5^{ab}	200	1.2 ± 0.2^{bc}	20	1.4 ± 0.4^{c}	25
TXB2	13.3 ± 0.8^{ab}	6	15.3 ± 1.0^{b}	6	12.4 ± 1.0^{ab}	8	14.0 ± 0.7^{ab}	5	11.2 ± 2.3^{a}	20	14.1 ± 2.9^{ab}	20
13-oxo-ODE	44.5 ± 5.3	12	43.8 ± 13.2	30	34.5 ± 18.0	52	47.0 ± 2.6	5	32.4 ± 3.0	9	27.6 ± 5.9	22
9-oxo-ODE	35.4 ± 3.9	11	33.9 ± 13.8	41	21.7 ± 10.7	49	28.3 ± 5.6	20	31.2 ± 4.3	14	27.0 ± 7.3	27
11-HETE	43.4 ± 3.8^{bc}	9	44.3 ± 11.7^{bc}	27	25.0 ± 3.1^{a}	12	32.4 ± 10.4^{ab}	32	58.4 ± 3.9^{cd}	7	61.6 ± 10.3^{d}	17
12-HEPE	58.2 ± 6.2^{b}	11	51.6 ± 27.3^{b}	53	12.3 ± 2.6^{a}	21	15.8 ± 11.6^{a}	73	60.8 ± 6.5^{b}	11	68.5 ± 2.1^{b}	3
12-HEPE	1252.4 ± 70.6^{cd}	6	925.5 ± 323.0^{bc}	35	476.4 ± 41.7^{a}	9	587.2 ± 286.3^{ab}	49	1346.7 ± 106.9^{d}	8	1220.4 ± 70.0^{cd}	6
15-HEPE	43.6 ± 3.2^{b}	7	37.7 ± 13.3^{b}	35	10.9 ± 3.1^{a}	29	15.5 ± 6.9^{a}	44	43.4 ± 4.4^{b}	10	43.7 ± 9.5^{b}	22
15-HETE	47.7 ± 4.9^{ab}	10	50.4 ± 13.7 ^{ab}	27	29.1 ± 4.2^{a}	15	35.5 ± 13.6^{a}	38	66.4 ± 5.6^{bc}	8	72.0 ± 13.0^{c}	18
15-oxo-ETE	4.3 ± 0.2^{ab}	4	4.3 ± 1.6^{ab}	37	3.3 ± 0.6^{a}	20	3.2 ± 1.2^{a}	38	3.9 ± 0.7^{ab}	17	6.0 ± 1.2^{b}	20
15(S)-HETrE	4.5 ± 0.4^{bc}	10	4.0 ± 1.2 ^{ab}	29	2.3 ± 0.3 ^{a}	12	3.3 ± 2.0 ^{ab}	60	5.2 ± 0.5^{bc}	9	6.1 ± 0.4^{c}	6
5-HEPE	7.9 ± 0.4^{ab}	5	7.1 ± 1.2^{ab}	18	5.5 ± 1.3^{a}	24	5.8 ± 0.9^{a}	16	8.8 ± 1.3^{b}	14	8.8 ± 2.1^{b}	24
5-HETE	79.7 ± 11.1	14	70.2 ± 17.2	24	51.0 ± 9.3	18	57.8 ± 12.5	22	80.3 ± 7.5	9	72.8 ± 19.9	27
5-oxo-ETE	9.3 ± 1.8^{b}	19	8.1 ± 2.8^{ab}	34	5.0 ± 0.4^{a}	8	5.4 ± 1.8^{ab}	34	7.1 ± 1.1^{ab}	15	7.2 ± 2.0^{ab}	27
8-HETE	136.9 ± 9.1^{c}	7	78.1 ± 38.4 ^{b}	49	29.5 ± 2.9^{a}	10	39.6 ± 31.3^{ab}	79	194.4 ± 10.2^{d}	5	137.1 ± 26.3^{c}	19
9-HETE	26.9 ± 2.8^{abc}	10	22.1 ± 11.3^{ab}	51	8.5 ± 1.5^{a}	18	12.2 ± 10.8^{a}	89	42.5 ± 6.1^{c}	14	38.1 ± 12.9^{bc}	34

Data are Mean ± Standard Deviation (SD); the coefficient of variation (CV) is reported for each treatment.100 µL of rat plasma were subjected to hydrolysis with different bases at various volumes and concentrations (n=4 / condition). Data were analyzed by one-way ANOVA followed by Tukey's multiple comparison post-hoc test. Values with different superscripts are statistically significant at $P<0.05$.

Supplement Table 5. Deuterated surrogate recovery from rat plasma hydrolyzed with NaOH or Na_2CO_3 at different volumes and concentrations.

	0.25M NaOH 300 µL	**0.25M NaOH 200 µL**	**0.25M Na_2CO_3 300 µL**	**0.25M Na_2CO_3 200 µL**	**0.4M NaOH 300 µL**	**0.4M NaOH 200 µL**
d-11-11(12)EpEtrE	69.2 ± 2.6	61.3 ± 2.5	70.4 ± 4.0	72.0 ± 8.4	68.4 ± 3.9	59.0 ± 4.7
d11-14,15-DiHETrE	94.4 ± 11.8	115.8 ± 14.7	111.7 ± 12.5	127.5 ± 12.9	95.6 ± 25.9	103.9 ± 7.9
d4-6-keto-PGF1a	74.6 ± 3.4	75.9 ± 9.1	88.4 ± 5.0	87.6 ± 16.2	62.8 ± 8.5	60.6 ± 1.9
d4-9HODE	94.5 ± 4.2	99.7 ± 5.8	106.7 ± 5.8	108.7 ± 11.7	83.4 ± 7.5	88.9 ± 4.5
d4-LTB4	94.1 ± 7.4	85.4 ± 14.0	78.0 ± 10.5	81.4 ± 4.8	88.2 ± 12.1	79.8 ± 5.2
d4-PGE2	0.0 ± 0.0	0.0 ± 0.0	0.0 ± 0.0	0.3 ± 0.6	0.0 ± 0.0	0.0 ± 0.0
d4-TXB2	23.5 ± 1.7	38.1 ± 22.2	67.1 ± 4.9	63.5 ± 27.5	9.9 ± 2.4	12.7 ± 0.5
d6-20-HETE	562.0 ± 48.6	428.0 ± 153.9	243.9 ± 124.0	238.0 ± 50.0	591.5 ± 24.5	503.2 ± 29.5
d8-5-HETE	96.4 ± 8.2	95.8 ± 5.8	96.3 ± 7.3	100.5 ± 8.6	84.7 ± 7.1	85.9 ± 5.9

Data are Mean ± Standard Deviation (SD) of n=4 per condition

Supplement Table 6. Effect of NaOH or Na_2CO_3 at different volumes and concentrations on rat brain oxylipin concentrations (pmol/mL)

	0.25M Na_2CO_3 200µL	CV	**0.4M NaOH 200 µL**	CV	**0.4M NaOH 300 µL**	CV
20-OH-LTB4	n.d.	n/a	0.452 ± 0.064	14	0.481 ± 0.096	20
LXA4	n.d.	n/a	0.035 ± 0.009	25	0.085 ± 0.035	42
8,15-DiHETE	n.d.	n/a	0.019 ± 0.005	25	0.020 ± 0.012	60
LTB4	n.d.	n/a	0.021 ± 0.005	25	0.019 ± 0.005	25
14,15-DiHETE	n.d.	n/a	0.100 ± 0.004	4	0.156 ± 0.025	16
12,13-DiHOME	0.071 ± 0.076	108	0.023 ± 0.019	84	0.007 ± 0.003	40
9,10-DiHOME	0.092 ± 0.097	106	0.048 ± 0.032	67	0.020 ± 0.006	31
14,15-DiHETrE	0.002 ± 0.001[a]	30	0.011 ± 0.003[b]	31	0.019 ± 0.003[c]	14
11,12-DiHETrE	0.001 ± 0.0003[a]	63	0.007 ± 0.002[b]	31	0.011 ± 0.002[c]	16
15-HEPE	0.027 ± 0.006[a]	22	0.072 ± 0.012[b]	16	0.079 ± 0.022[b]	28
5,6-DiHETrE	0.002 ± 0.001[a]	51	0.008 ± 0.002[b]	22	0.004 ± 0.003[ab]	75
13-HODE	0.199 ± 0.143	72	0.824 ± 1.068	130	0.109 ± 0.042	39
9-HODE	0.130 ± 0.103	79	0.598 ± 0.791	132	0.065 ± 0.025	39
15-HETE	0.038 ± 0.003[a]	9	0.084 ± 0.018[b]	22	0.084 ± 0.006[b]	7
17-HDoHE	0.086 ± 0.015[a]	17	0.165 ± 0.032[ab]	19	0.210 ± 0.070[b]	33
11-HETE	0.024 ± 0.001[a]	4	0.049 ± 0.010[b]	20	0.051 ± 0.005[b]	9
9-oxo-ODE	0.189 ± 0.194	102	0.033 ± 0.032	95	0.008 ± 0.005	60
15-oxo-ETE	0.003 ± 0.0004 [a]	13	0.025 ± 0.008[b]	33	0.017 ± 0.006[b]	36
14(15)-EpETE	n.d.	n/a	0.027 ± 0.004	15	0.024 ± 0.003	14
8-HETE	0.010 ± 0.001[a]	7	0.155 ± 0.036[b]	23	0.258 ± 0.030[c]	12
12-HETE	0.206 ± 0.006[a]	3	1.096 ± 0.239[b]	22	1.517 ± 0.178[c]	12
11(12)-EpETE	0.004 ± 0.002[a]	69	0.029 ± 0.004[b]	14	0.030 ± 0.007[b]	23
9-HETE	0.012 ± 0.002[a]	18	0.031 ± 0.007[b]	23	0.035 ± 0.002[b]	6
15(S)-HETrE	0.005 ± 0.0004[a]	9	0.024 ± 0.002[b]	9	0.022 ± 0.003[b]	15
5-HETE	0.052 ± 0.003[a]	6	0.081 ± 0.016[b]	20	0.068 ± 0.005[ab]	7
12(13)-EpOME	0.887 ± 1.335	150	0.221 ± 0.289	131	0.156 ± 0.041	26
19(20)-EpDPE	0.180 ± 0.044[a]	25	0.506 ± 0.139[b]	27	1.406 ± 0.204[c]	15
9(10)-EpOME	9.611 ± 13.315	139	1.039 ± 1.290	124	0.374 ± 0.048	13
14(15)-EpETrE	2.821 ± 0.296[a]	11	3.188 ± 0.415[a]	13	4.107 ± 0.114[b]	3
16(17)-EpDPE	1.956 ± 0.190[a]	10	2.656 ± 0.350[b]	13	4.018 ± 0.187[c]	5
13(14)-EpDPE	1.750 ± 0.165[a]	9	2.684 ± 0.324[b]	12	4.037 ± 0.137[c]	3
10(11)-EpDPE	0.646 ± 0.133[a]	21	2.057 ± 0.383[b]	19	3.510 ± 0.169[c]	5
11(12)-EpETrE	0.054 ± 0.006[a]	11	0.236 ± 0.065[b]	27	0.561 ± 0.068[c]	12
7(8)-EpDPE	0.077 ± 0.052	68	0.014 ± 0.014	99	0.049 ± 0.020	40

8(9)-EpETrE	0.567 ± 0.070	12	0.429 ± 0.109	26	0.430 ± 0.058	13
5(6)-EpETrE	0.906 ± 0.133[a]	15	1.363 ± 0.160[b]	12	1.774 ± 0.029[c]	2

Data are Mean ± Standard Deviation (SD); the coefficient of variation (CV) is reported for each treatment. 8.45mg rat brain were subjected to hydrolysis with different bases at various volumes and concentrations following Folch extraction (n=4 / condition). Data were analyzed by one-way ANOVA followed by Tukey's multiple comparison post-hoc test. Values with different superscripts are statistically significant at $P<0.05$. Two replicates from Na_2CO_3 group for 12(13) EpOME are replaced with LOQ/sqrt(2) for statistical analysis because they were not detected. N.d. stands for not detected in all 4 samples per condition, and n/a stands for not available.

Supplement Table 7. Deuterated surrogate standard recovery from rat brain hydrolyzed with NaOH or Na_2CO_3 at different volumes and concentrations.

	0.25M Na_2CO_3 200µL	**0.4M NaOH 200µL**	**0.4M NaOH 300µL**
d4-LTB4	76.2 ± 7.8	80.5 ± 4.3	86.6 ± 5.5
d4-6-keto-PGF1a	81.9 ± 15.3	71.7 ± 3.1	70.1 ± 6.6
d4-PGE2	0.0 ± 0.0	0.0 ± 0.0	0.0 ± 0.0
d4-TXB2	78.7 ± 15.0	25.3 ± 4.6	11.7 ± 1.0
d11-14,15-DiHETrE	109.1 ± 19.5	126.4 ± 9.2	178.4 ± 42.4
d4-9HODE	115.7 ± 1.6	107.5 ± 4.1	105.2 ± 10.1
d6-20-HETE	126.7 ± 2.5	688.2 ± 27.2	587.6 ± 73.3
d8-5-HETE	117.0 ± 6.5	96.9 ± 9.0	100.5 ± 7.6
d-11-11(12)EpEtrE	65.1 ± 9.6	74.1 ± 6.5	73.7 ± 6.2

Data are Mean ± Standard Deviation (SD) of n=4 per condition

Supplement Table 8. Ion suppression/enhancement after NaOH or Na_2CO_3 hydrolysis of rat brain at different volumes and concentrations.

	0.25M Na_2CO_3 200µL	**0.4M NaOH 200µL**	**0.4M NaOH 300µL**
20-COOH-LTB4	66.0	95.5	94.9
6-keto-PGF1a	75.9	90.3	90.2
Resolvin E1	63.8	75.9	77.8
20-OH-LTB4	63.5	83.7	80.5
TXB2	81.5	85.5	83.3
PGE3	81.9	90.6	89.0
PGD3	74.0	73.6	77.9
9,12,13-TriHOME	83.5	86.0	81.3
9,10,13-TriHOME	77.9	77.3	72.0
PGF2a	77.6	81.0	71.7
PGE2	89.1	85.0	78.2
PGE1	87.1	93.8	93.0
PGD1	86.6	93.6	92.4
PGD2	96.4	95.1	98.1

LTD4	0.0	4.5	9.8
LXA4	87.2	85.1	90.0
LTC4	0.0	0.0	4.0
LTE4	0.5	0.0	1.5
PGJ2	75.9	106.8	98.8
PGB2	66.7	76.3	79.5
8,15-DiHETE	95.2	89.0	87.1
6-trans-LTB4	72.5	83.5	84.8
5,15-DiHETE	97.8	115.0	117.5
5,6-DiHETE	94.8	104.9	110.0
17,18-DiHETE	113.3	118.1	108.0
LTB4	84.5	110.8	114.4
14,15-DiHETE	109.1	120.1	118.5
12,13-DiHOME	88.9	95.2	89.3
9,10-DiHOME	95.6	120.5	111.1
14,15-DiHETrE	87.1	102.8	103.4
LTB3	89.6	107.3	97.2

11,12-DiHETrE	91.4	106.7	109.5
9-HOTrE	92.5	116.3	110.3
8,9-DiHETrE	109.0	126.2	122.5
13-HOTrE	95.8	132.4	122.3
15-deoxy-PGJ2	95.9	185.1	202.9
20-HETE	101.0	175.3	206.1
15-HEPE	103.5	160.1	156.2
5,6-DiHETrE	92.2	85.1	87.0
8-HEPE	90.9	99.9	100.4
12-HEPE	116.4	161.6	146.0
5-HEPE	116.4	144.6	138.7
d4-13-HODE	97.3	107.7	105.3
13-HODE	103.0	116.2	116.1
9-HODE	92.9	109.6	112.4
15-HETE	106.3	119.7	114.4
17(18)-EpETE	85.0	99.5	94.7
13-oxo-ODE	64.8	81.3	84.4
17-HDoHE	95.8	113.0	105.1
11-HETE	100.3	131.6	124.8
9-oxo-ODE	100.0	97.3	111.5

15-oxo-ETE	107.6	114.1	118.3
14(15)-EpETE	105.6	109.6	119.0
8-HETE	107.0	140.7	173.7
12-HETE	106.8	133.1	173.0
8(9)-EpETE	100.0	117.9	115.0
11(12)-EpETE	105.4	134.2	185.6
9-HETE	105.6	115.5	118.4
15(S)-HETrE	116.7	121.7	124.3
12-oxo-ETE	83.5	107.0	107.1
5-HETE	94.1	102.3	99.0
12(13)-EpOME	65.5	34.6	24.1
19(20)-EpDPE	53.4	71.0	71.3
9(10)-EpOME	98.6	109.8	103.8
14(15)-EpETrE	95.5	95.8	87.2
16(17)-EpDPE	96.2	95.4	85.9

13(14)-EpDPE	91.7	86.4	81.7
5-oxo-ETE	83.3	101.3	103.6
10(11)-EpDPE	77.7	73.6	75.1
11(12)-EpETrE	30.3	38.1	47.5
7(8)-EpDPE	79.6	76.3	89.1
8(9)-EpETrE	100.7	81.8	83.9
5(6)-EpETrE	95.2	102.6	103.3

Supplementary Table 9. Brain concentrations of endogenous free and total 9-HODE and 9,12,13-TriHOME (pmol/mg) in rats fed a low, moderate and high LNA diet.

	Low LNA diet	Moderate LNA diet	High LNA diet
9-HODE (pmol/g)			
Free	3.452±1.852	2.936±0.628	3.015±0.936
Total	3.913±1.573	4.132±1.490	4.000±0.563
9,12,13-TriHOME (pmol/mg)			
Free	0.848±0.351	0.695±0.048	0.587±0.101
Total	1.408±0.311	1.192±0.298	1.139±0.156

Data are mean ± SD. Sample size of low, moderate, and high LNA dietary groups was 6, 5, and 4 respectively. Data were analyzed by one-Way ANOVA followed by Tukey's test was applied. No significant differences were detected at $p<0.05$.

Supplementary Table 10. Brain concentrations of labeled ^{13}C-9-HODE and ^{13}C -9,12,13-TriHOME (pmol/g) in rats fed a low, moderate, and high LNA diet.

	Low LNA diet	Moderate LNA diet	High LNA diet
^{13}C-9-HODE (pmol/g)			
Free	0.067±0.053	0.046±0.028	0.025±0.004
Total	0.099±0.065	0.049±0.026	0.050±0.021
d-9,12,13-TriHOME (pmol/g)			
Free	0.036±0.029	0.025±0.015	0.019±0.008
Total	0.036±0.029	0.027±0.012	0.016±0.008

Data are mean ± SD. Sample size of low, moderate, and high LNA dietary groups was 6, 5, and 4 respectively. Data were analyzed by one-Way ANOVA followed by Tukey's test was applied. No significant differences were detected at $p<0.05$.

Supplement Figure 1: Natural log (ln) transformed plasma concentration vs time plots for UE and total (UE + ES) d4-13-HODE from 1 to 5 min in IV injected rats. Data are the mean of 2-3 rats per time-point.

(A) UE d4-13-HODE

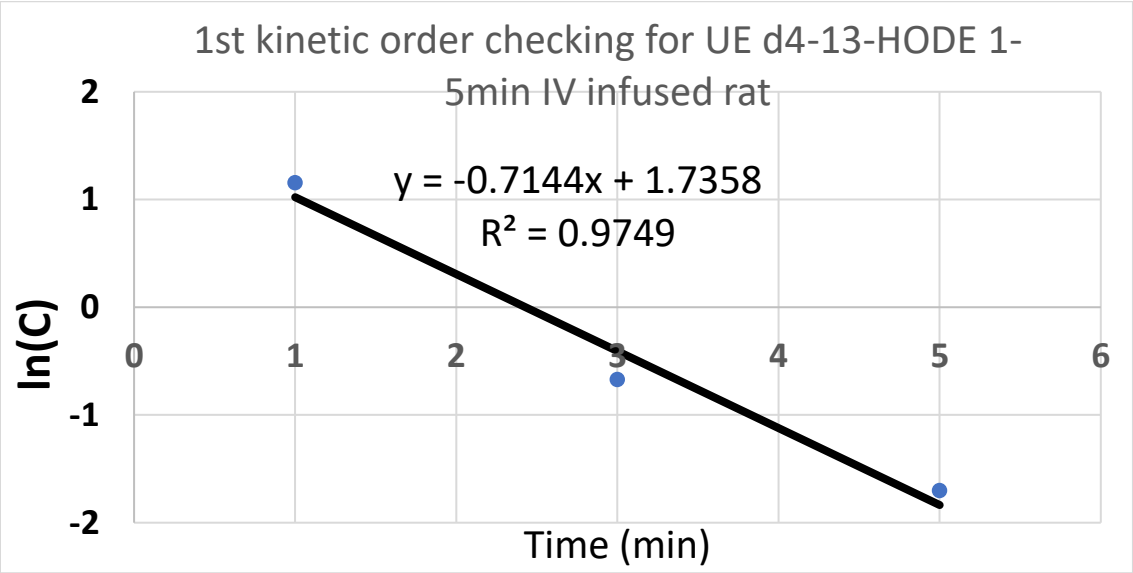

(B) total d4-13-HODE

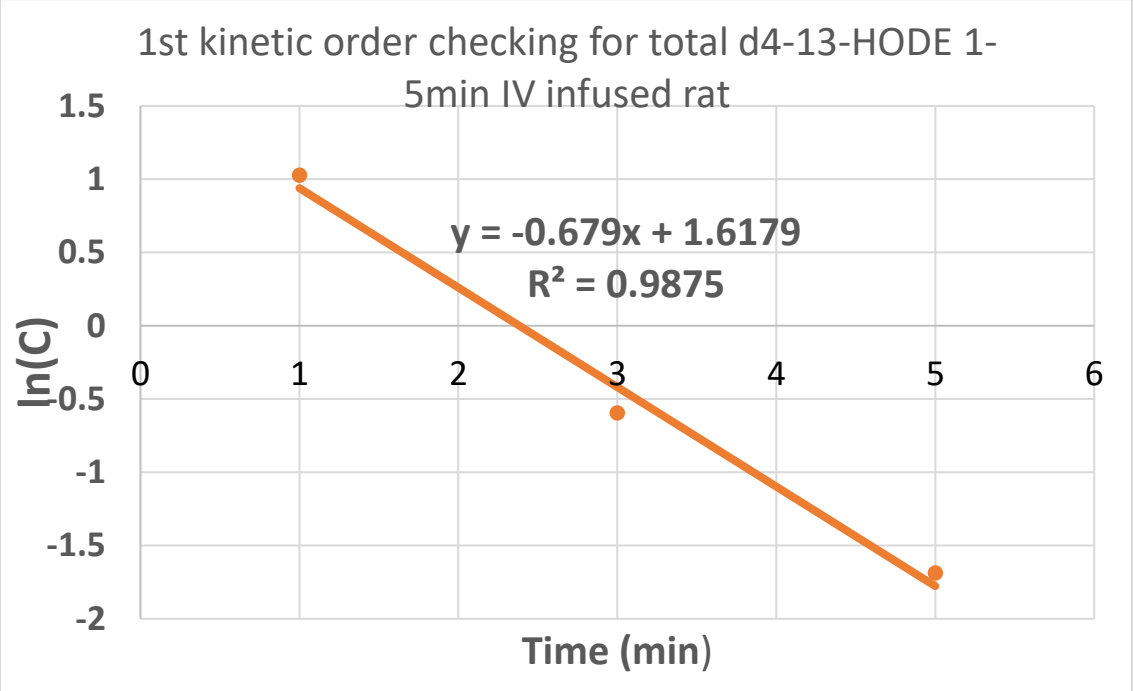

Supplement Figure 2: UE and total d4-13-HODE Concentration-time plot for each rat injected IV or gavaged with UE d4-13-HODE

Rat #4 (Gavage)

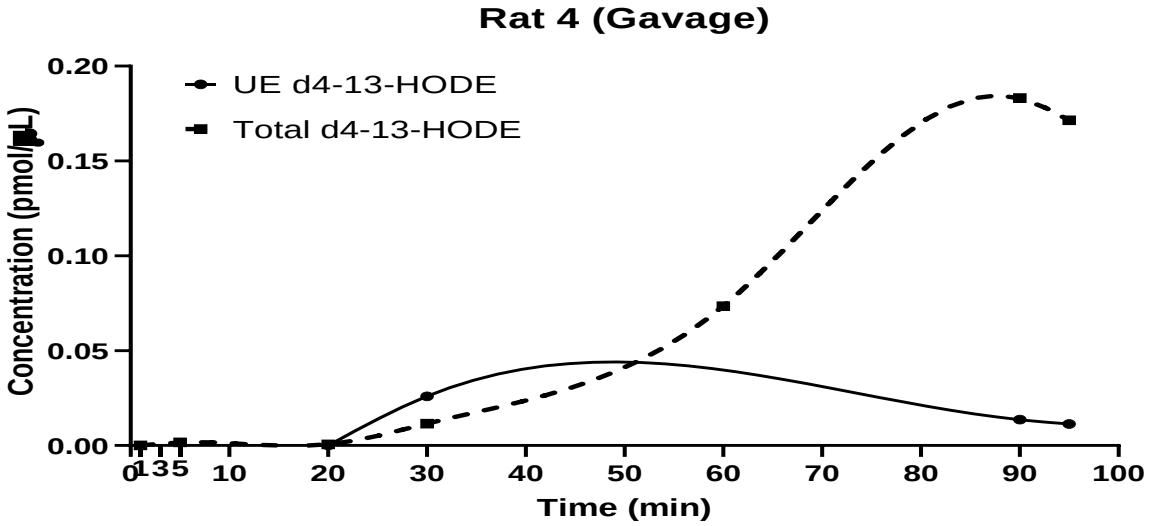

Rat #5 (IV)

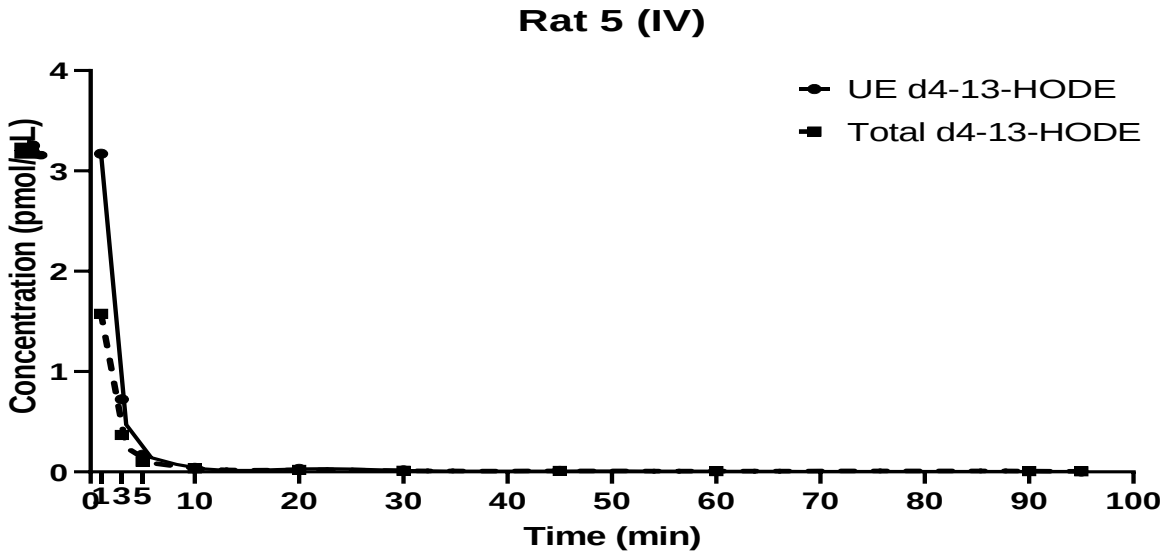

Rat #6 (Gavage)

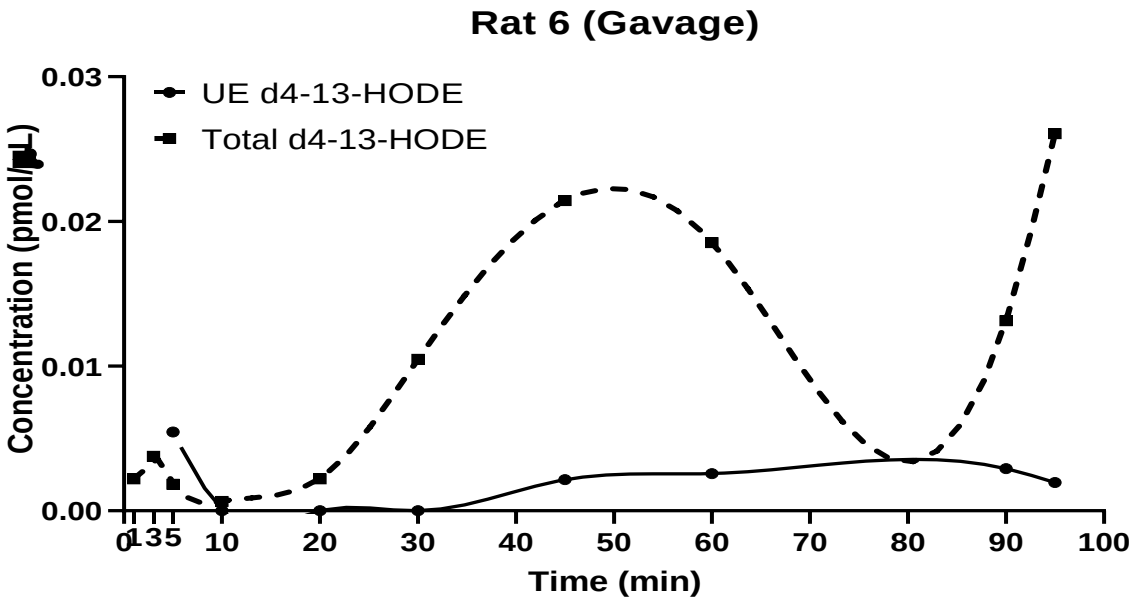

Rat #7 (IV)

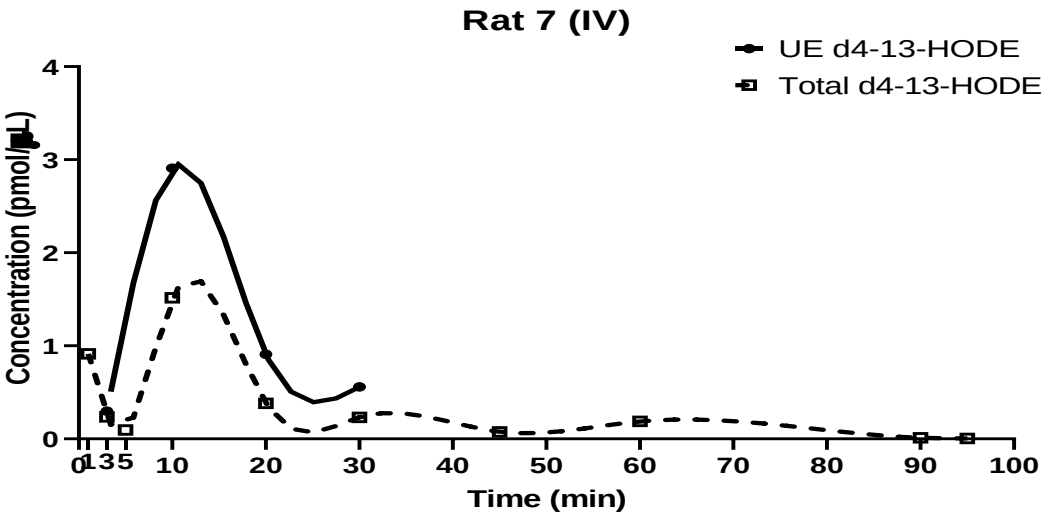

Rat #8 (Gavage)

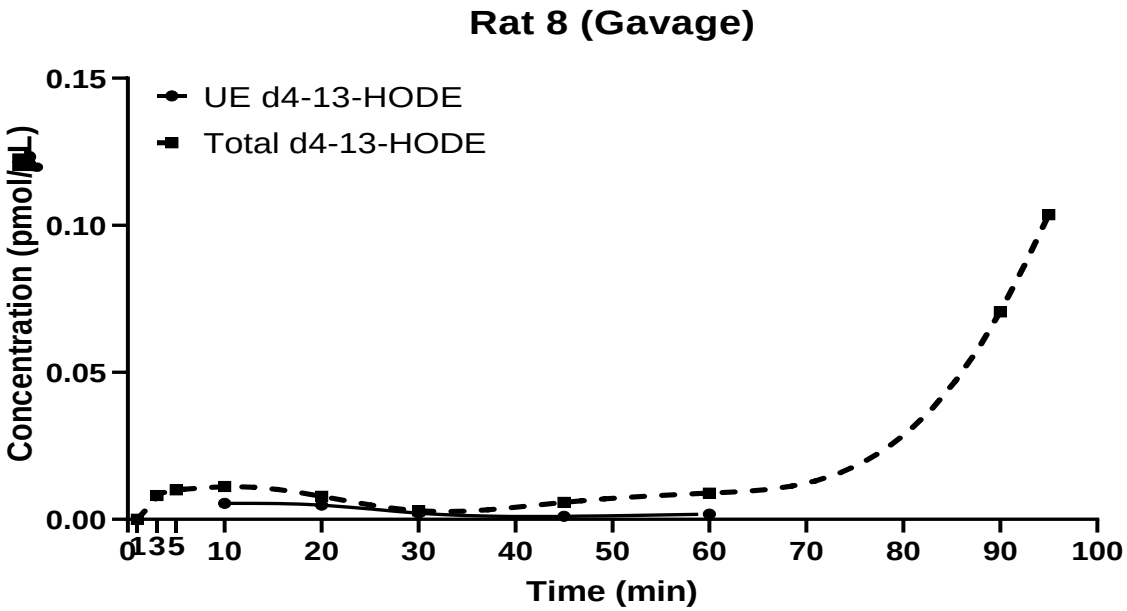
Rat 8 (Gavage)
UE d4-13-HODE
Total d4-13-HODE
Concentration (pmol/mL)
0.15
0.10
0.05
0.00
0
1
3
5
10
20
30
40
50
60
70
80
90
100
Time (min)

Rat #9 (IV)

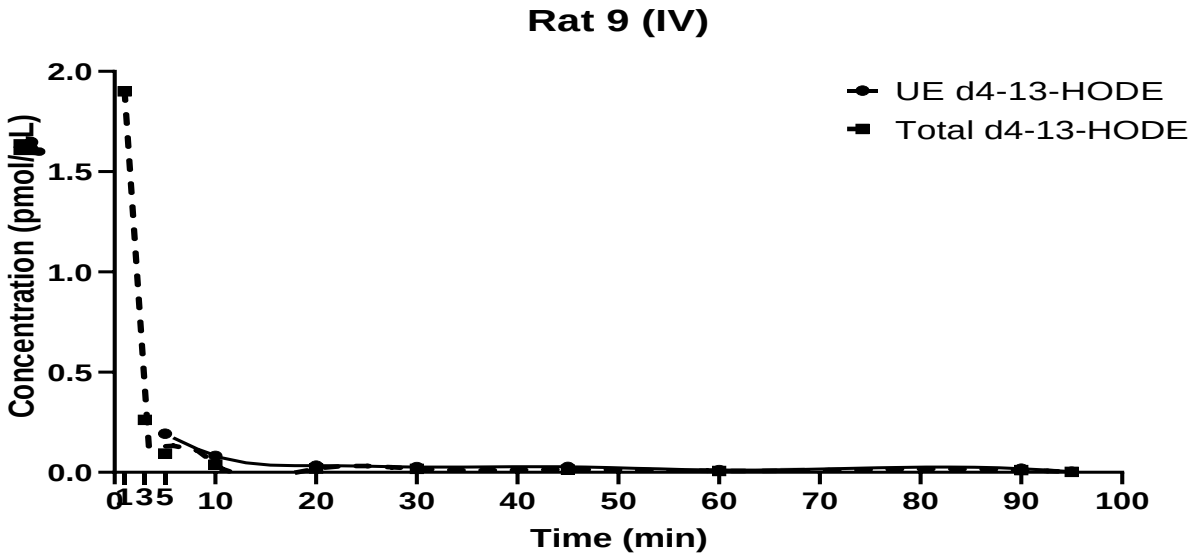
Rat 9 (IV)
UE d4-13-HODE
Total d4-13-HODE
Concentration (pmol/mL)
2.0
1.5
1.0
0.5
0.0
0
1
3
5
10
20
30
40
50
60
70
80
90
100
Time (min)

Supplement Figure 3: Concentration-Time plot of unlabeled 13-HODE in plasma of rats injected (IV) or gavaged with the tracer.

(A) IV-injected rats

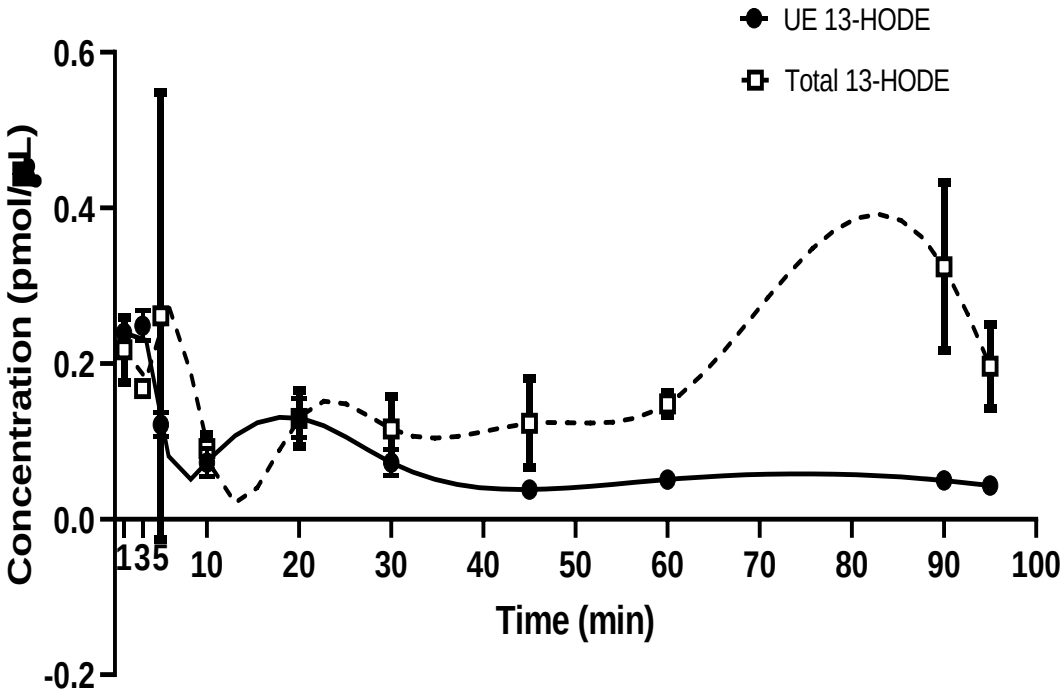

(B) Gavaged rats

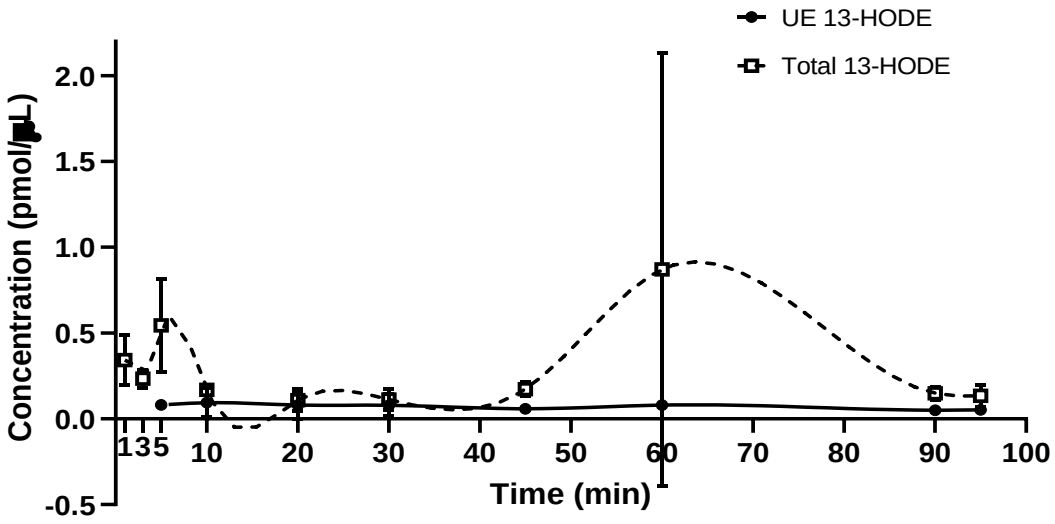

Supplement Figure 4: First derivative of plasma d4-13-HODE total concentration over time in gavage rats

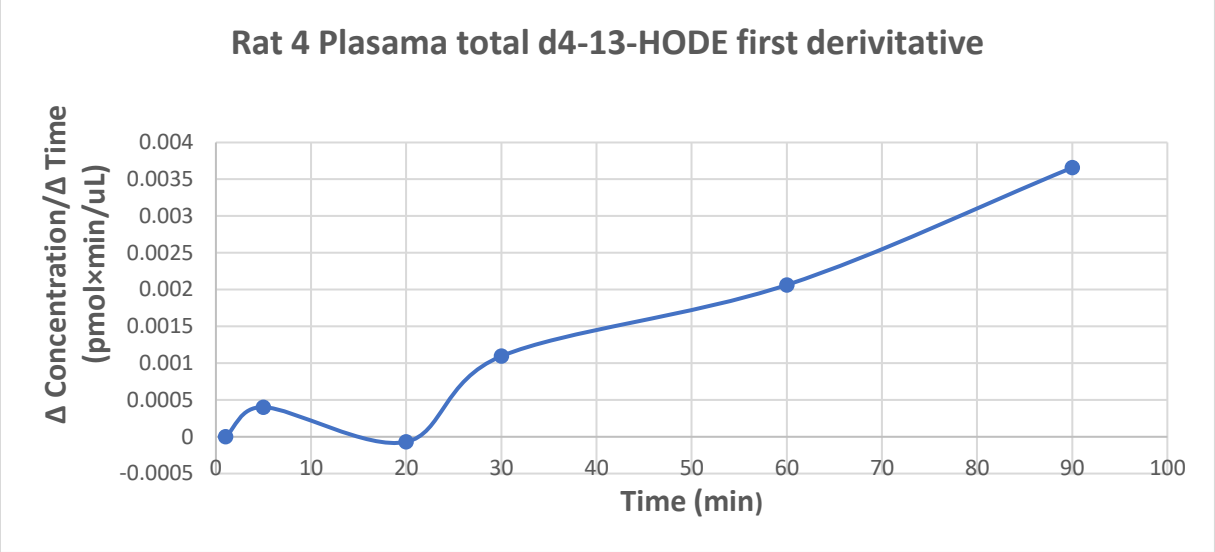
Rat 4 Plasama total d4-13-HODE first derivitative
Δ Concentration/Δ Time (pmol×min/uL)
0.004
0.0035
0.003
0.0025
0.002
0.0015
0.001
0.0005
0
-0.0005
0
10
20
30
40
50
60
70
80
90
100
Time (min)

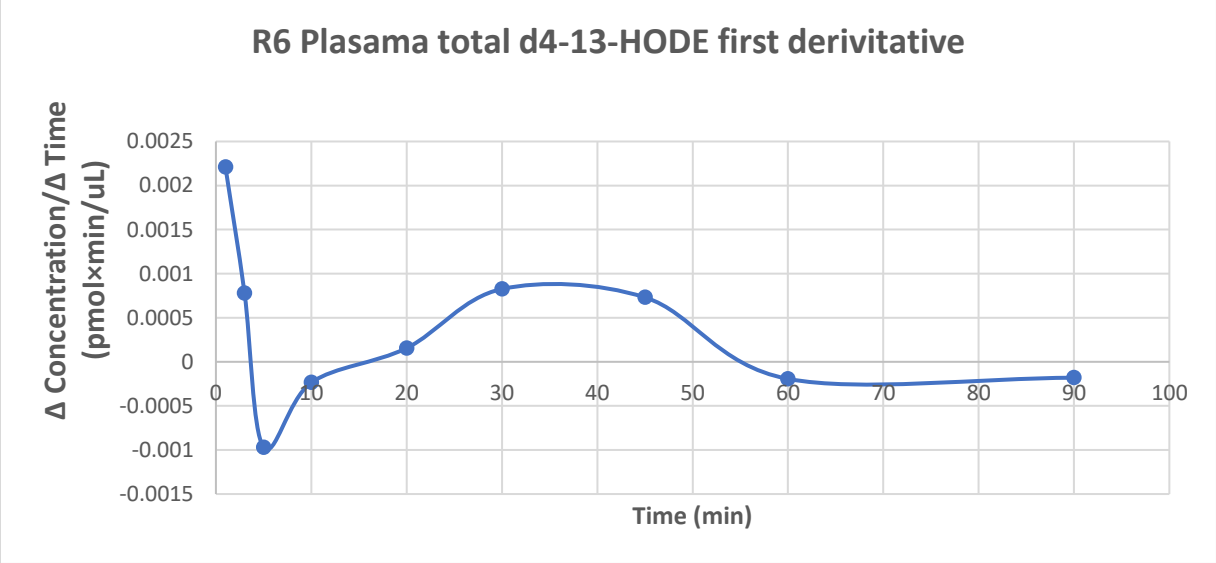
R6 Plasama total d4-13-HODE first derivitative
Δ Concentration/Δ Time (pmol×min/uL)
0.0025
0.002
0.0015
0.001
0.0005
0
-0.0005
-0.001
-0.0015
0
10
20
30
40
50
60
70
80
90
100
Time (min)

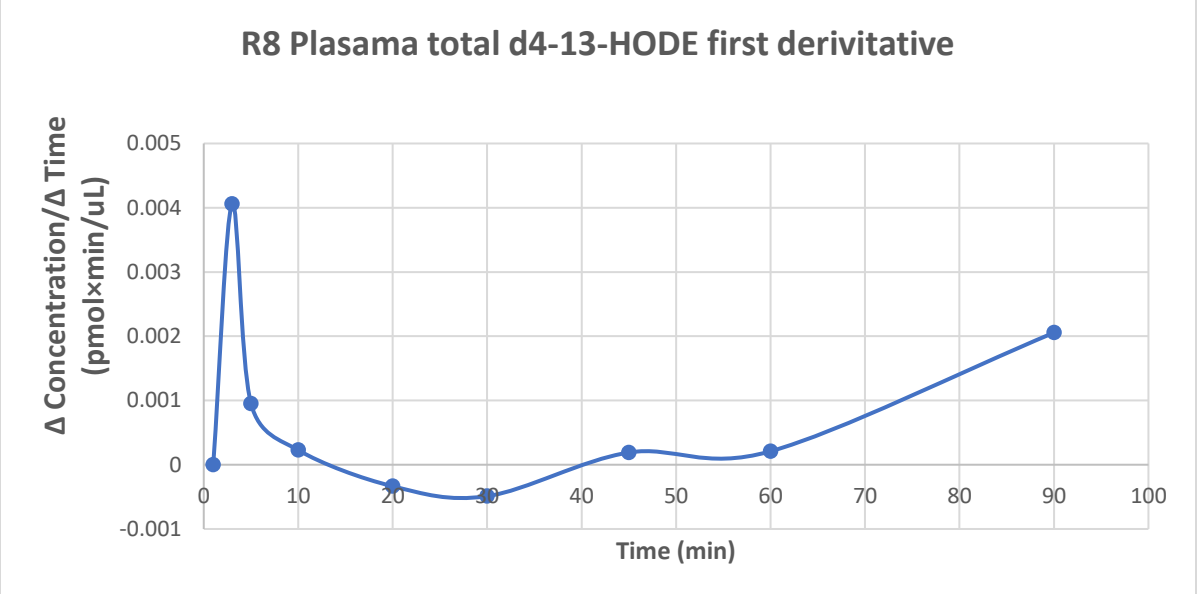
R8 Plasama total d4-13-HODE first derivitative
Δ Concentration/Δ Time (pmol×min/uL)
0.005
0.004
0.003
0.002
0.001
0
-0.001
0
10
20
30
40
50
60
70
80
90
100
Time (min)

Supplement Figure 5: UPLC-MS/MS chromatograms of tracer incorporation into perirenal adipose tissue, visceral adipose tissue, heart liver, and brain following IV or gavage**.**

(A) <u>Perirenal adipose tissue</u>

Rat 2 (Vehicle, gavage)

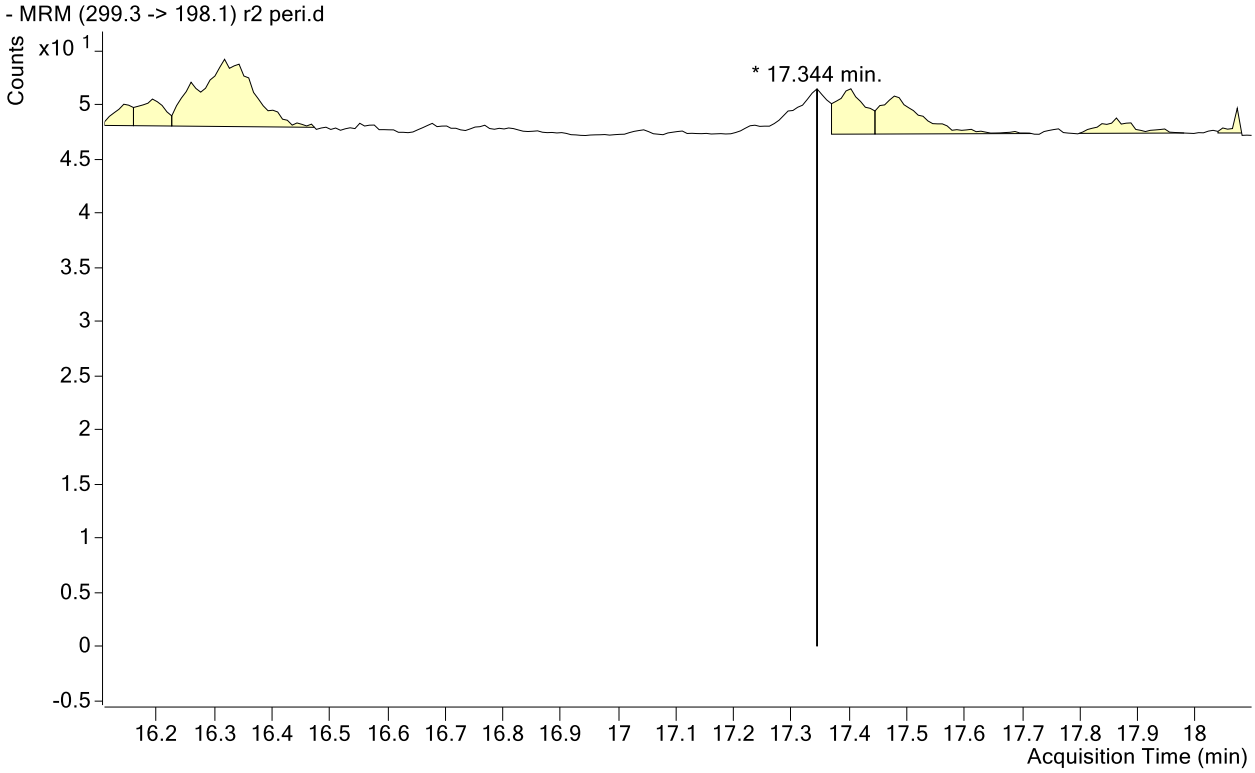

Rat 3 (Vehicle, IV)

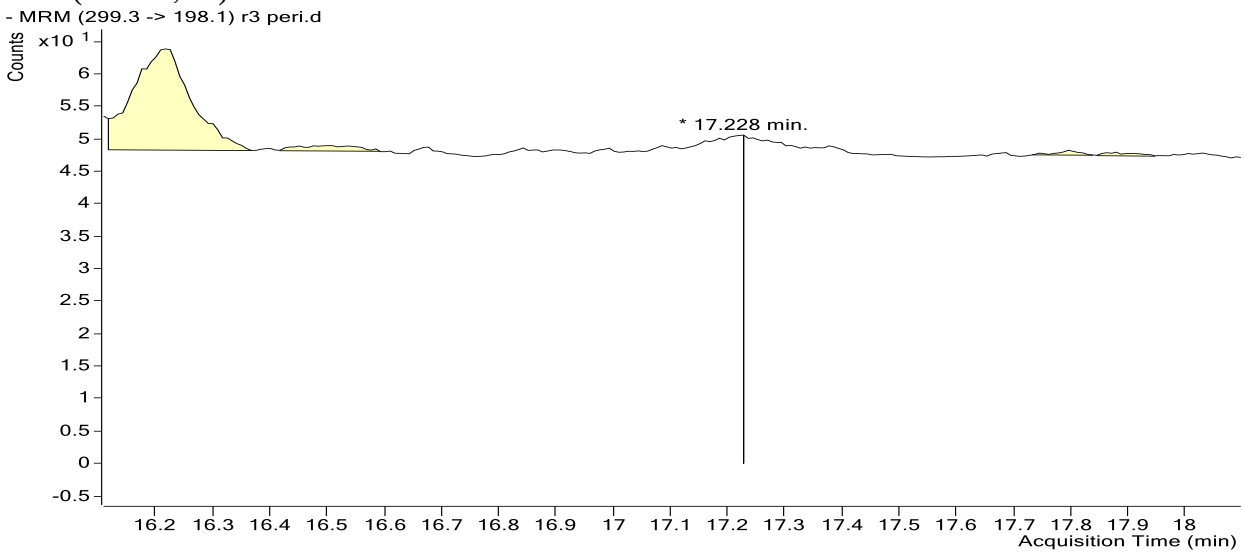

Rat 4 (Gavage)

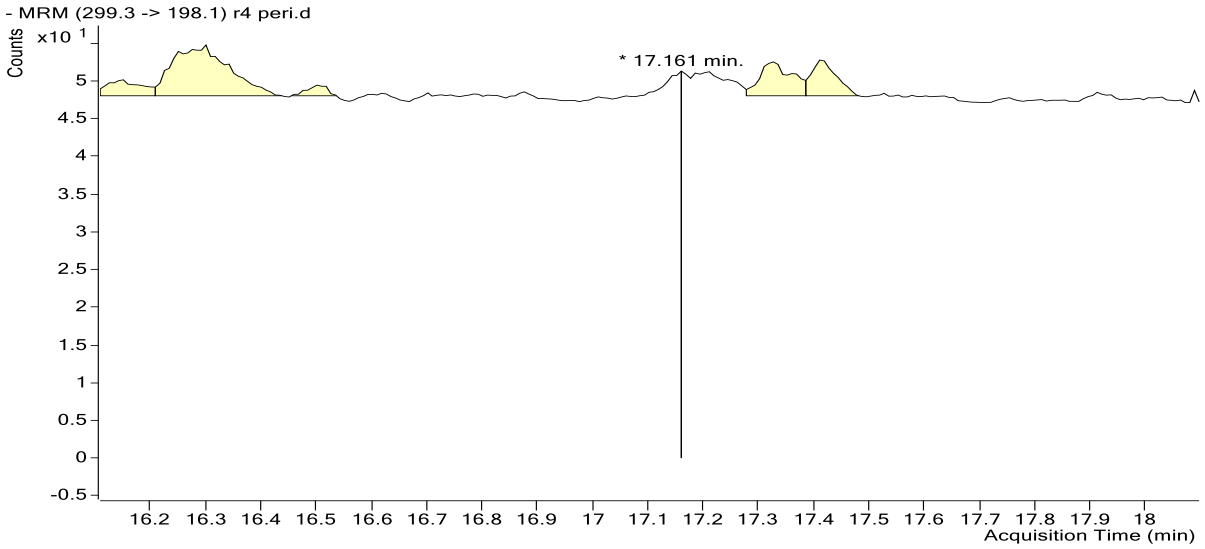

Rat 6 (Gavage)

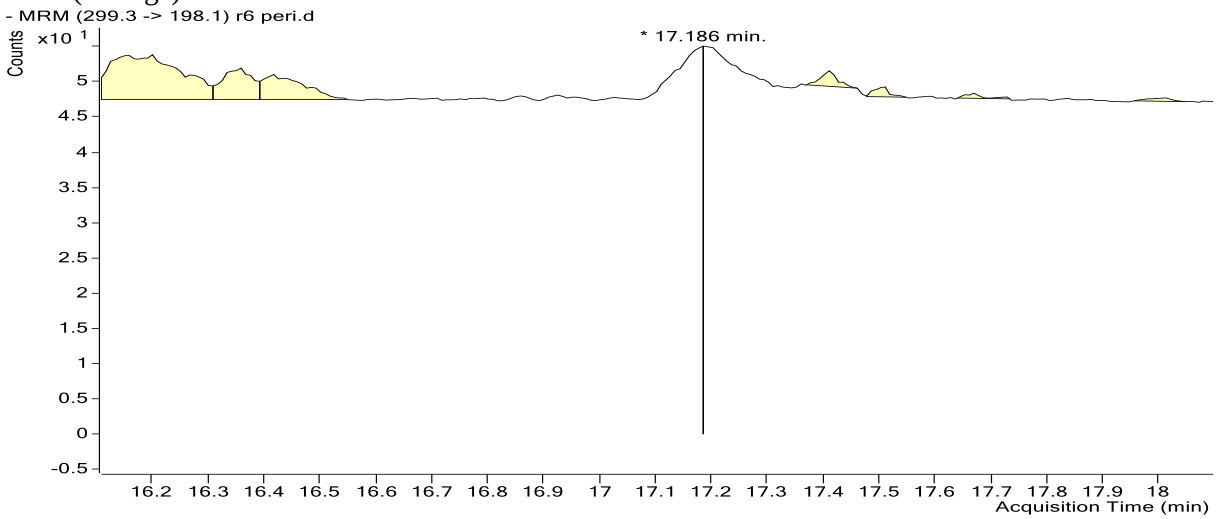

Rat 8 (Gavage)

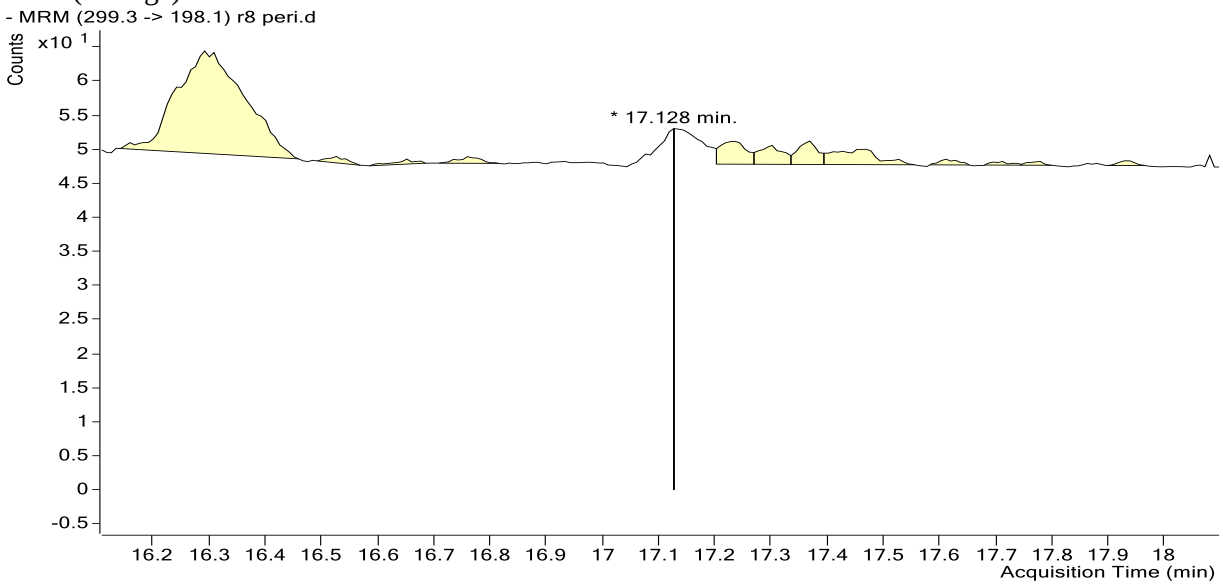

Rat 5 (IV-injected)

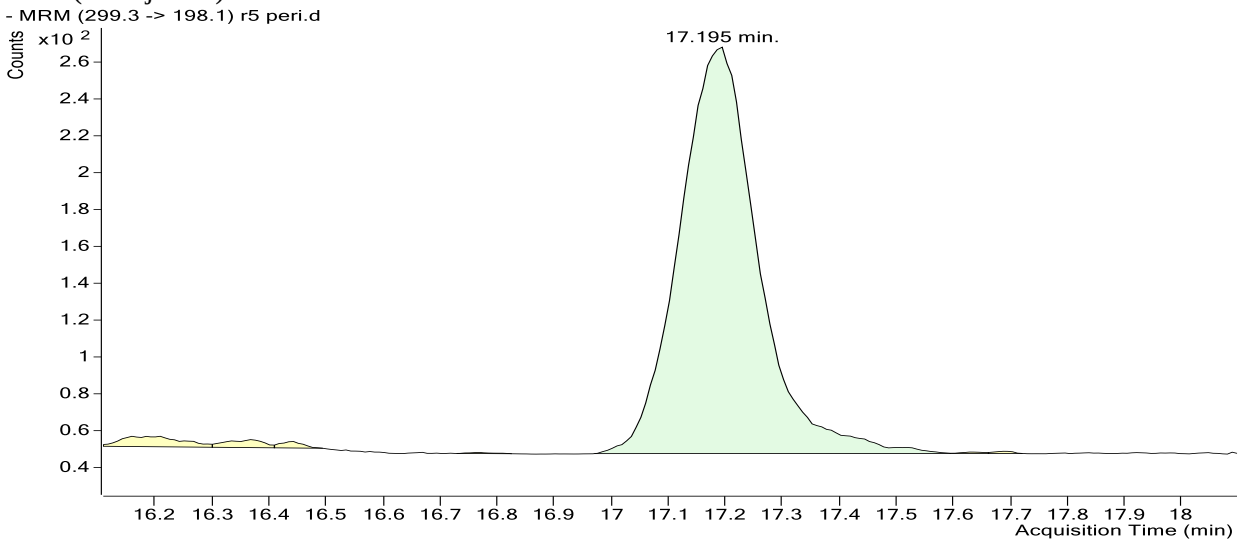

Rat 7 (IV-injected)

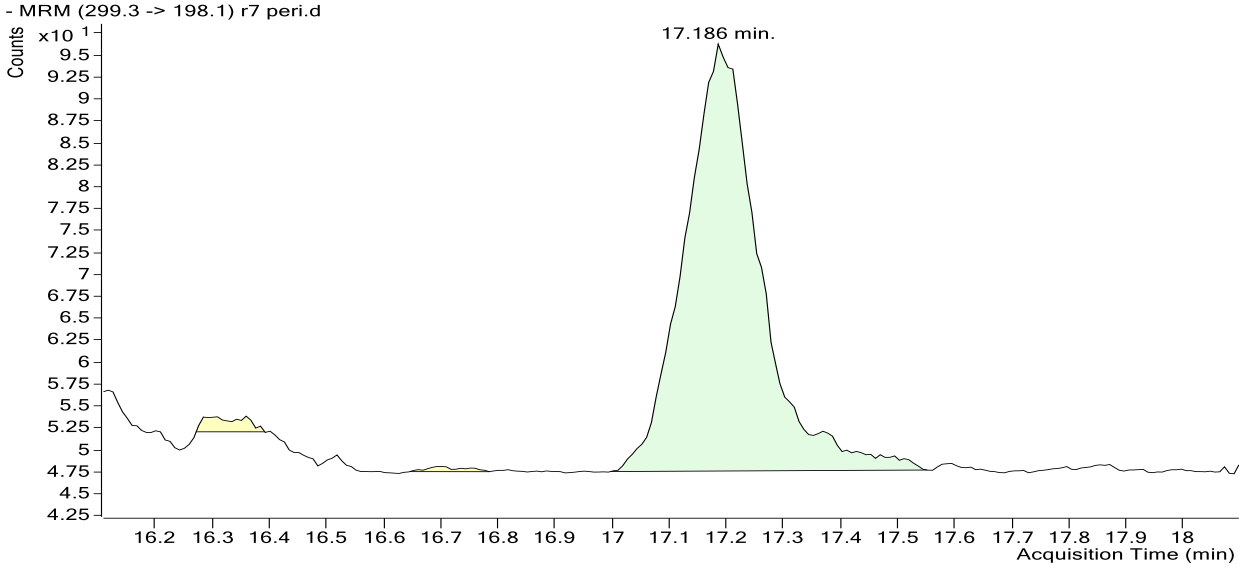

Rat 9 (IV-injected)

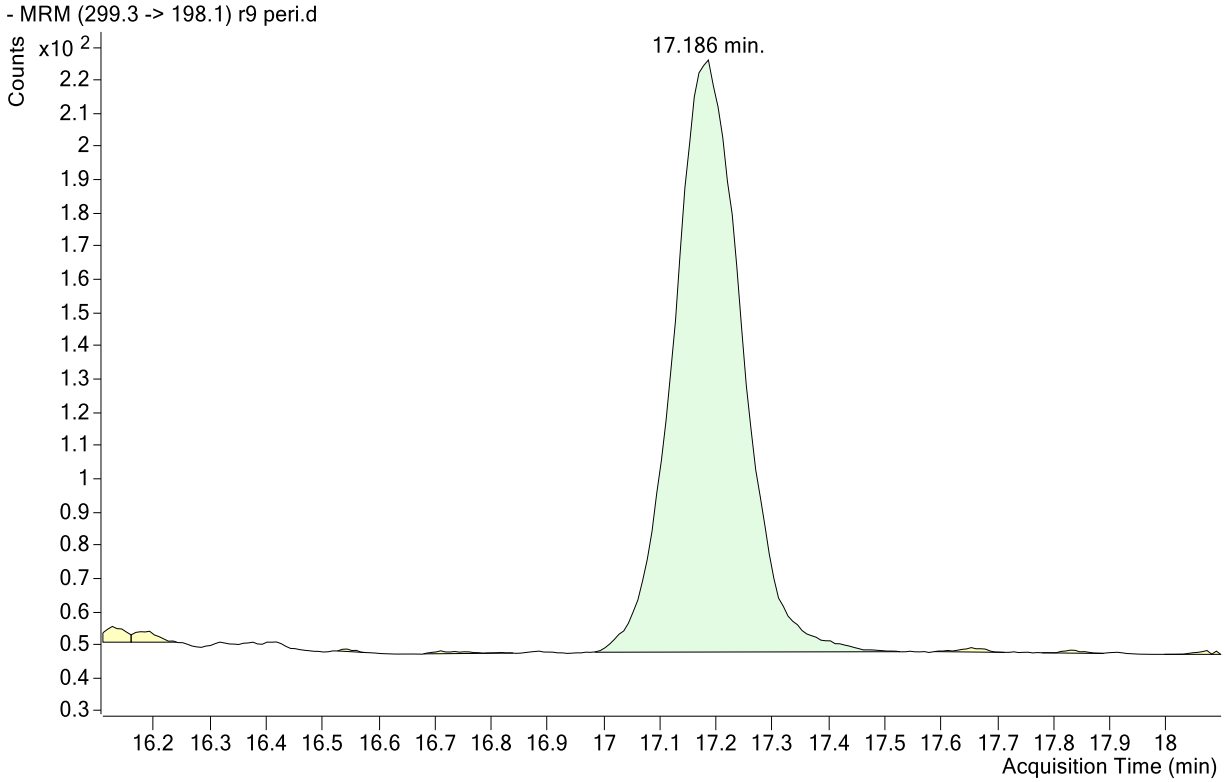

(B) <u>Visceral adipose</u>

Rat 2 (Vehicle, gavage)

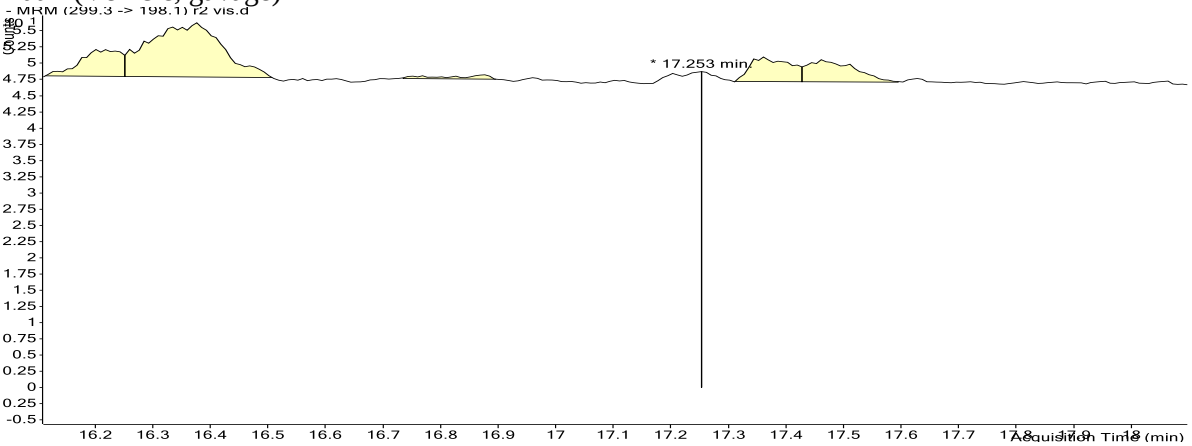

Rat 3 (Vehicle, IV)

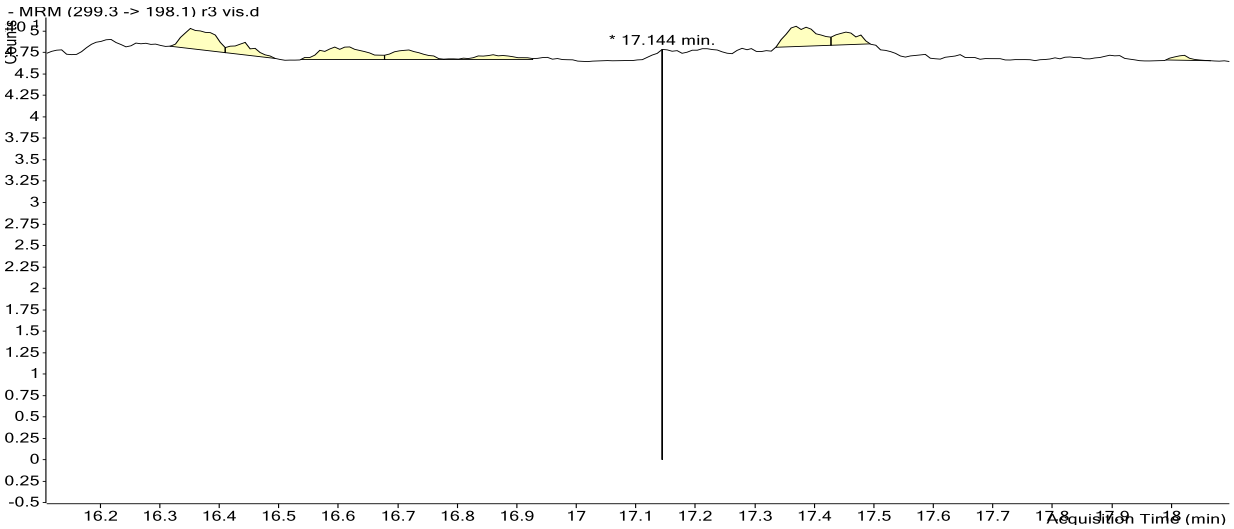

Rat 4 (Gavage)

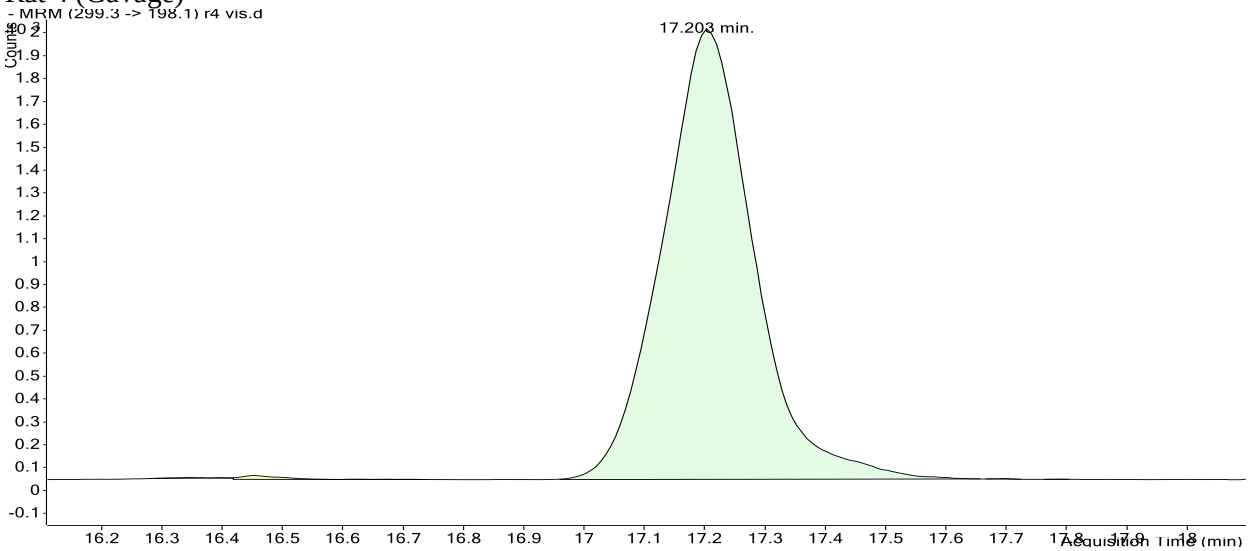

Rat 6 (Gavage)

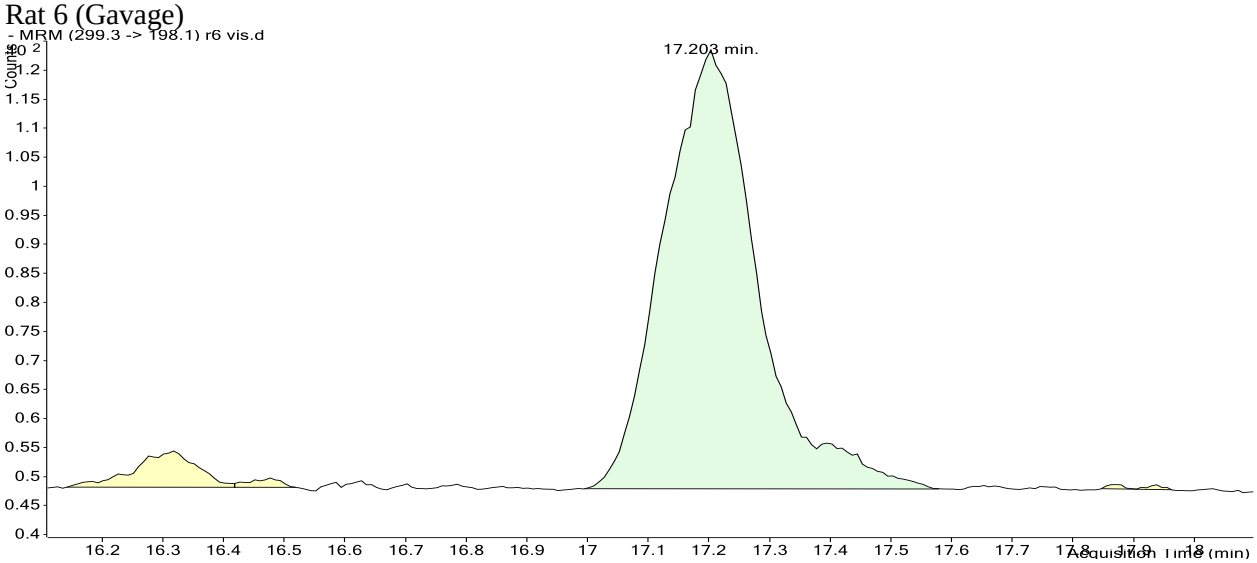

Rat 8 (Gavage)

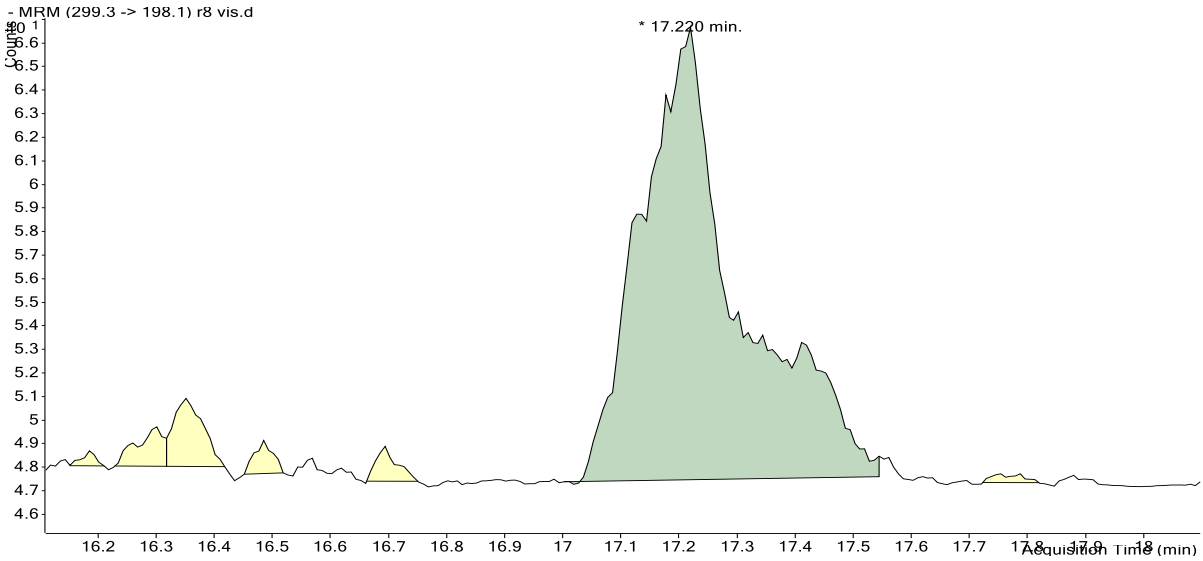

Rat 5 (IV-injected)

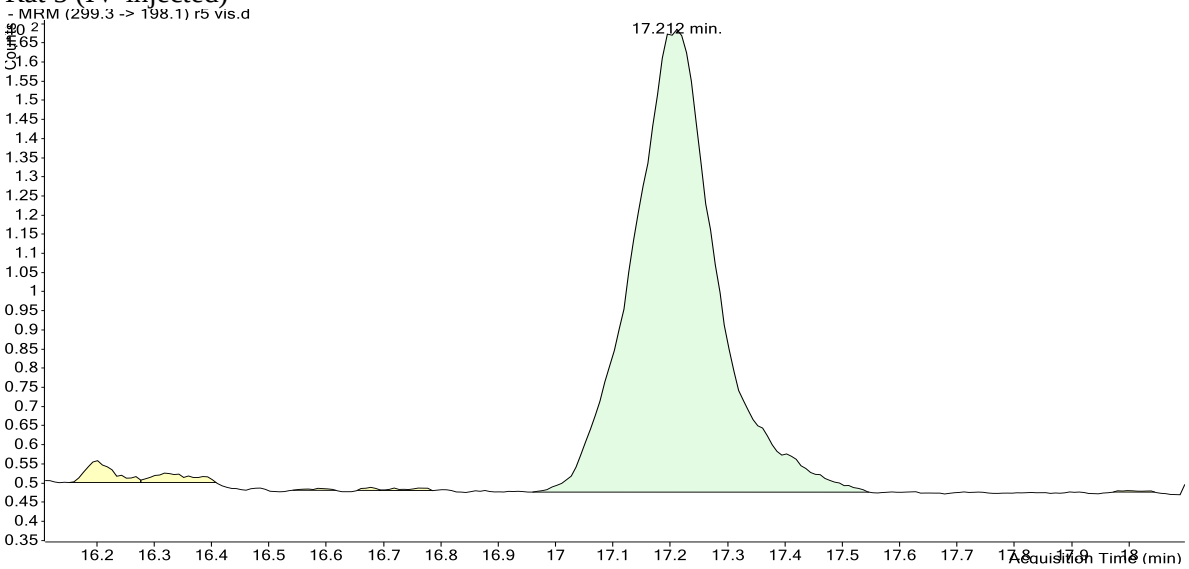

Rat 7 (IV-injected)

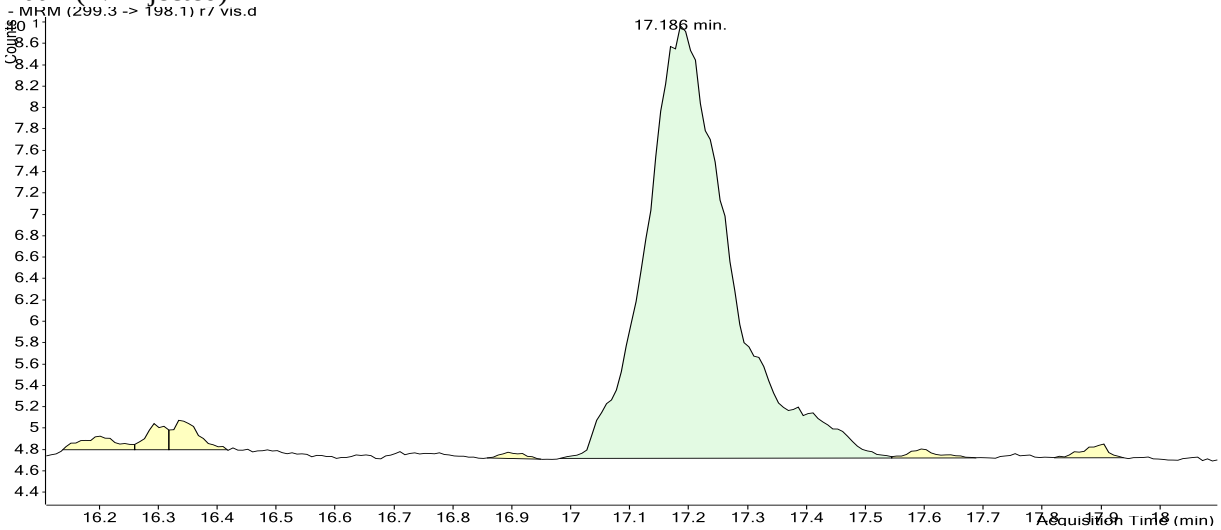

Rat 9 (IV-injected)

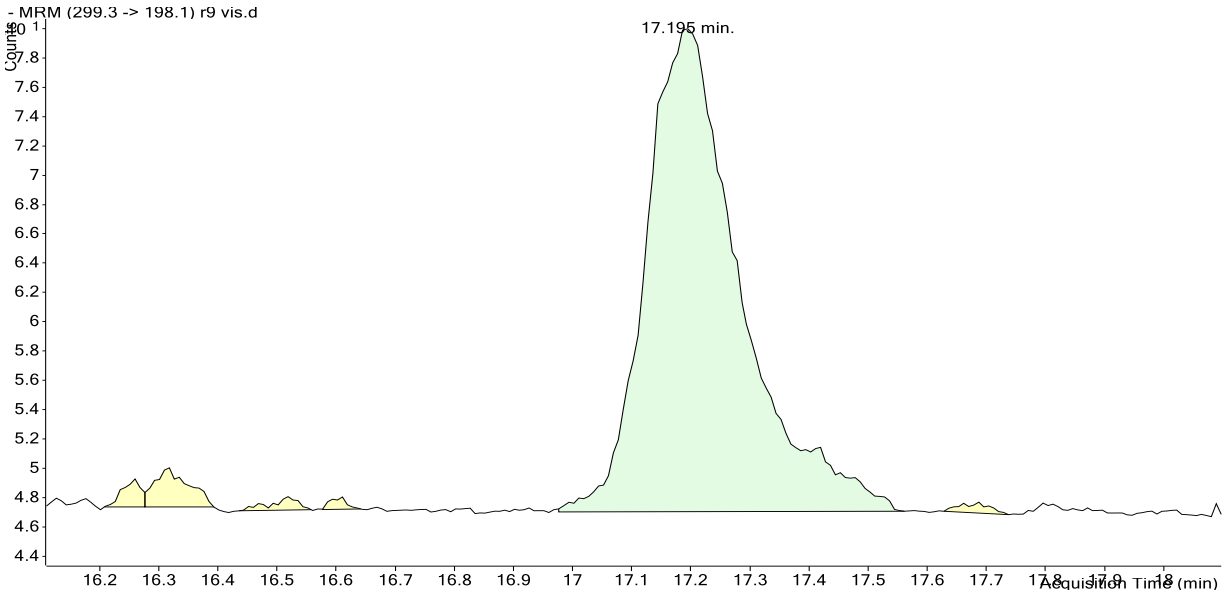

(C) <u>Liver</u>

Rat 2 (Vehicle, gavage)

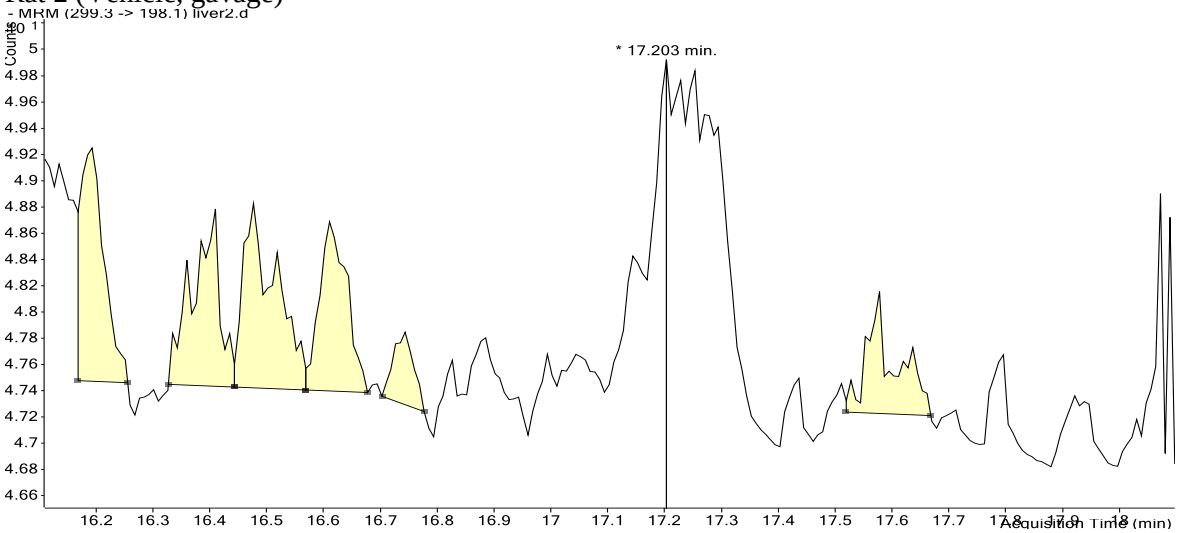

Rat 3 (Vehicle, IV)

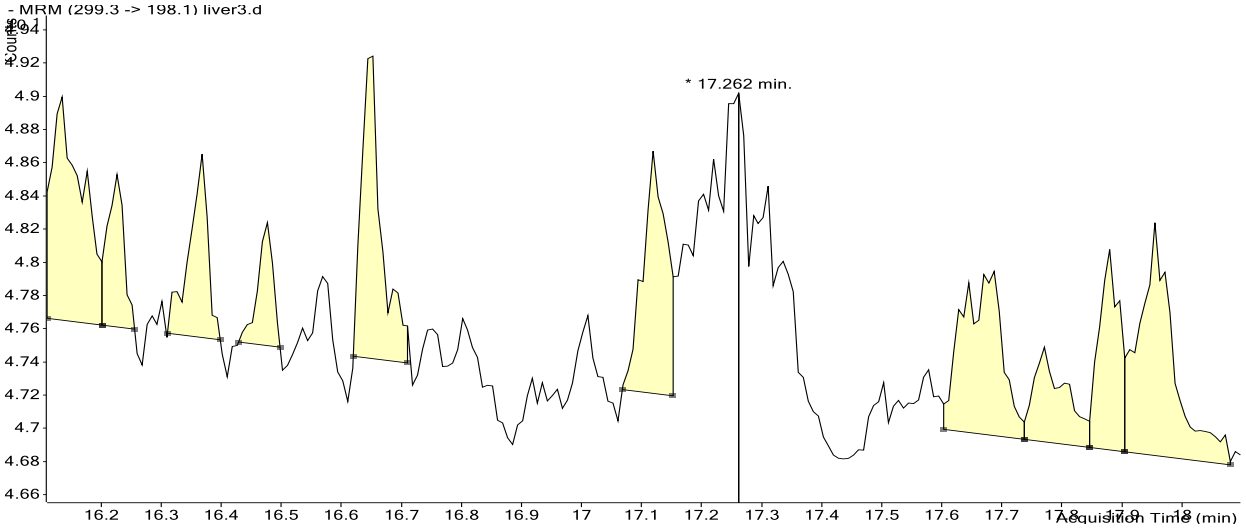

Rat 4 (Gavage)

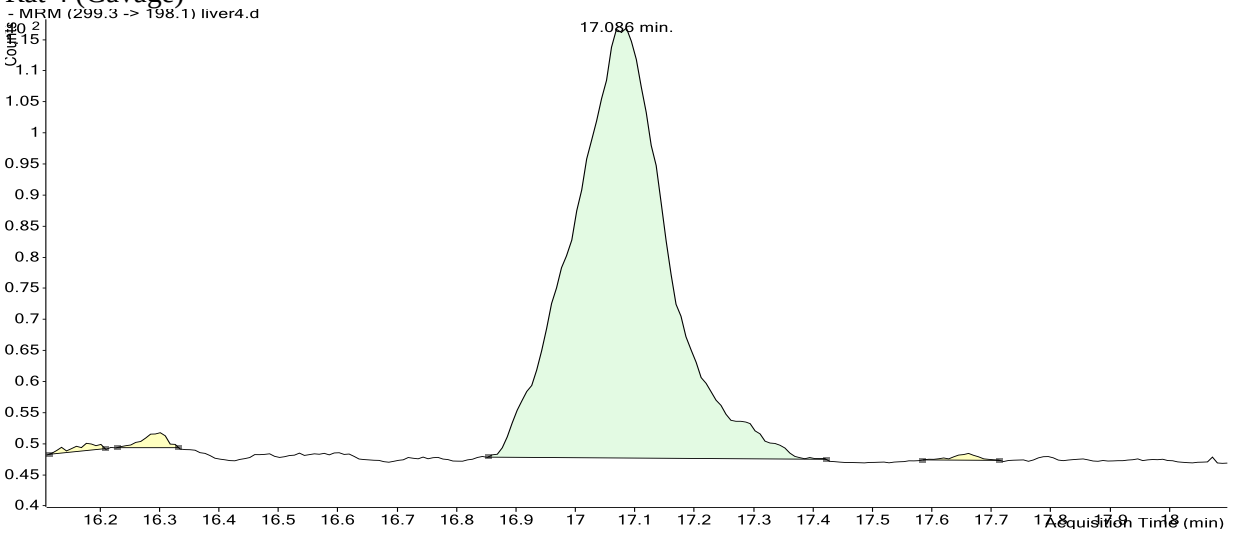

Rat 6 (Gavage)

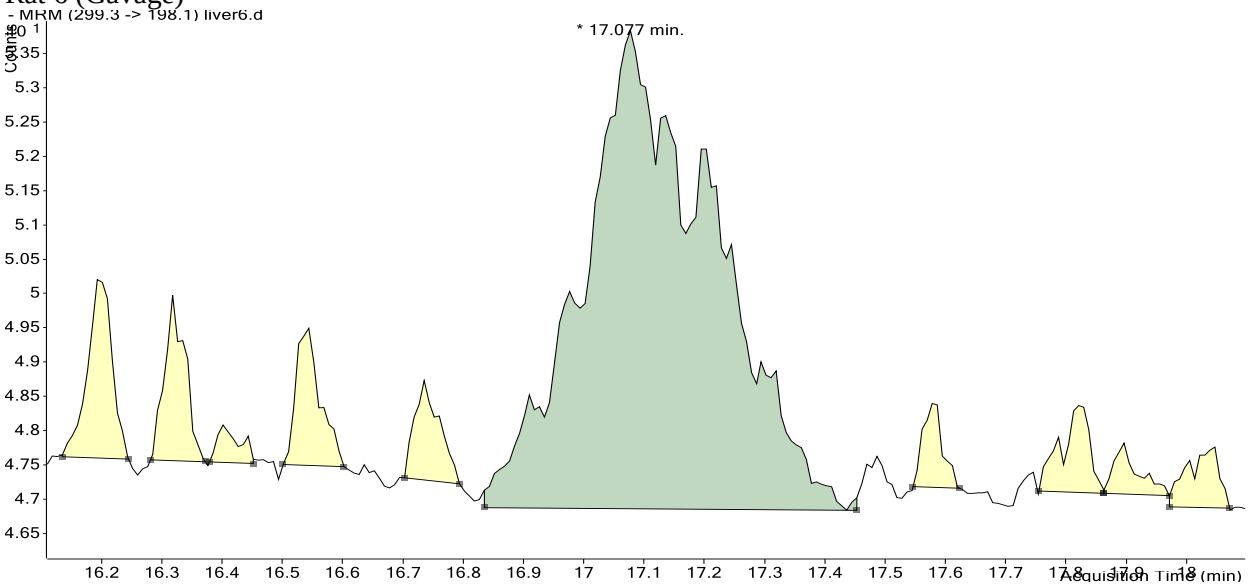

Rat 8 (Gavage)

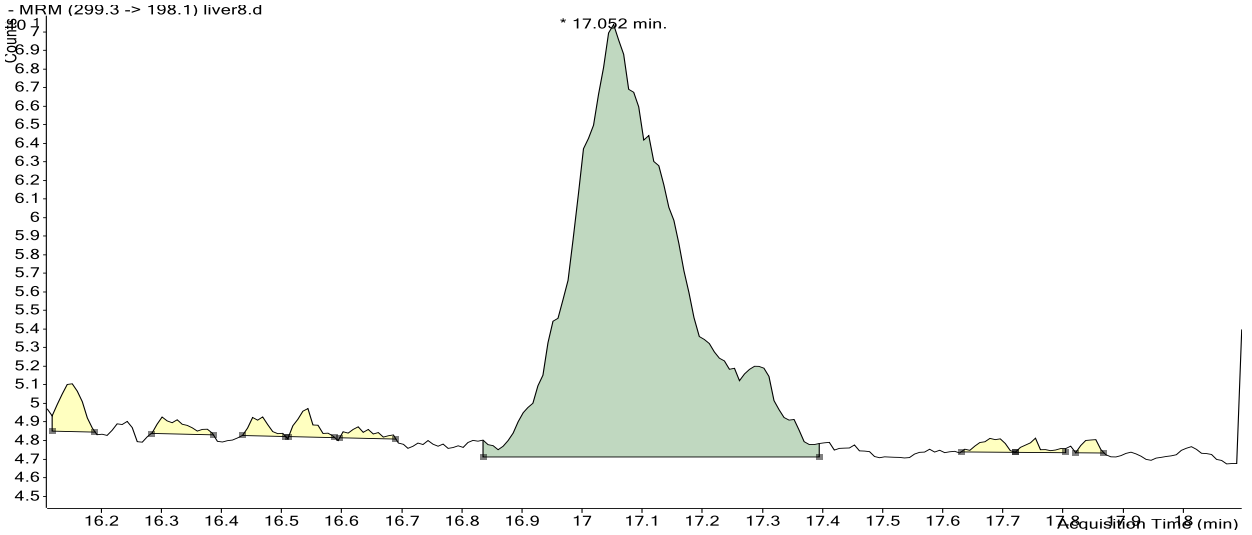

Rat 5 (IV-injected)

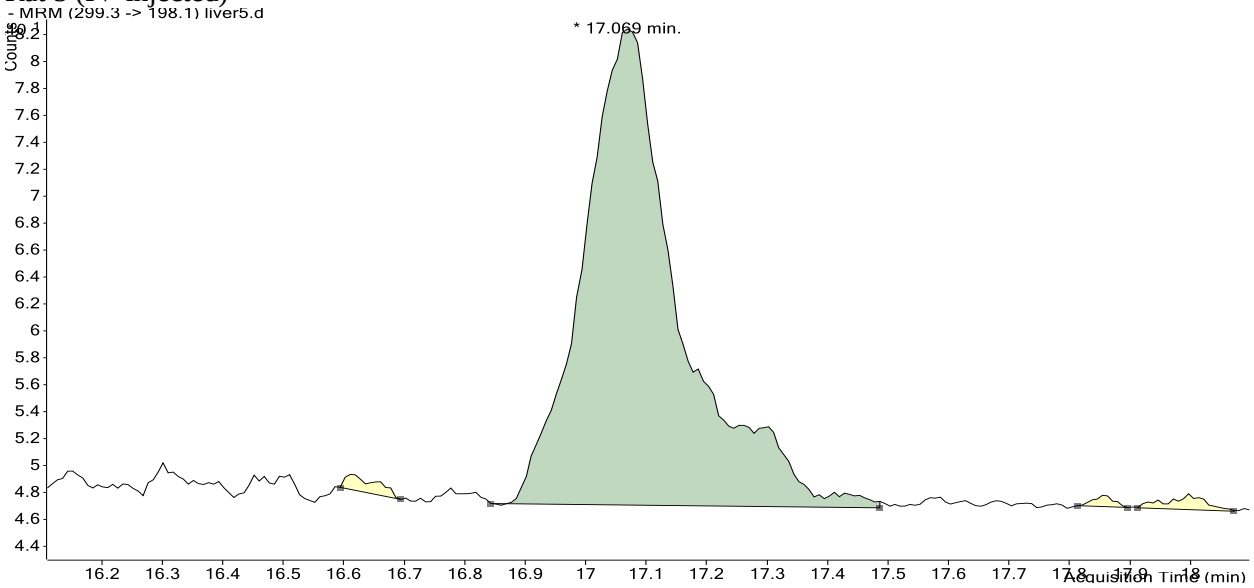

Rat 7 (IV-injected)

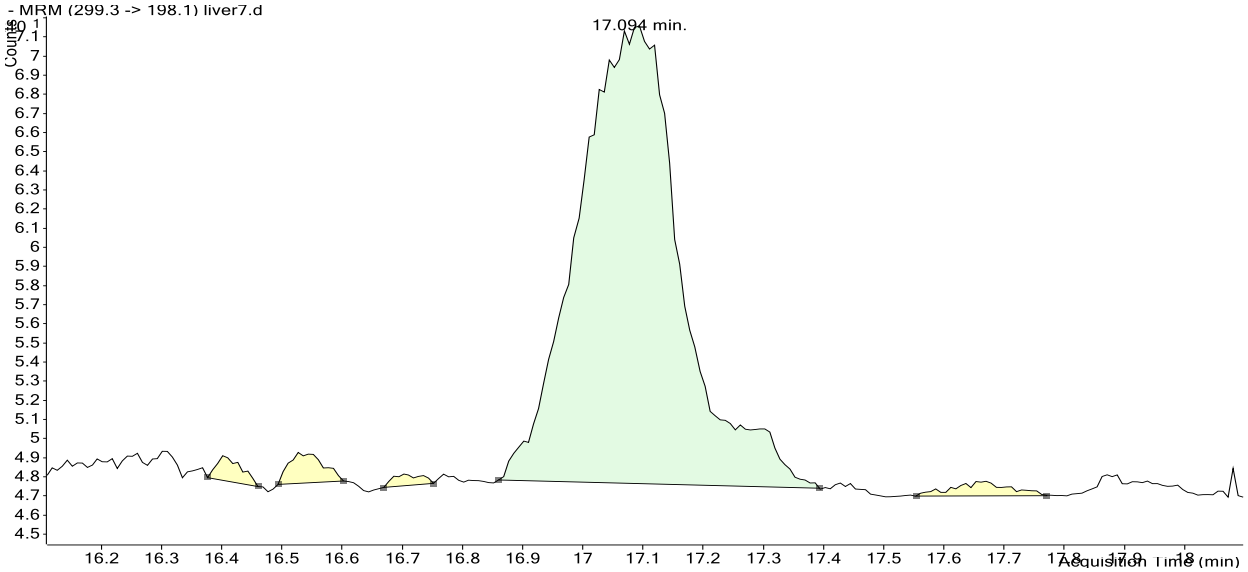

Rat 9 (IV-injected)

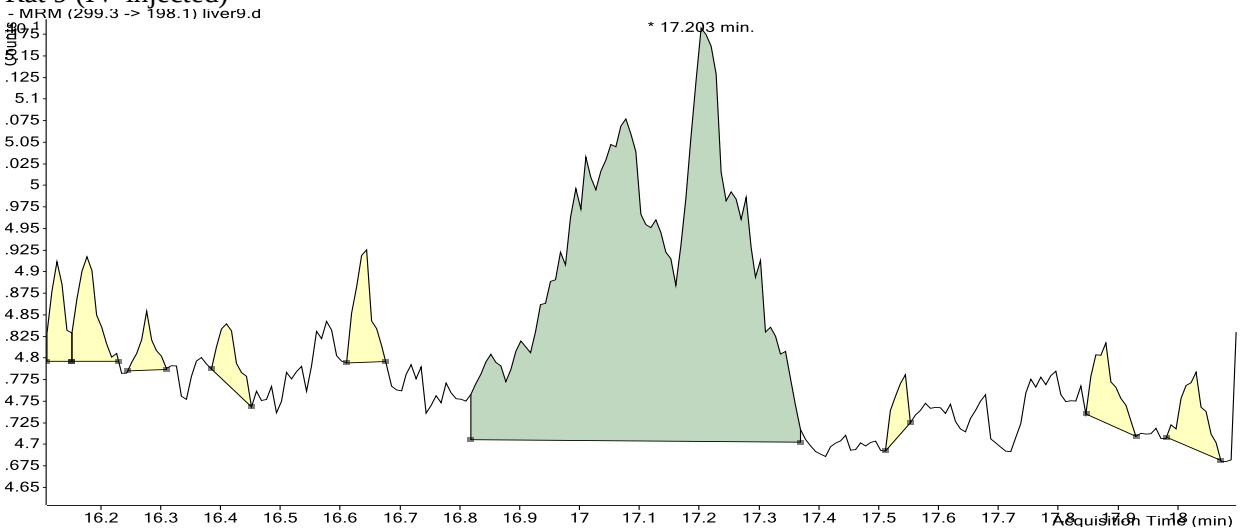

(D) <u>Heart</u>

Rat 2 (Vehicle, gavage)

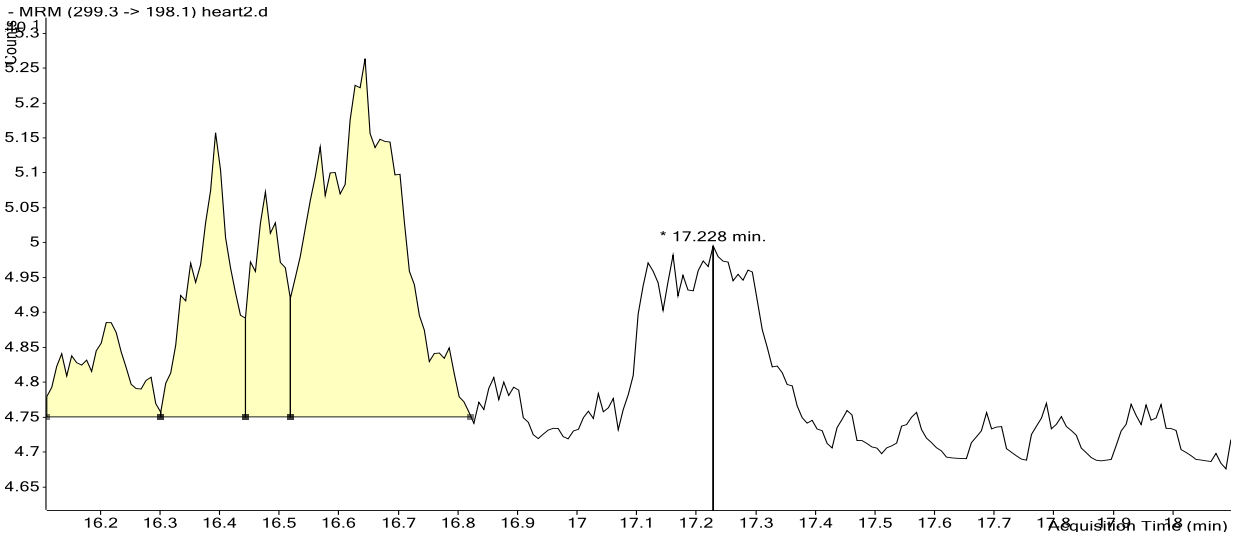

Rat 3 (Vehicle, IV)

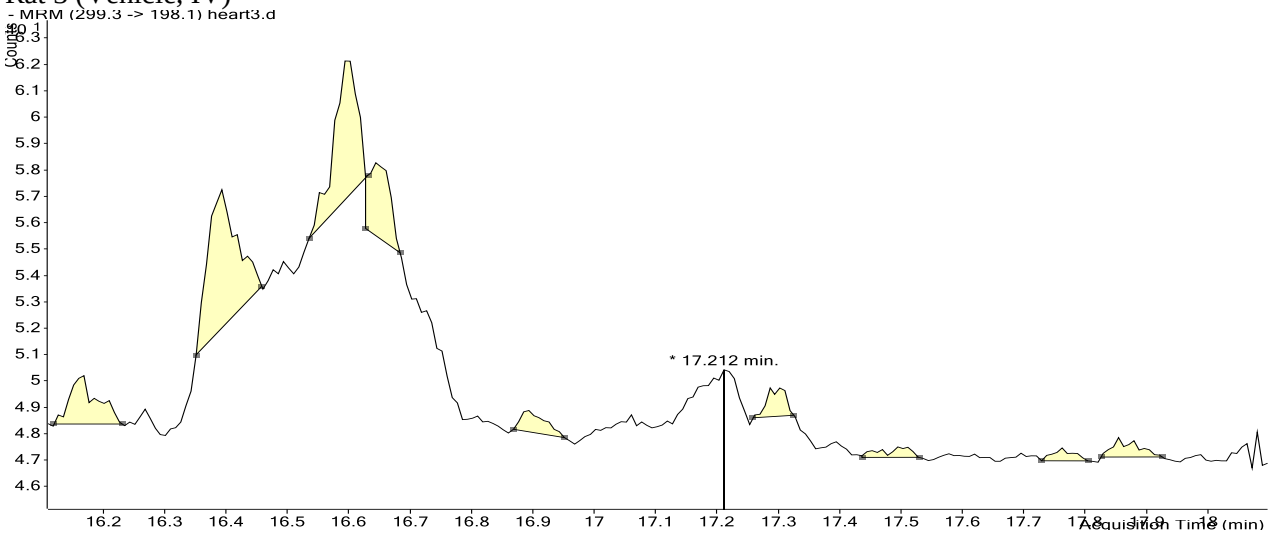

Rat 4 (Gavage)

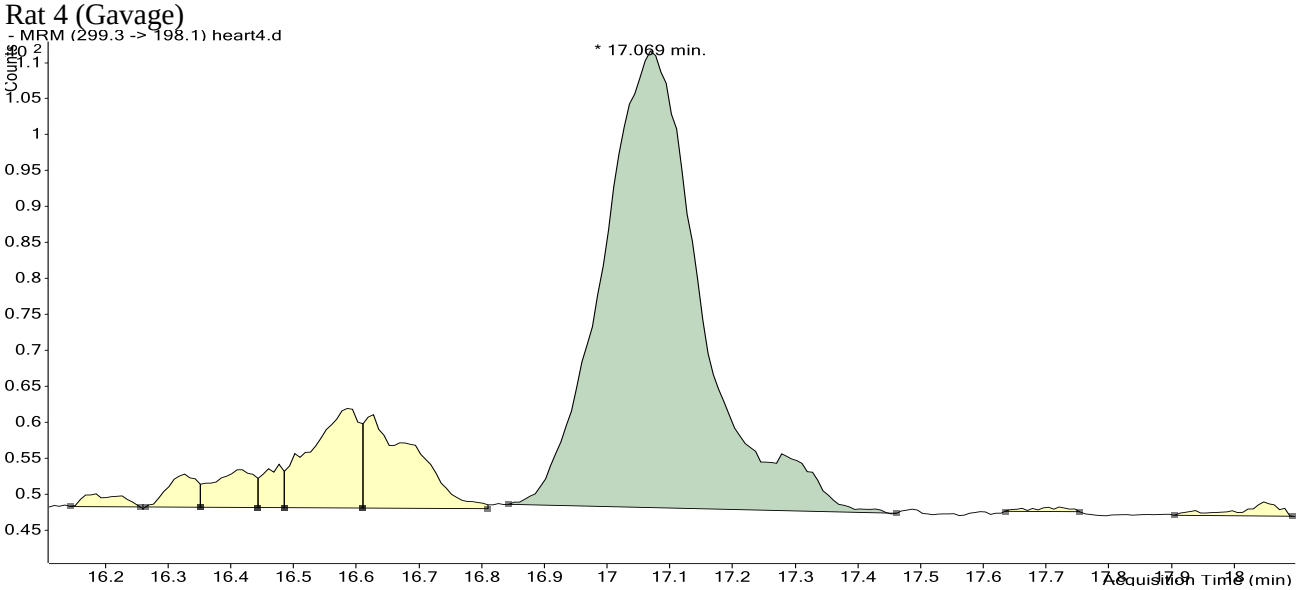

Rat 6 (Gavage)

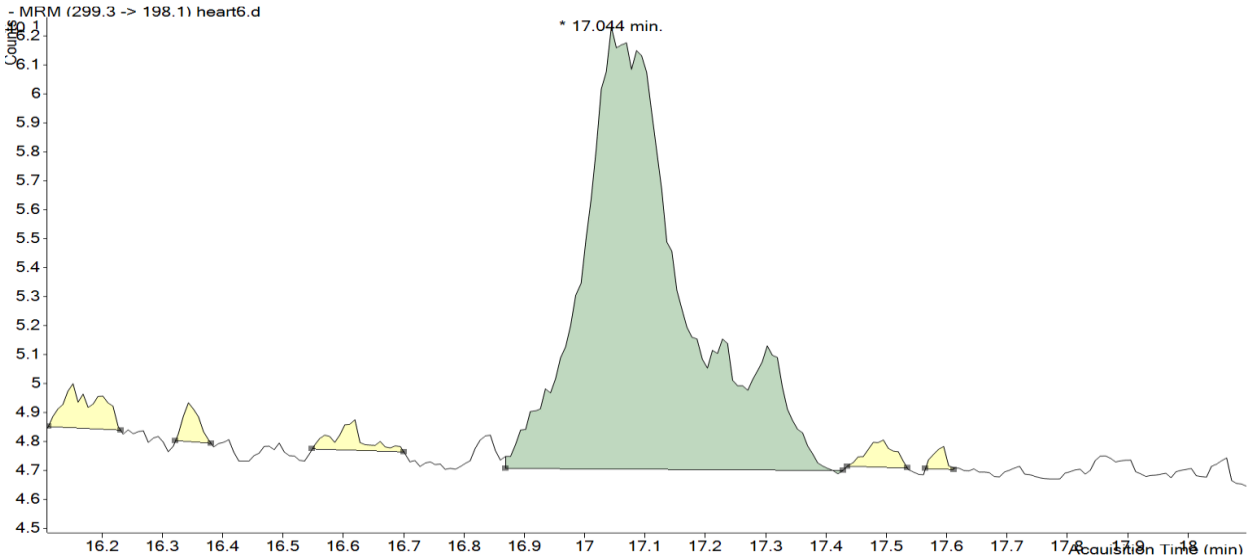

Rat 8 (Gavage)

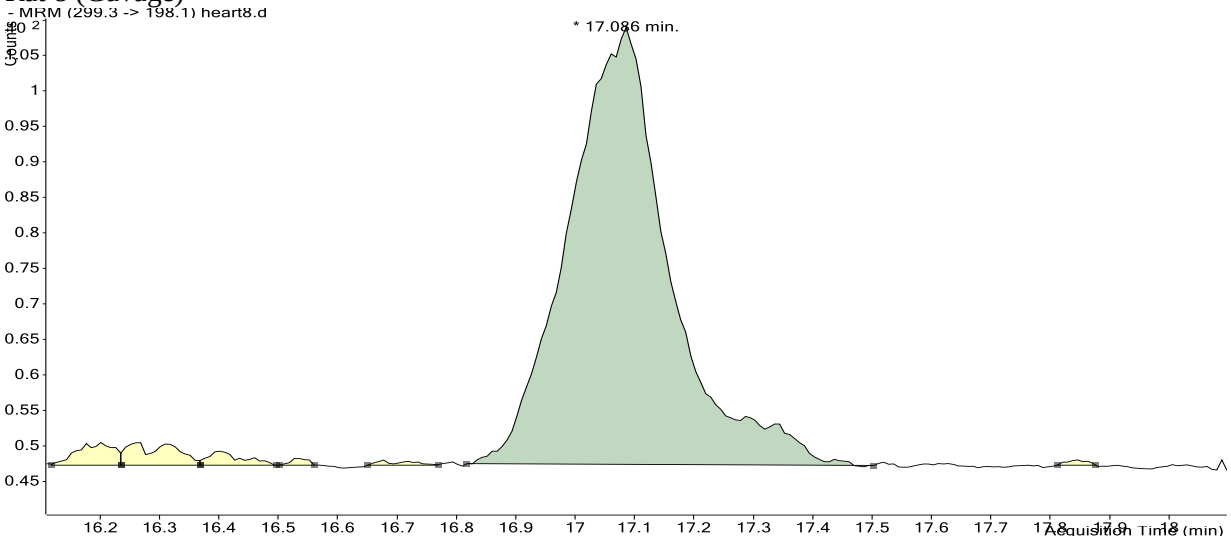

Rat 5 (IV-injected)

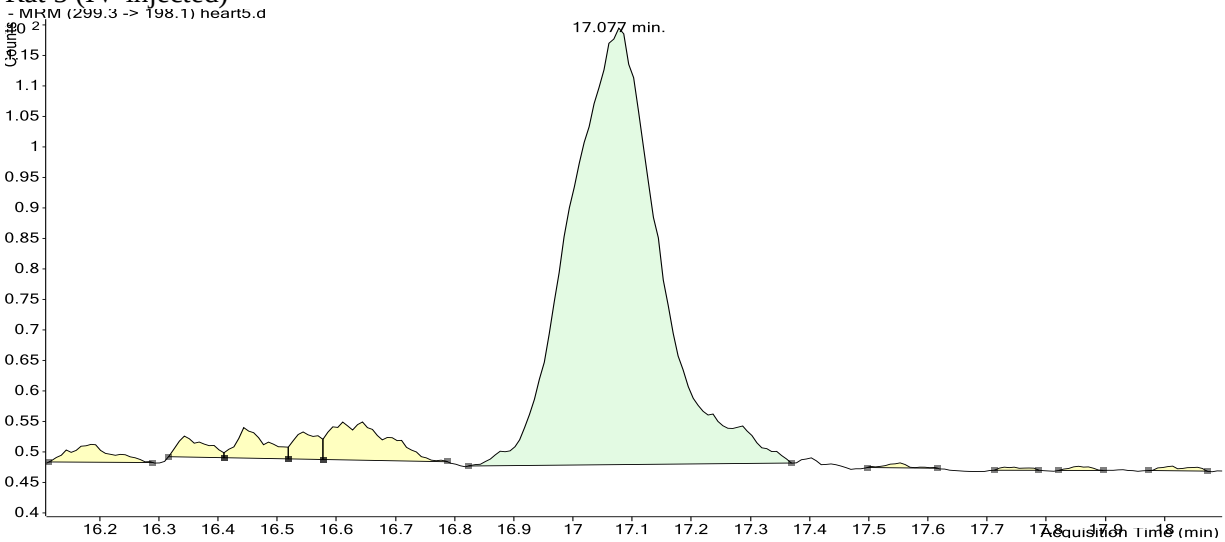

Rat 7 (IV-injected)

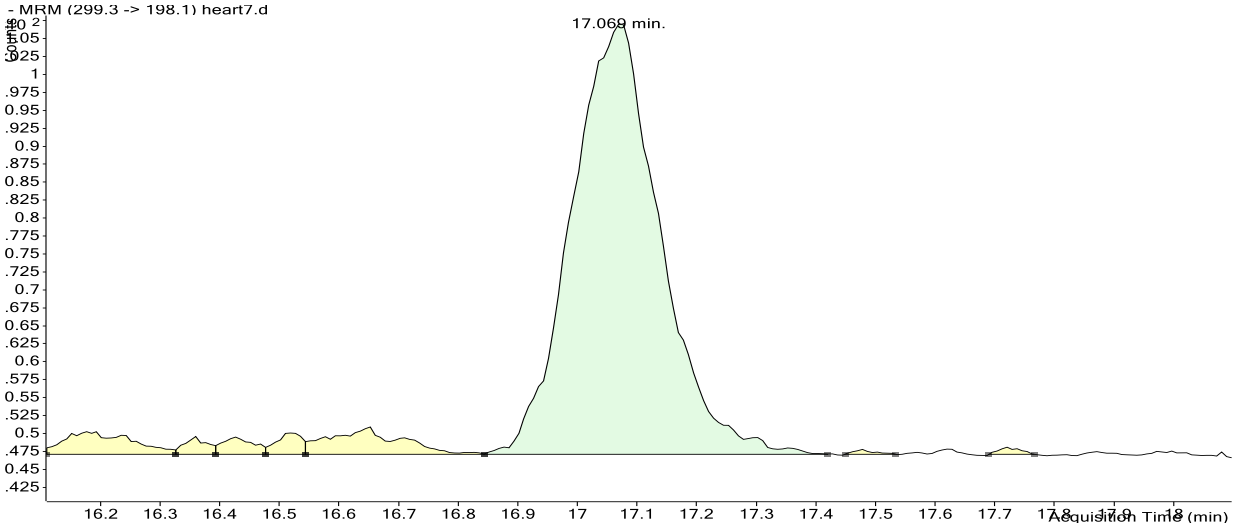

Rat 9 (IV-injected)

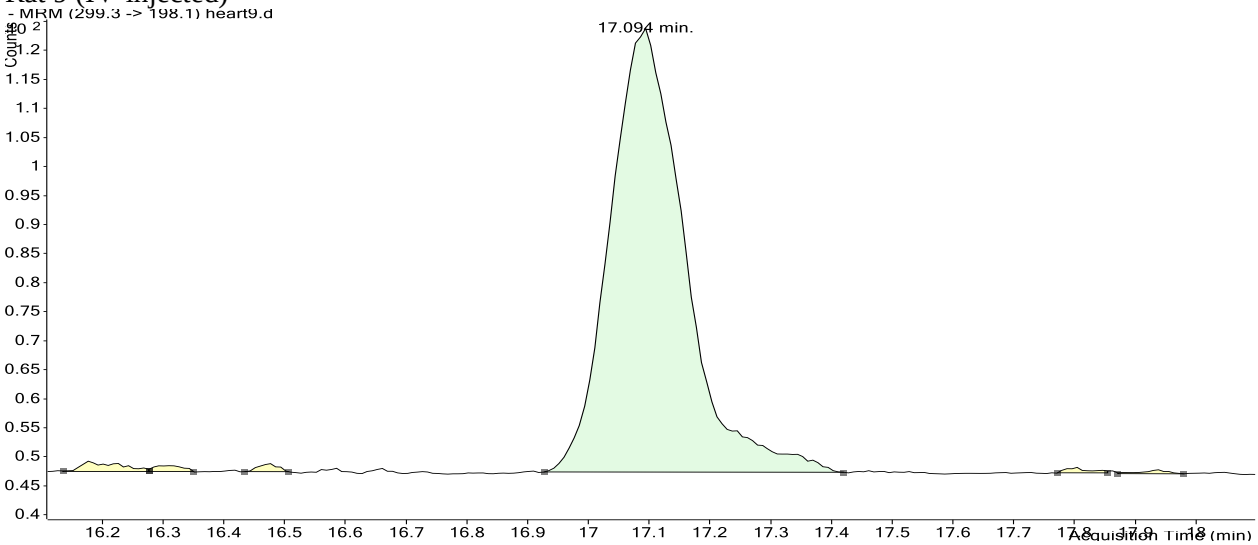

(E) <u>brain</u>

Rat 2 (Vehicle, gavage)

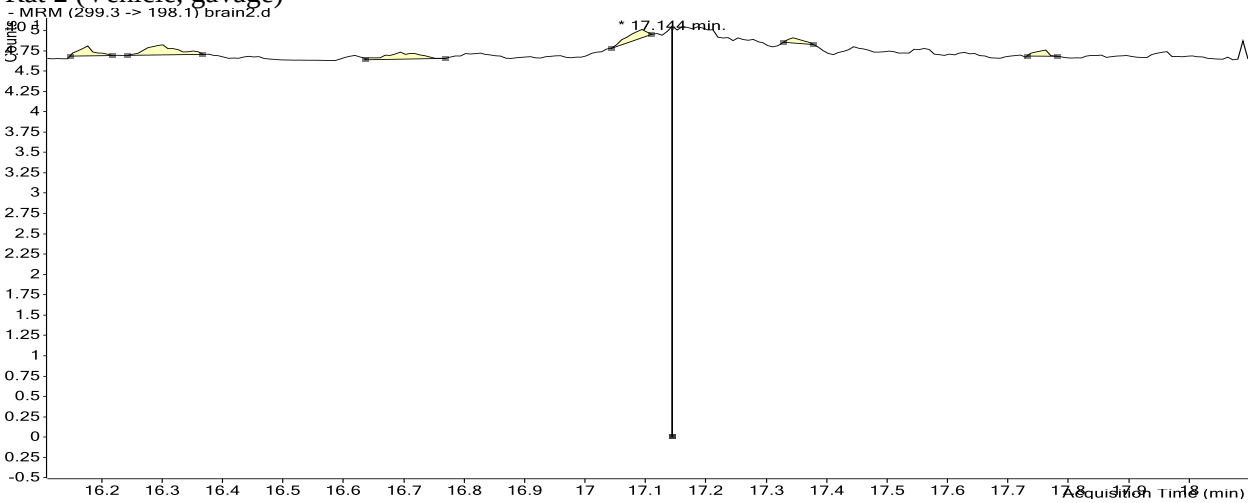

Rat 3 (Vehicle, IV)

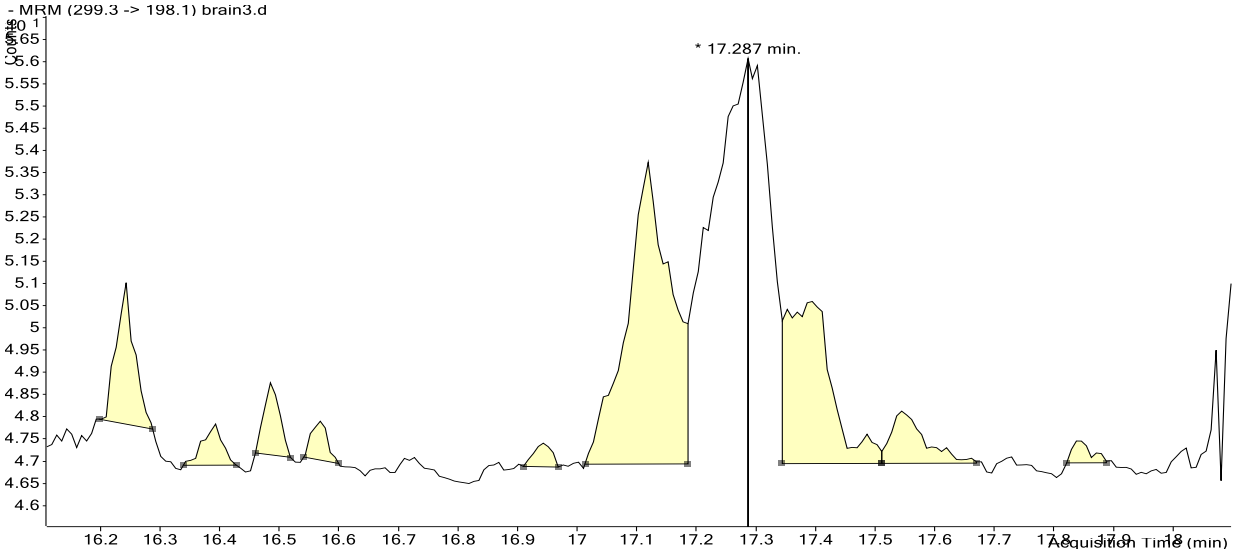

Rat 4 (Gavage)

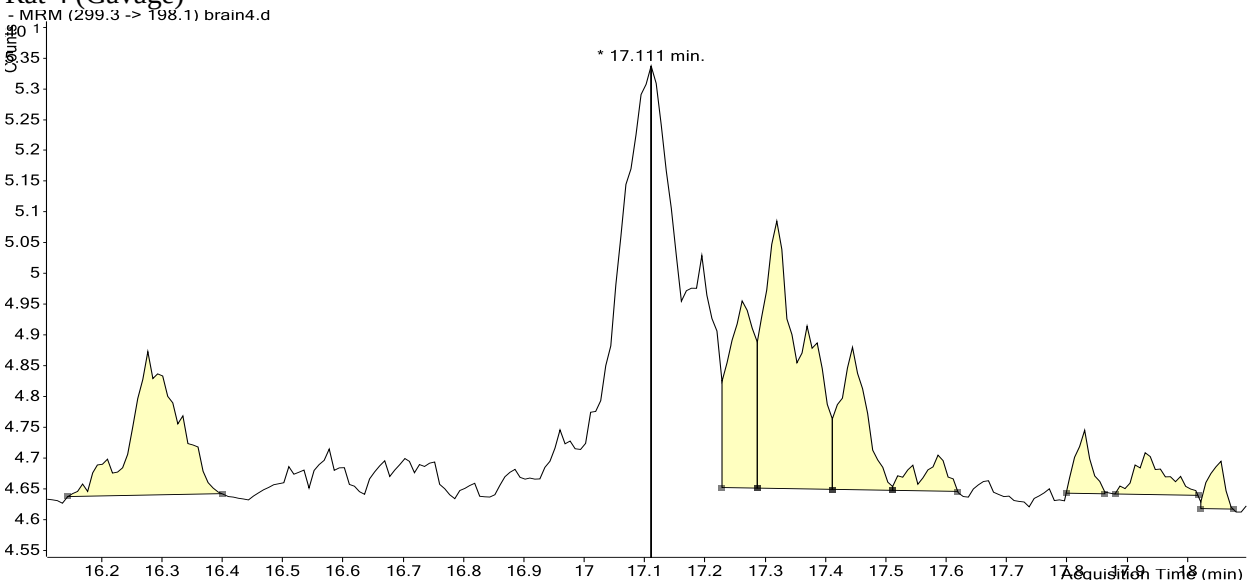

Rat 6 (Gavage)

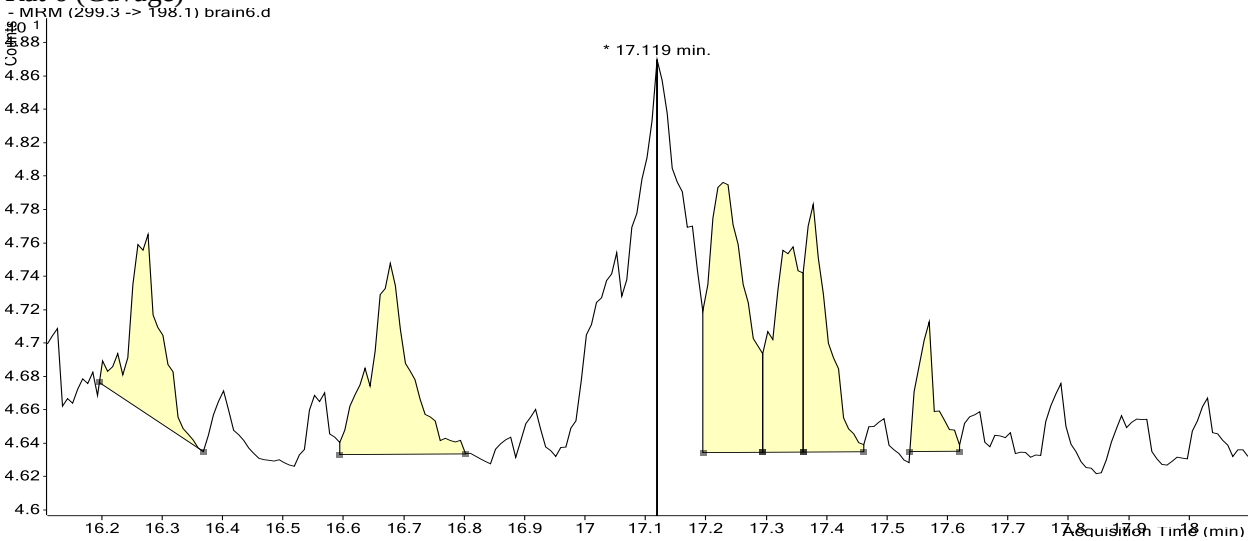

Rat 8 (Gavage)

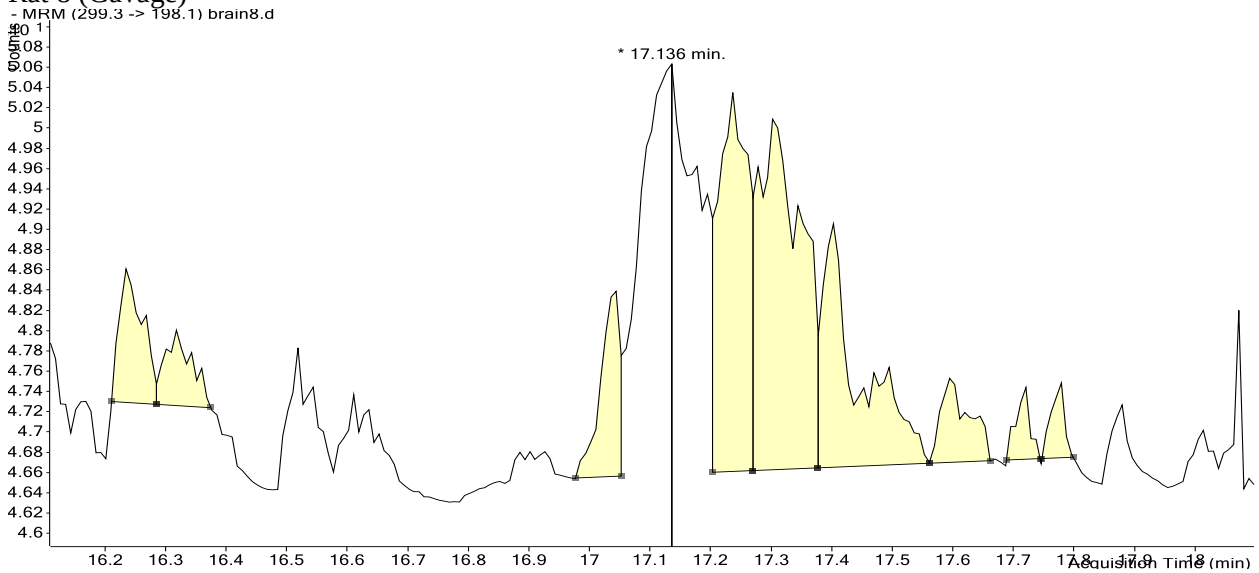

Rat 5 (IV-injected)

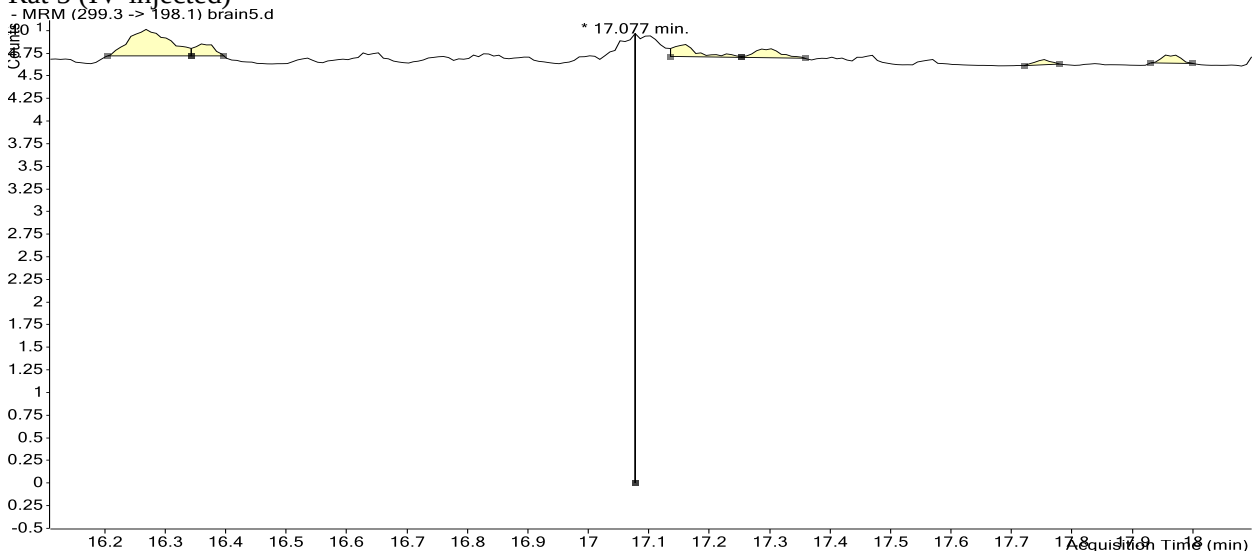

Rat 7 (IV-injected)

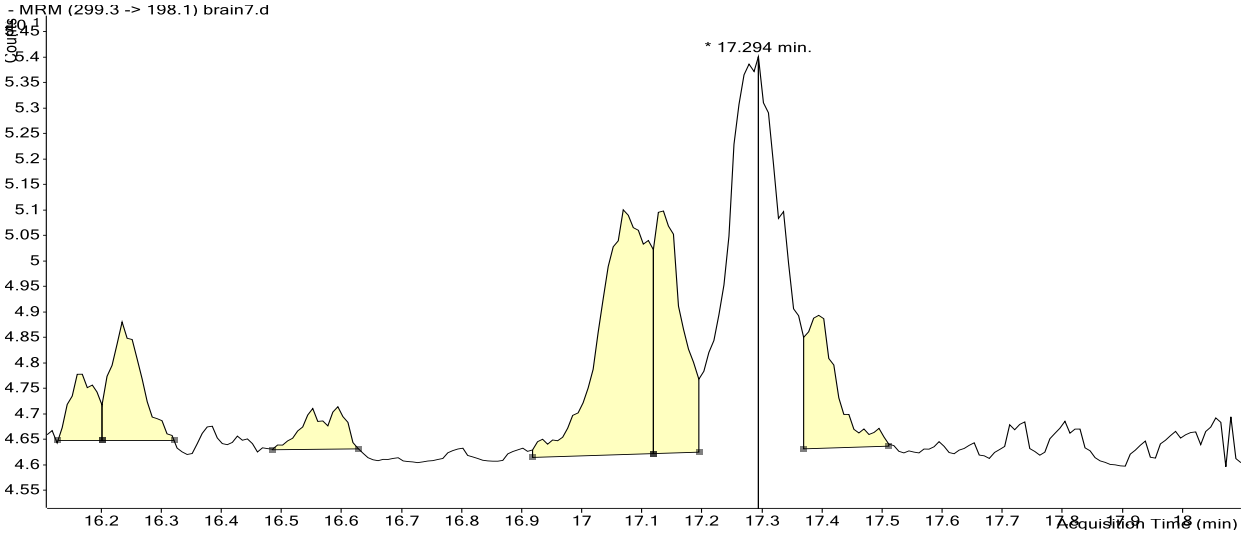

Rat 9 (IV-injected)

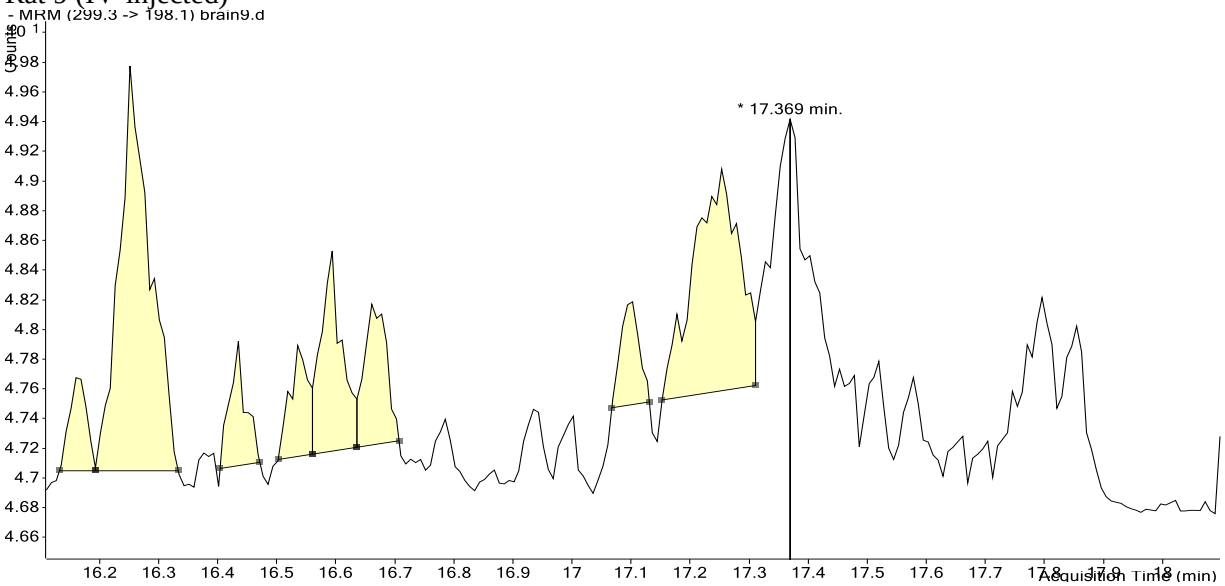

Supplement Figure 6. Predicated downstream metabolites chromatograms of brain, liver, heart, perirenal and visceral adipose tissues in both gavage and IV rats

A) <u>d-9,10,13-TriHOME (333.2-172.1/171.1) and d-13-oxo-ODE (296.2-198.1) in brain</u>

Rat 2 (Vehicle, gavage)

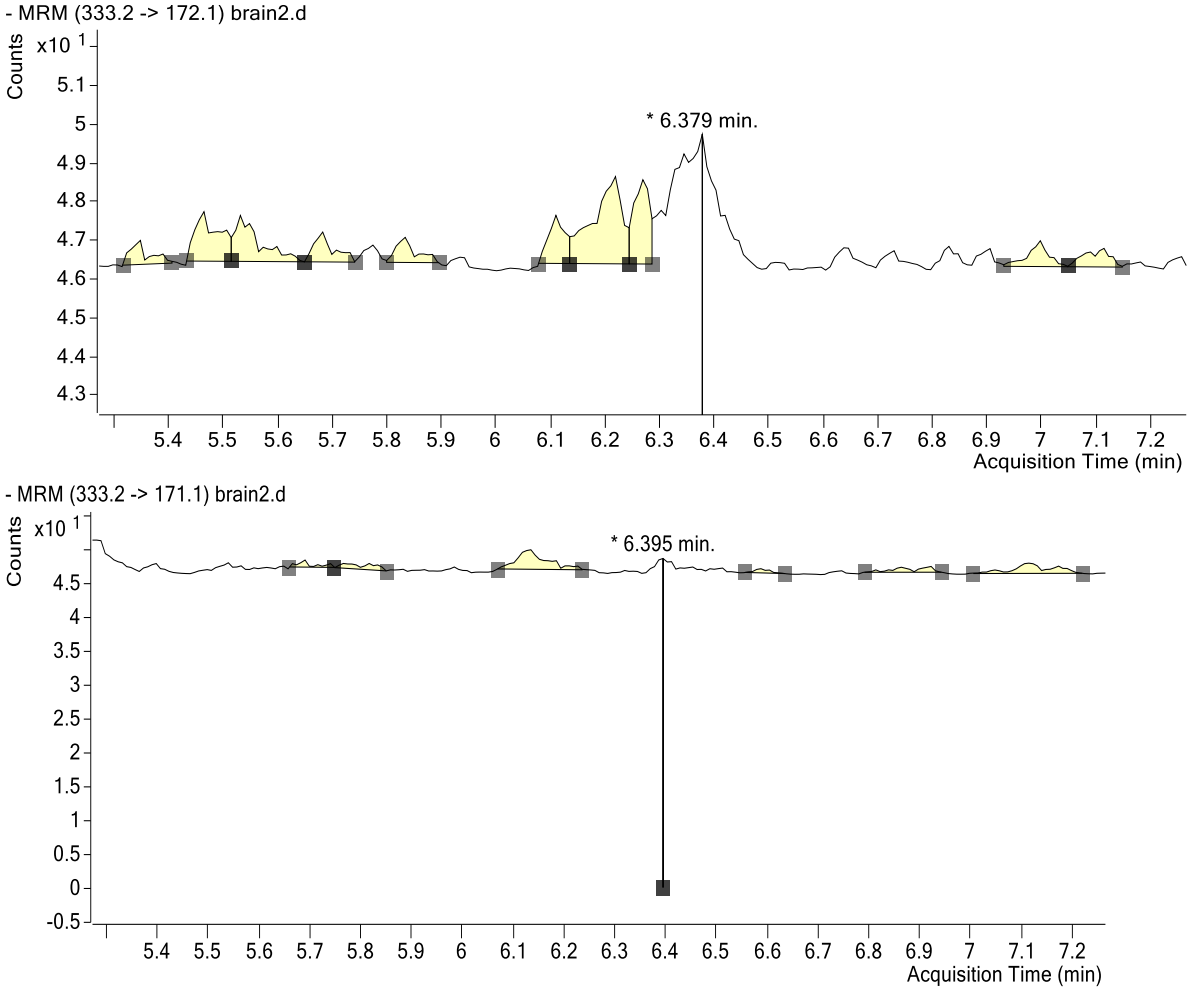

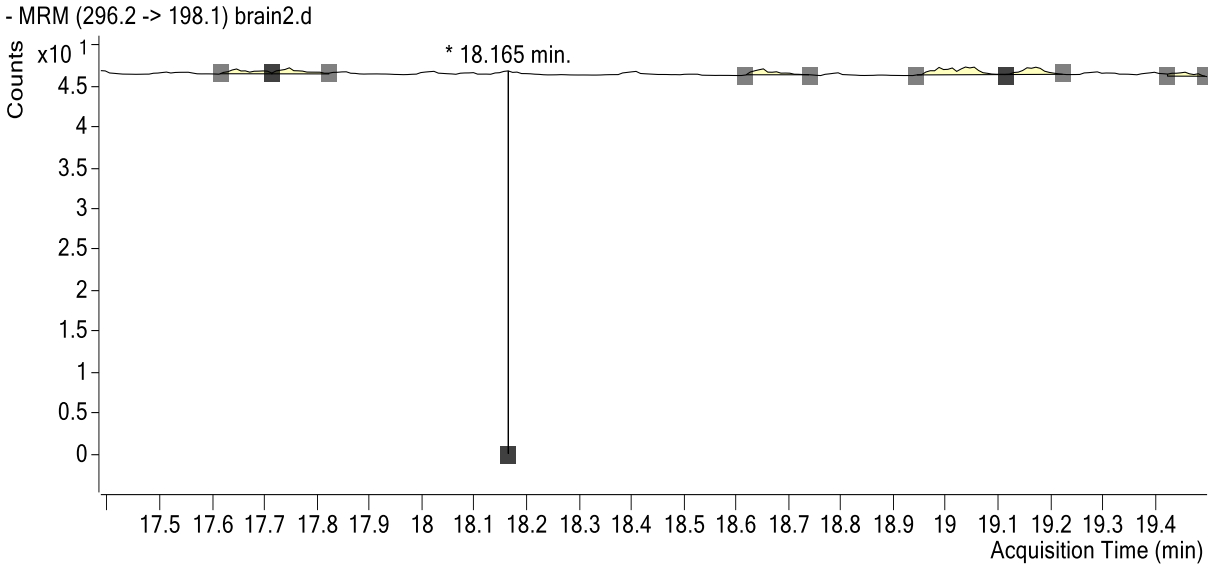

Rat 3 (Vehicle, IV)

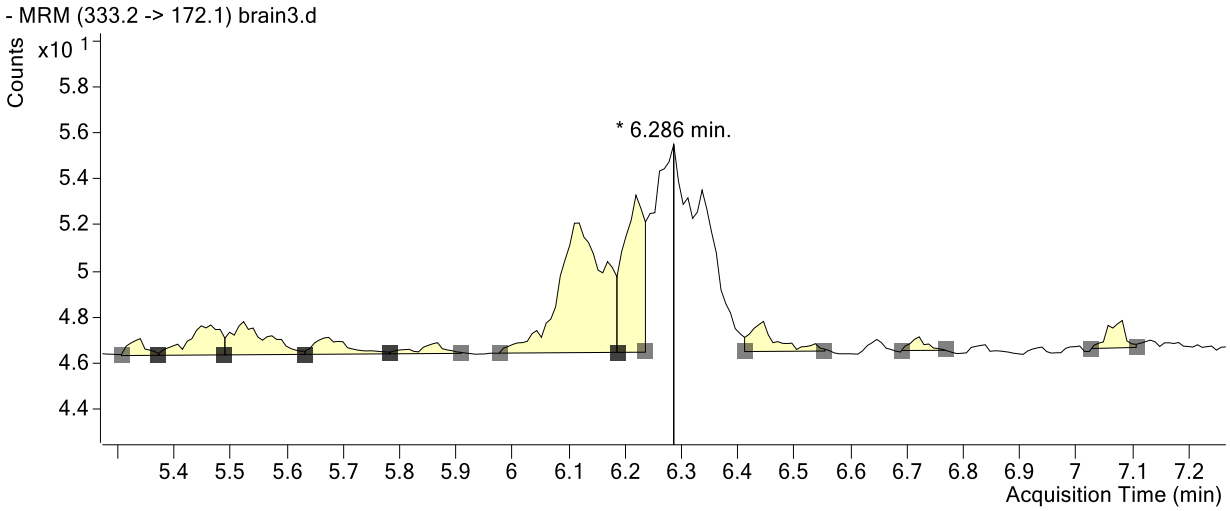

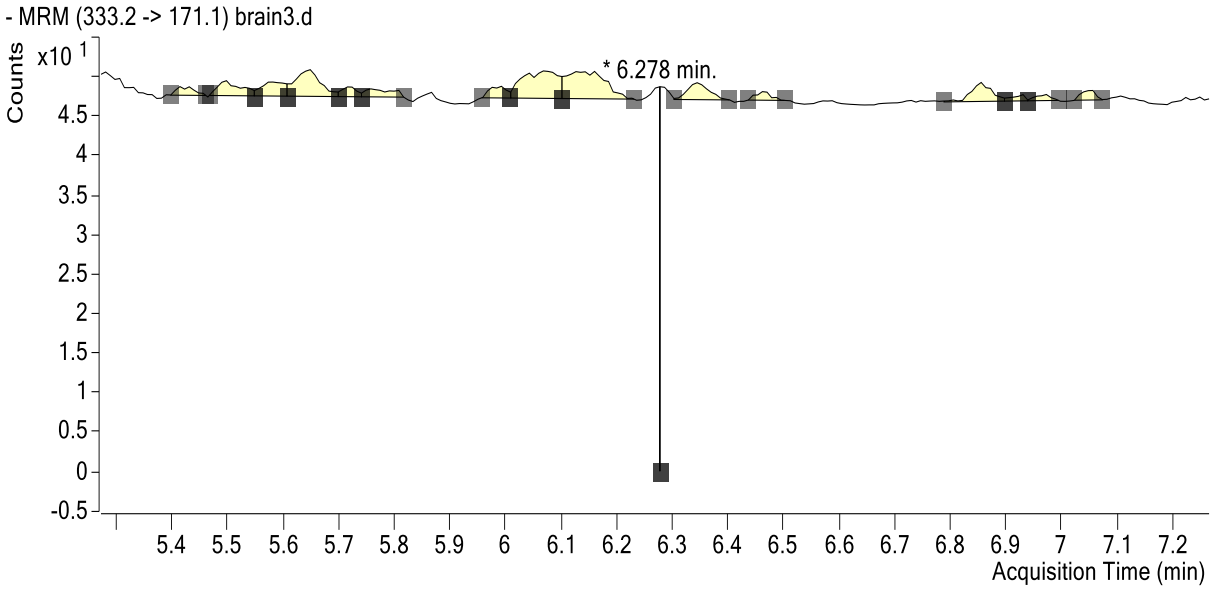
- MRM (333.2 -> 171.1) brain3.d
Counts
x10 1
* 6.278 min.
4.5
4
3.5
3
2.5
2
1.5
1
0.5
0
-0.5
5.4 5.5 5.6 5.7 5.8 5.9 6 6.1 6.2 6.3 6.4 6.5 6.6 6.7 6.8 6.9 7 7.1 7.2
Acquisition Time (min)

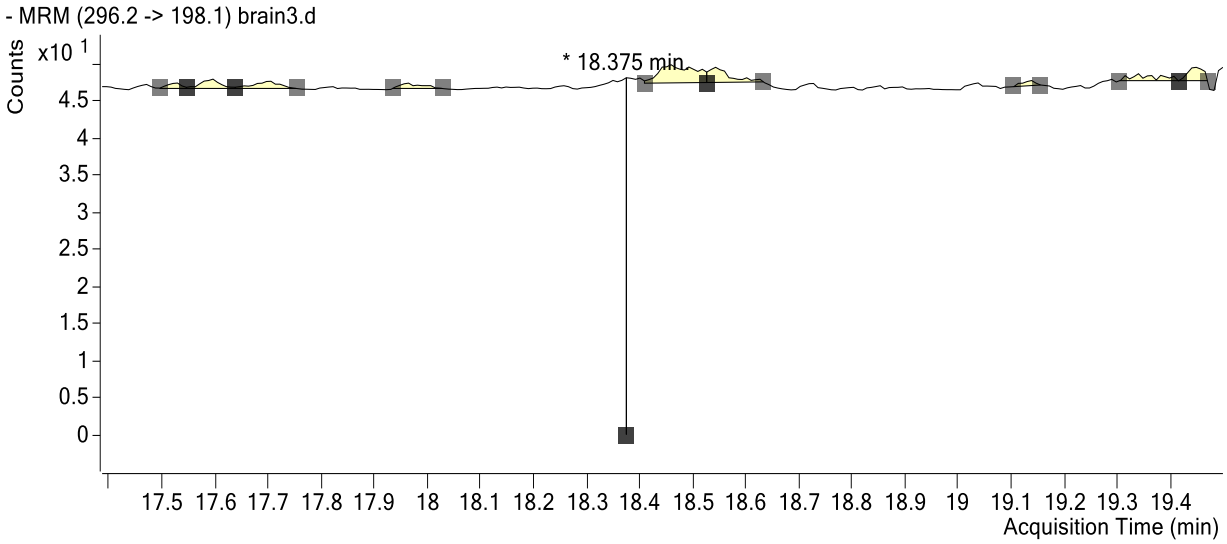
- MRM (296.2 -> 198.1) brain3.d
Counts
x10 1
* 18.375 min.
4.5
4
3.5
3
2.5
2
1.5
1
0.5
0
17.5 17.6 17.7 17.8 17.9 18 18.1 18.2 18.3 18.4 18.5 18.6 18.7 18.8 18.9 19 19.1 19.2 19.3 19.4
Acquisition Time (min)

Rat 4 (gavage)

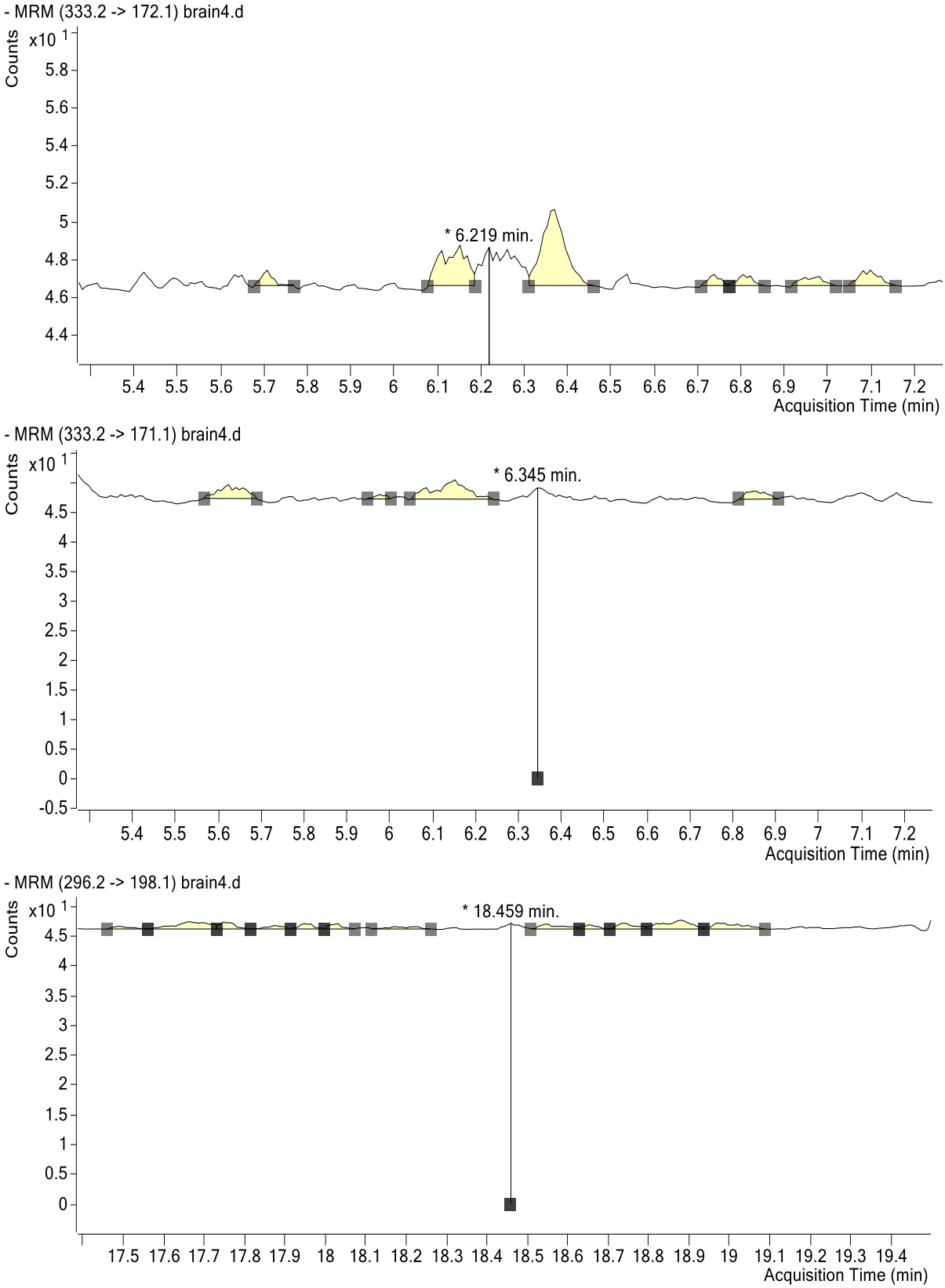
- MRM (333.2 -> 172.1) brain4.d
Counts
x10 1
* 6.219 min.
Acquisition Time (min)
- MRM (333.2 -> 171.1) brain4.d
Counts
x10 1
* 6.345 min.
Acquisition Time (min)
- MRM (296.2 -> 198.1) brain4.d
Counts
x10 1
* 18.459 min.
Acquisition Time (min)

Rat 6 (gavage)

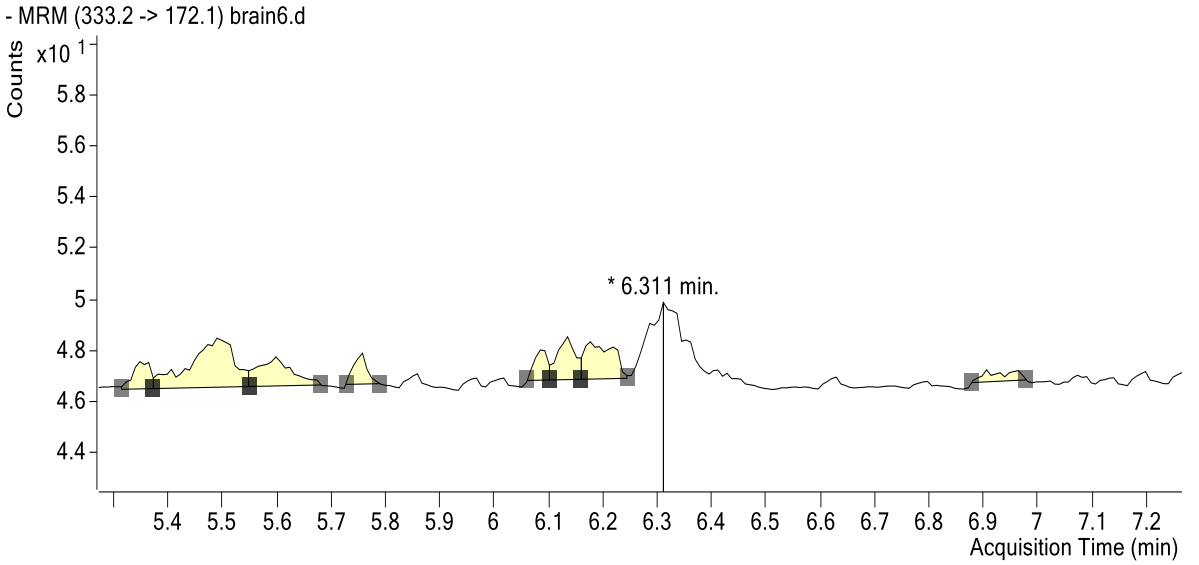
- MRM (333.2 -> 172.1) brain6.d
Counts
x10 1
5.8
5.6
5.4
5.2
5
4.8
4.6
4.4
* 6.311 min.
5.4 5.5 5.6 5.7 5.8 5.9 6 6.1 6.2 6.3 6.4 6.5 6.6 6.7 6.8 6.9 7 7.1 7.2
Acquisition Time (min)

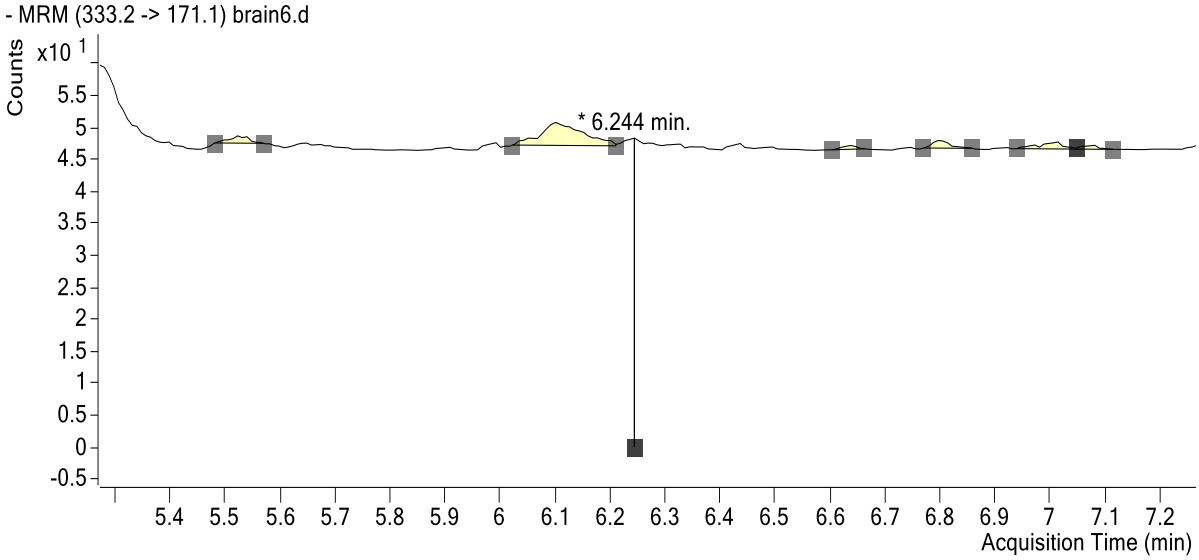
- MRM (333.2 -> 171.1) brain6.d
Counts
x10 1
5.5
5
4.5
4
3.5
3
2.5
2
1.5
1
0.5
0
-0.5
* 6.244 min.
5.4 5.5 5.6 5.7 5.8 5.9 6 6.1 6.2 6.3 6.4 6.5 6.6 6.7 6.8 6.9 7 7.1 7.2
Acquisition Time (min)

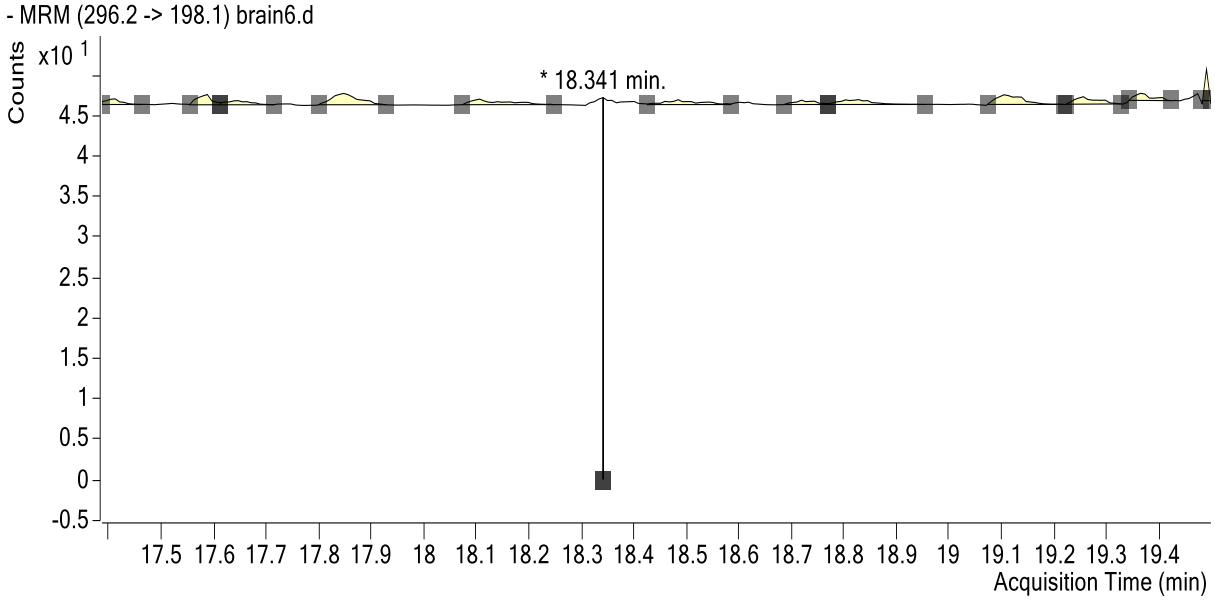
- MRM (296.2 -> 198.1) brain6.d
Counts
x10 1
* 18.341 min.
4.5
4
3.5
3
2.5
2
1.5
1
0.5
0
-0.5
17.5 17.6 17.7 17.8 17.9 18 18.1 18.2 18.3 18.4 18.5 18.6 18.7 18.8 18.9 19 19.1 19.2 19.3 19.4
Acquisition Time (min)

Rat 8 (gavage)

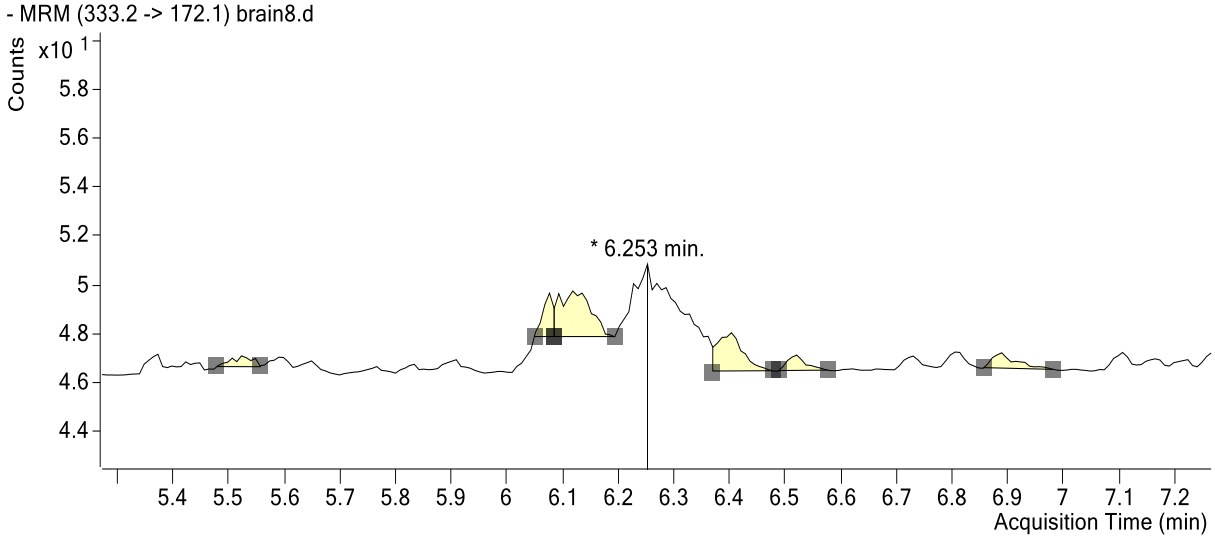
- MRM (333.2 -> 172.1) brain8.d
Counts
x10 1
* 6.253 min.
5.8
5.6
5.4
5.2
5
4.8
4.6
4.4
5.4 5.5 5.6 5.7 5.8 5.9 6 6.1 6.2 6.3 6.4 6.5 6.6 6.7 6.8 6.9 7 7.1 7.2
Acquisition Time (min)

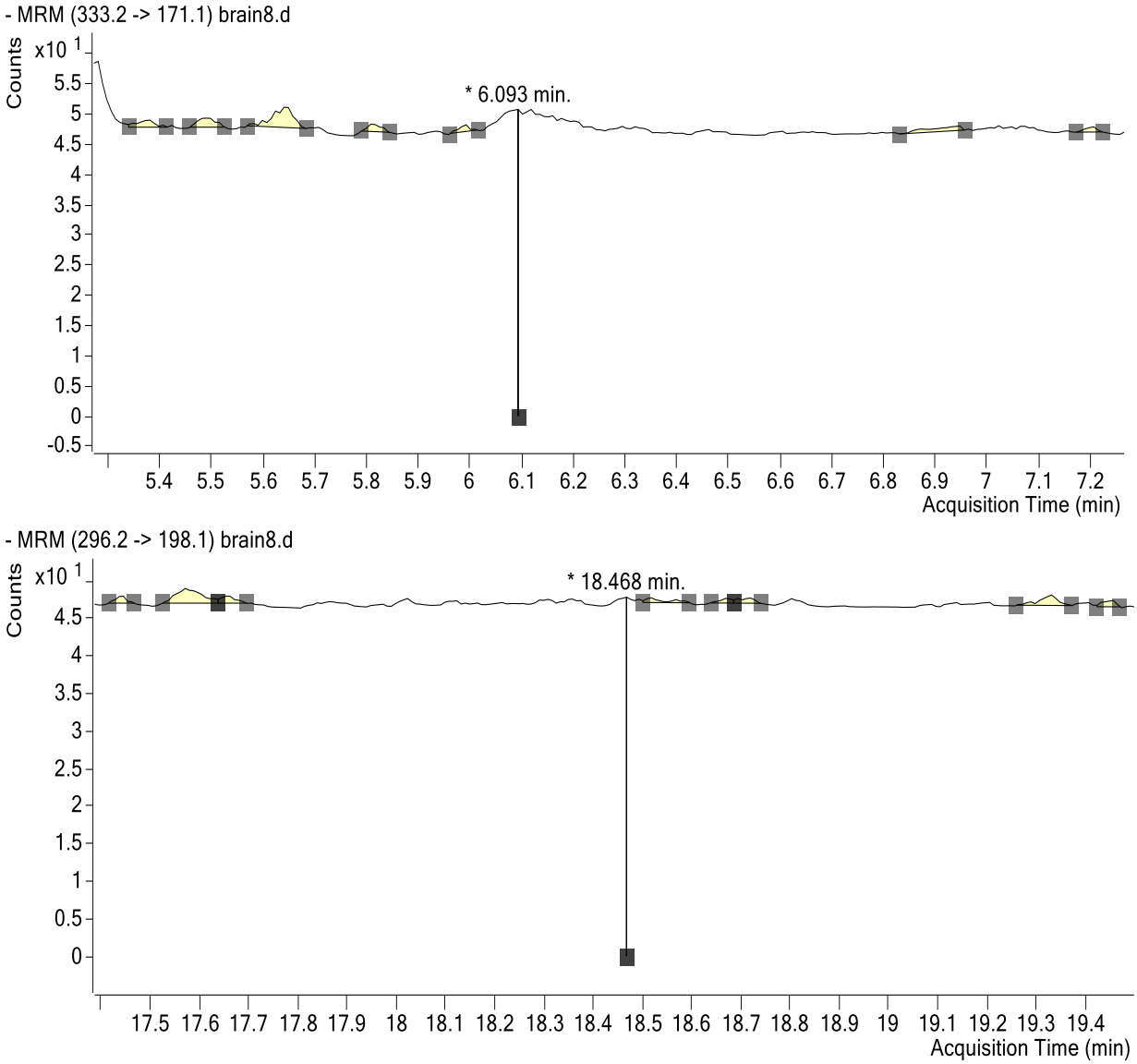
- MRM (333.2 -> 171.1) brain8.d
Counts
x10 1
* 6.093 min.
Acquisition Time (min)
- MRM (296.2 -> 198.1) brain8.d
Counts
x10 1
* 18.468 min.
Acquisition Time (min)

Rat 5 (IV)

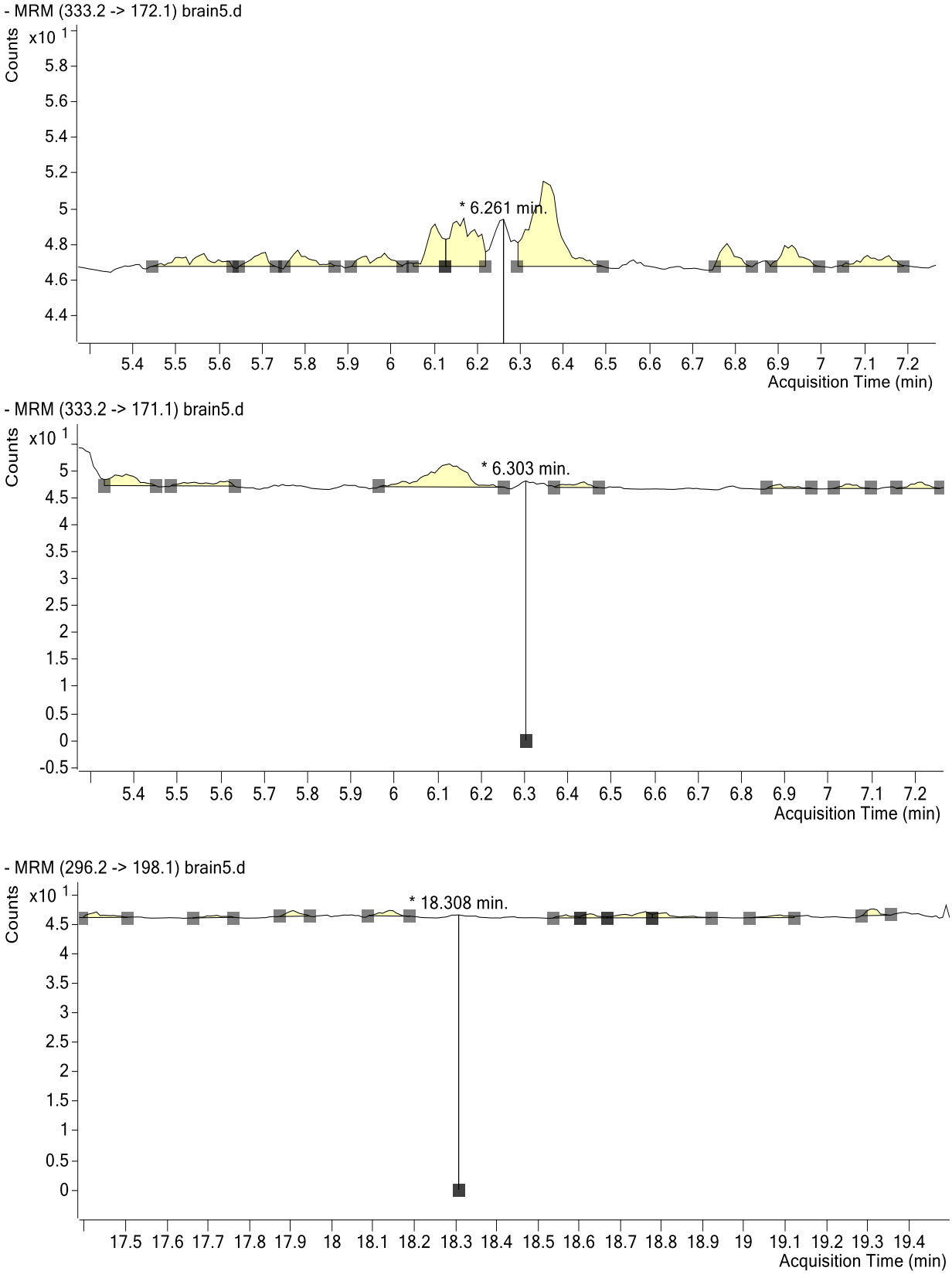
- MRM (333.2 -> 172.1) brain5.d
Counts
x10 1
* 6.261 min.
Acquisition Time (min)
- MRM (333.2 -> 171.1) brain5.d
Counts
x10 1
* 6.303 min.
Acquisition Time (min)
- MRM (296.2 -> 198.1) brain5.d
Counts
x10 1
* 18.308 min.
Acquisition Time (min)

Rat 7 (IV)

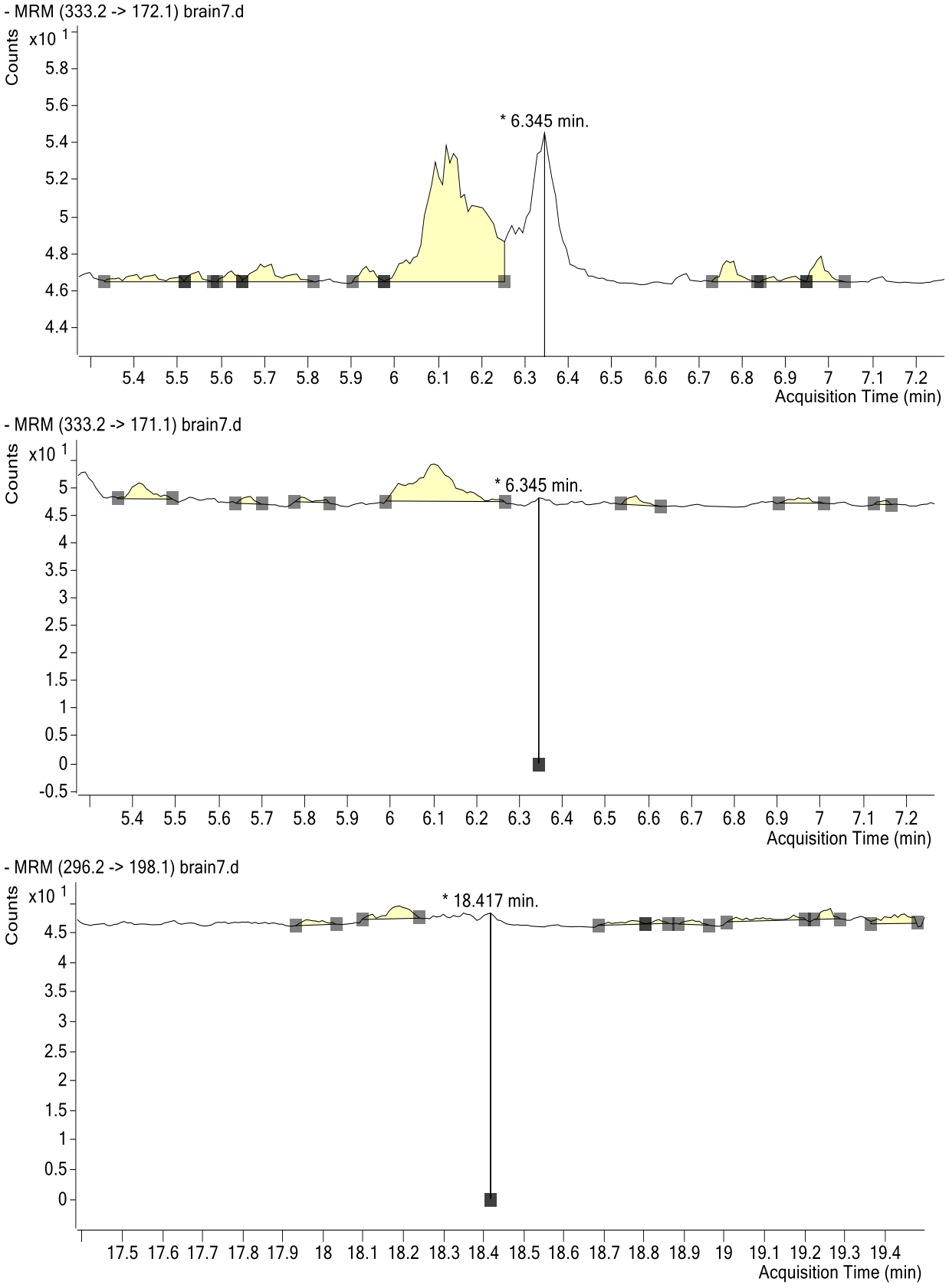
- MRM (333.2 -> 172.1) brain7.d
Counts
x10 1
* 6.345 min.
Acquisition Time (min)
- MRM (333.2 -> 171.1) brain7.d
Counts
x10 1
* 6.345 min.
Acquisition Time (min)
- MRM (296.2 -> 198.1) brain7.d
Counts
x10 1
* 18.417 min.
Acquisition Time (min)

Rat 9 (IV)

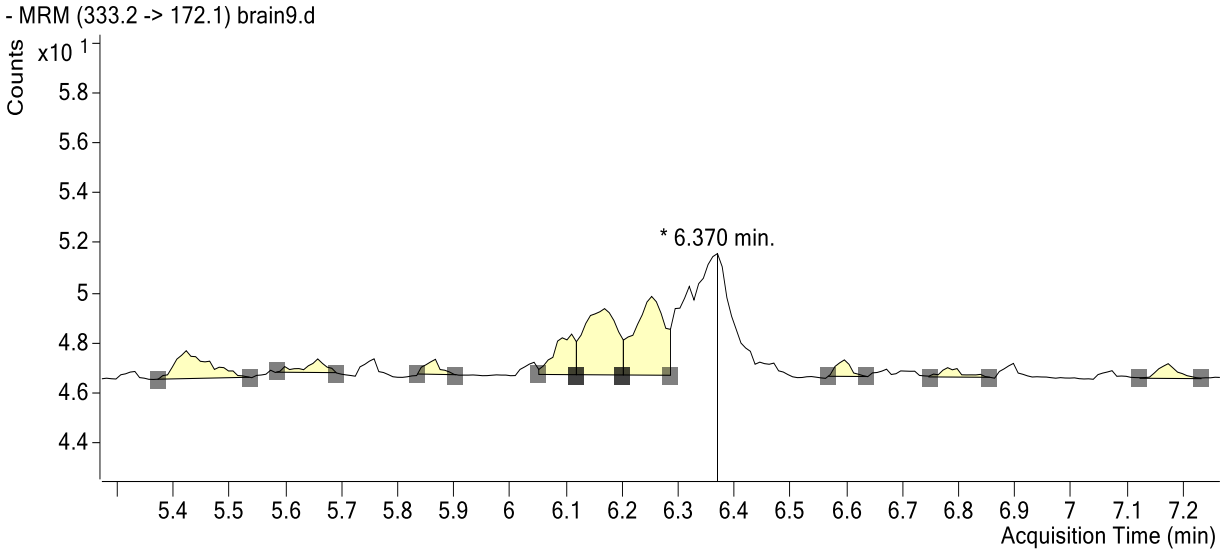
- MRM (333.2 -> 172.1) brain9.d
Counts
x10 1
5.8
5.6
5.4
5.2
5
4.8
4.6
4.4
* 6.370 min.
5.4 5.5 5.6 5.7 5.8 5.9 6 6.1 6.2 6.3 6.4 6.5 6.6 6.7 6.8 6.9 7 7.1 7.2
Acquisition Time (min)

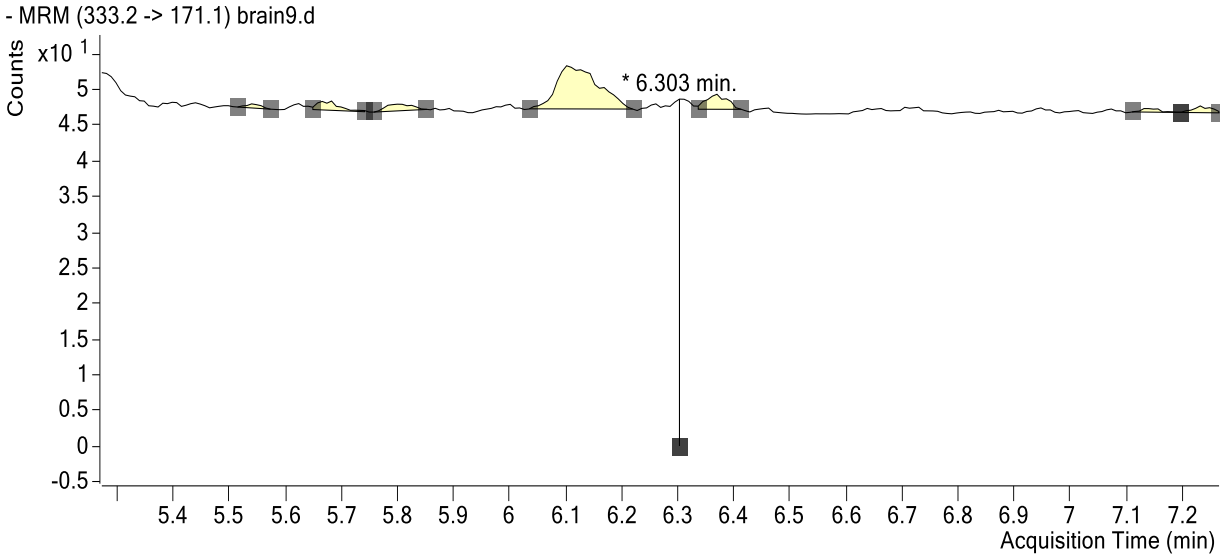
- MRM (333.2 -> 171.1) brain9.d
Counts
x10 1
5
4.5
4
3.5
3
2.5
2
1.5
1
0.5
0
-0.5
* 6.303 min.
5.4 5.5 5.6 5.7 5.8 5.9 6 6.1 6.2 6.3 6.4 6.5 6.6 6.7 6.8 6.9 7 7.1 7.2
Acquisition Time (min)

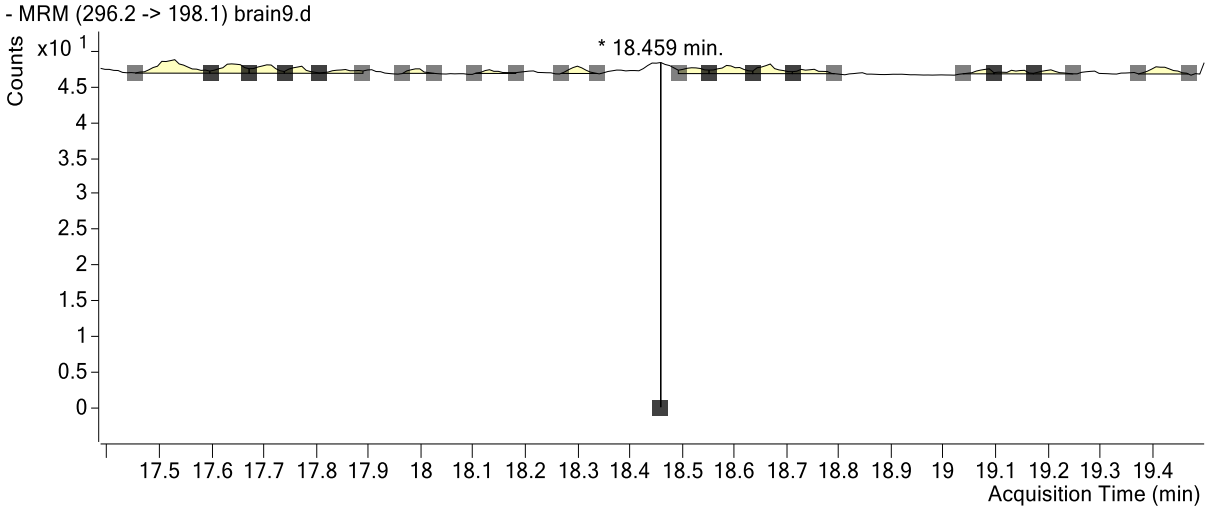
- MRM (296.2 -> 198.1) brain9.d
Counts
x10 1
4.5
4
3.5
3
2.5
2
1.5
1
0.5
0
* 18.459 min.
17.5 17.6 17.7 17.8 17.9 18 18.1 18.2 18.3 18.4 18.5 18.6 18.7 18.8 18.9 19 19.1 19.2 19.3 19.4
Acquisition Time (min)

B) <u>d-9,10,13-TriHOME (333.2-172.1/171.1) and d-13-oxo-ODE (296.2-198.1) in heart.</u>

Rat 2 (Vehicle, gavage)

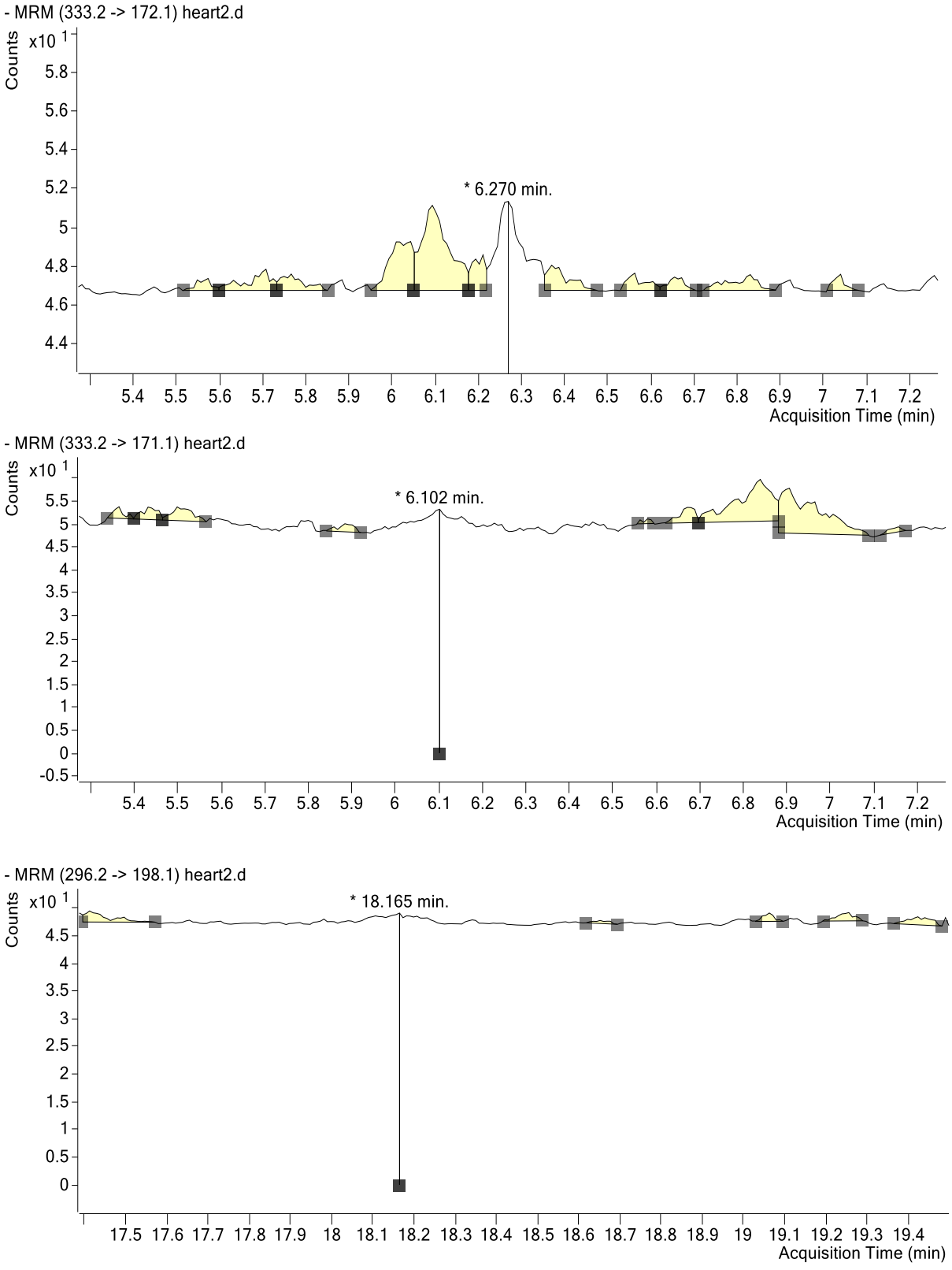

Rat 3 (Vehicle, IV)

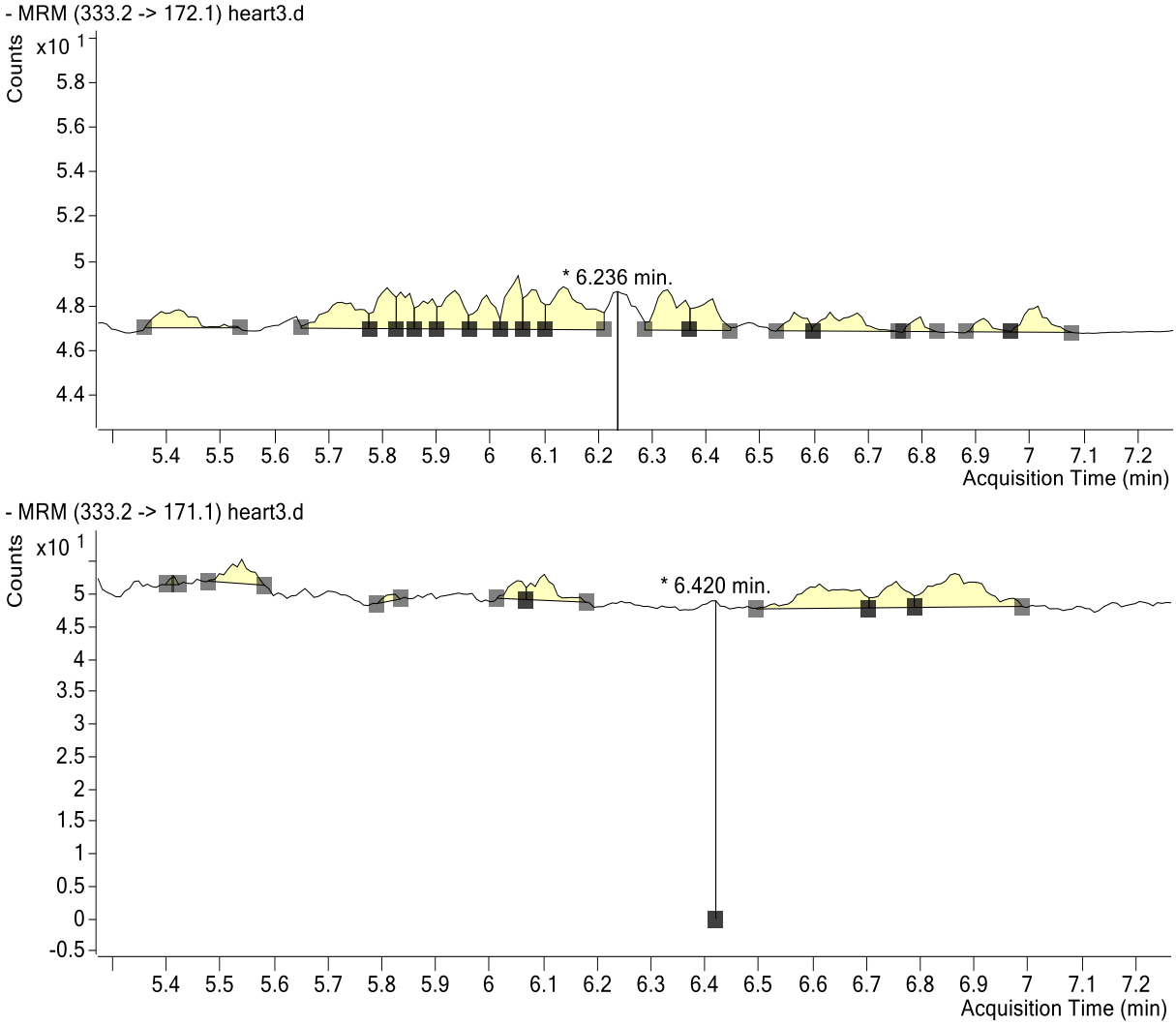

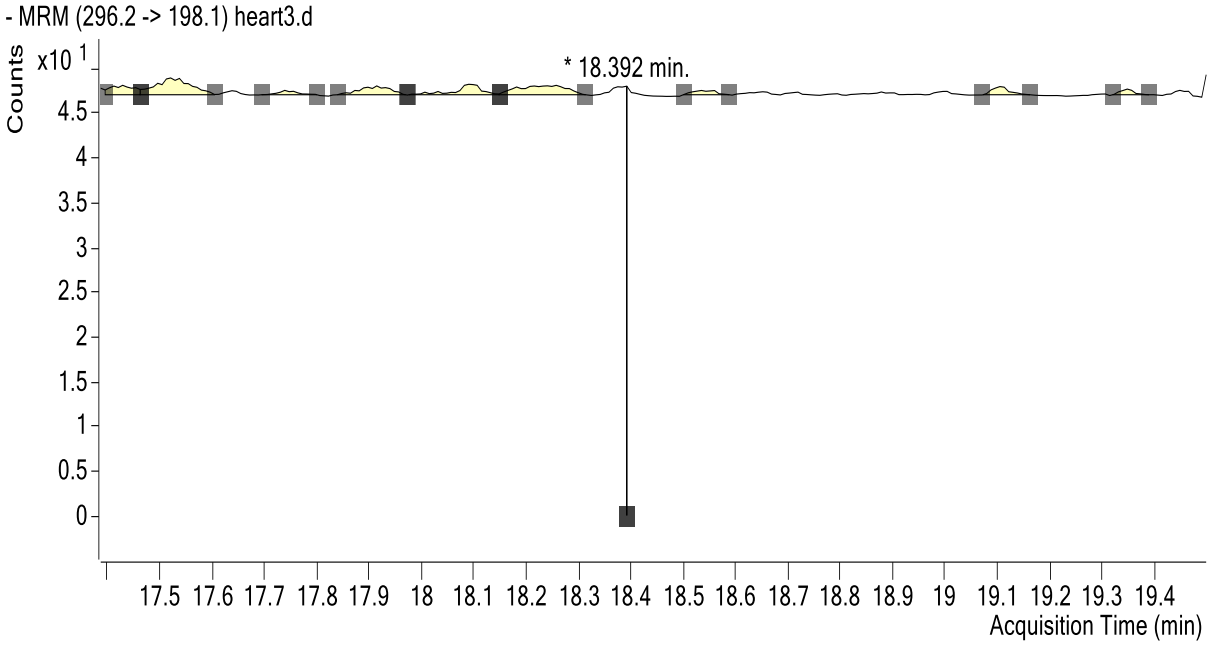
- MRM (296.2 -> 198.1) heart3.d
Counts
x10 1
* 18.392 min.
4.5
4
3.5
3
2.5
2
1.5
1
0.5
0
17.5 17.6 17.7 17.8 17.9 18 18.1 18.2 18.3 18.4 18.5 18.6 18.7 18.8 18.9 19 19.1 19.2 19.3 19.4
Acquisition Time (min)

Rat 4 (gavage)

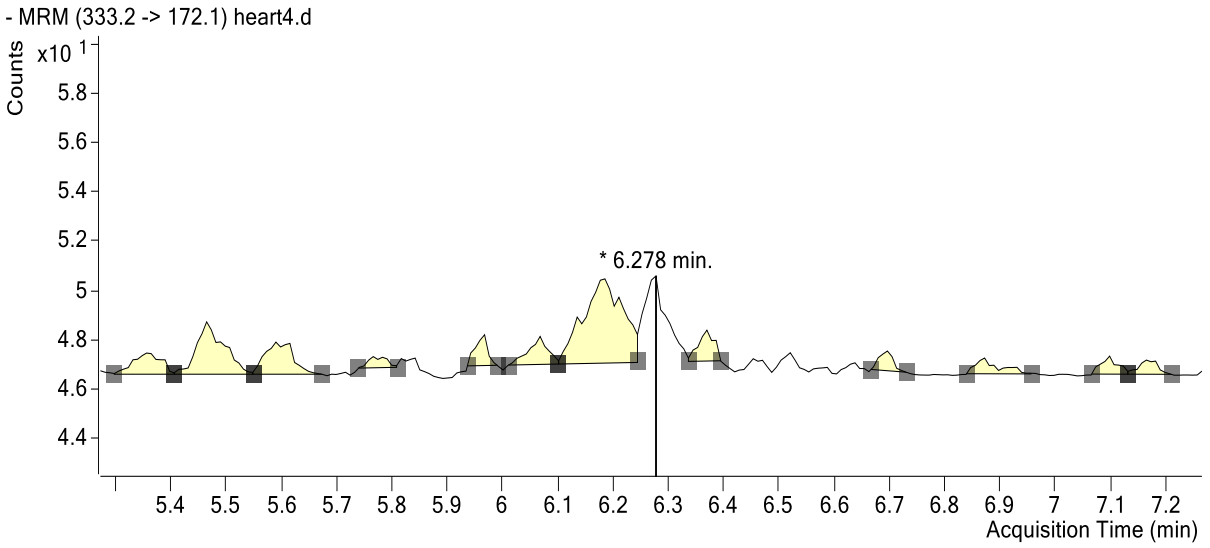
- MRM (333.2 -> 172.1) heart4.d
Counts
x10 1
* 6.278 min.
5.8
5.6
5.4
5.2
5
4.8
4.6
4.4
5.4 5.5 5.6 5.7 5.8 5.9 6 6.1 6.2 6.3 6.4 6.5 6.6 6.7 6.8 6.9 7 7.1 7.2
Acquisition Time (min)

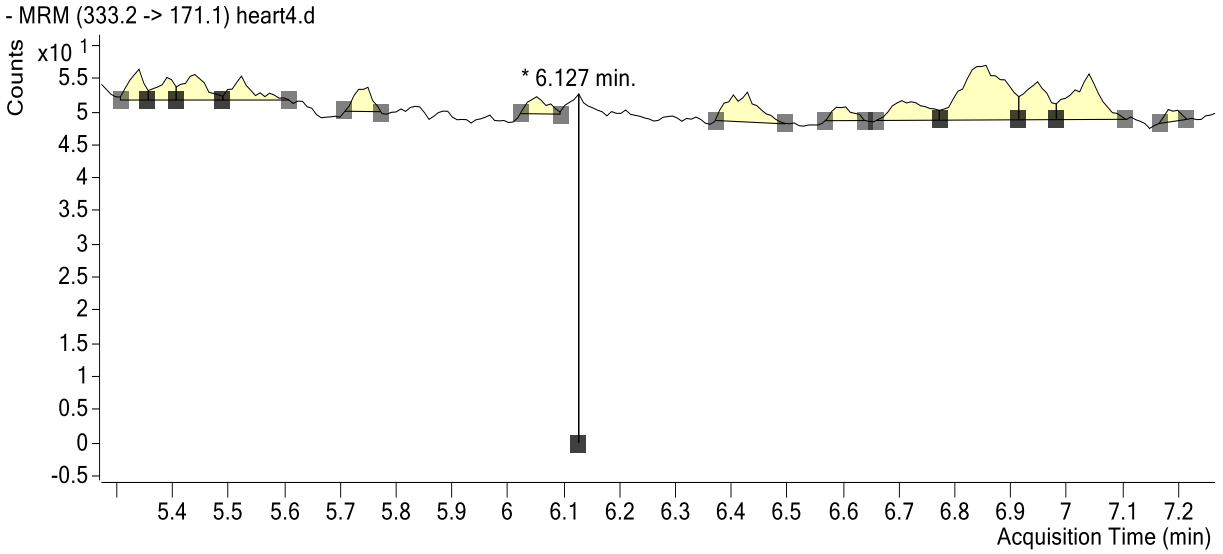
- MRM (333.2 -> 171.1) heart4.d
Counts
x10 1
* 6.127 min.
Acquisition Time (min)

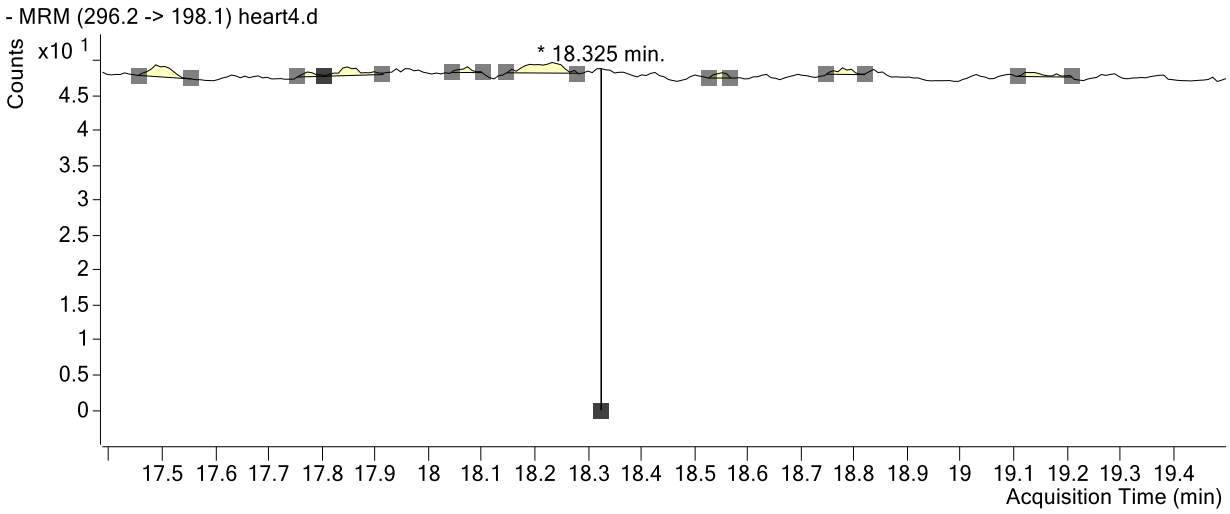
- MRM (296.2 -> 198.1) heart4.d
Counts
x10 1
* 18.325 min.
Acquisition Time (min)

Rat 6 (gavage)

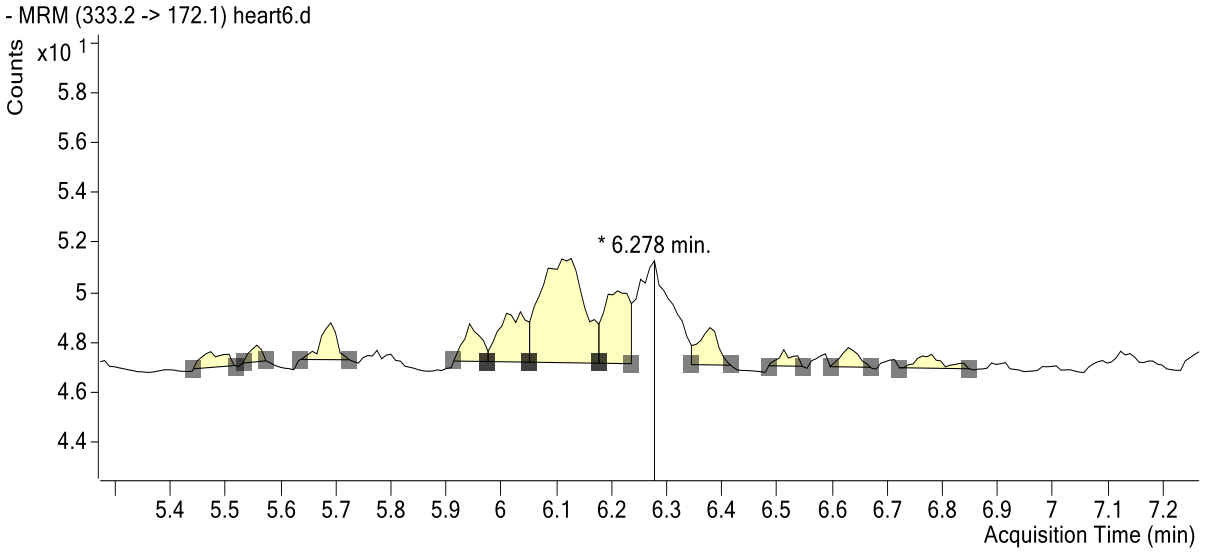
- MRM (333.2 -> 172.1) heart6.d
Counts
x10 1
5.8
5.6
5.4
5.2
5
4.8
4.6
4.4
* 6.278 min.
5.4 5.5 5.6 5.7 5.8 5.9 6 6.1 6.2 6.3 6.4 6.5 6.6 6.7 6.8 6.9 7 7.1 7.2
Acquisition Time (min)

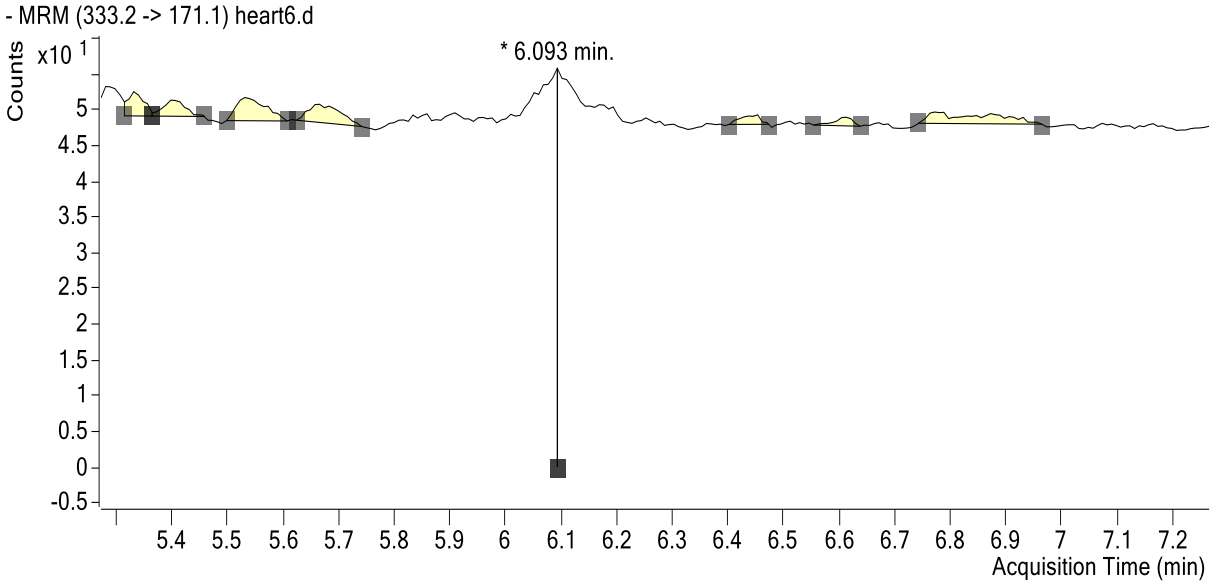
- MRM (333.2 -> 171.1) heart6.d
Counts
x10 1
5
4.5
4
3.5
3
2.5
2
1.5
1
0.5
0
-0.5
* 6.093 min.
5.4 5.5 5.6 5.7 5.8 5.9 6 6.1 6.2 6.3 6.4 6.5 6.6 6.7 6.8 6.9 7 7.1 7.2
Acquisition Time (min)

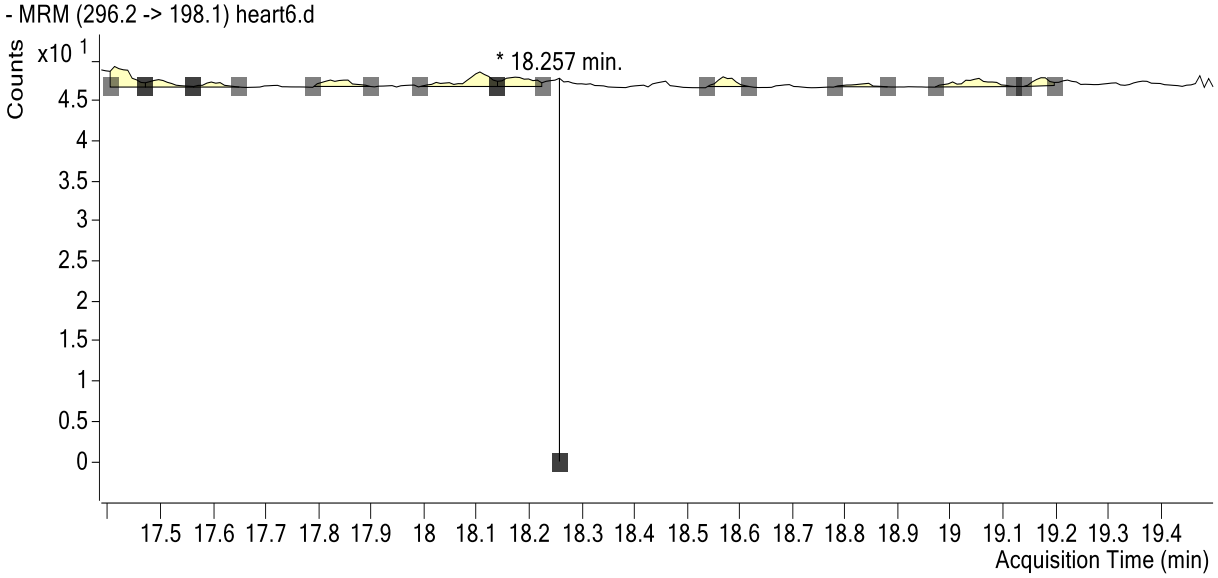
- MRM (296.2 -> 198.1) heart6.d
Counts
x10 1
* 18.257 min.
4.5
4
3.5
3
2.5
2
1.5
1
0.5
0
17.5 17.6 17.7 17.8 17.9 18 18.1 18.2 18.3 18.4 18.5 18.6 18.7 18.8 18.9 19 19.1 19.2 19.3 19.4
Acquisition Time (min)

Rat 8 (gavage)

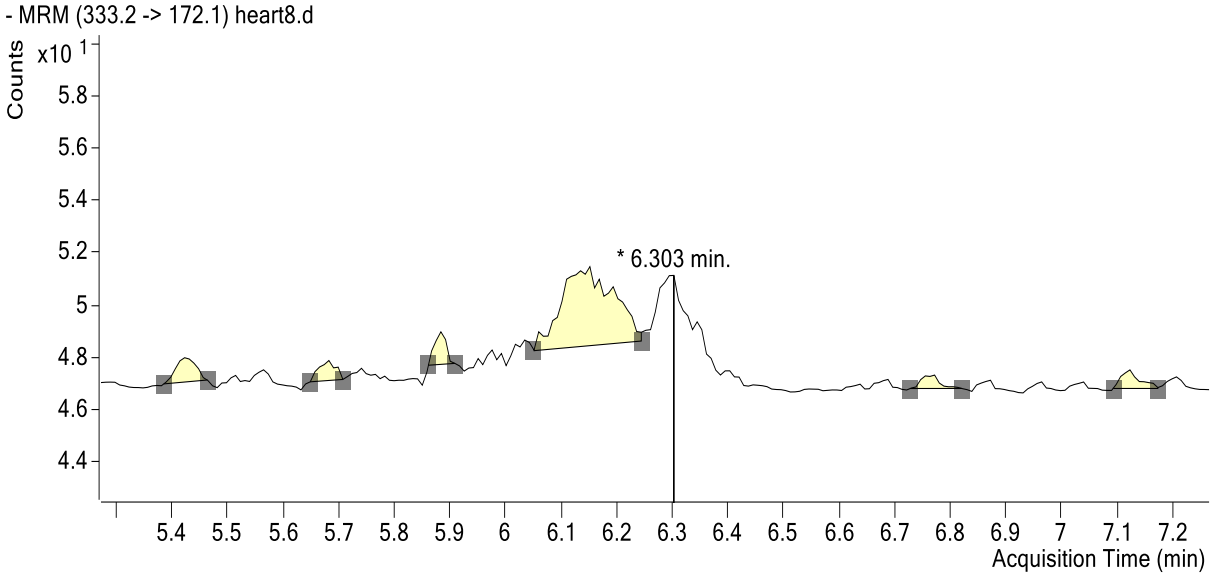
- MRM (333.2 -> 172.1) heart8.d
Counts
x10 1
5.8
5.6
5.4
5.2
5
4.8
4.6
4.4
* 6.303 min.
5.4 5.5 5.6 5.7 5.8 5.9 6 6.1 6.2 6.3 6.4 6.5 6.6 6.7 6.8 6.9 7 7.1 7.2
Acquisition Time (min)

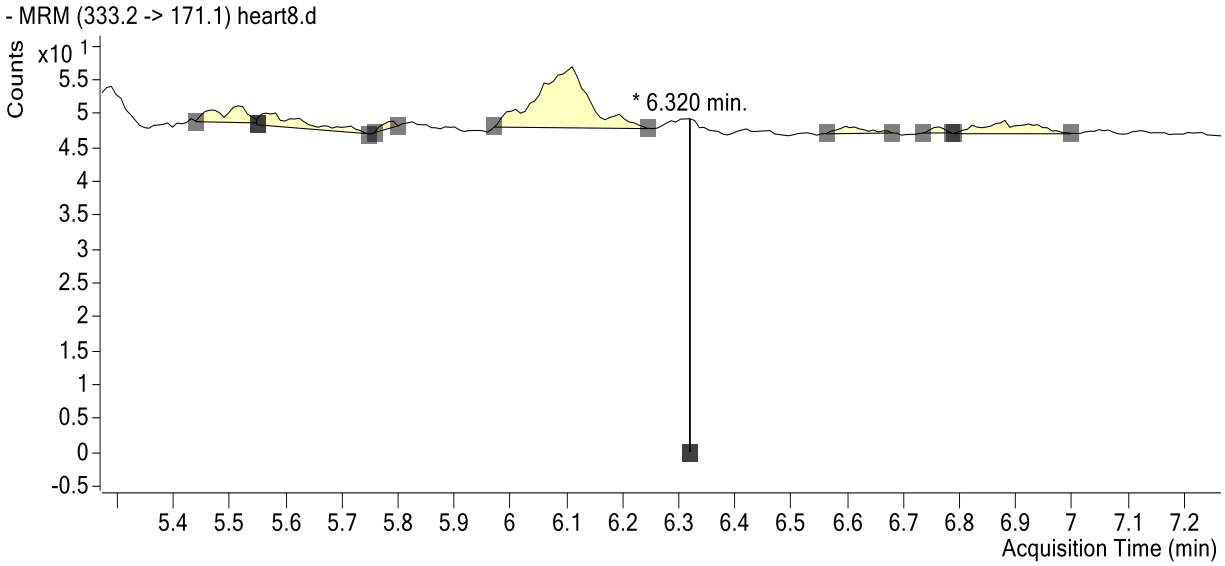
- MRM (333.2 -> 171.1) heart8.d
Counts
x10 1
5.5
5
4.5
4
3.5
3
2.5
2
1.5
1
0.5
0
-0.5
* 6.320 min.
5.4 5.5 5.6 5.7 5.8 5.9 6 6.1 6.2 6.3 6.4 6.5 6.6 6.7 6.8 6.9 7 7.1 7.2
Acquisition Time (min)

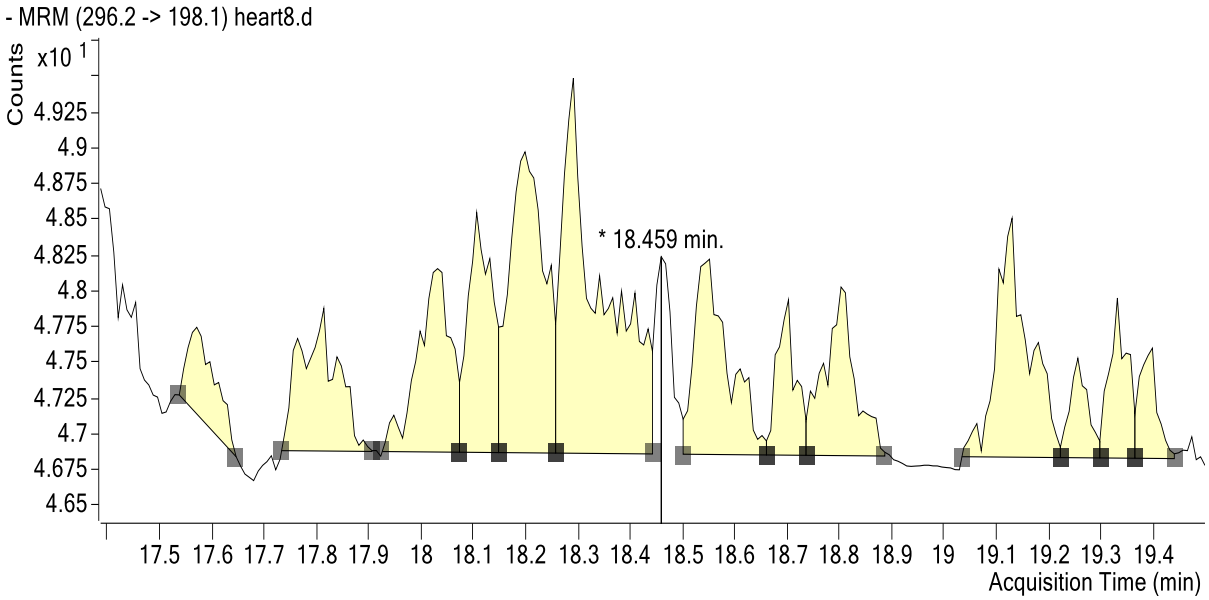
- MRM (296.2 -> 198.1) heart8.d
Counts
x10 1
4.925
4.9
4.875
4.85
4.825
4.8
4.775
4.75
4.725
4.7
4.675
4.65
* 18.459 min.
17.5 17.6 17.7 17.8 17.9 18 18.1 18.2 18.3 18.4 18.5 18.6 18.7 18.8 18.9 19 19.1 19.2 19.3 19.4
Acquisition Time (min)

Rat 5 (IV)

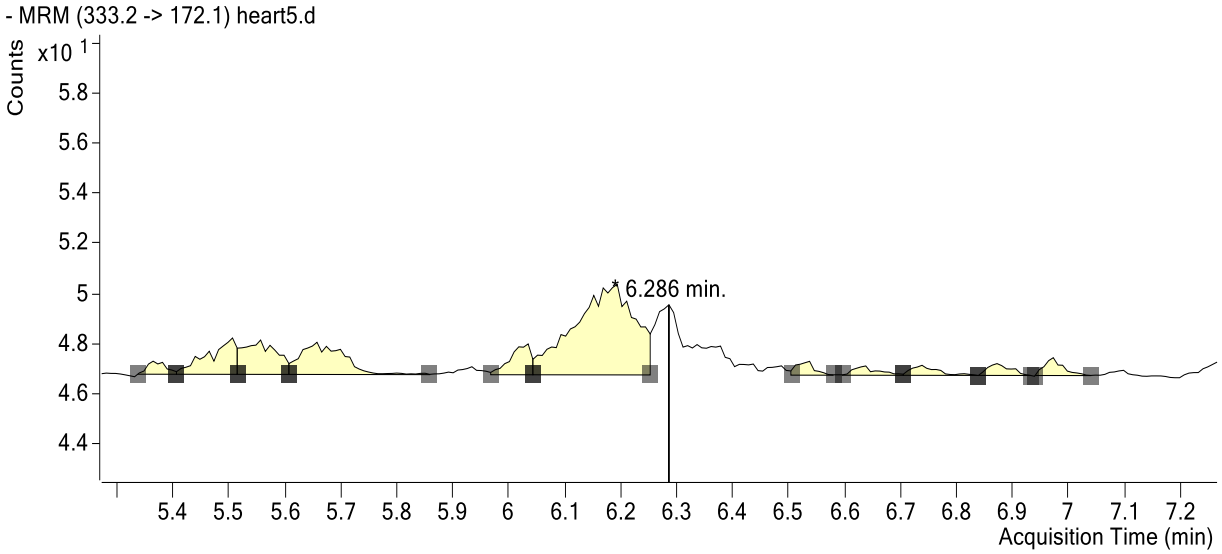
- MRM (333.2 -> 172.1) heart5.d
Counts
x10 1
5.8
5.6
5.4
5.2
5
4.8
4.6
4.4
* 6.286 min.
5.4 5.5 5.6 5.7 5.8 5.9 6 6.1 6.2 6.3 6.4 6.5 6.6 6.7 6.8 6.9 7 7.1 7.2
Acquisition Time (min)

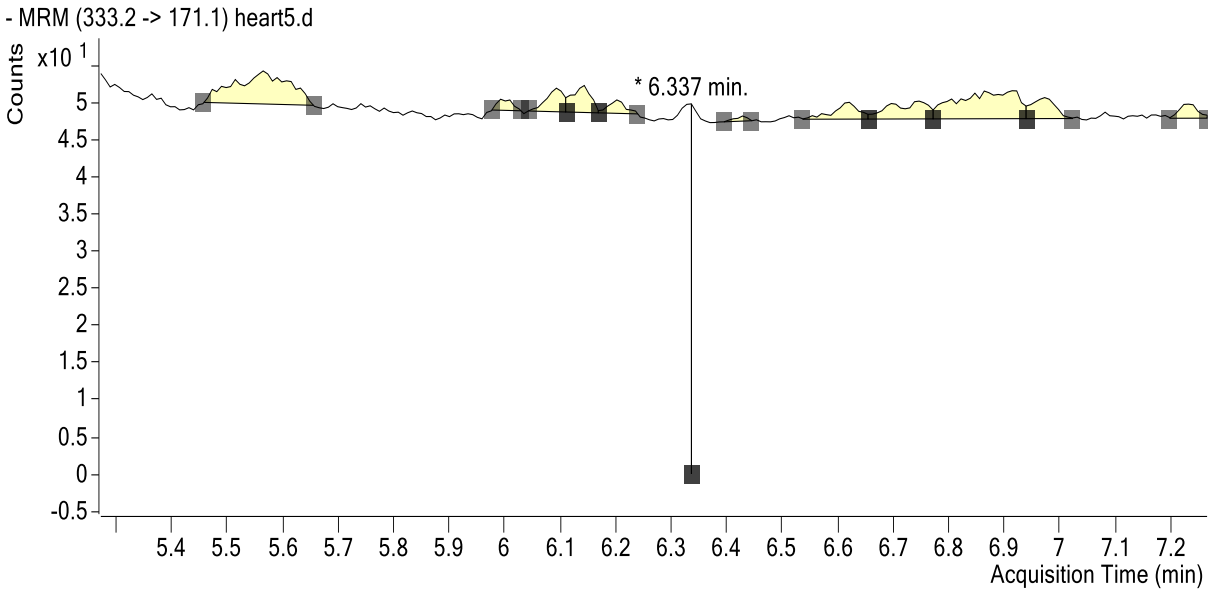
- MRM (333.2 -> 171.1) heart5.d
Counts
x10 1
5
4.5
4
3.5
3
2.5
2
1.5
1
0.5
0
-0.5
* 6.337 min.
5.4 5.5 5.6 5.7 5.8 5.9 6 6.1 6.2 6.3 6.4 6.5 6.6 6.7 6.8 6.9 7 7.1 7.2
Acquisition Time (min)

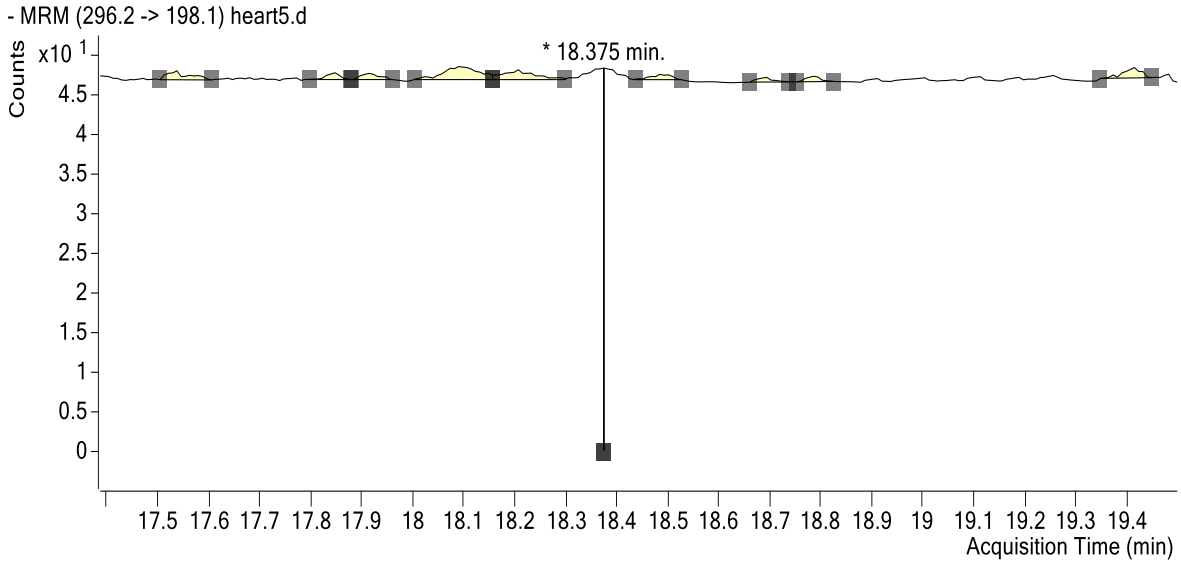
- MRM (296.2 -> 198.1) heart5.d
Counts
x10 1
* 18.375 min.
4.5
4
3.5
3
2.5
2
1.5
1
0.5
0
17.5 17.6 17.7 17.8 17.9 18 18.1 18.2 18.3 18.4 18.5 18.6 18.7 18.8 18.9 19 19.1 19.2 19.3 19.4
Acquisition Time (min)

Rat 7 (IV)

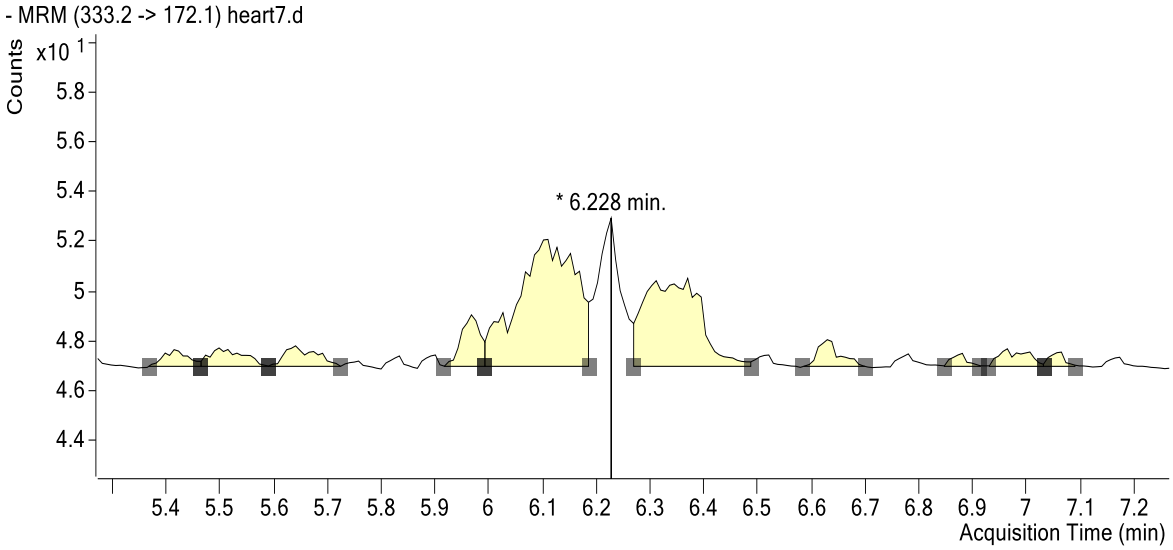
- MRM (333.2 -> 172.1) heart7.d
Counts
x10 1
5.8
5.6
5.4
* 6.228 min.
5.2
5
4.8
4.6
4.4
5.4 5.5 5.6 5.7 5.8 5.9 6 6.1 6.2 6.3 6.4 6.5 6.6 6.7 6.8 6.9 7 7.1 7.2
Acquisition Time (min)

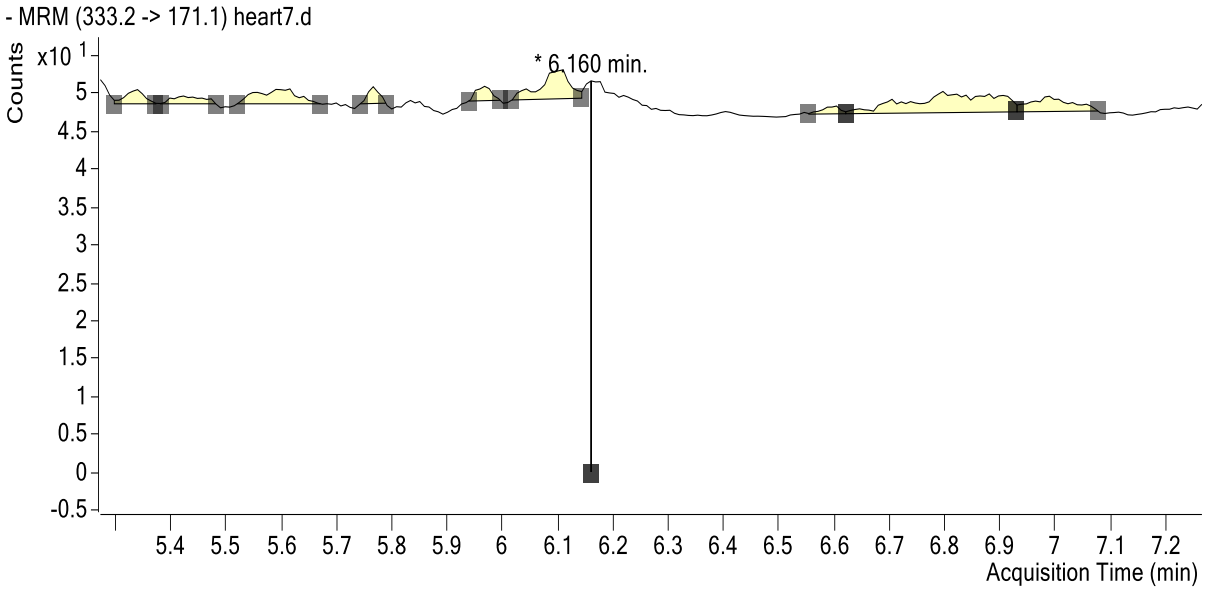
- MRM (333.2 -> 171.1) heart7.d
Counts
x10 1
* 6.160 min.
Acquisition Time (min)

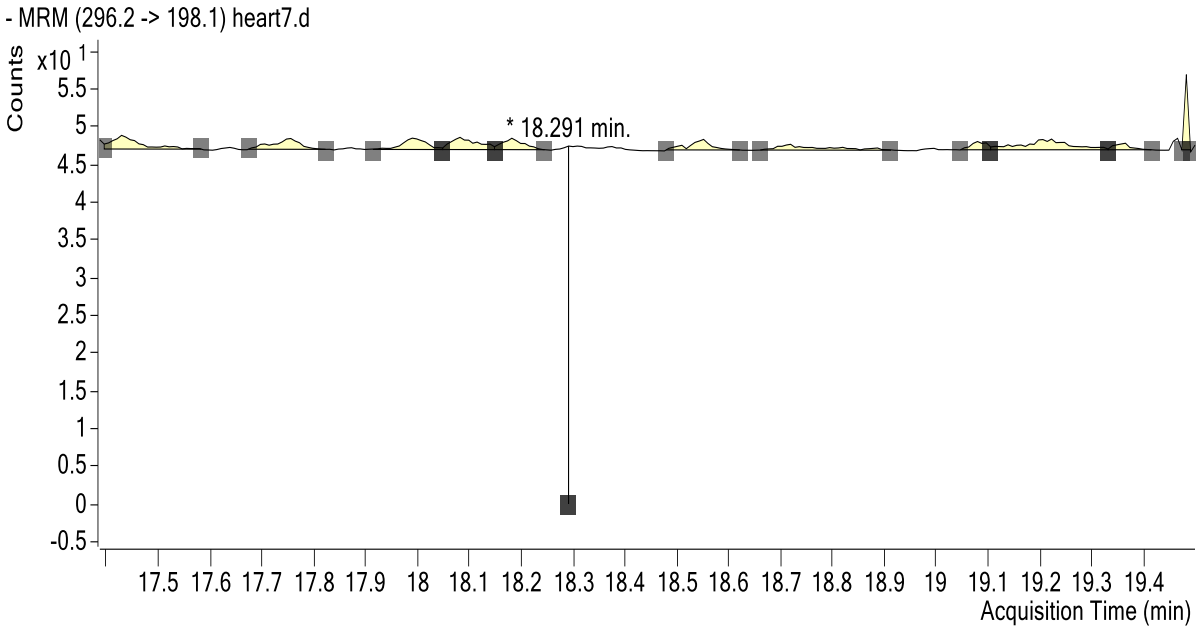
- MRM (296.2 -> 198.1) heart7.d
Counts
x10 1
* 18.291 min.
Acquisition Time (min)

Rat 9 (IV)

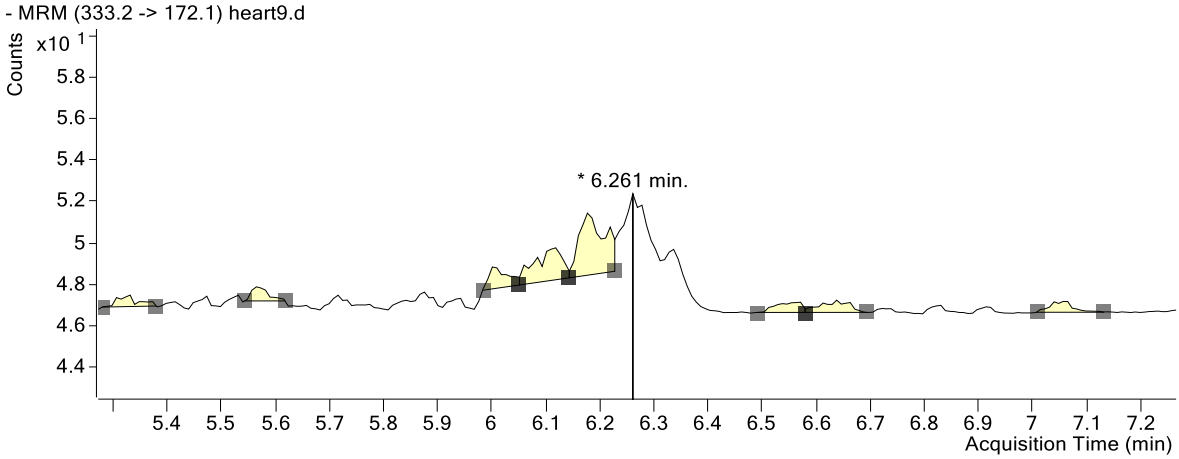
- MRM (333.2 -> 172.1) heart9.d
Counts
x10 1
* 6.261 min.
Acquisition Time (min)

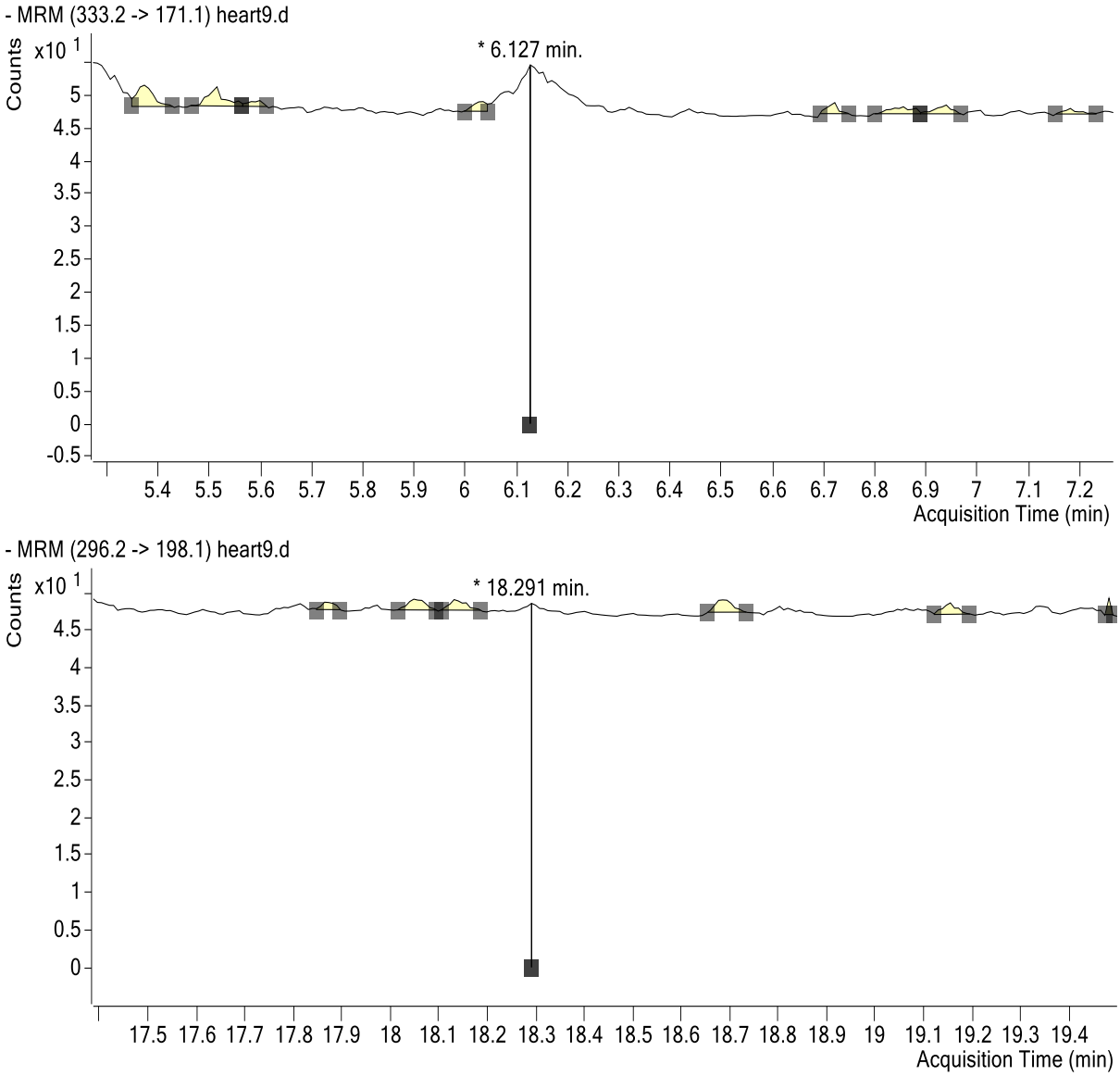

C) <u>d-9,10,13-TriHOME (333.2-172.1/171.1) and d-13-oxo-ODE (296.2-198.1) in liver</u>

Rat 2 (Vehicle, gavage)

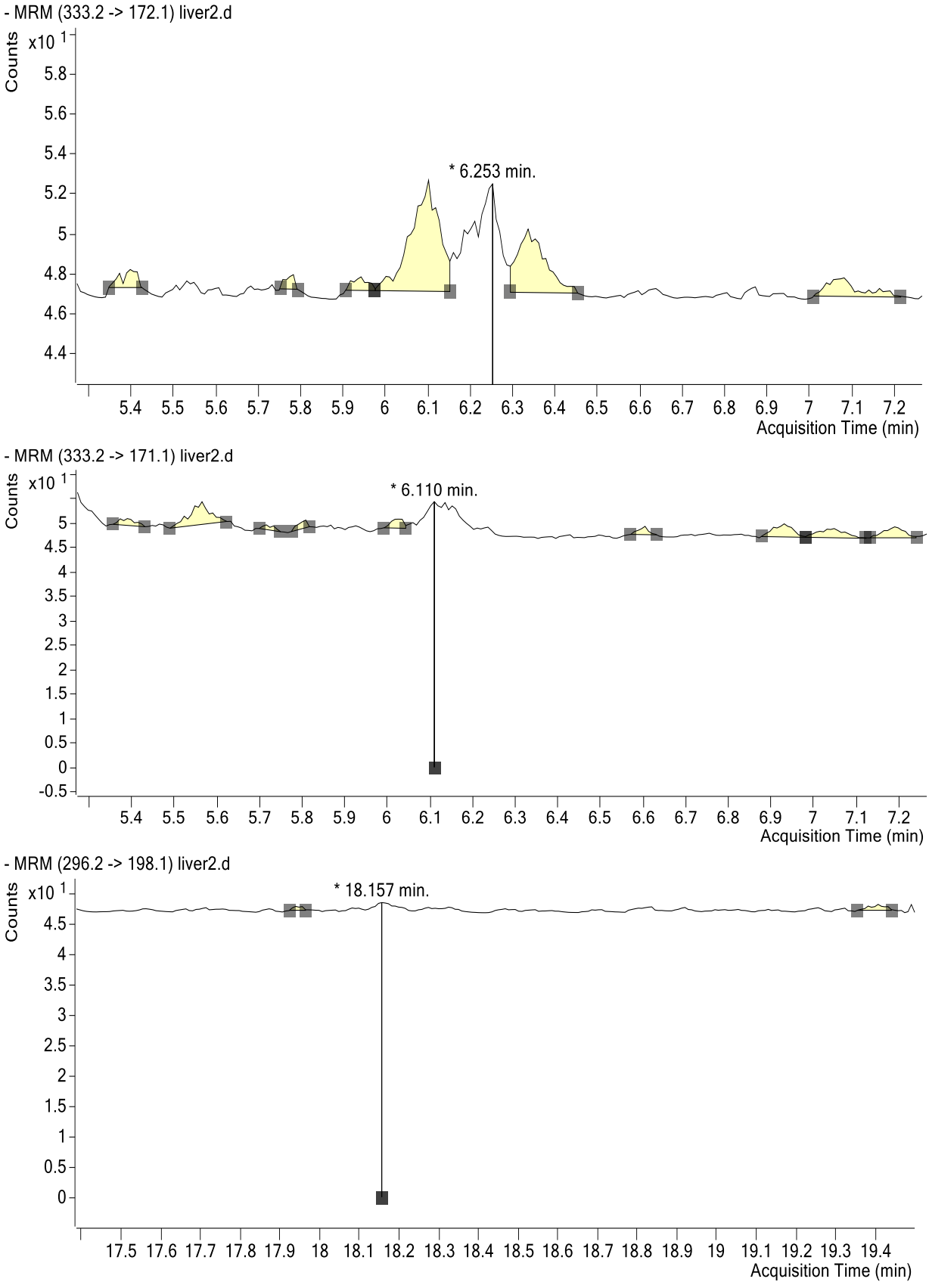
- MRM (333.2 -> 172.1) liver2.d
Counts
x10 1
* 6.253 min.
Acquisition Time (min)
- MRM (333.2 -> 171.1) liver2.d
Counts
x10 1
* 6.110 min.
Acquisition Time (min)
- MRM (296.2 -> 198.1) liver2.d
Counts
x10 1
* 18.157 min.
Acquisition Time (min)

Rat 3 (Vehicle, IV)

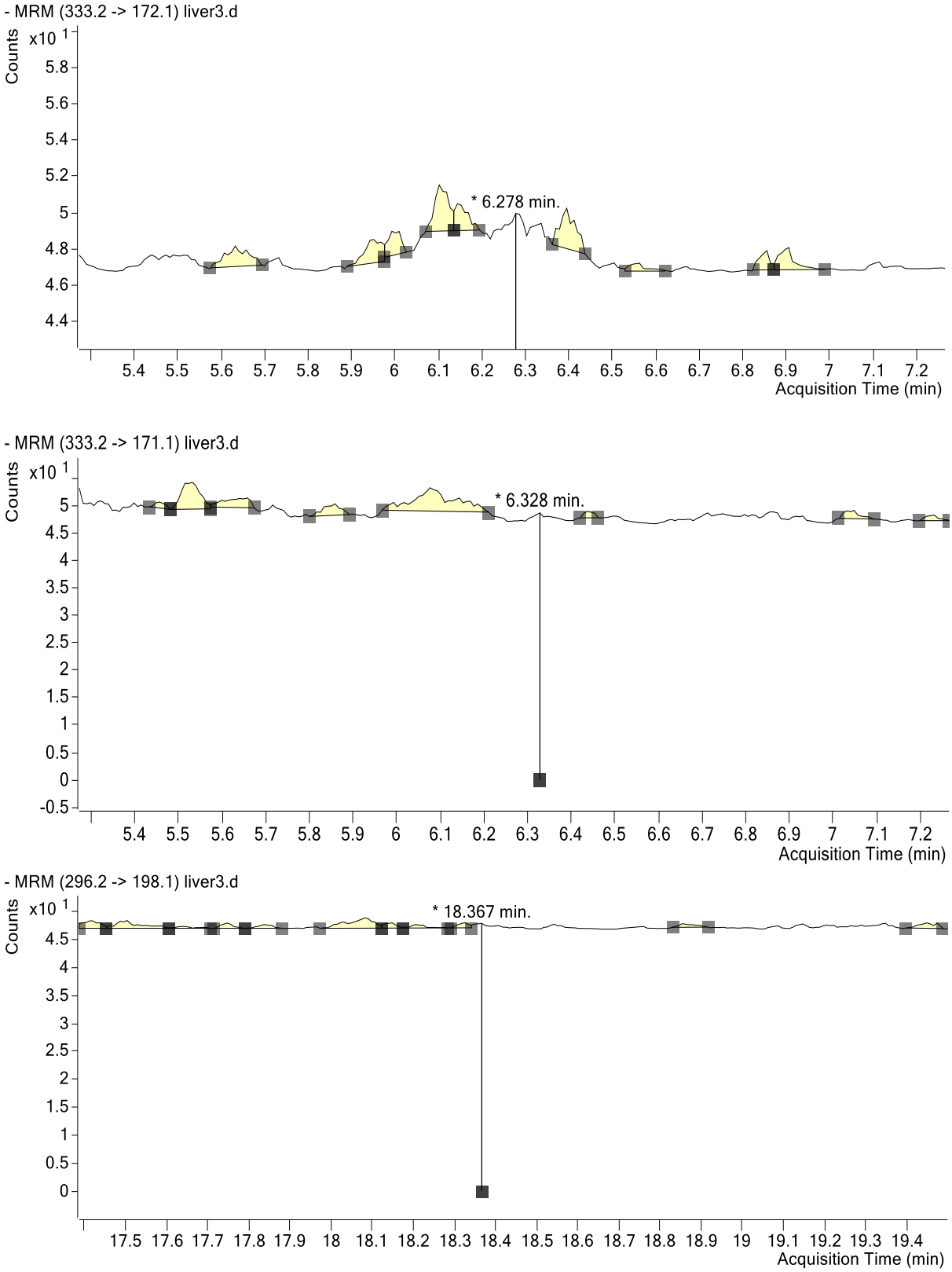

Rat 4 (gavage)

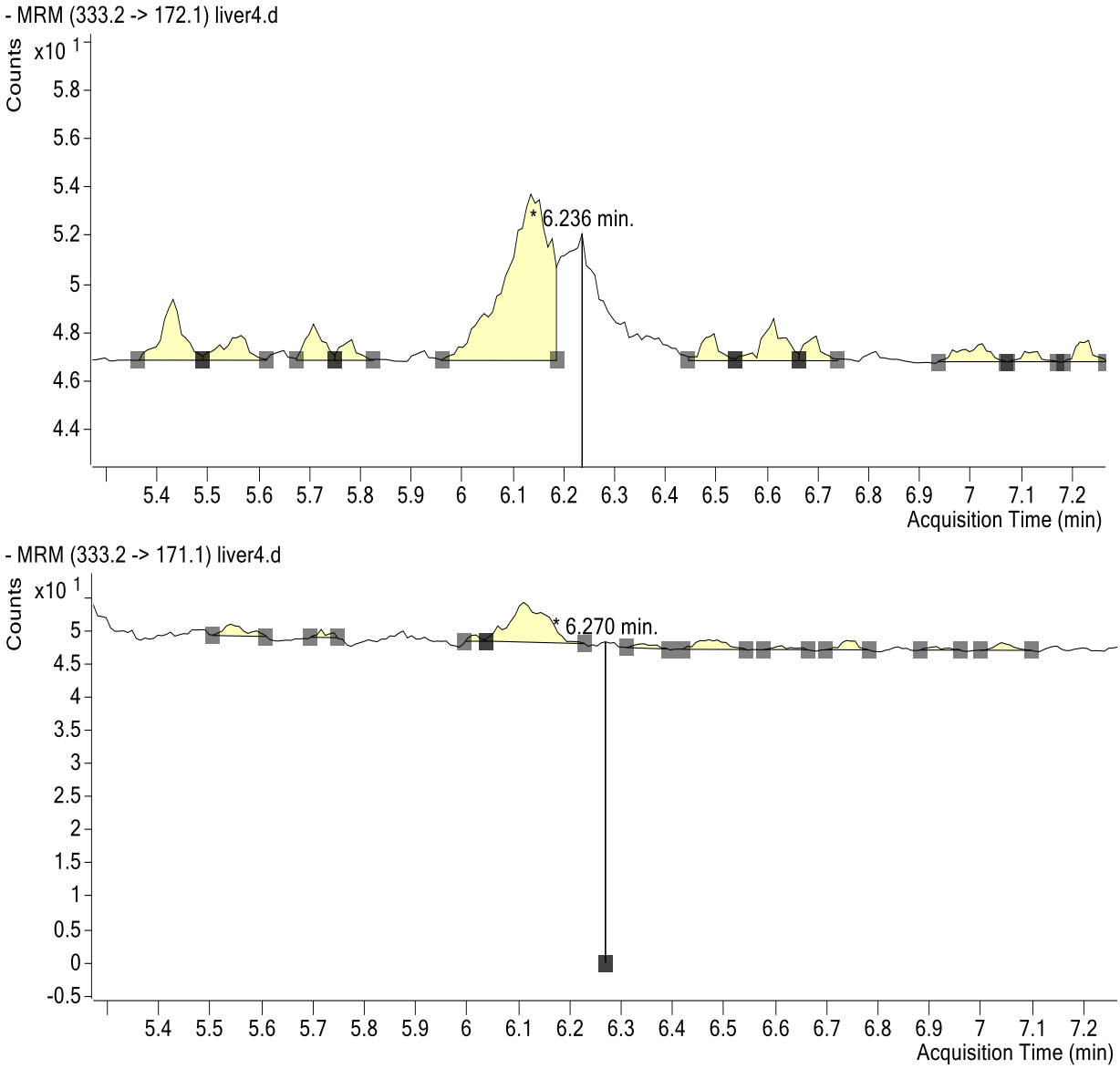
- MRM (333.2 -> 172.1) liver4.d
Counts
x10 1
5.8
5.6
5.4
5.2
5
4.8
4.6
4.4
* 6.236 min.
5.4 5.5 5.6 5.7 5.8 5.9 6 6.1 6.2 6.3 6.4 6.5 6.6 6.7 6.8 6.9 7 7.1 7.2
Acquisition Time (min)
- MRM (333.2 -> 171.1) liver4.d
Counts
x10 1
5
4.5
4
3.5
3
2.5
2
1.5
1
0.5
0
-0.5
* 6.270 min.
5.4 5.5 5.6 5.7 5.8 5.9 6 6.1 6.2 6.3 6.4 6.5 6.6 6.7 6.8 6.9 7 7.1 7.2
Acquisition Time (min)

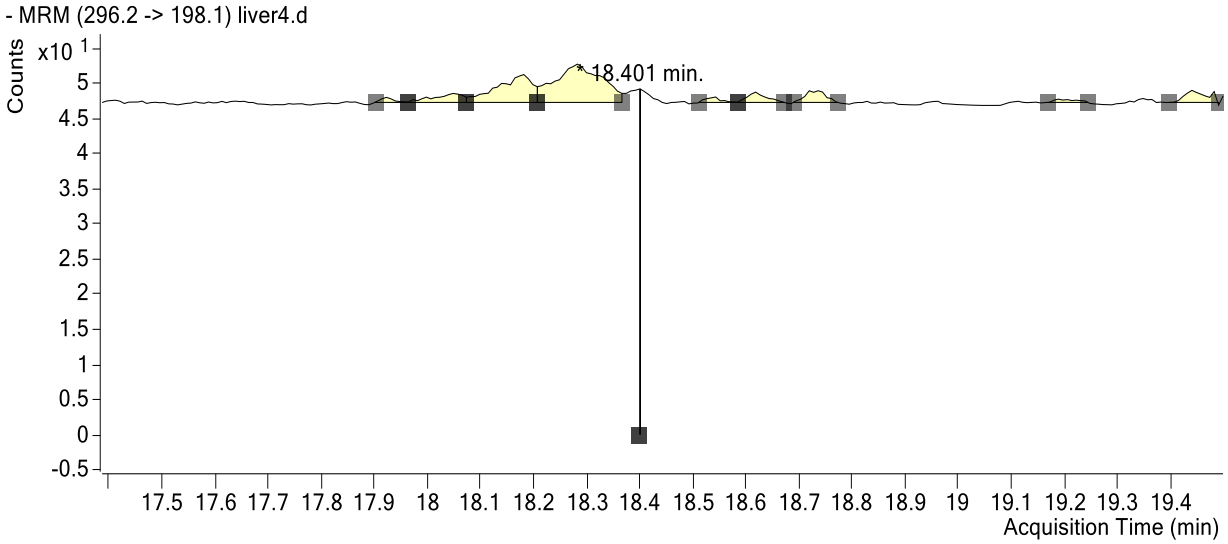
- MRM (296.2 -> 198.1) liver4.d
Counts
x10 1
* 18.401 min.
Acquisition Time (min)

Rat 6 (gavage)

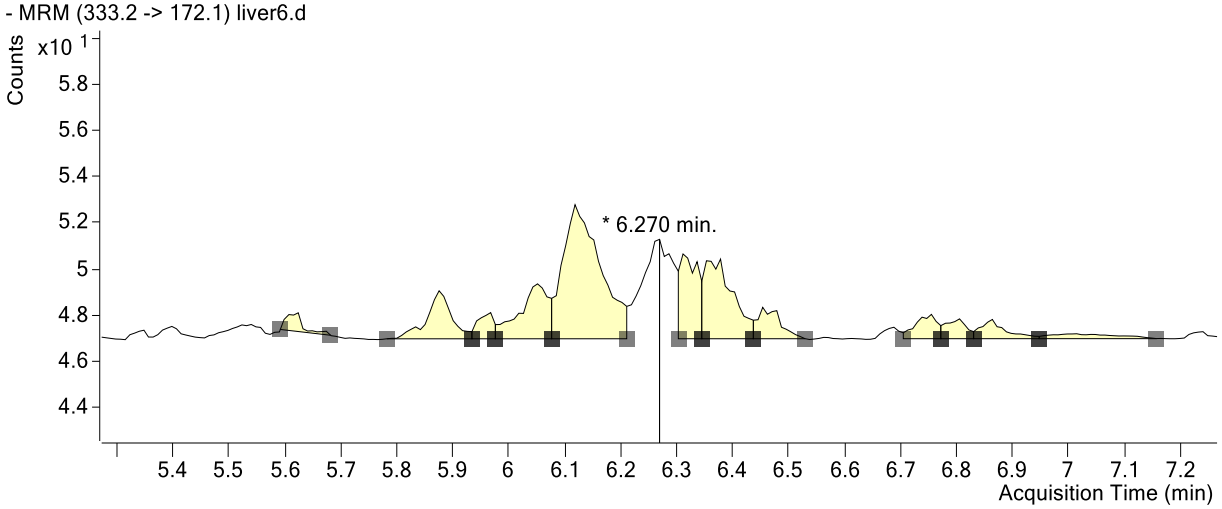
- MRM (333.2 -> 172.1) liver6.d
Counts
x10 1
* 6.270 min.
Acquisition Time (min)

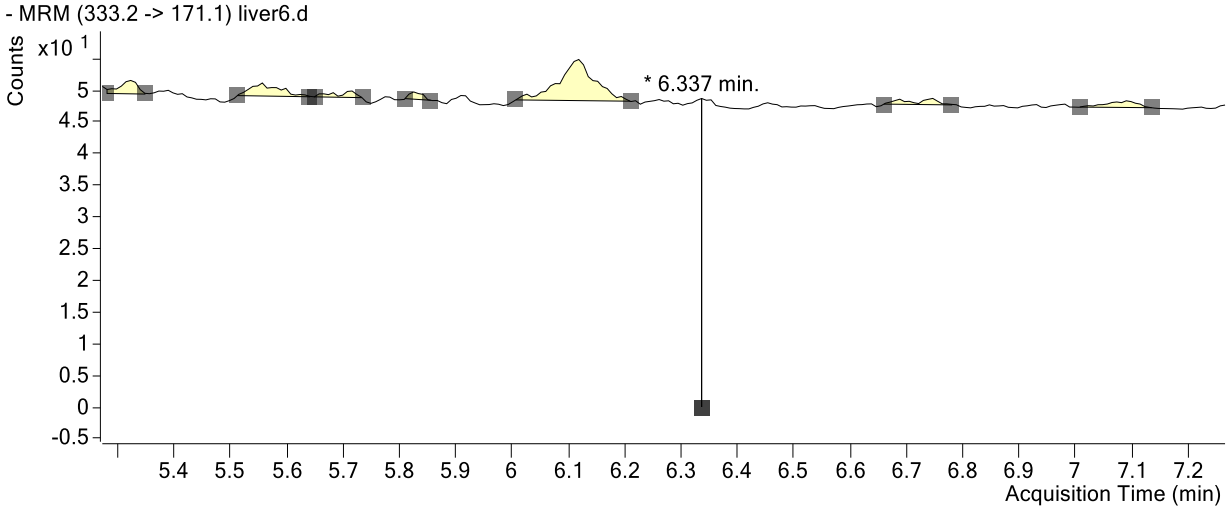
- MRM (333.2 -> 171.1) liver6.d
Counts
x10 1
* 6.337 min.
Acquisition Time (min)

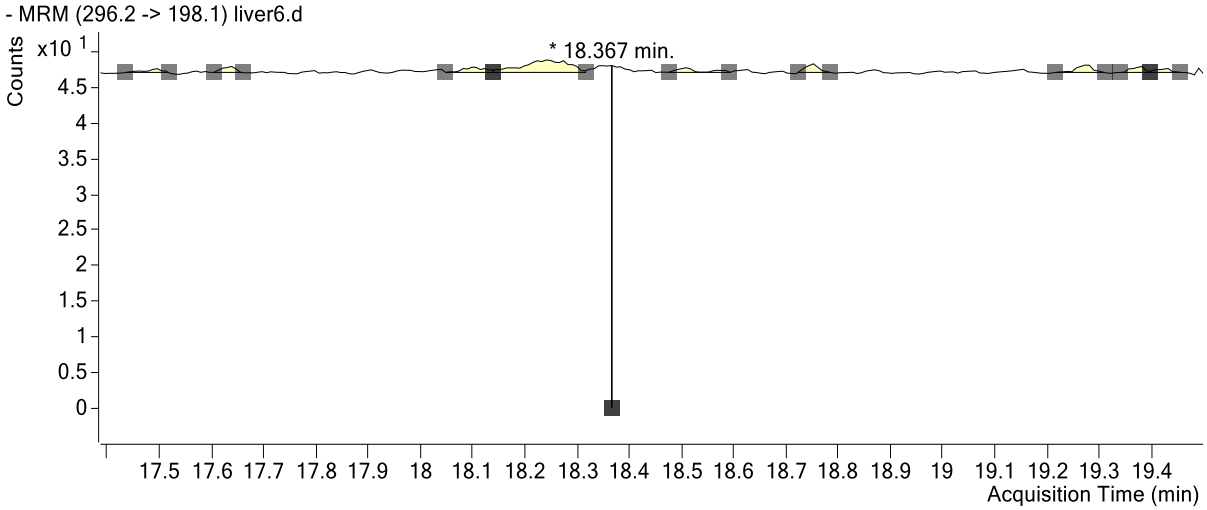
- MRM (296.2 -> 198.1) liver6.d
Counts
x10 1
* 18.367 min.
Acquisition Time (min)

Rat 8 (gavage)

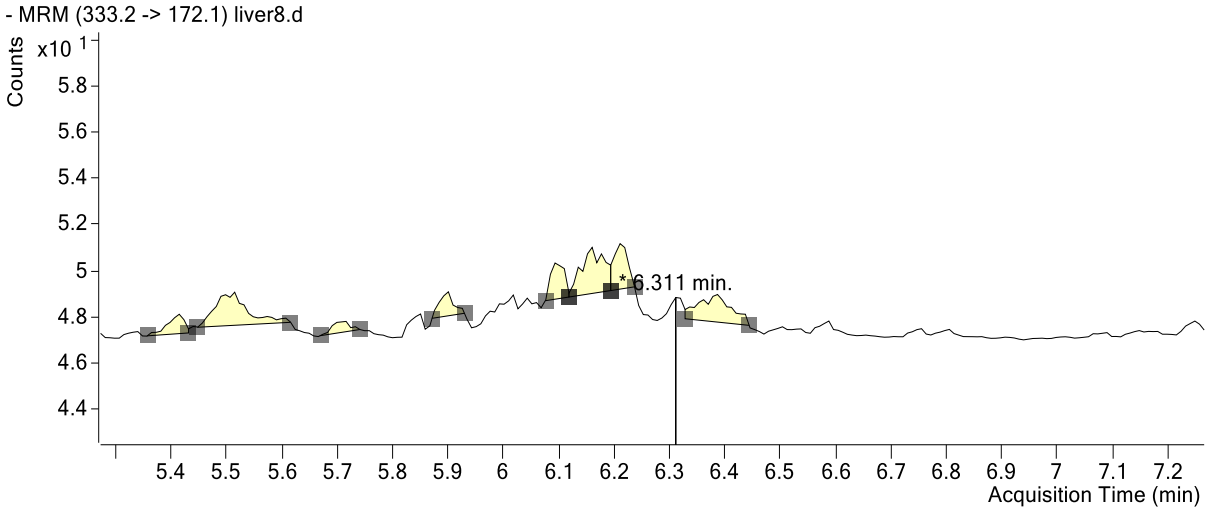
- MRM (333.2 -> 172.1) liver8.d
Counts
x10 1
* 6.311 min.
Acquisition Time (min)

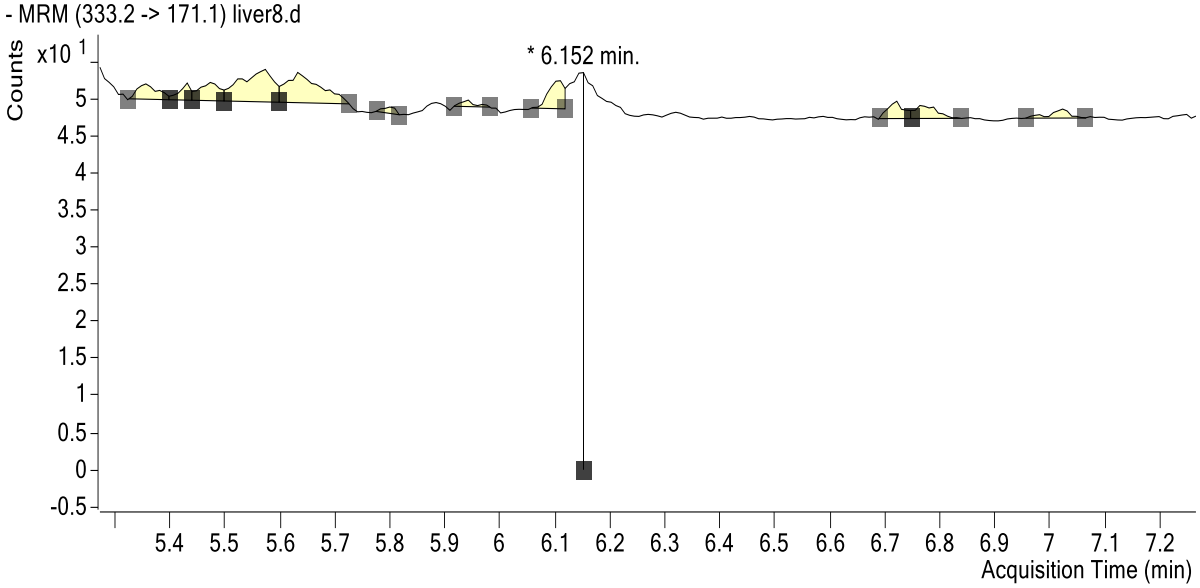
- MRM (333.2 -> 171.1) liver8.d
Counts
x10 1
* 6.152 min.
Acquisition Time (min)

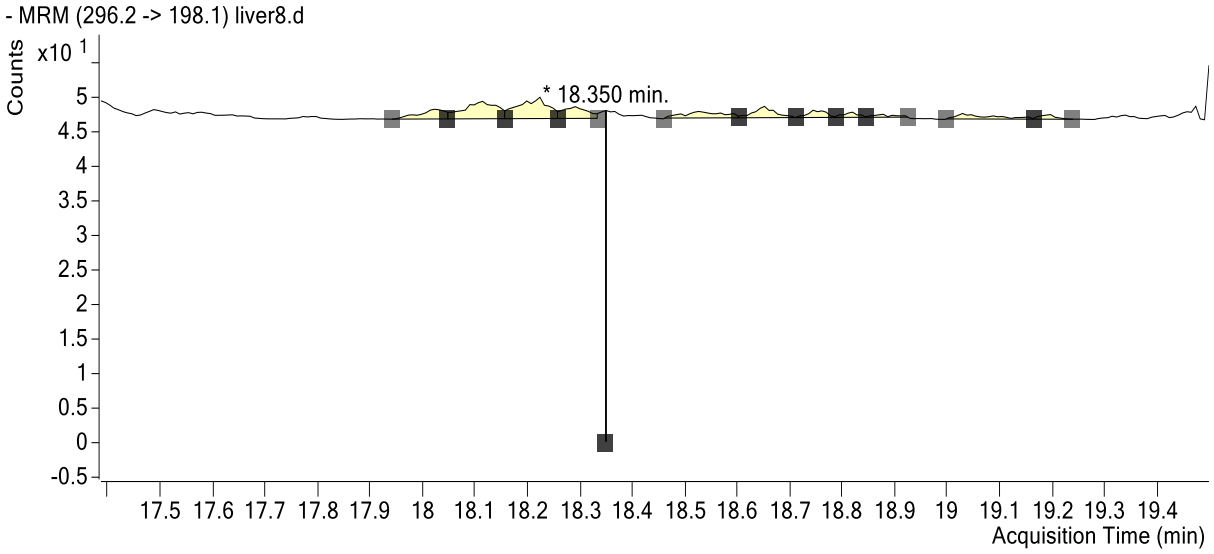
- MRM (296.2 -> 198.1) liver8.d
Counts
x10 1
* 18.350 min.
Acquisition Time (min)

Rat 5 (IV)

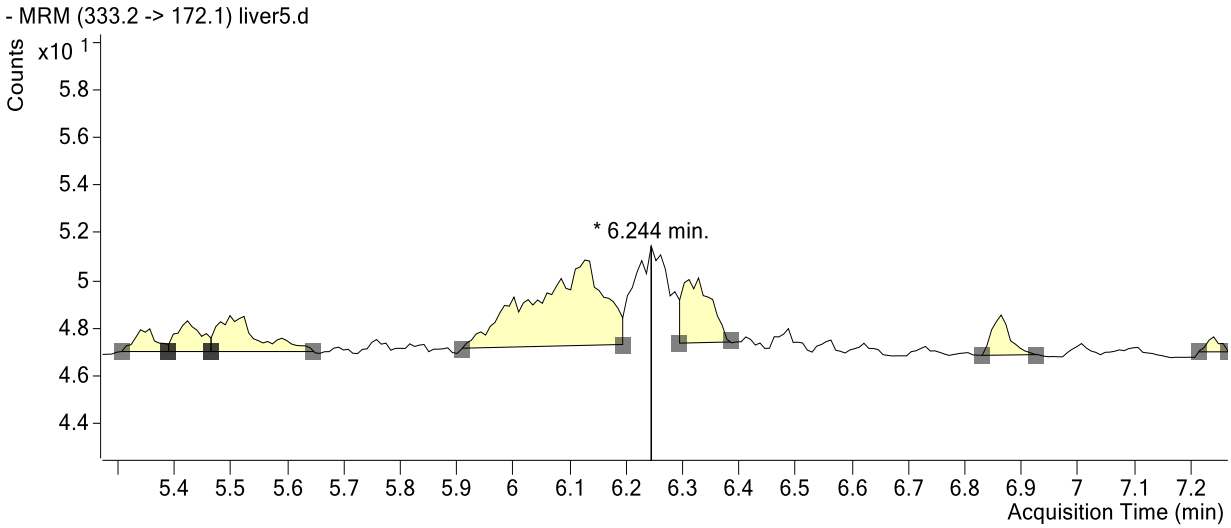
- MRM (333.2 -> 172.1) liver5.d
Counts
x10 1
* 6.244 min.
Acquisition Time (min)

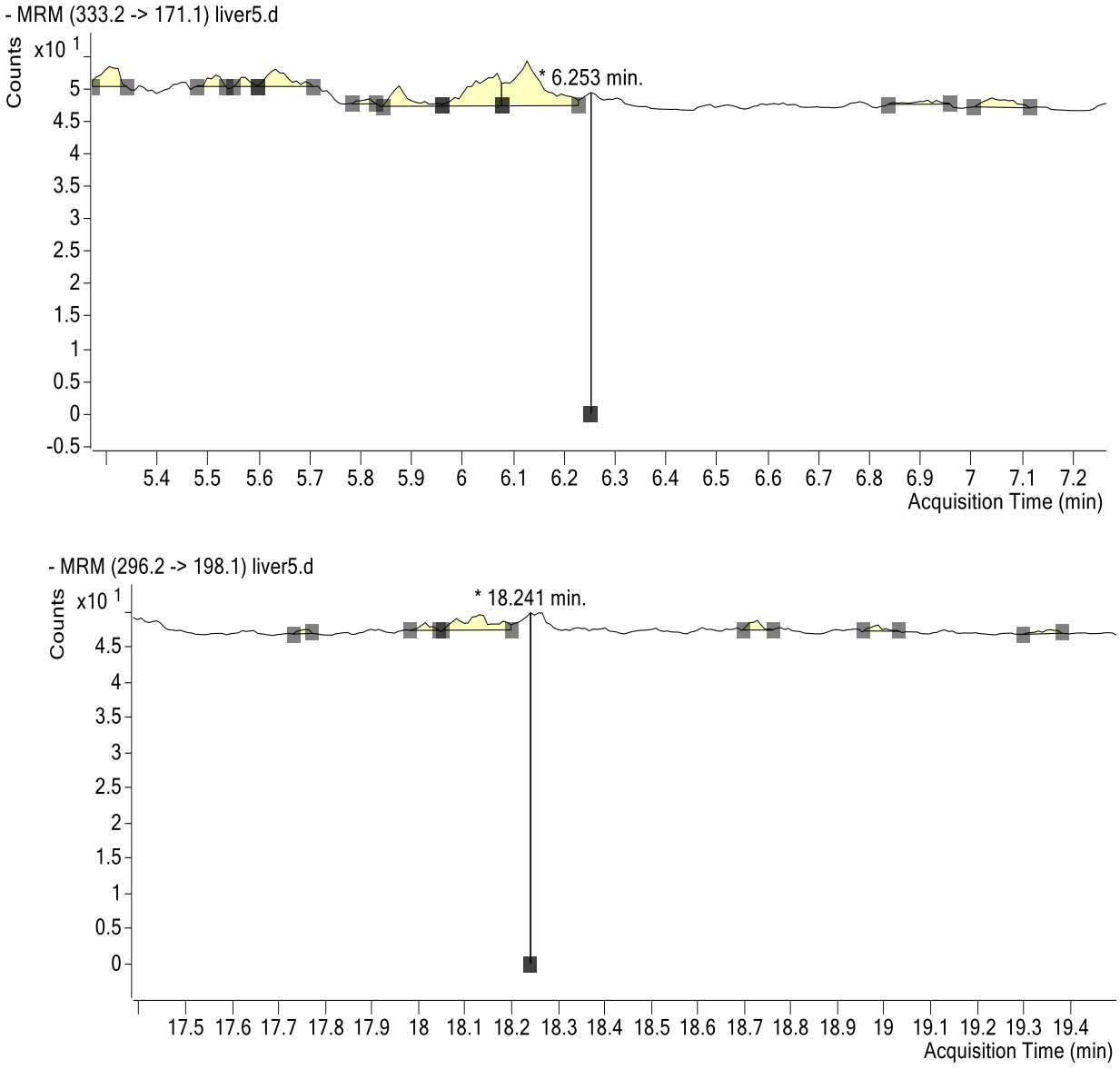
- MRM (333.2 -> 171.1) liver5.d
Counts
x10 1
* 6.253 min.
Acquisition Time (min)
- MRM (296.2 -> 198.1) liver5.d
Counts
x10 1
* 18.241 min.
Acquisition Time (min)

Rat 7 (IV)

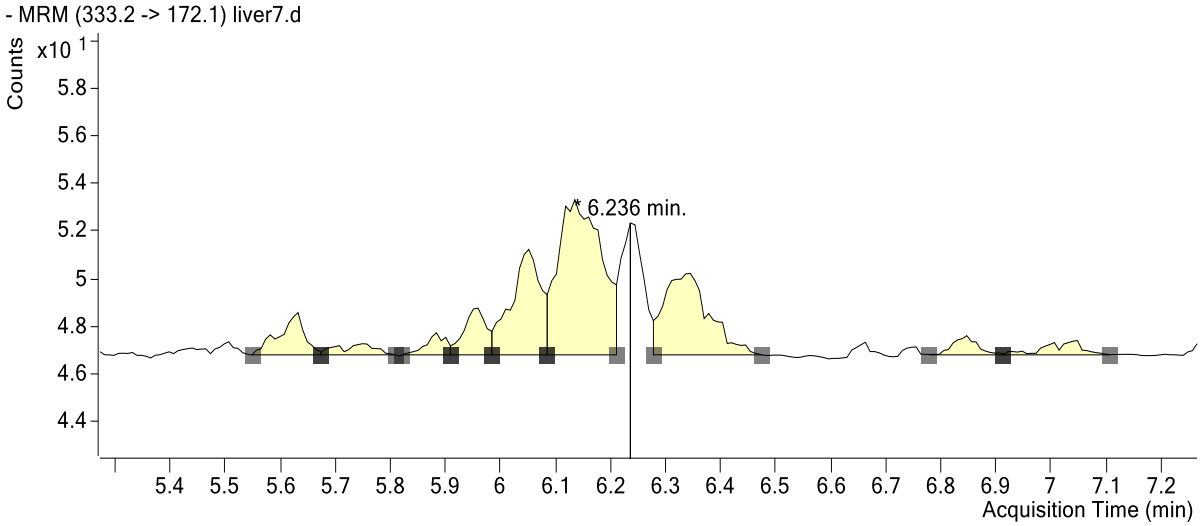
- MRM (333.2 -> 172.1) liver7.d
Counts
x10 1
5.8
5.6
5.4
5.2
5
4.8
4.6
4.4
* 6.236 min.
5.4 5.5 5.6 5.7 5.8 5.9 6 6.1 6.2 6.3 6.4 6.5 6.6 6.7 6.8 6.9 7 7.1 7.2
Acquisition Time (min)

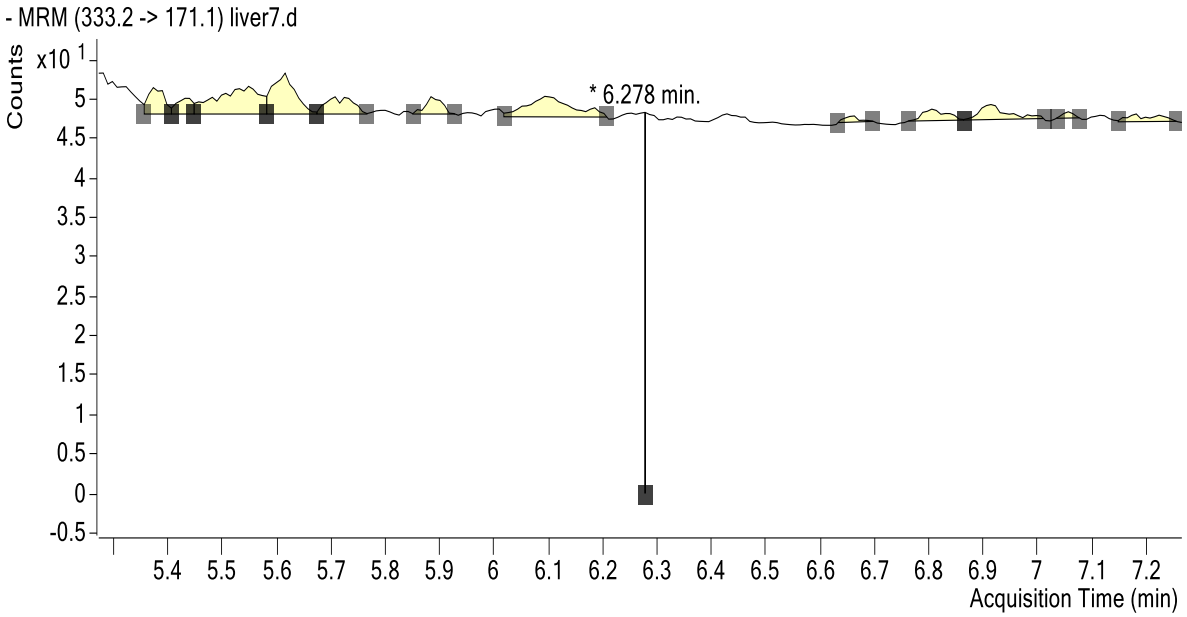
- MRM (333.2 -> 171.1) liver7.d
Counts
x10 1
5
4.5
4
3.5
3
2.5
2
1.5
1
0.5
0
-0.5
* 6.278 min.
5.4 5.5 5.6 5.7 5.8 5.9 6 6.1 6.2 6.3 6.4 6.5 6.6 6.7 6.8 6.9 7 7.1 7.2
Acquisition Time (min)

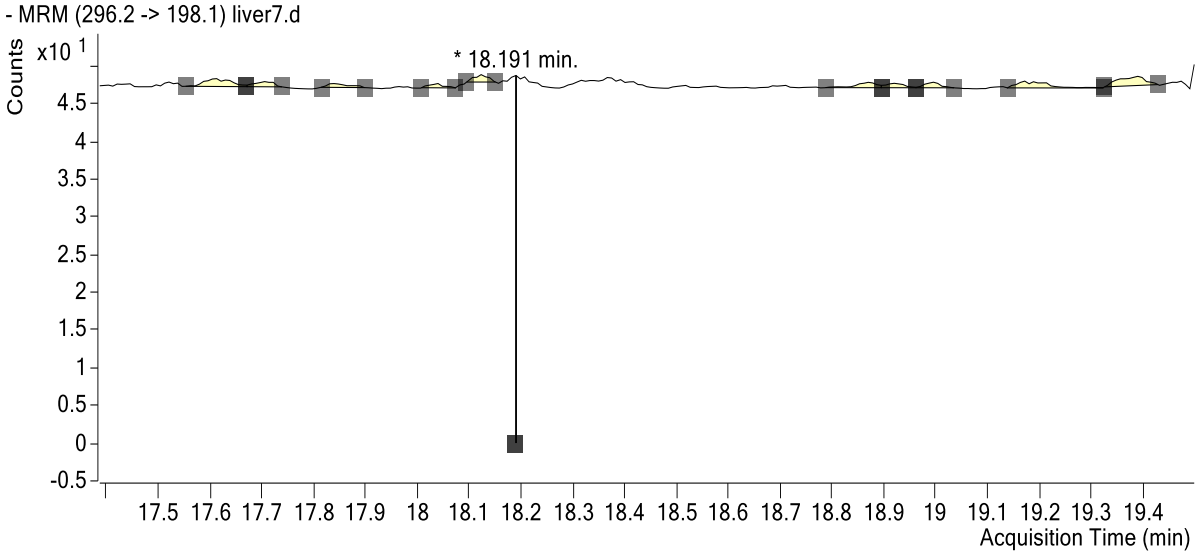
- MRM (296.2 -> 198.1) liver7.d
Counts
x10 1
4.5
4
3.5
3
2.5
2
1.5
1
0.5
0
-0.5
* 18.191 min.
17.5 17.6 17.7 17.8 17.9 18 18.1 18.2 18.3 18.4 18.5 18.6 18.7 18.8 18.9 19 19.1 19.2 19.3 19.4
Acquisition Time (min)

Rat 9 (IV)

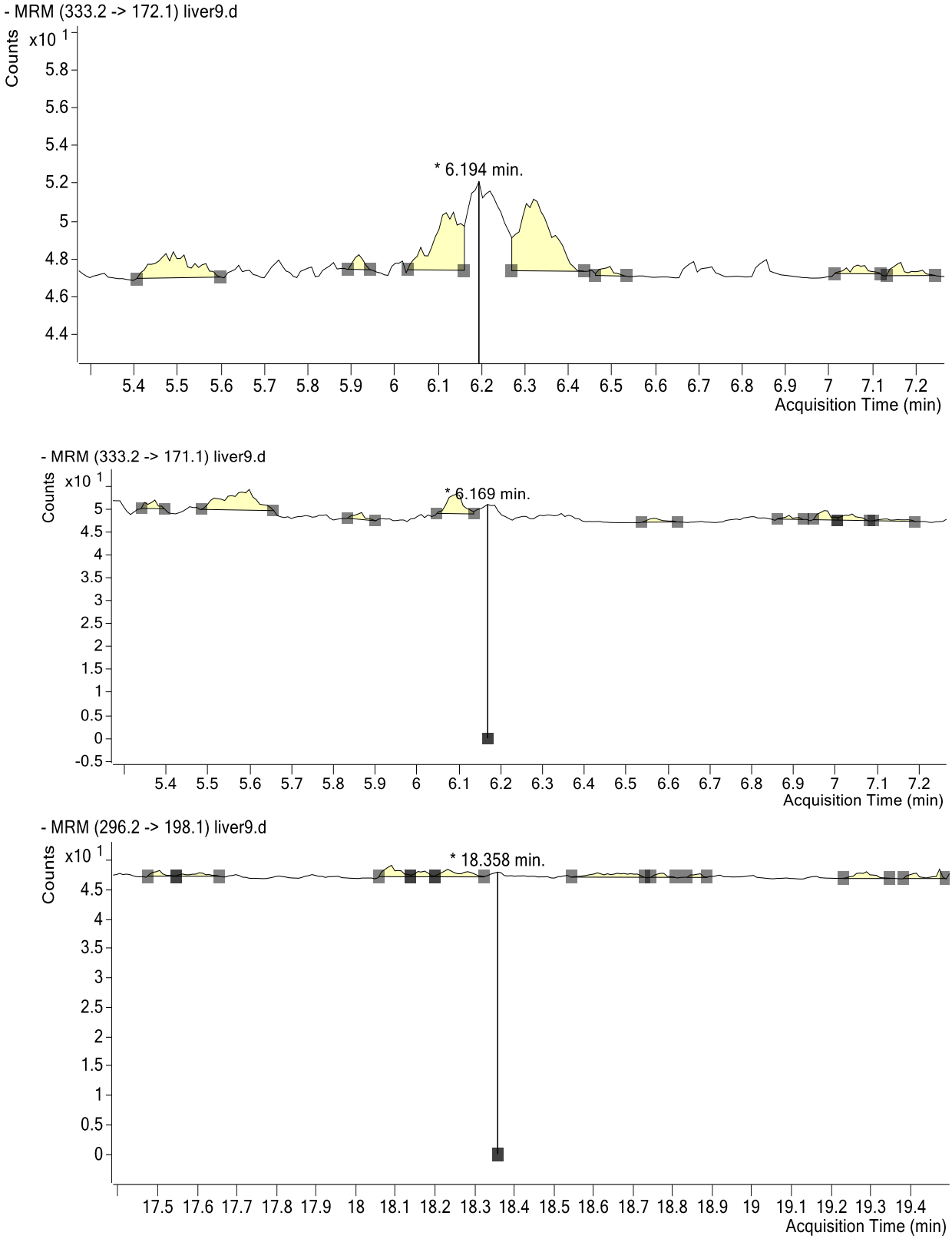
- MRM (333.2 -> 172.1) liver9.d
Counts
x10 1
* 6.194 min.
Acquisition Time (min)
- MRM (333.2 -> 171.1) liver9.d
Counts
x10 1
* 6.169 min.
Acquisition Time (min)
- MRM (296.2 -> 198.1) liver9.d
Counts
x10 1
* 18.358 min.
Acquisition Time (min)

D) <u>d-9,10,13-TriHOME (333.2-172.1/171.1) and d-13-oxo-ODE (296.2-198.1) in perirenal adipose tissue</u>

Rat 2 (Vehicle, gavage)

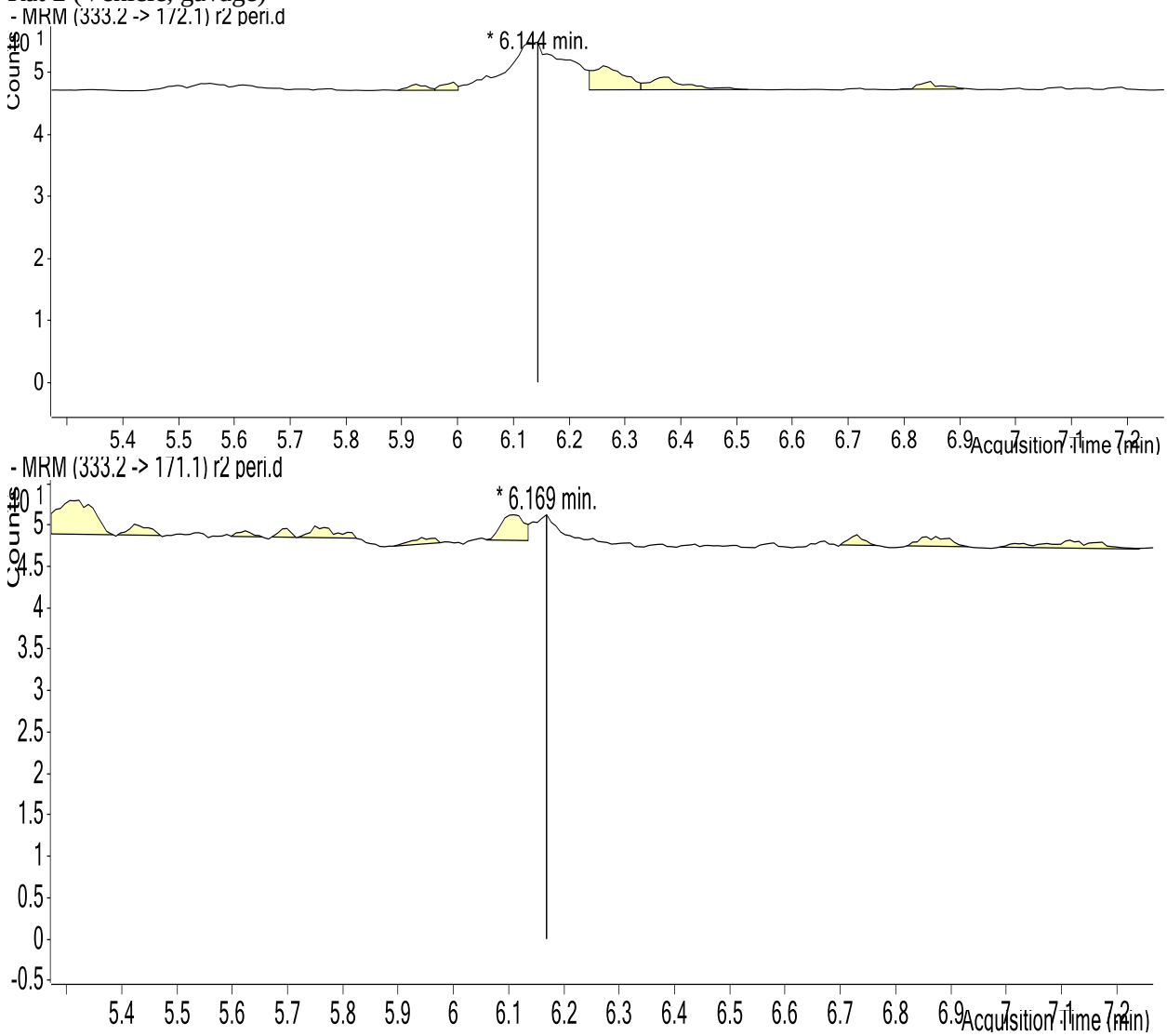

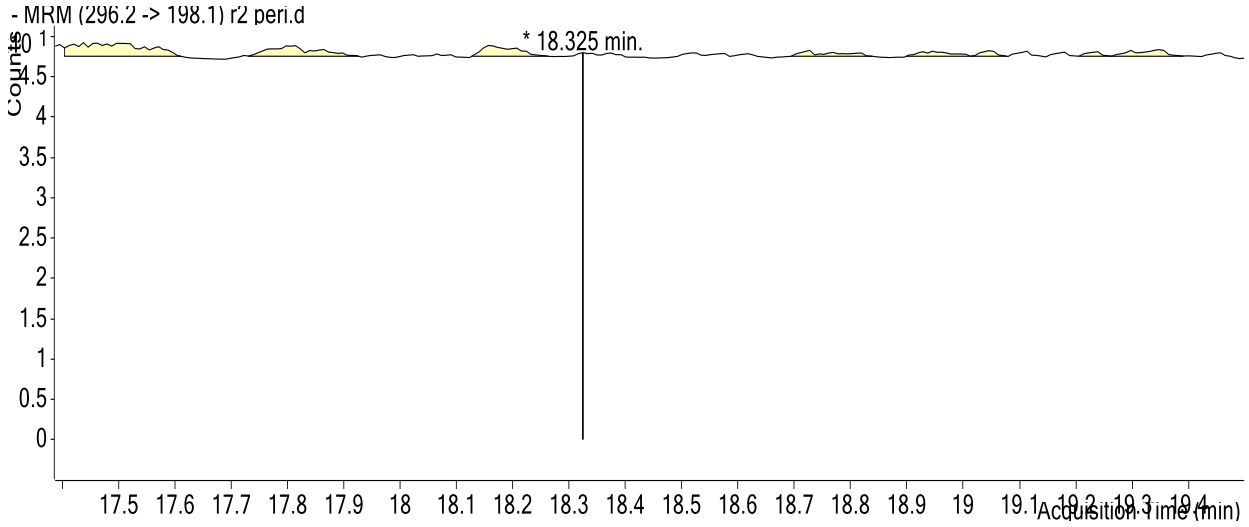

Rat 3 (Vehicle, IV)

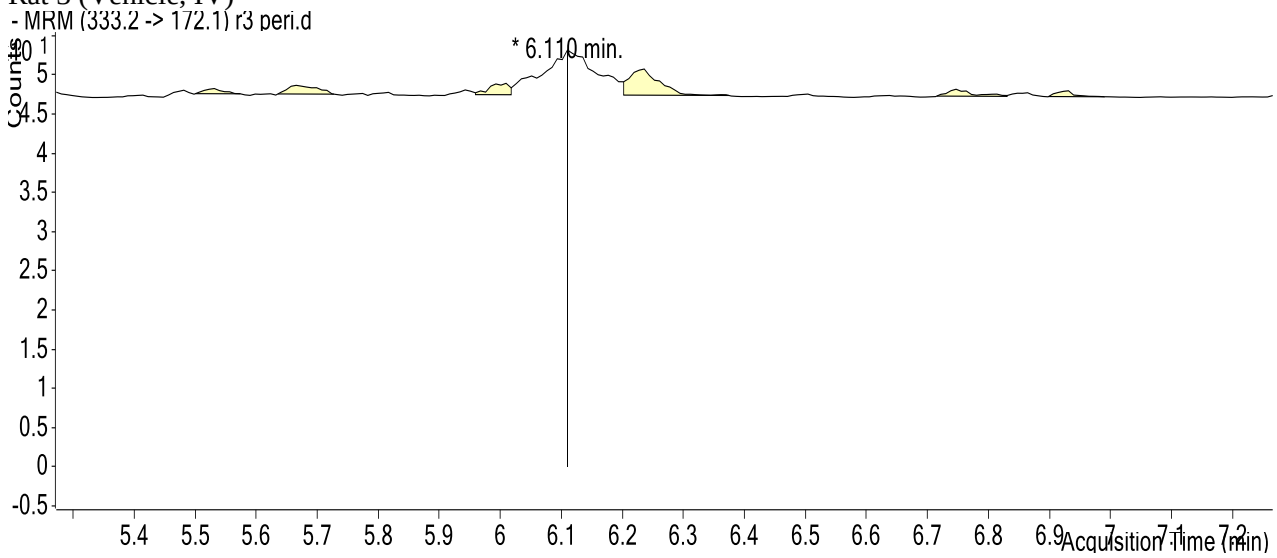

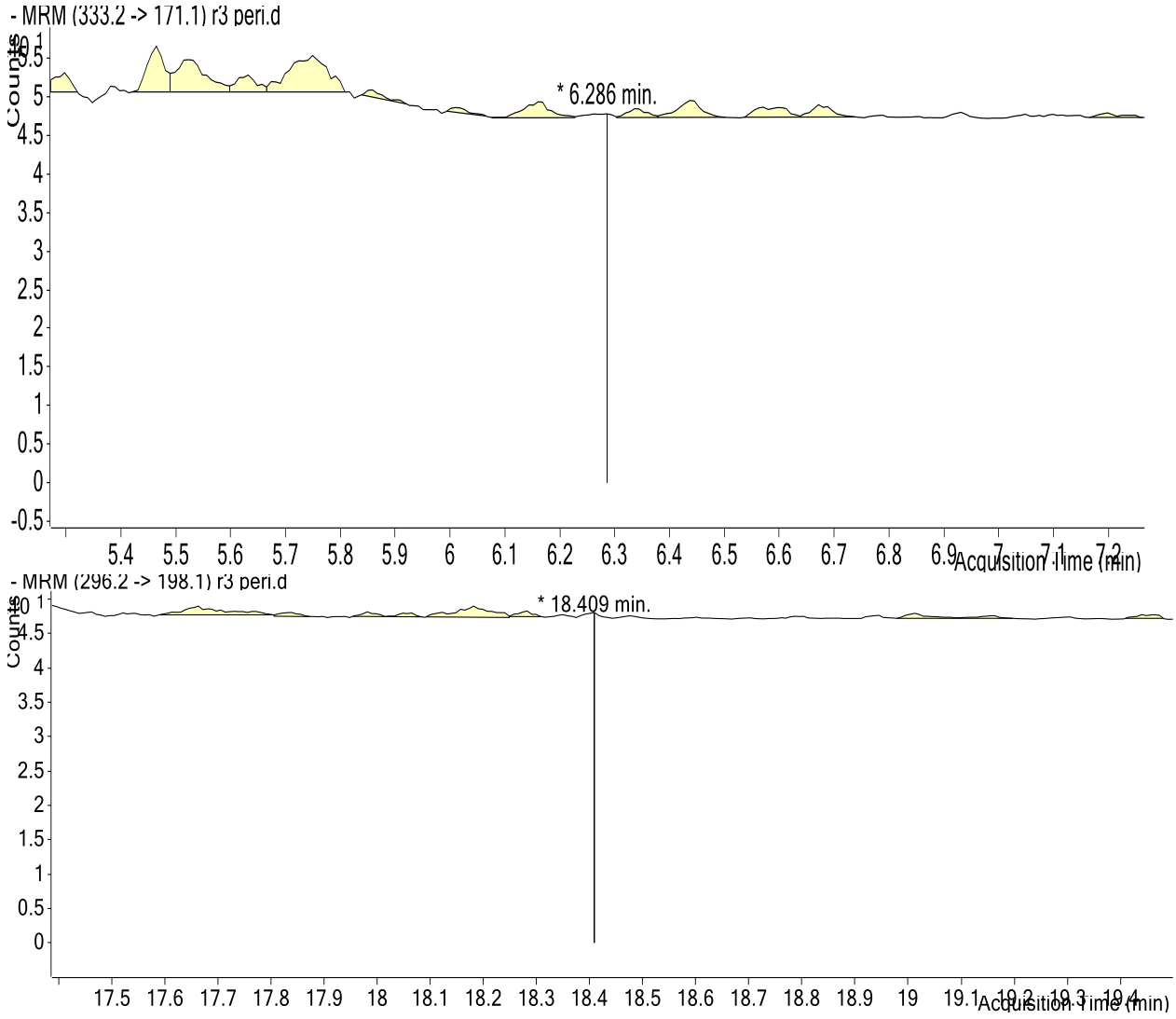
- MRM (333.2 -> 171.1) r3 peri.d
Counts
* 6.286 min.
Acquisition Time (min)
- MRM (296.2 -> 198.1) r3 peri.d
Counts
* 18.409 min.
Acquisition Time (min)

Rat 4 (gavage)

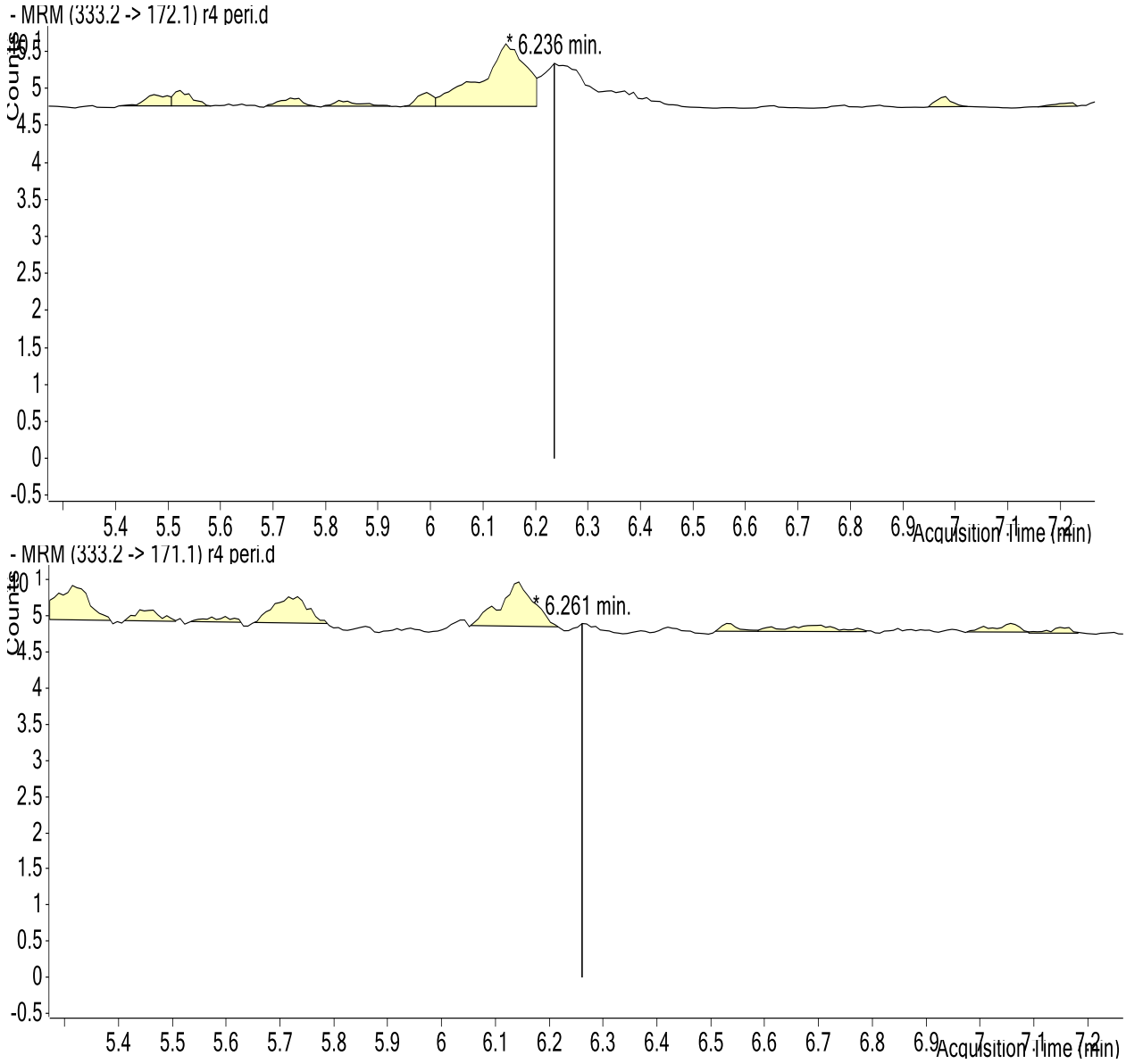
- MRM (333.2 -> 172.1) r4 peri.d
* 6.236 min.
Counts
Acquisition Time (min)
- MRM (333.2 -> 171.1) r4 peri.d
* 6.261 min.
Counts
Acquisition Time (min)

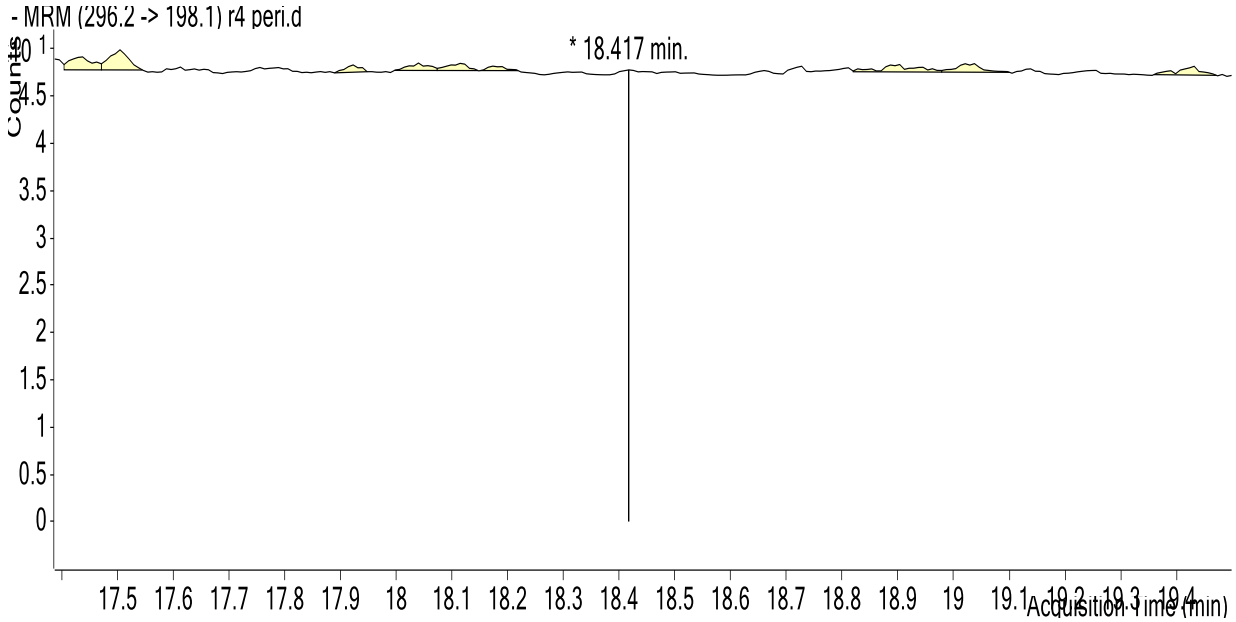
- MRM (296.2 -> 198.1) r4 peri.d
* 18.417 min.
Counts
Acquisition Time (min)

Rat 6 (gavage)

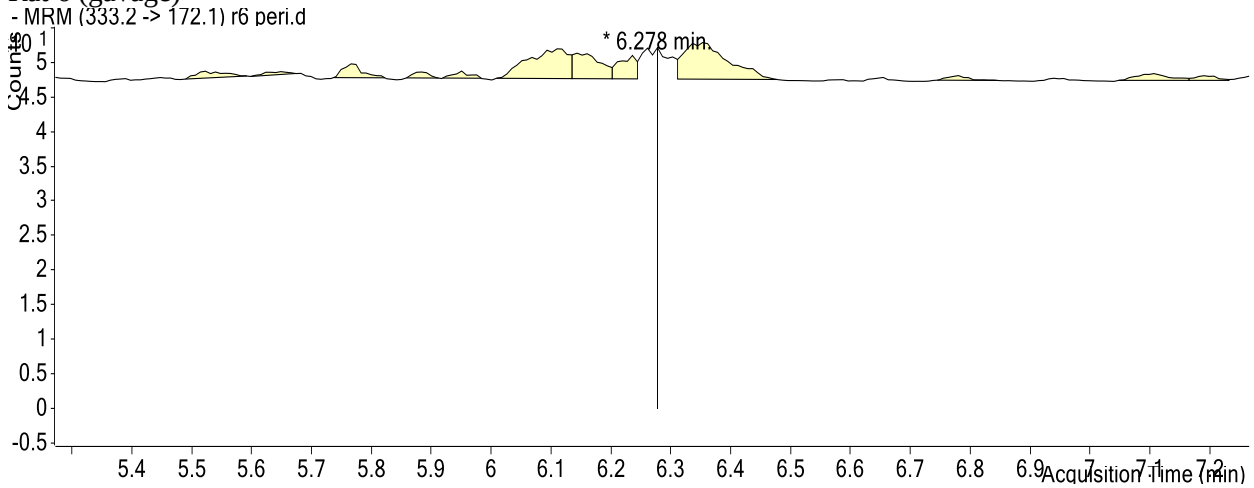
- MRM (333.2 -> 172.1) r6 peri.d
* 6.278 min.
Counts
Acquisition Time (min)

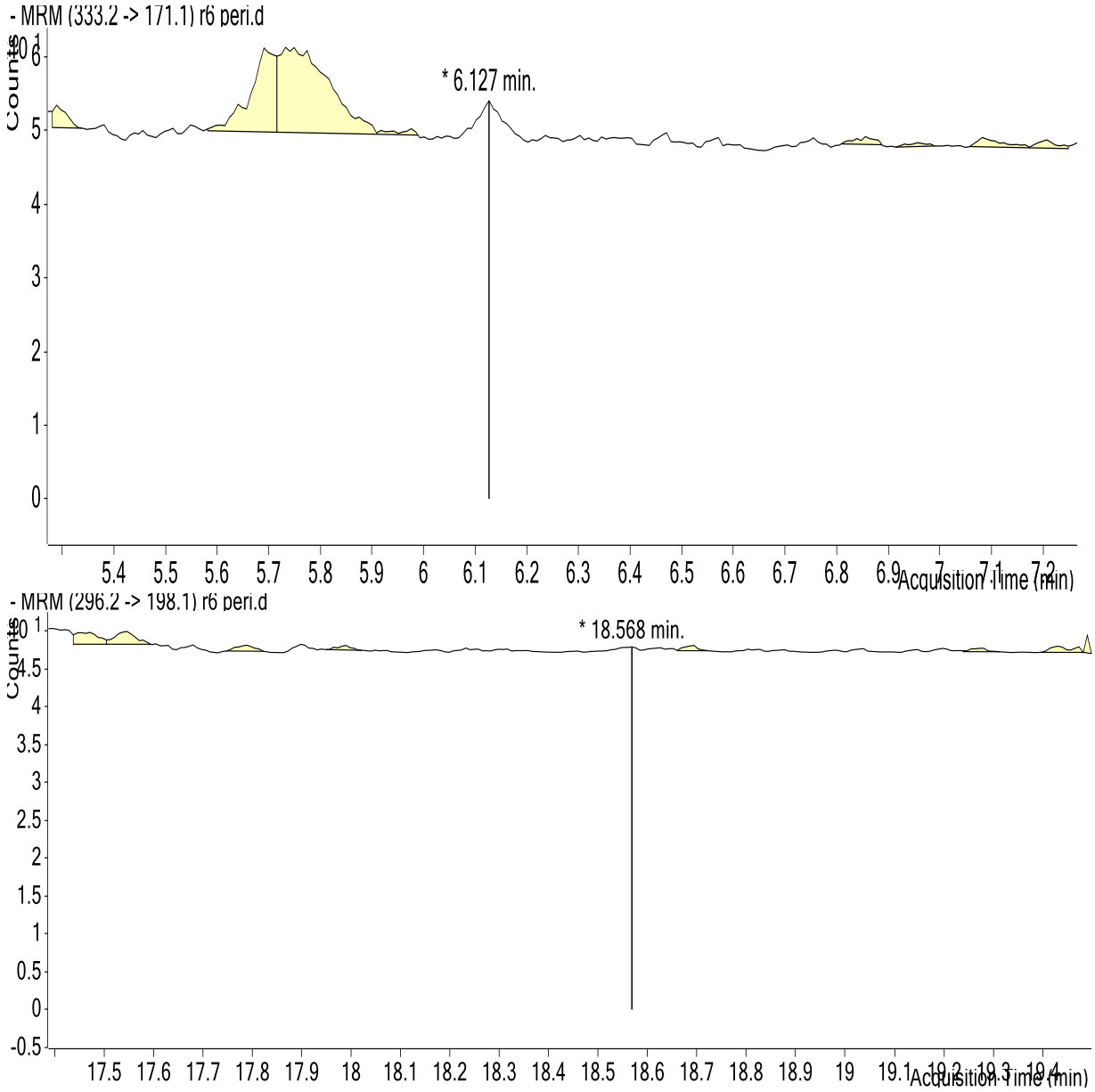
- MRM (333.2 -> 171.1) r6 peri.d
Counts
* 6.127 min.
Acquisition Time (min)
- MRM (296.2 -> 198.1) r6 peri.d
Counts
* 18.568 min.
Acquisition Time (min)

Rat 8 (gavage)

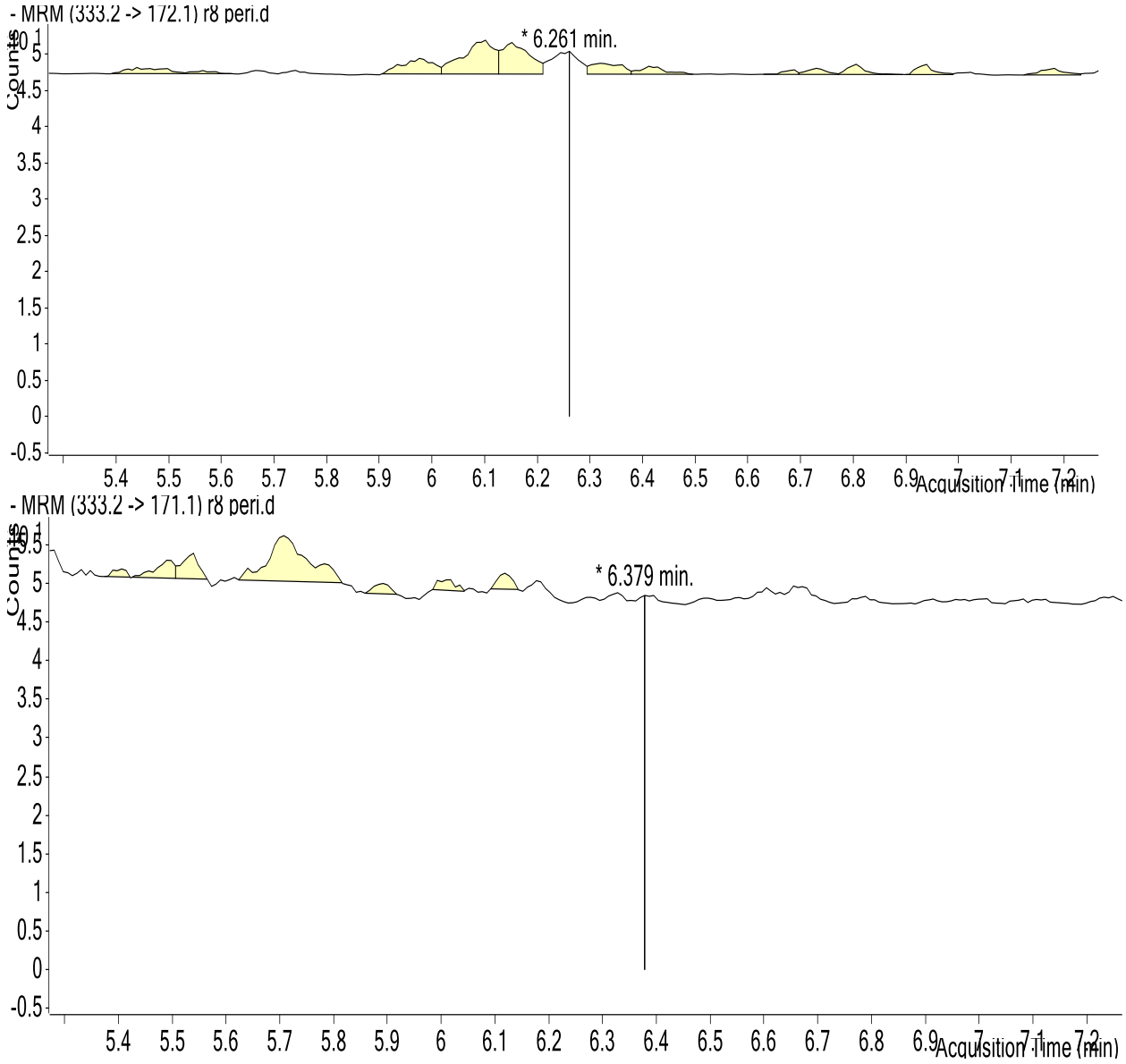
- MRM (333.2 -> 172.1) r8 peri.d
* 6.261 min.
Counts
Acquisition Time (min)
- MRM (333.2 -> 171.1) r8 peri.d
* 6.379 min.
Counts
Acquisition Time (min)

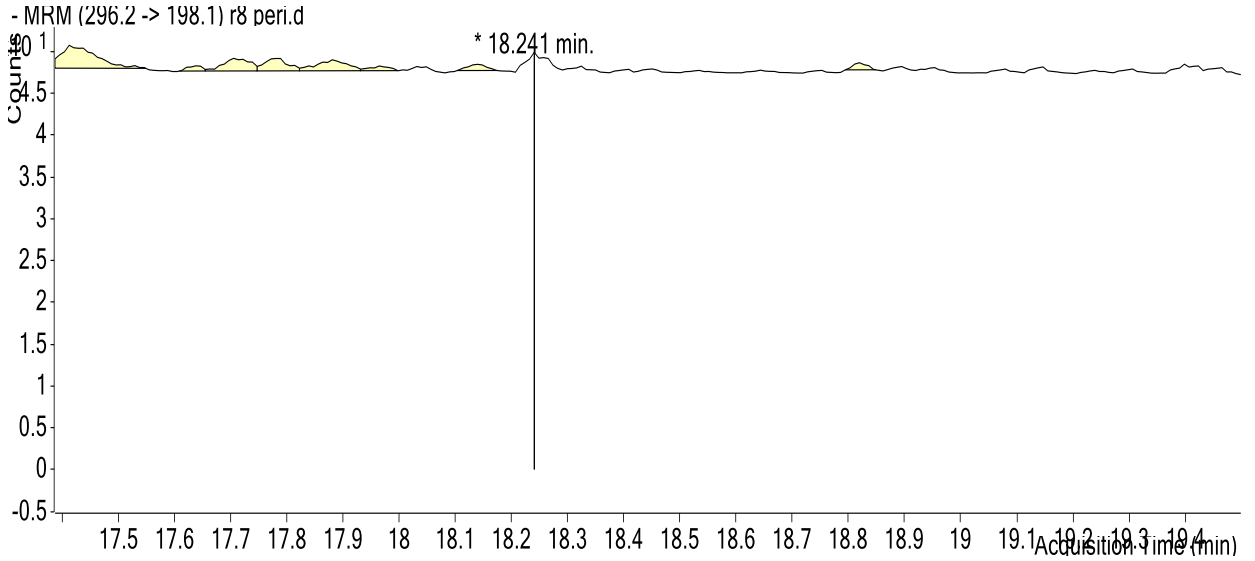
- MRM (296.2 -> 198.1) r8 peri.d
* 18.241 min.
Counts
Acquisition Time (min)

Rat 5 (IV)

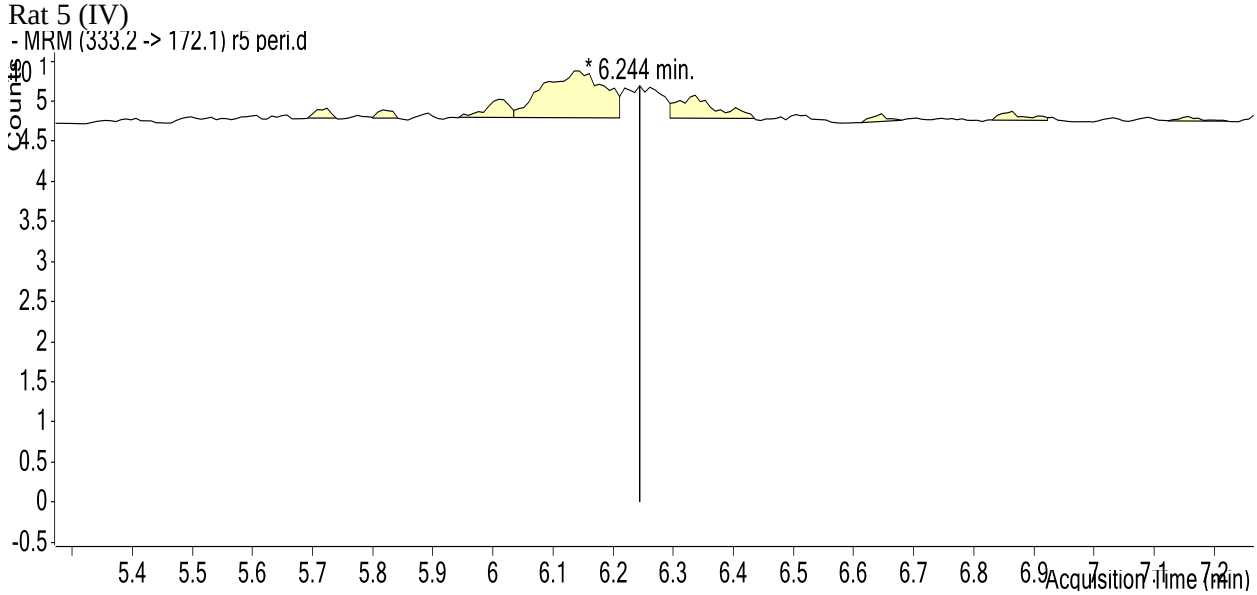
- MRM (333.2 -> 172.1) r5 peri.d
* 6.244 min.
Counts
Acquisition Time (min)

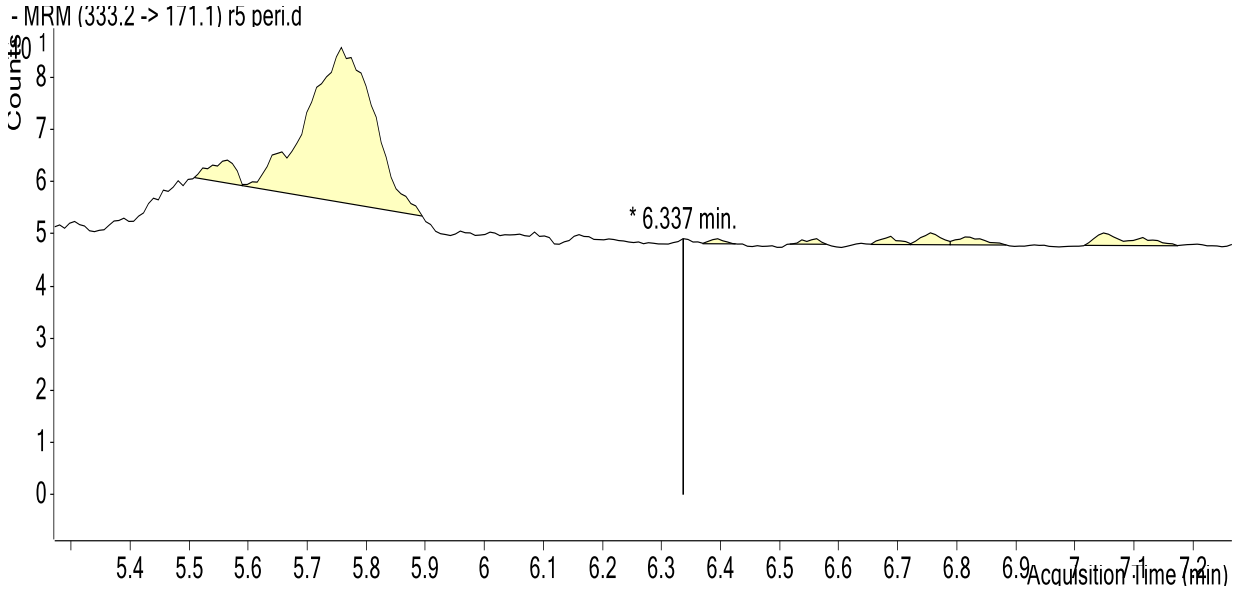
- MRM (333.2 -> 171.1) r5 peri.d
Counts
* 6.337 min.
Acquisition Time (min)

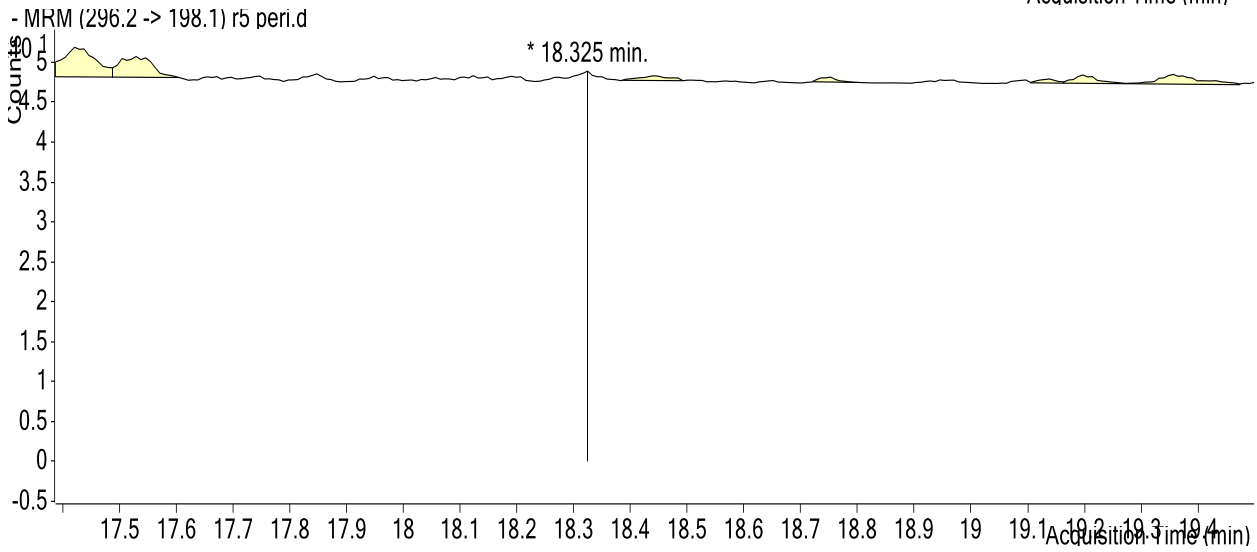
- MRM (296.2 -> 198.1) r5 peri.d
Counts
* 18.325 min.
Acquisition Time (min)

Rat 7 (IV)

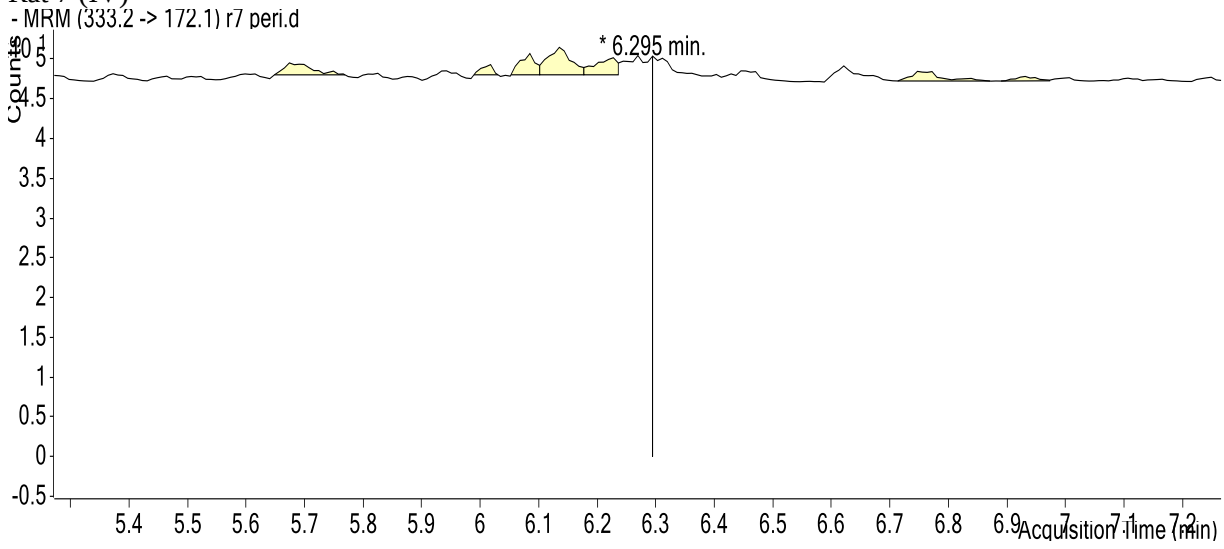
- MRM (333.2 -> 172.1) r7 peri.d
Counts
* 6.295 min.
Acquisition Time (min)

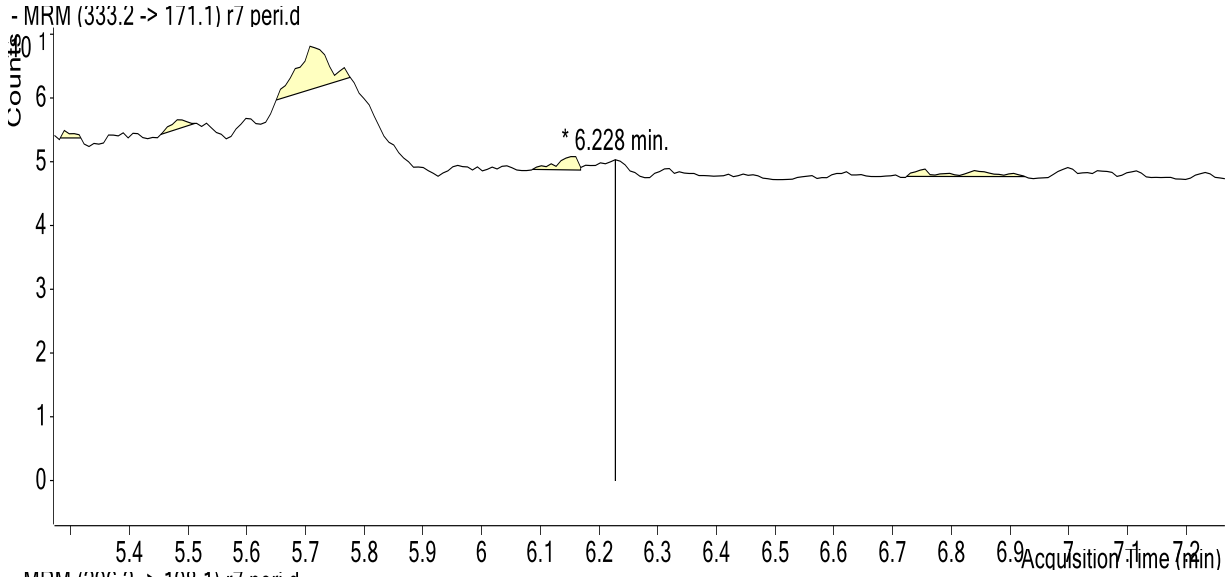
- MRM (333.2 -> 171.1) r7 peri.d
Counts
* 6.228 min.
Acquisition Time (min)

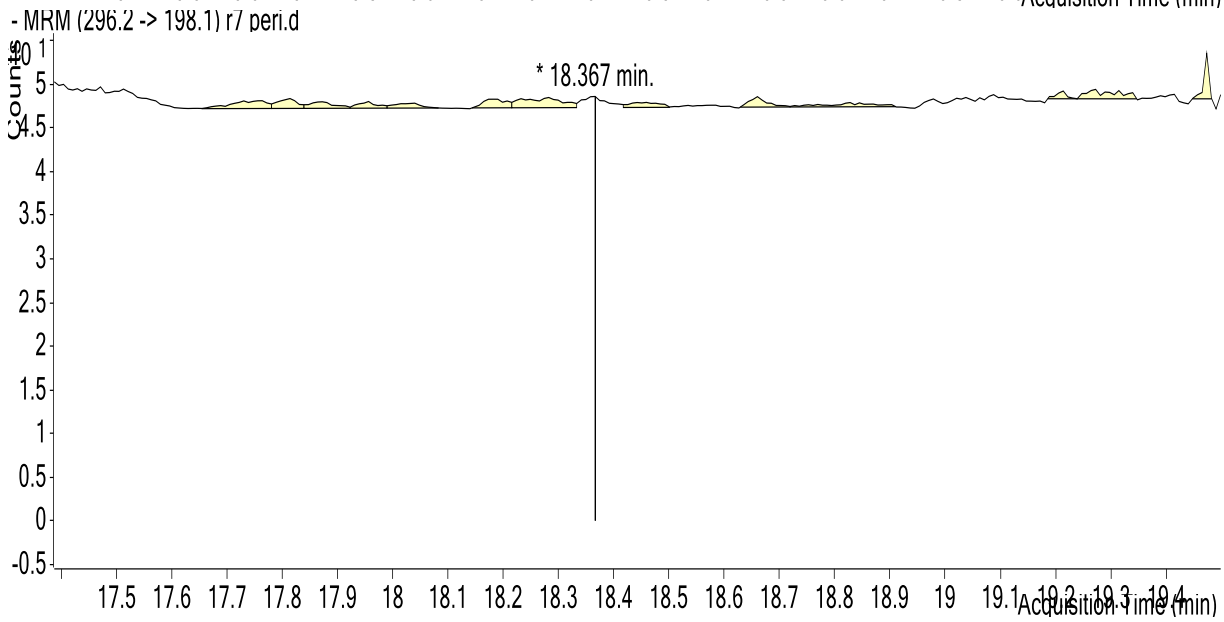
- MRM (296.2 -> 198.1) r7 peri.d
Counts
* 18.367 min.
Acquisition Time (min)

Rat 9 (IV)

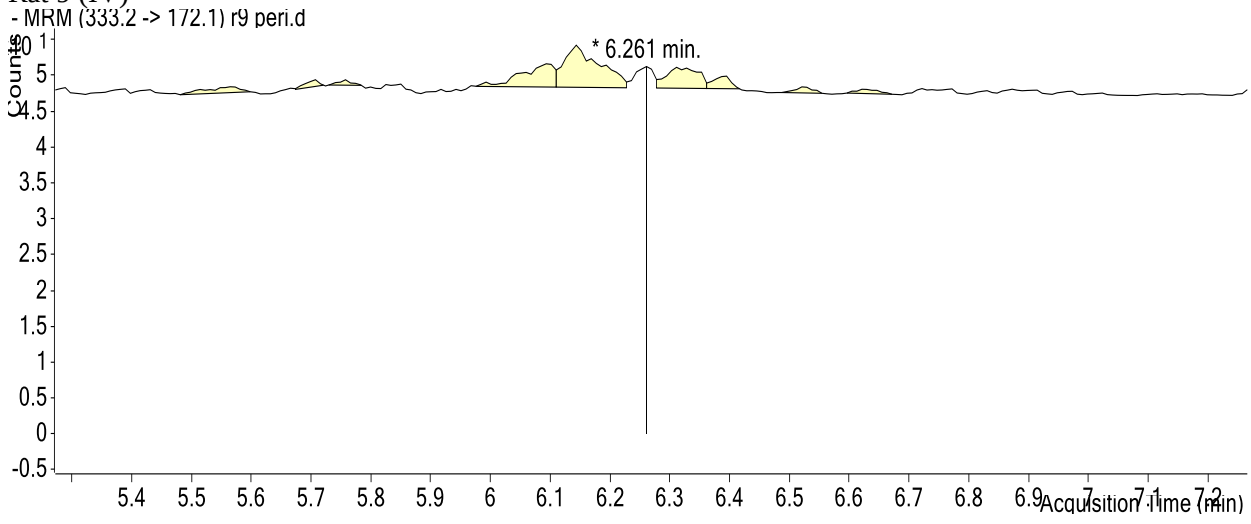
- MRM (333.2 -> 172.1) r9 peri.d
Counts
* 6.261 min.
Acquisition Time (min)

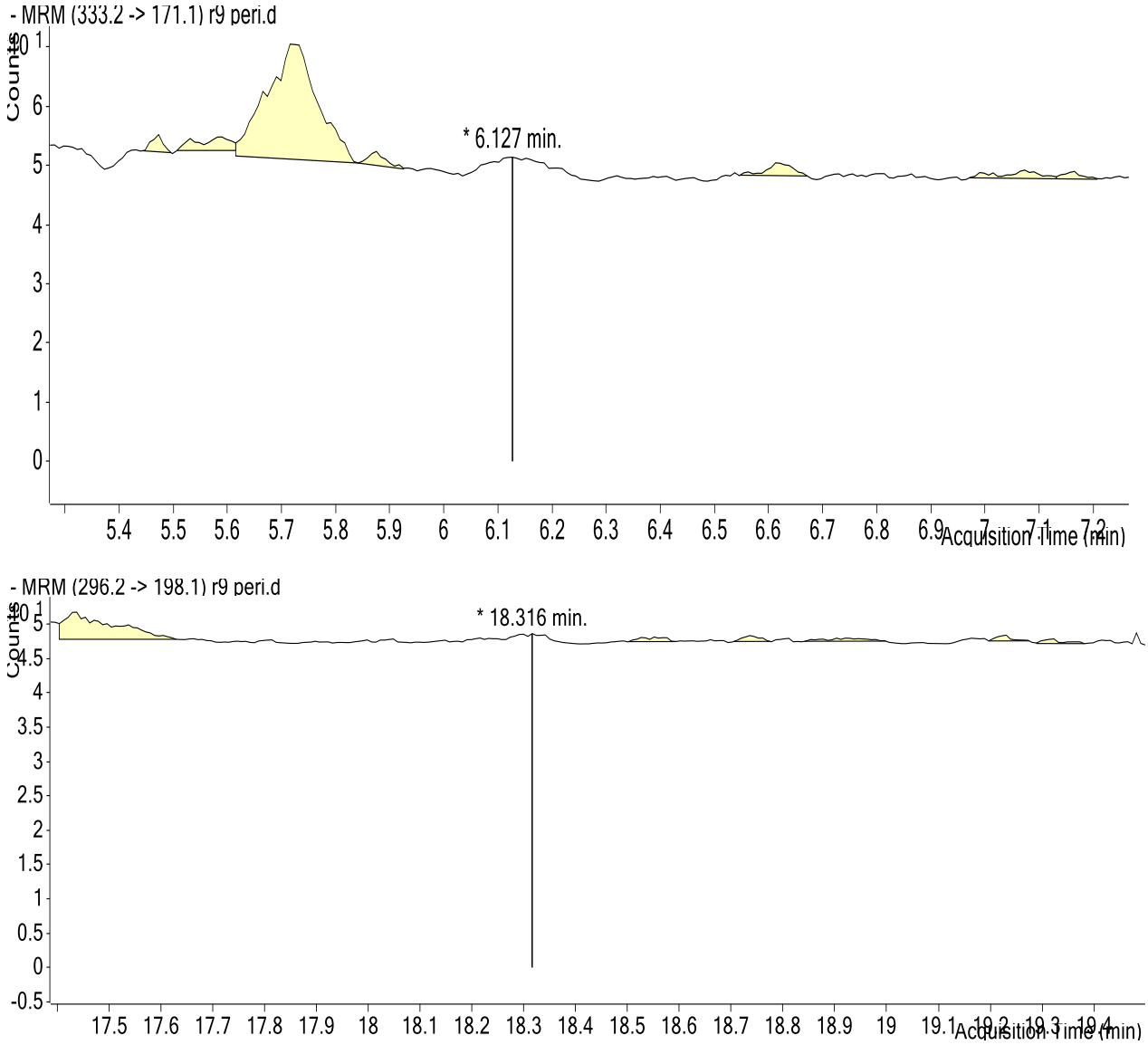

E) <u>d-9,10,13-TriHOME (333.2-172.1/171.1) and d-13-oxo-ODE (296.2-198.1) in visceral adipose tissue</u>

Rat 2 (Vehicle, gavage)

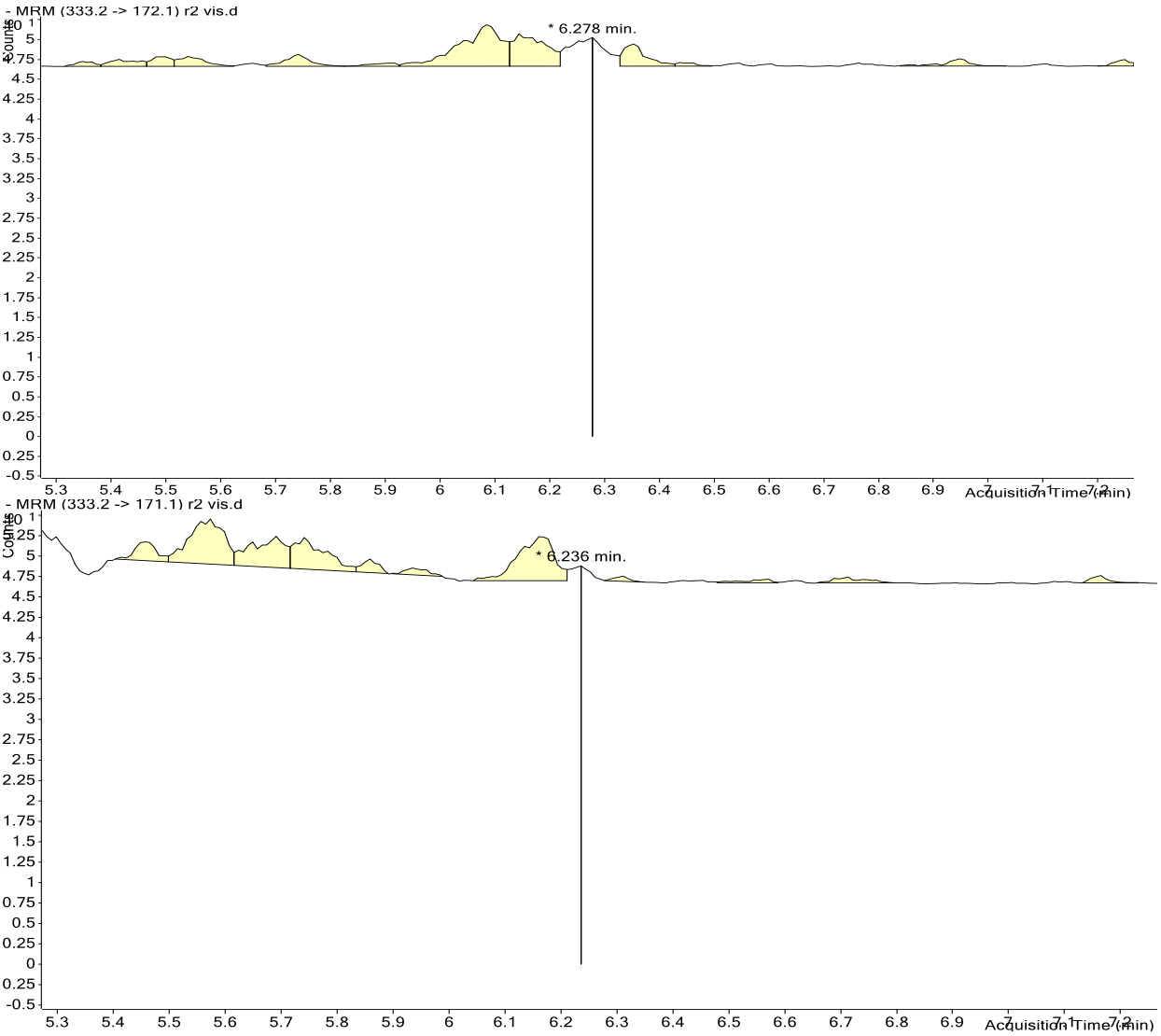
- MRM (333.2 -> 172.1) r2 vis.d
* 6.278 min.
Counts
Acquisition Time (min)
- MRM (333.2 -> 171.1) r2 vis.d
* 6.236 min.
Counts
Acquisition Time (min)

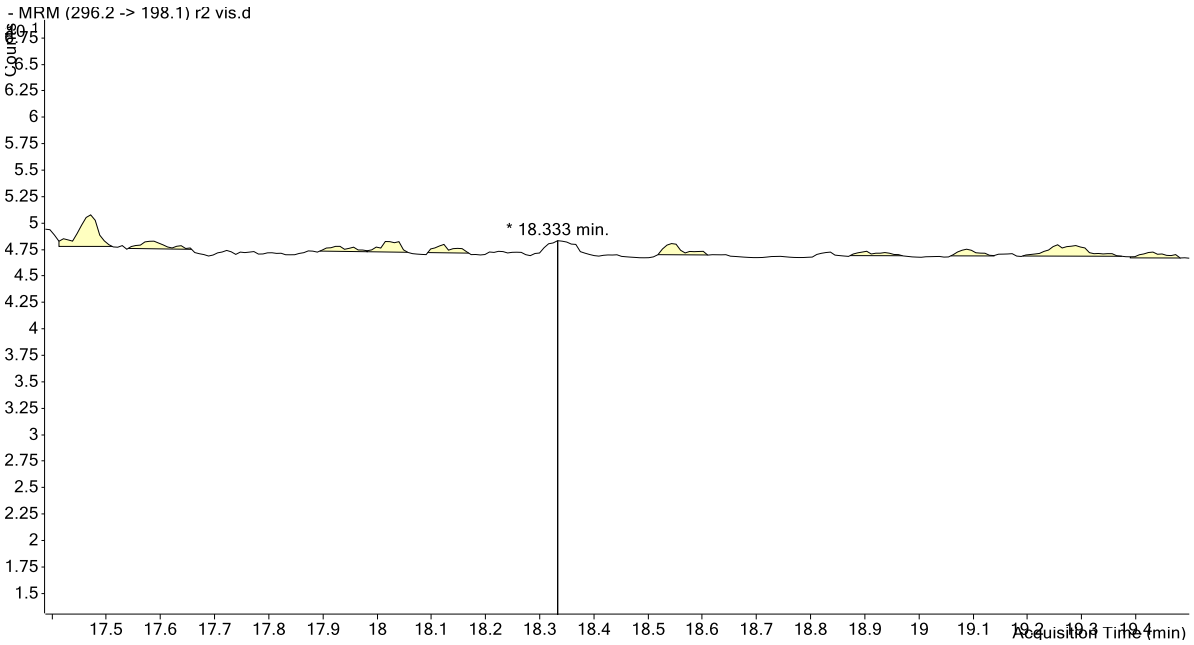

Rat 3 (IV, vehicle)

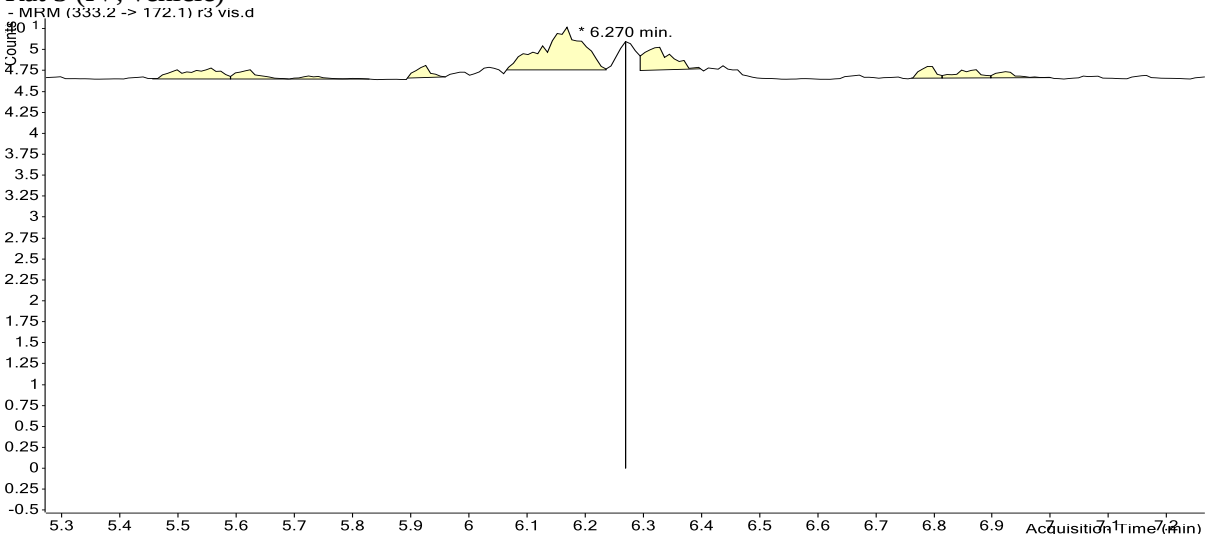

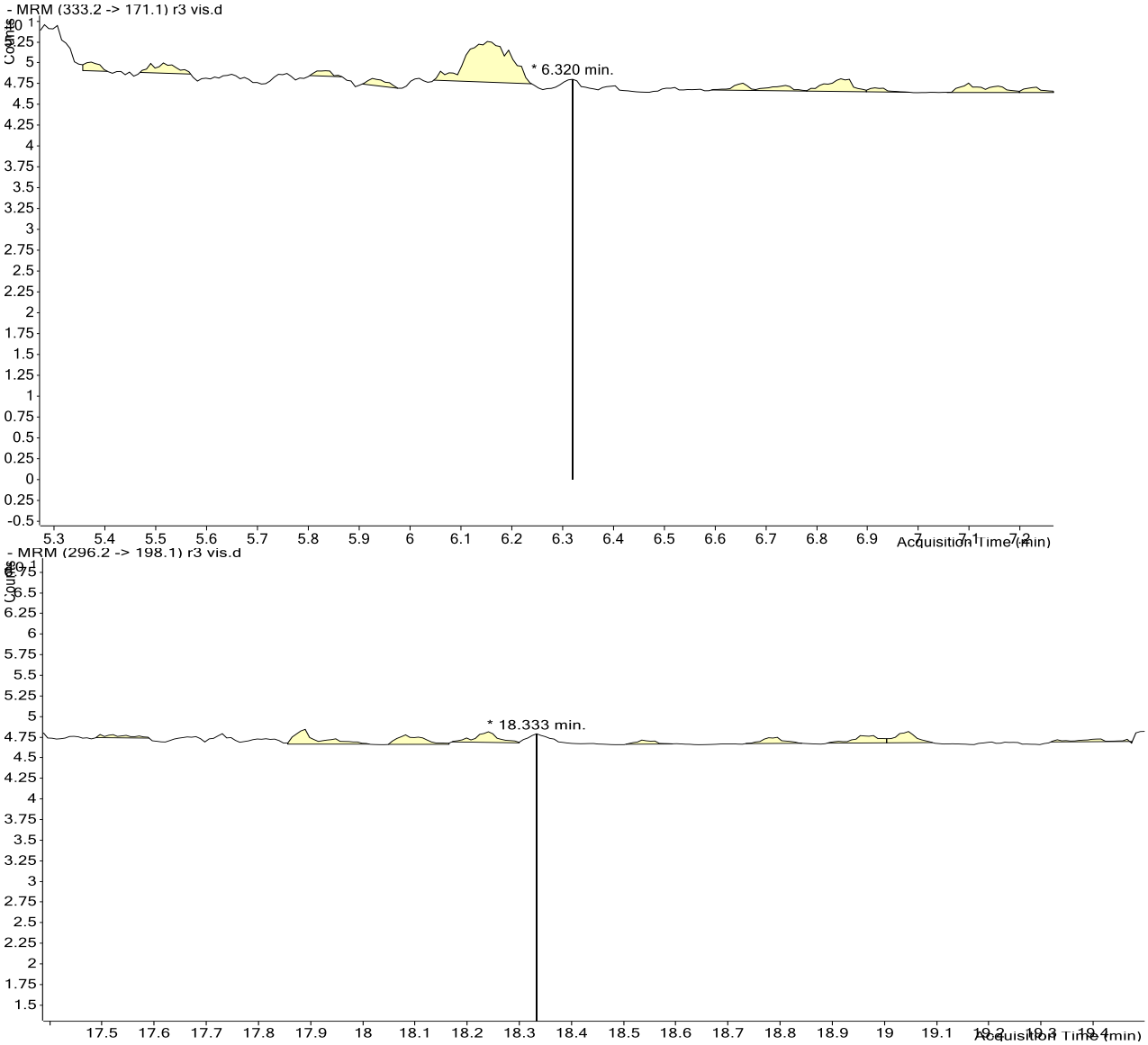
- MRM (333.2 -> 171.1) r3 vis.d
Counts
* 6.320 min.
Acquisition Time (min)
- MRM (296.2 -> 198.1) r3 vis.d
Counts
* 18.333 min.
Acquisition Time (min)

Rat 4 (gavage)

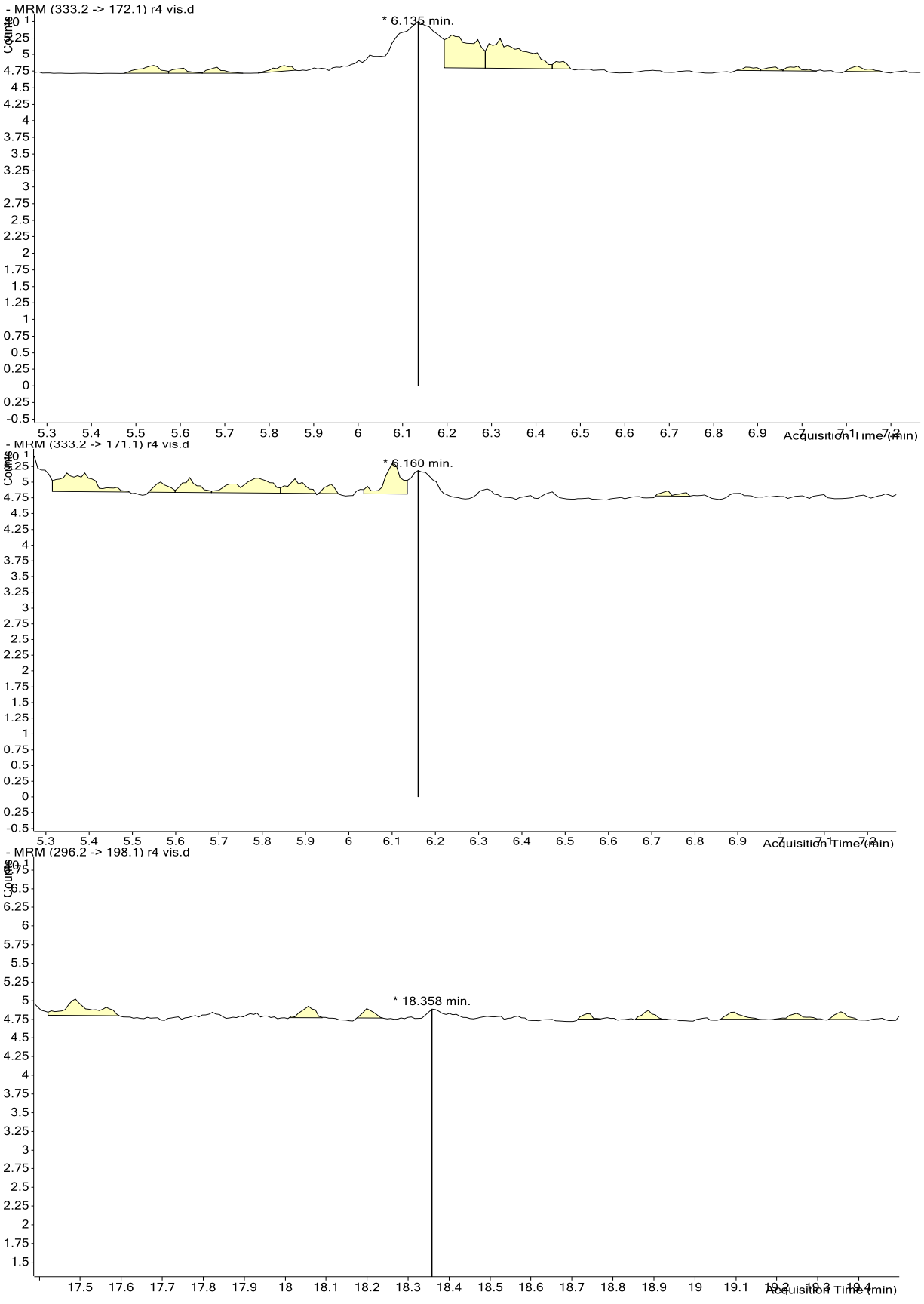
- MRM (333.2 -> 172.1) r4 vis.d
* 6.135 min.
Counts
Acquisition Time (min)
- MRM (333.2 -> 171.1) r4 vis.d
* 6.160 min.
Counts
Acquisition Time (min)
- MRM (296.2 -> 198.1) r4 vis.d
* 18.358 min.
Counts
Acquisition Time (min)

Rat 6 (gavage)

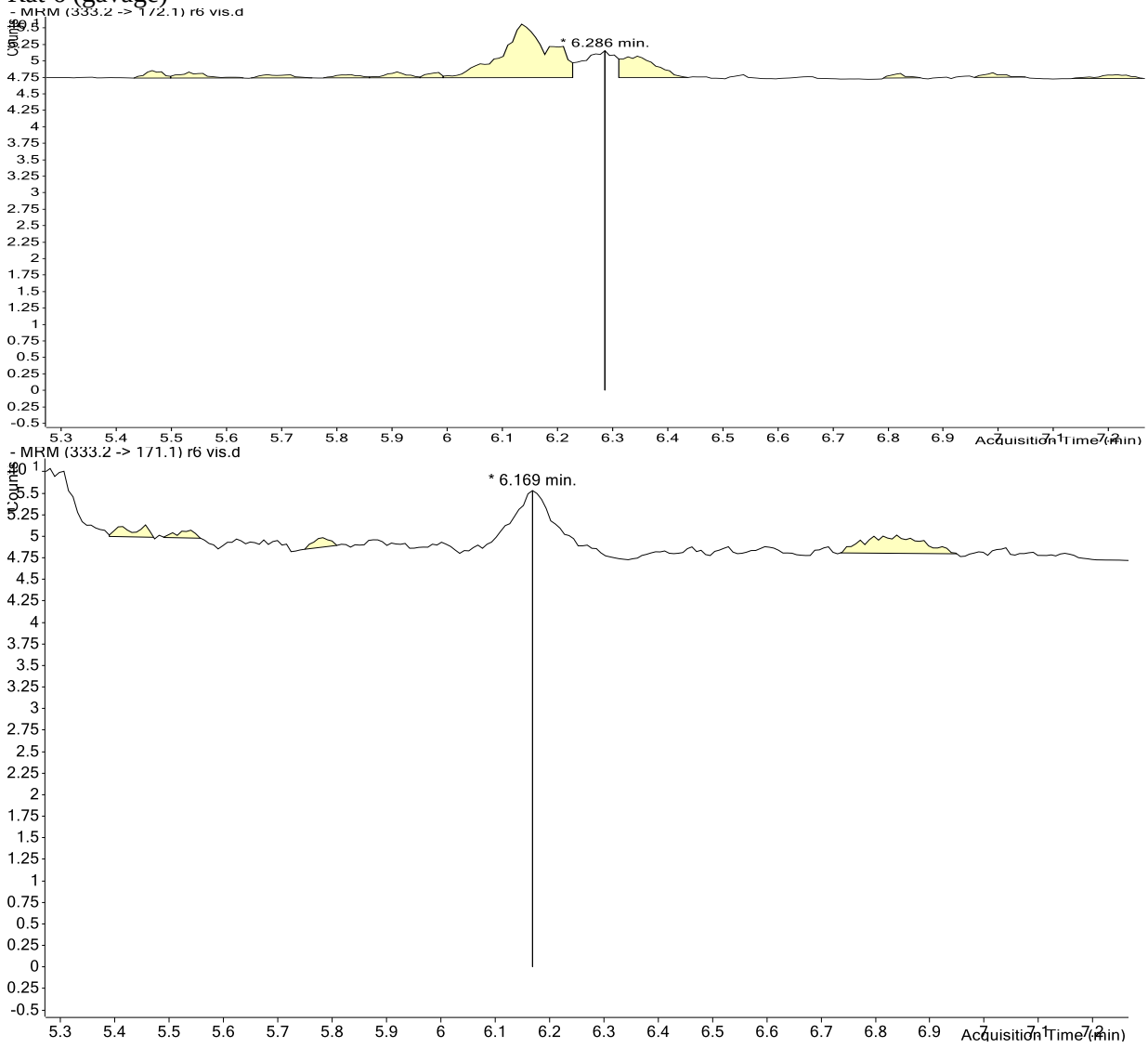
- MRM (333.2 -> 172.1) r6 vis.d
* 6.286 min.
Counts
Acquisition Time (min)
- MRM (333.2 -> 171.1) r6 vis.d
* 6.169 min.
Counts
Acquisition Time (min)

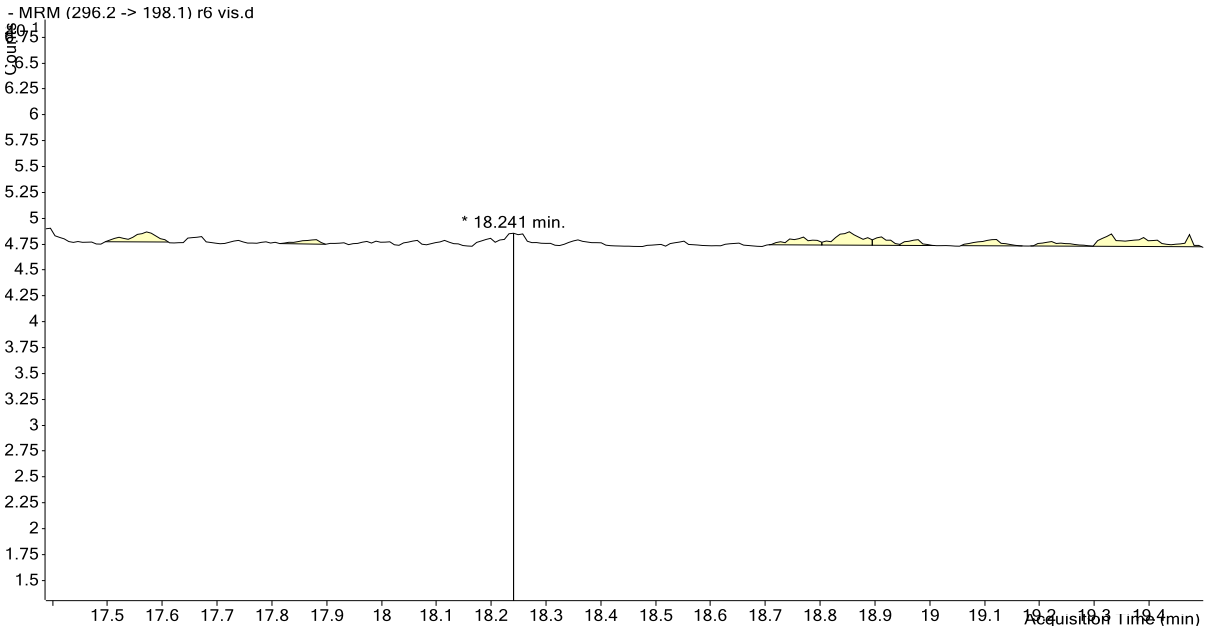
- MRM (296.2 -> 198.1) r6 vis.d
Counts
* 18.241 min.
Acquisition Time (min)

Rat 8 (gavage)

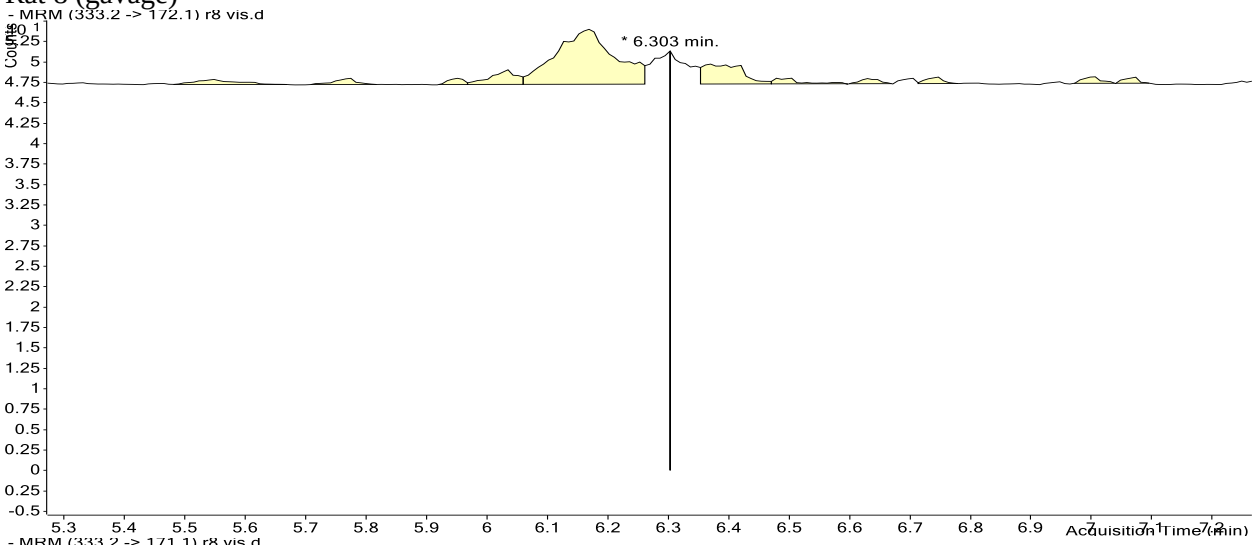
- MRM (333.2 -> 172.1) r8 vis.d
Counts
* 6.303 min.
Acquisition Time (min)

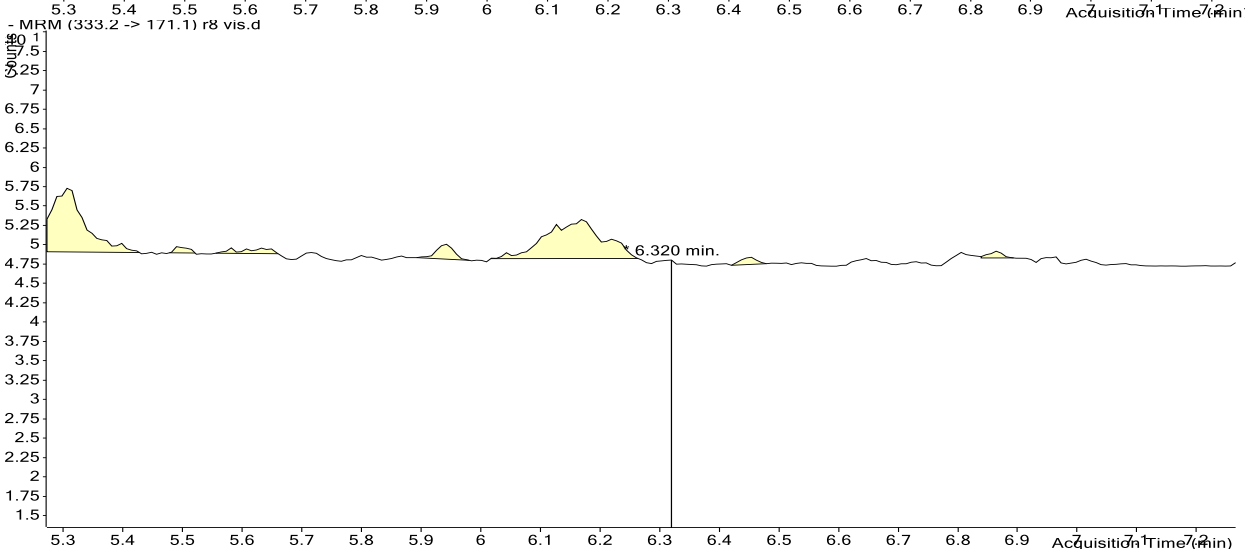
- MRM (333.2 -> 171.1) r8 vis.d
Counts
* 6.320 min.
Acquisition Time (min)

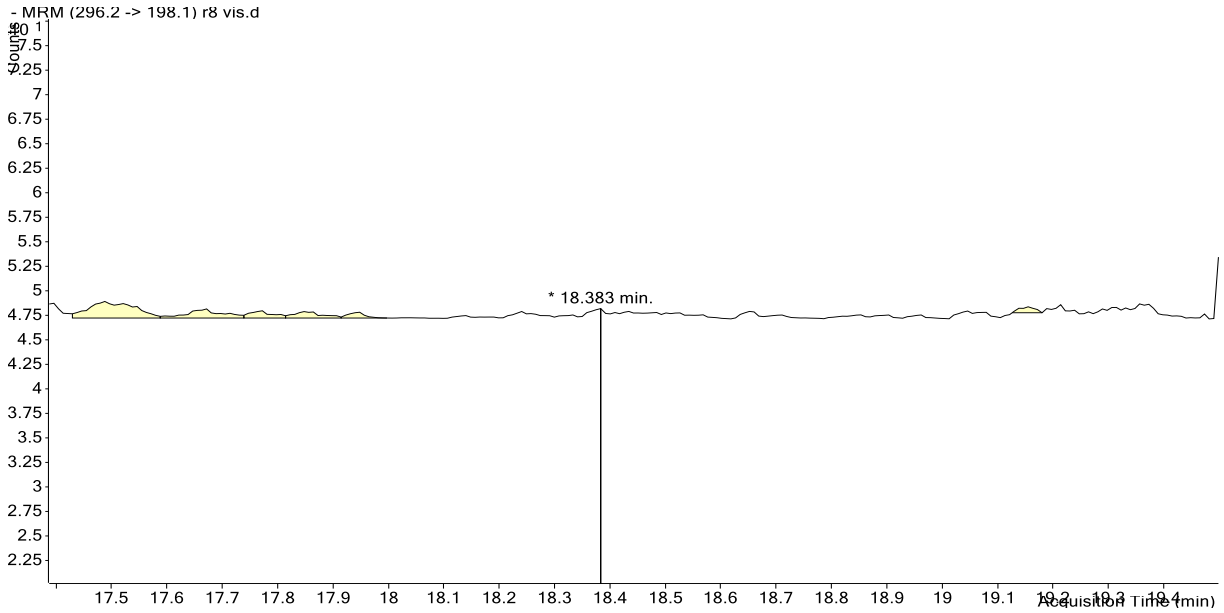
- MRM (296.2 -> 198.1) r8 vis.d
Counts
* 18.383 min.
Acquisition Time (min)

Rat 5 (IV)

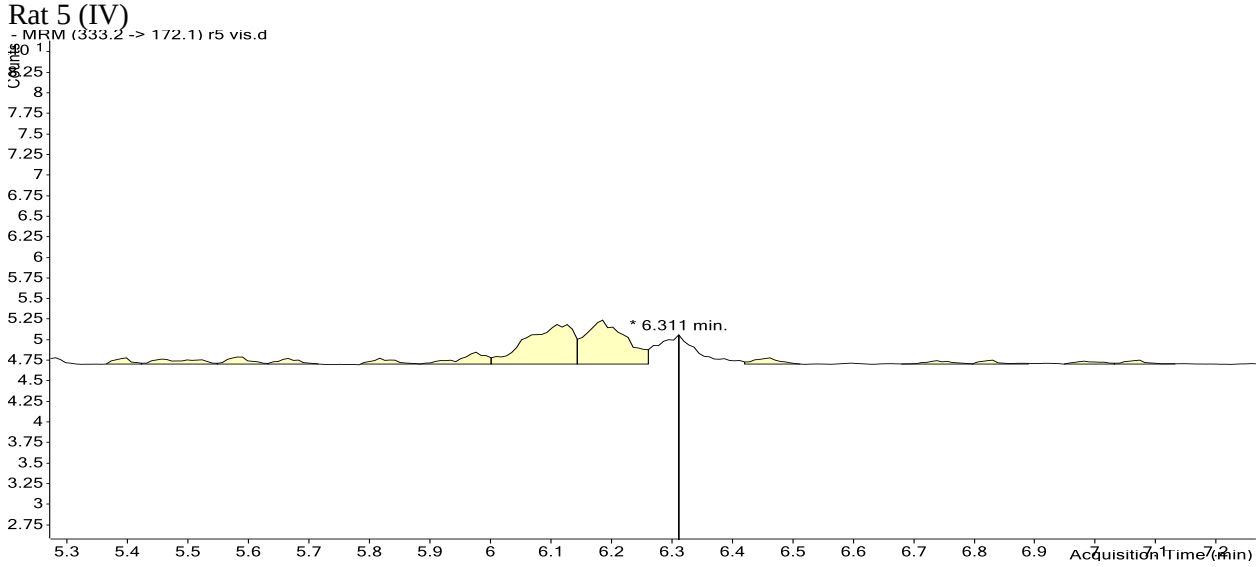
- MRM (333.2 -> 172.1) r5 vis.d
Counts
* 6.311 min.
Acquisition Time (min)

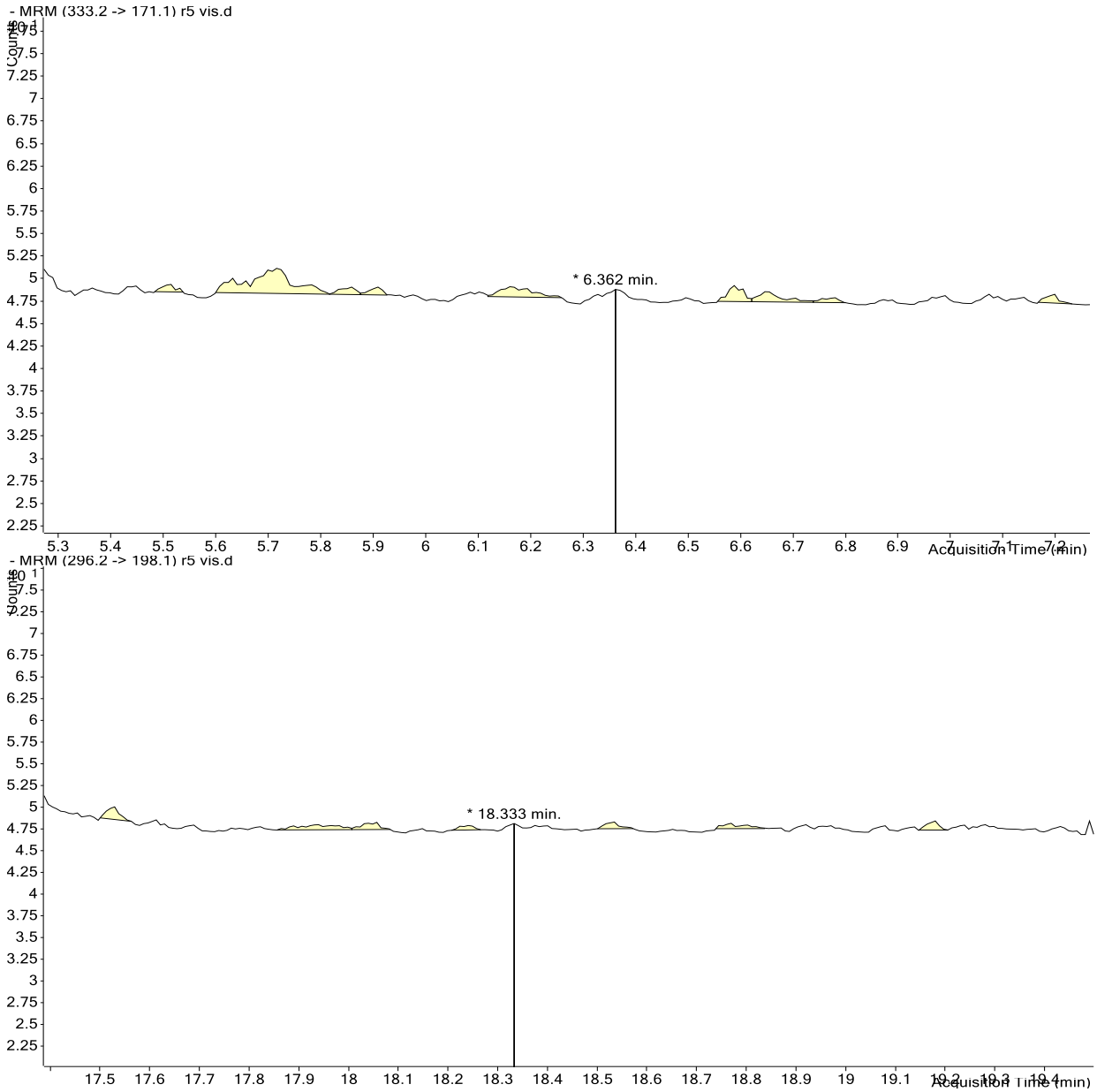
- MRM (333.2 -> 171.1) r5 vis.d
Counts
* 6.362 min.
Acquisition Time (min)
- MRM (296.2 -> 198.1) r5 vis.d
Counts
* 18.333 min.
Acquisition Time (min)

Rat 7 (IV)

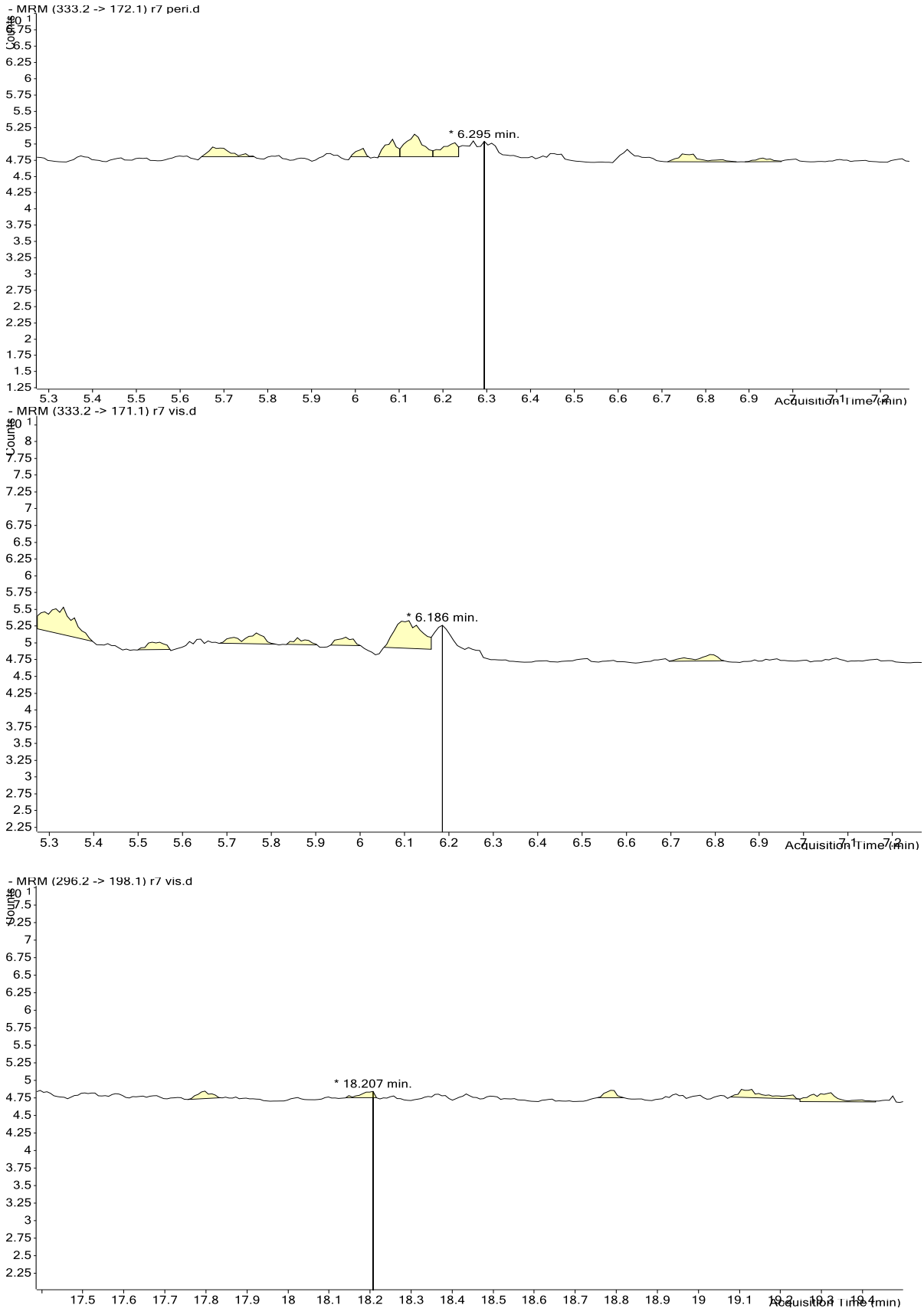
- MRM (333.2 -> 172.1) r7 peri.d
Counts
* 6.295 min.
Acquisition Time (min)
- MRM (333.2 -> 171.1) r7 vis.d
Counts
* 6.186 min.
Acquisition Time (min)
- MRM (296.2 -> 198.1) r7 vis.d
Counts
* 18.207 min.
Acquisition Time (min)

Rat 9 (IV)

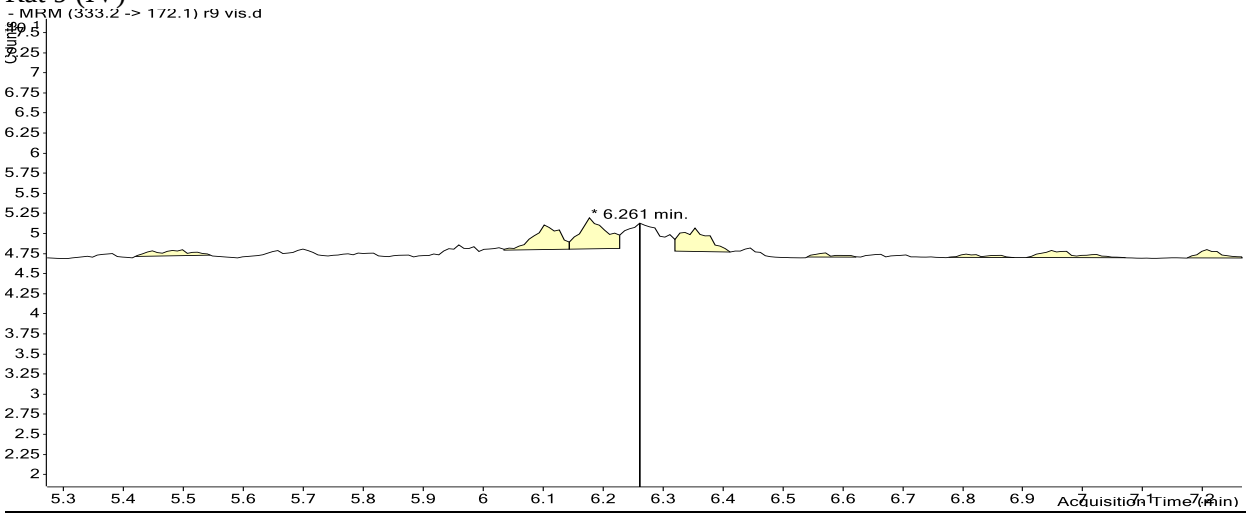
- MRM (333.2 -> 172.1) r9 vis.d
Counts
* 6.261 min.
Acquisition Time (min)

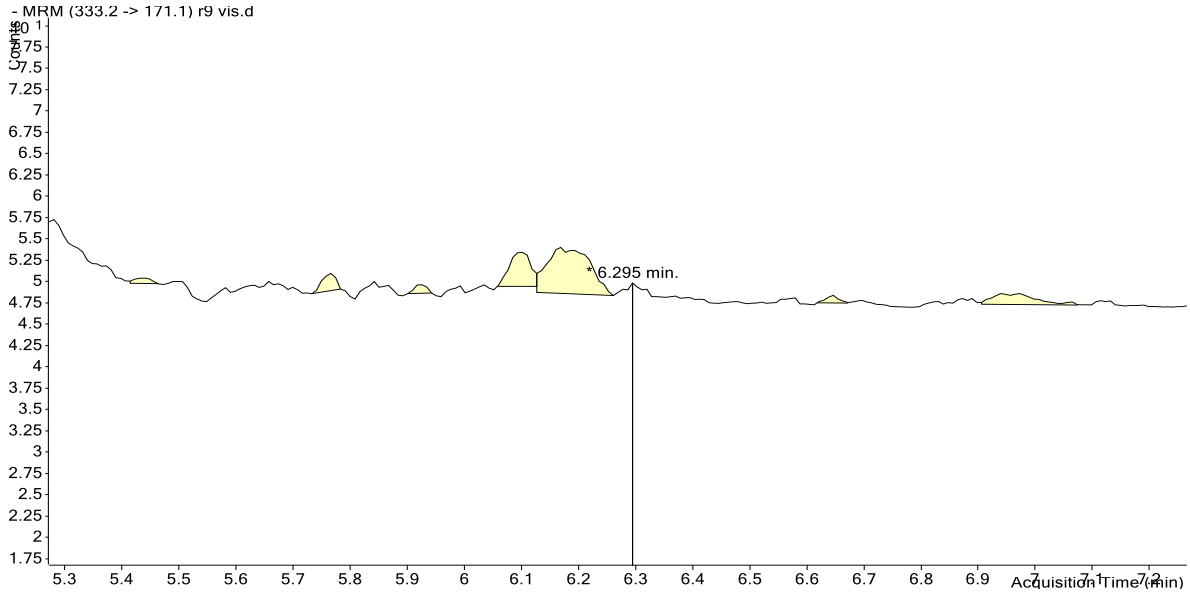
- MRM (333.2 -> 171.1) r9 vis.d
Counts
* 6.295 min.
Acquisition Time (min)

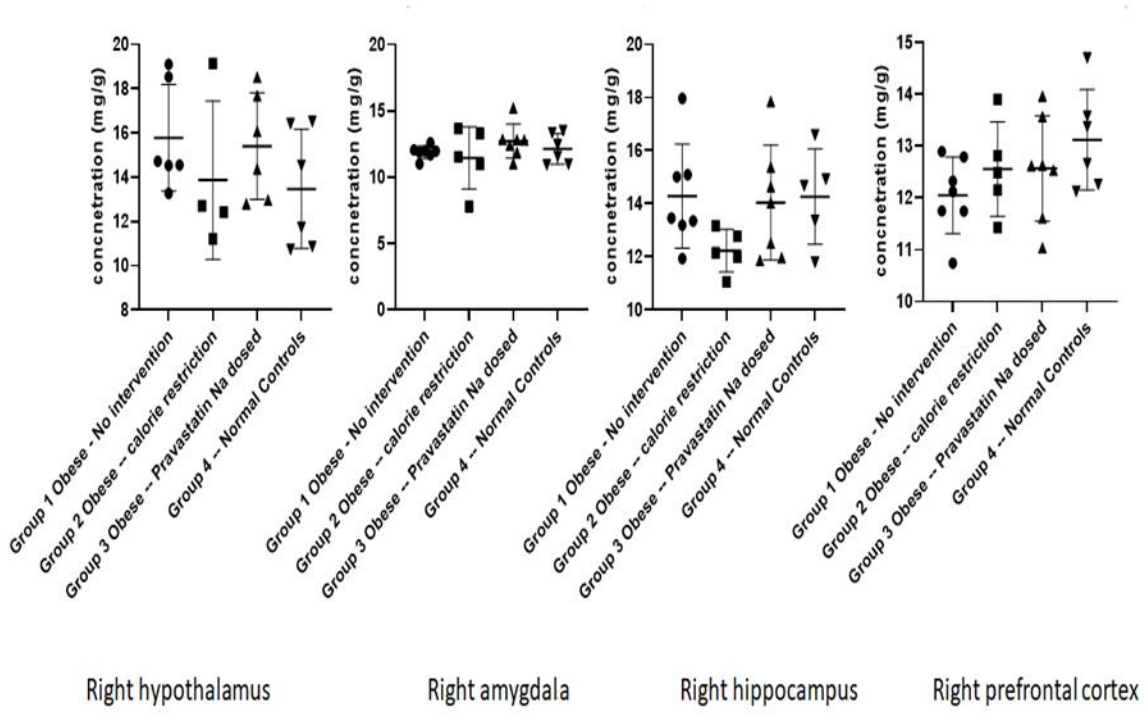

Supplemental Figure 7. Scatter plot of male offspring right hypothalamus, hippocampus, amygdala, and prefrontal cortex cholesterol concetration at 6 months. Data were expressed as mean ± SD. Data were analyzed using Kruskal-Wallis test followed by Dunn's multiple comparison post-hoc test. No significant differences were observed.

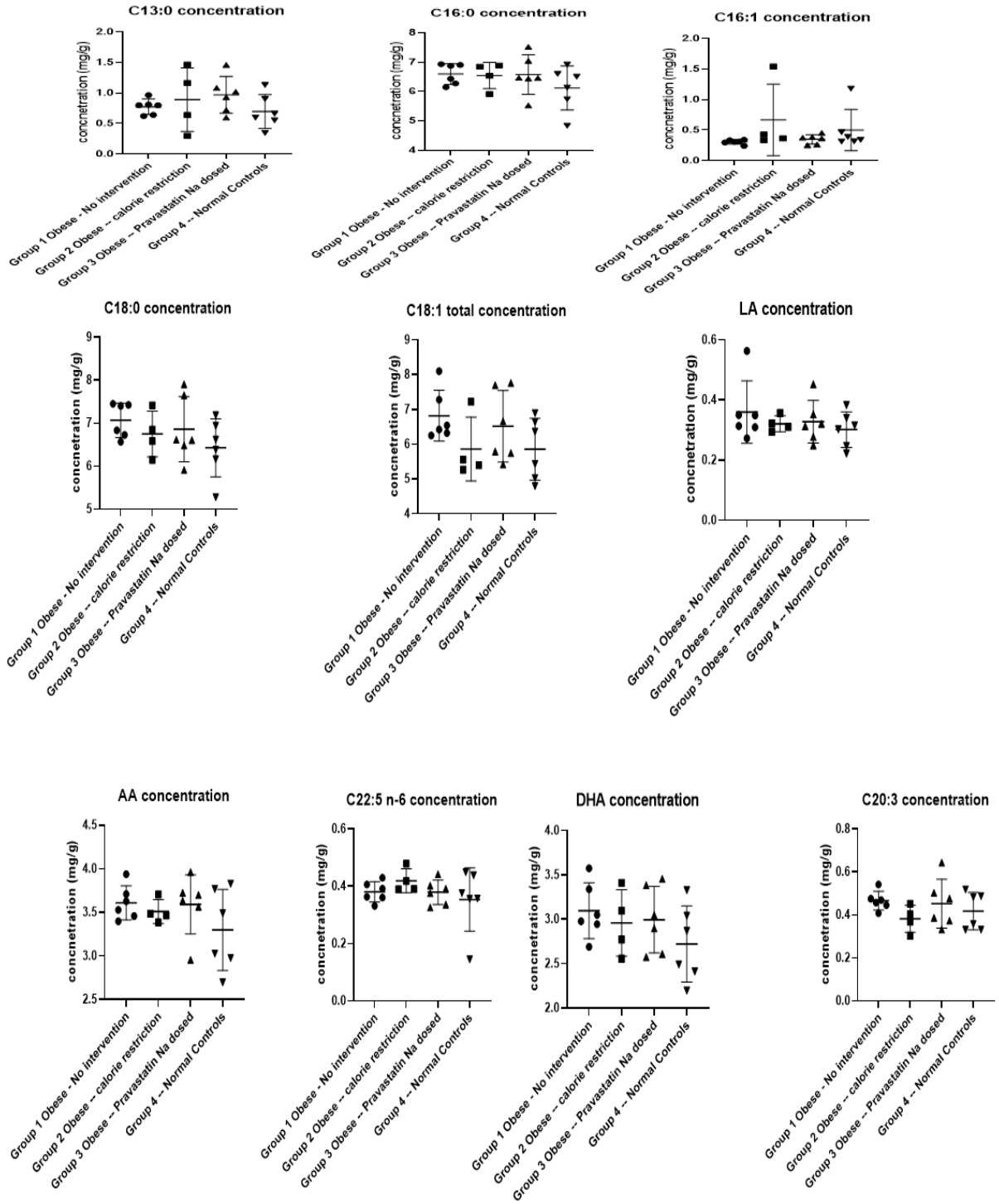

Supplemental Figure 8. Scatter plot of male offspring right hypothalamus fatty acid concentrations at 6 months. Data were expressed as mean ± SD. Data were analyzed using Kruskal-Wallis test followed by Dunn's multiple comparison post-hoc test. No significant differences were observed.

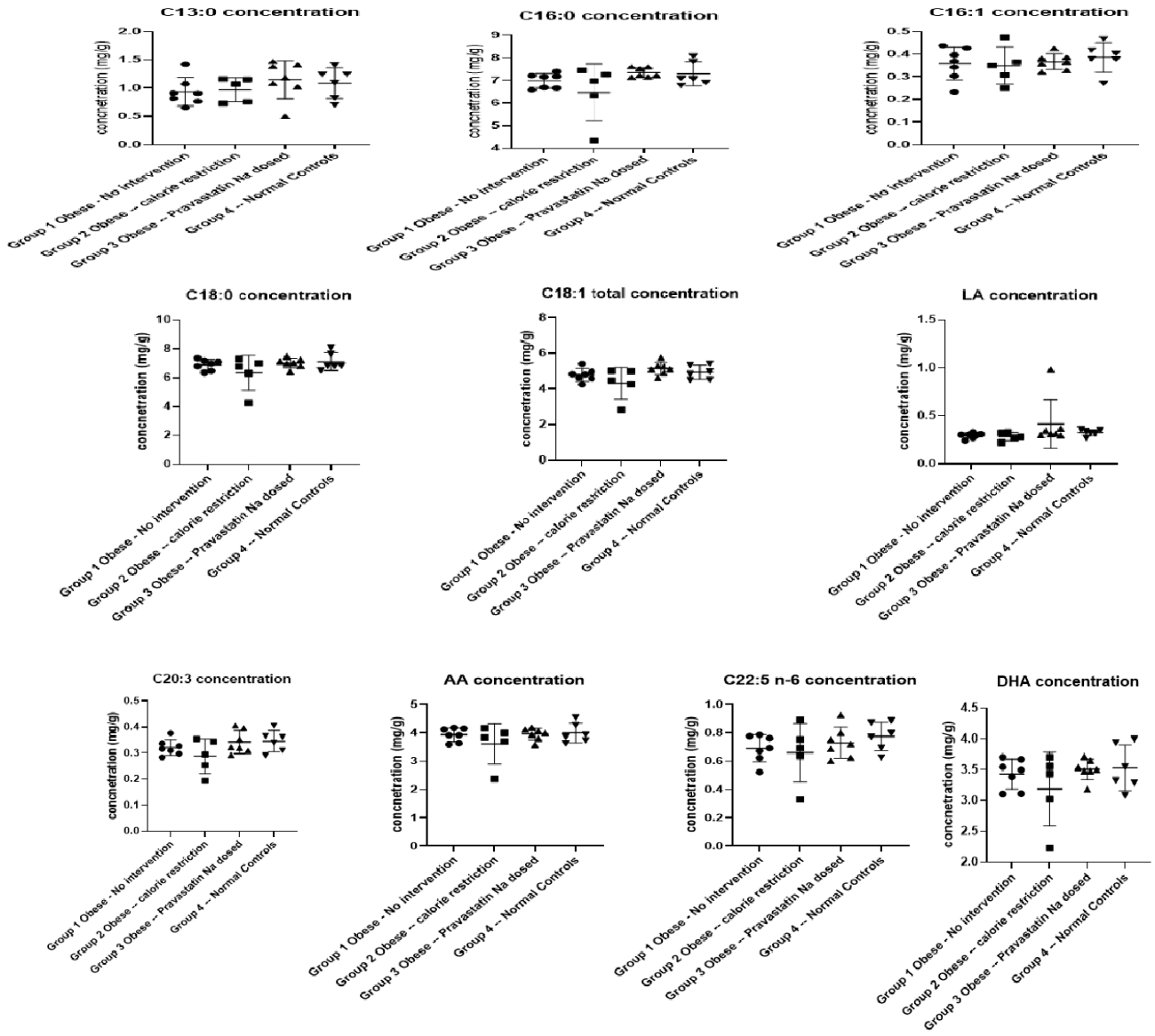

Supplemental Figure 9. Scatter plot of male offspring right amygdala fatty acid concentrations at 6 months. Data were expressed as mean ± SD. Data were analyzed using Kruskal-Wallis test followed by Dunn's multiple comparison post-hoc test. No significant differences were observed.

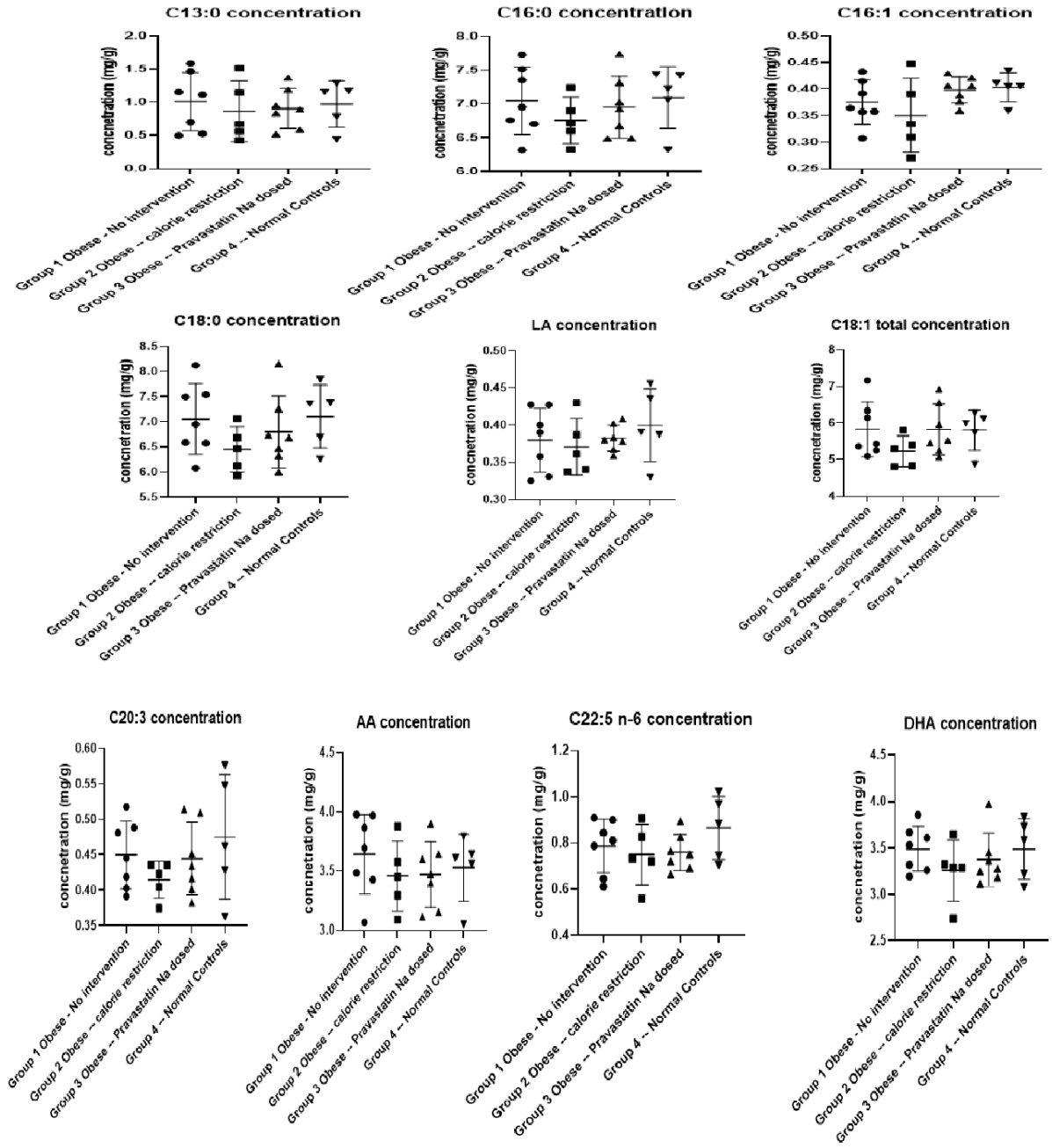

Supplemental Figure 10. Scatter plot of male offspring right hippocampus fatty acid concentrations at 6 months. Data were expressed as mean ± SD. Data were analyzed using Kruskal-Wallis test followed by Dunn's multiple comparison post-hoc test. No significant differences were observed.

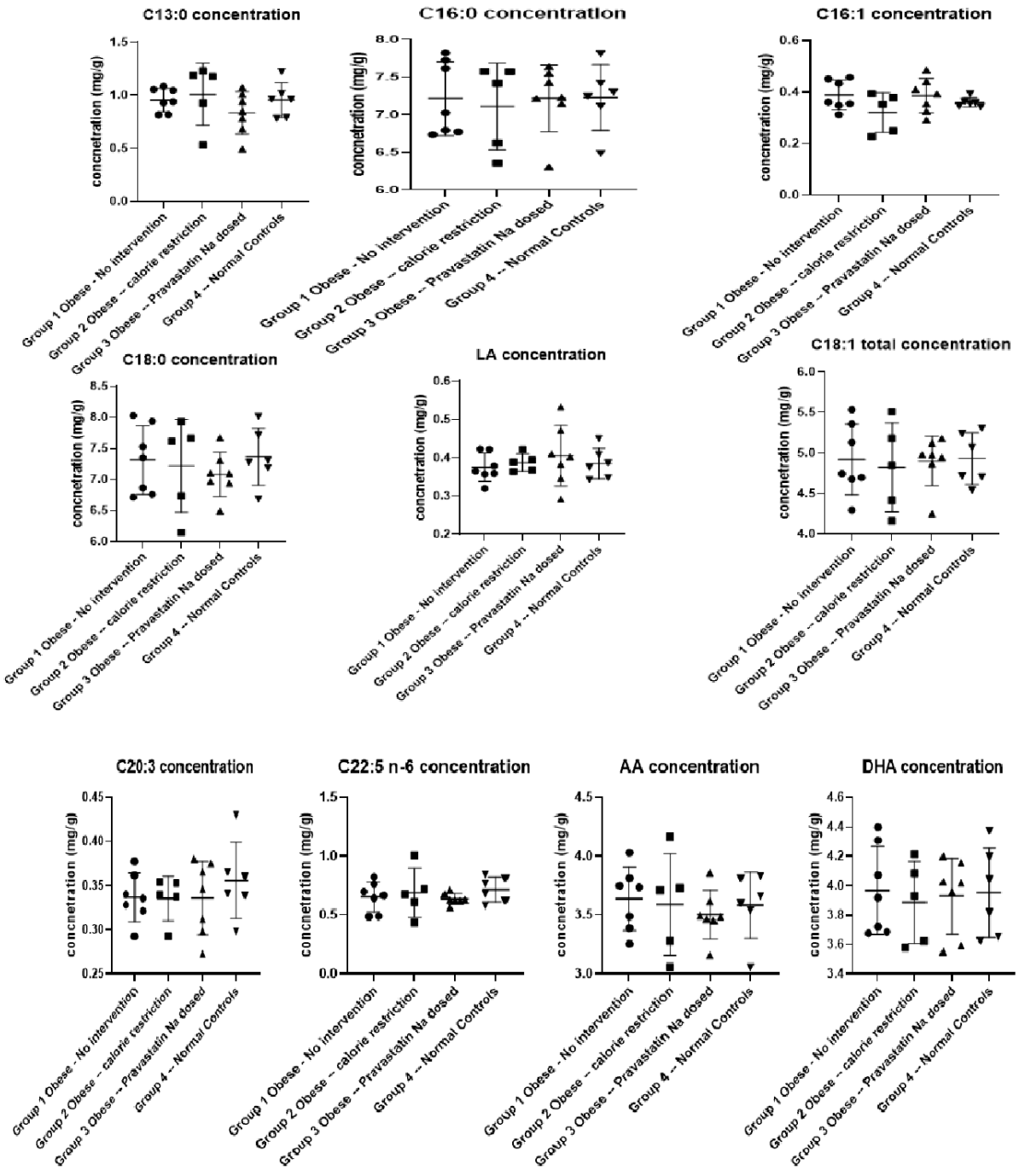

Supplemental Figure 11. Scatter plot of male offspring right prefrontal cortex fatty acid concentrations at 6 months. Data were expressed as mean ± SD. Data were analyzed using Kruskal-Wallis test followed by Dunn's multiple comparison post-hoc test. No significant differences were observed.

References:

Agrawal, K., Hassoun, L. A., Foolad, N., Pedersen, T. L., Sivamani, R. K., & Newman, J. W. (2017). Sweat lipid mediator profiling: a noninvasive approach for cutaneous research. *Journal of Lipid Research, 58*(1), 188-195. Retrieved from <Go to ISI>://WOS:000392408700015. doi:10.1194/jlr.M071738

Ailhaud, G., & Guesnet, P. (2004). Fatty acid composition of fats is an early determinant of childhood obesity: a short review and an opinion. *Obesity Reviews, 5*(1), 21-26. Retrieved from https://onlinelibrary.wiley.com/doi/abs/10.1111/j.1467-789X.2004.00121.x. doi:10.1111/j.1467-789X.2004.00121.x

Alexandre-Gouabau, M.-C., Moyon, T., Cariou, V., Antignac, J.-P., Qannari, E. M., Croyal, M., . . . Boquien, C.-Y. (2018). Breast milk lipidome is associated with early growth trajectory in preterm infants. *Nutrients, 10*(2), 164. doi:10.3390/nu10020164

Anthon, G. E., & Barrett, D. M. (2002). Kinetic parameters for the thermal inactivation of quality-related enzymes in carrots and potatoes. *J Agric Food Chem, 50*(14), 4119-4125. Retrieved from http://www.ncbi.nlm.nih.gov/pubmed/12083894.

Arnardottir, H., Orr, S. K., Dalli, J., & Serhan, C. N. (2016). Human milk proresolving mediators stimulate resolution of acute inflammation. *Mucosal Immunology, 9*(3), 757-766. Retrieved from <Go to ISI>://WOS:000375275300016

https://www.nature.com/articles/mi201599.pdf. doi:10.1038/mi.2015.99

Arnold, C., Markovic, M., Blossey, K., Wallukat, G., Fischer, R., Dechend, R., . . . Schunck, W. H. (2010). Arachidonic acid-metabolizing cytochrome P450 enzymes are targets of {omega}-3 fatty acids. *J Biol Chem, 285*(43), 32720-32733. Retrieved from https://www.ncbi.nlm.nih.gov/pubmed/20732876. doi:10.1074/jbc.M110.118406

Balas, L., Rise, P., Gandrath, D., Rovati, G., Bolego, C., Stellari, F., . . . Sala, A. (2019). Rapid Metabolization of Protectin D1 by beta-Oxidation of Its Polar Head Chain. *J Med Chem, 62*(21), 9961-9975. Retrieved from https://www.ncbi.nlm.nih.gov/pubmed/31626541. doi:10.1021/acs.jmedchem.9b01463

Ballou, L. R., Botting, R. M., Goorha, S., Zhang, J., & Vane, J. R. (2000). Nociception in cyclooxygenase isozyme-deficient mice. *Proc Natl Acad Sci U S A, 97*(18), 10272-10276. Retrieved from https://www.ncbi.nlm.nih.gov/pubmed/10954756. doi:10.1073/pnas.180319297

Bao, W., Tobias, D. K., Hu, F. B., Chavarro, J. E., & Zhang, C. L. (2016). Pre-pregnancy potato consumption and risk of gestational diabetes mellitus: prospective cohort study. *Bmj-British Medical Journal, 352*. Retrieved from <Go to ISI>://WOS:000368375500001. doi:ARTN h6898 10.1136/bmj.h6898

Bartov, I., & Bornstein, S. (1980). Susceptibility of Chicks to Nutritional Encephalopathy - Effect of Fat and Alpha-Tocopherol Content of the Breeder Diet. *Poultry Science, 59*(2), 264-267. Retrieved from <Go to ISI>://WOS:A1980JF25100011. doi:DOI 10.3382/ps.0590264

Bergan, J. G., & Draper, H. H. (1970). Absorption and metabolism of 1-14C-methyl linoleate hydroperoxide. *Lipids, 5*(12), 976-982. Retrieved from https://www.ncbi.nlm.nih.gov/pubmed/5500184. doi:10.1007/bf02533200

Bernard, J. Y., Armand, M., Garcia, C., Forhan, A., De Agostini, M., Charles, M. A., . . . Grp, E. M.-C. C. S. (2015). The association between linoleic acid levels in colostrum and child cognition at 2 and 3 y in the EDEN cohort (vol 77, pg 829, 2015). *Pediatric Research, 78*(3), 356-356. Retrieved from <Go to ISI>://WOS:000359752500018.

Bjerve, K. S., Thoresen, L., Mostad, I. L., & Alme, K. (1987). Alpha-linolenic acid deficiency in man: effect of essential fatty acids on fatty acid composition. *Adv Prostaglandin Thromboxane Leukot Res, 17B*, 862-865. Retrieved from https://www.ncbi.nlm.nih.gov/pubmed/2890285.

Blasbalg, T. L., Hibbeln, J. R., Ramsden, C. E., Majchrzak, S. F., & Rawlings, R. R. (2011a). Changes in consumption of omega-3 and omega-6 fatty acids in the United States during the 20th century.

American Journal of Clinical Nutrition, 93(5), 950-962. Retrieved from <Go to ISI>://WOS:000289770500008. doi:10.3945/ajcn.110.006643

Blasbalg, T. L., Hibbeln, J. R., Ramsden, C. E., Majchrzak, S. F., & Rawlings, R. R. (2011b). Changes in consumption of omega-3 and omega-6 fatty acids in the United States during the 20th century. *Am J Clin Nutr, 93*(5), 950-962. Retrieved from https://www.ncbi.nlm.nih.gov/pubmed/21367944. doi:10.3945/ajcn.110.006643

Bonaccio, M., Di Castelnuovo, A., Costanzo, S., De Curtis, A., Persichillo, M., Sofi, F., . . . Investigators, M.-s. S. (2021). Ultra-processed food consumption is associated with increased risk of all-cause and cardiovascular mortality in the Moli-sani Study. *American Journal of Clinical Nutrition, 113*(2), 446-455. Retrieved from <Go to ISI>://WOS:000628690200023.

Borgi, L., Rimm, E. B., Willett, W. C., & Forman, J. P. (2016). Potato intake and incidence of hypertension: results from three prospective US cohort studies. *BMJ, 353*, i2351. Retrieved from http://www.ncbi.nlm.nih.gov/pubmed/27189229. doi:10.1136/bmj.i2351

Borgstrom, B., & Olivecrona, T. (1961). Metabolism of Palmitic Acid-L-C14 in Functionally Hepatectomized Rats. *Journal of Lipid Research, 2*(3), 263-&. Retrieved from <Go to ISI>://WOS:A19615592B00002.

Bourlieu, C., Menard, O., Bouzerzour, K., Mandalari, G., Macierzanka, A., Mackie, A. R., & Dupont, D. (2014). Specificity of infant digestive conditions: some clues for developing relevant in vitro models. *Critical Reviews in Food Science and Nutrition, 54*(11), 1427-1457. Retrieved from <Go to ISI>://WOS:000335931500003

http://www.tandfonline.com/doi/pdf/10.1080/10408398.2011.640757. doi:10.1080/10408398.2011.640757

Bourlieu, C., Menard, O., De La Chevasnerie, A., Sams, L., Rousseau, F., Madec, M. N., . . . Dupont, D. (2015). The structure of infant formulas impacts their lipolysis, proteolysis and disintegration during in vitro gastric digestion. *Food Chemistry, 182*, 224-235. Retrieved from <Go to ISI>://WOS:000353731400032

http://ac.els-cdn.com/S0308814615003507/1-s2.0-S0308814615003507-main.pdf?_tid=d403ea9c-cb20-11e5-82dc-00000aab0f26&acdnat=1454577936_00cb2e2071799459ed80a1aa955a0463. doi:10.1016/j.foodchem.2015.03.001

Bourre, J. M., Francois, M., Youyou, A., Dumont, O., Piciotti, M., Pascal, G., & Durand, G. (1989). The effects of dietary alpha-linolenic acid on the composition of nerve membranes, enzymatic activity, amplitude of electrophysiological parameters, resistance to poisons and performance of learning tasks in rats. *J Nutr, 119*(12), 1880-1892. Retrieved from https://www.ncbi.nlm.nih.gov/pubmed/2576038. doi:10.1093/jn/119.12.1880

Bourre, J. M., Piciotti, M., Dumont, O., Pascal, G., & Durand, G. (1990). Dietary linoleic acid and polyunsaturated fatty acids in rat brain and other organs. Minimal requirements of linoleic acid. *Lipids, 25*(8), 465-472. Retrieved from https://www.ncbi.nlm.nih.gov/pubmed/2120529. doi:10.1007/BF02538090

Branchi, A., Fiorenza, A. M., Rovellini, A., Torri, A., Muzio, F., Macor, S., & Sommariva, D. (1999). Lowering effects of four different statins on serum triglyceride level. *European Journal of Clinical Pharmacology, 55*(7), 499-502. Retrieved from <Go to ISI>://WOS:000082848500002. doi:DOI 10.1007/s002280050663

Brans, G., Schroen, C., van der Sman, R. G. M., & Boom, R. M. (2004). Membrane fractionation of milk: state of the art and challenges. *Journal of Membrane Science, 243*(1-2), 263-272. Retrieved from <Go to ISI>://WOS:000224366100028

http://ac.els-cdn.com/S0376738804004557/1-s2.0-S0376738804004557-main.pdf?_tid=ef6b9fd6-9bc3-11e6-a80d-00000aacb35f&acdnat=1477517832_dea5b3620658bfdefa427a56b7941916. doi:10.1016/j.memsci.2004.06.029

Breder, C. D., Dewitt, D., & Kraig, R. P. (1995). Characterization of inducible cyclooxygenase in rat brain. *J Comp Neurol, 355*(2), 296-315. Retrieved from https://www.ncbi.nlm.nih.gov/pubmed/7608344. doi:10.1002/cne.903550208

Bronte-Stewart, B. (1958). The effect of dietary fats on the blood lipids and their relation to ischaemic heart disease. *Br Med Bull, 14*(3), 243-252. Retrieved from https://www.ncbi.nlm.nih.gov/pubmed/13584797. doi:10.1093/oxfordjournals.bmb.a069691

Budowski, P., Bartov, I., Dror, Y., & Frankel, E. N. (1979). Lipid oxidation products and chick nutritional encephalopathy. *Lipids, 14*(9), 768-772. Retrieved from https://www.ncbi.nlm.nih.gov/pubmed/491861. doi:10.1007/BF02533514

Burr, G. O., & Burr, M. M. (1929). A new deficiency disease produced by the rigid exclusion of fat from the diet. *Journal of Biological Chemistry, 82*(2), 345-367. Retrieved from <Go to ISI>://WOS:000187543300010.

Burr, G. O., & Burr, M. M. (1930). On the nature and role of the fatty acids essential in nutrition. *Journal of Biological Chemistry, 86*(2), 0587-0621. Retrieved from <Go to ISI>://WOS:000187544400014.

Cayer, L. G. J., Mendonca, A. M., Pauls, S. D., Winter, T., Leng, S., Taylor, C. G., . . . Aukema, H. M. (2019). Adipose tissue oxylipin profiles vary by anatomical site and are altered by dietary linoleic acid in rats. *Prostaglandins Leukot Essent Fatty Acids, 141*, 24-32. Retrieved from https://www.ncbi.nlm.nih.gov/pubmed/30661602. doi:10.1016/j.plefa.2018.12.004

Chen, C. T., Green, J. T., Orr, S. K., & Bazinet, R. P. (2008). Regulation of brain polyunsaturated fatty acid uptake and turnover. *Prostaglandins Leukot Essent Fatty Acids, 79*(3-5), 85-91. Retrieved from https://www.ncbi.nlm.nih.gov/pubmed/18938067. doi:10.1016/j.plefa.2008.09.003

Chinnici, C. M., Yao, Y., & Pratico, D. (2007). The 5-lipoxygenase enzymatic pathway in the mouse brain: young versus old. *Neurobiol Aging, 28*(9), 1457-1462. Retrieved from https://www.ncbi.nlm.nih.gov/pubmed/16930777. doi:10.1016/j.neurobiolaging.2006.06.007

Cho, Y. H., & Ziboh, V. A. (1994). Incorporation of 13-Hydroxyoctadecadienoic Acid (13-Hode) into Epidermal Ceramides and Phospholipids - Phospholipase C-Catalyzed Release of Novel 13-Hode-Containing Diacylglycerol. *Journal of Lipid Research, 35*(2), 255-262. Retrieved from <Go to ISI>://WOS:A1994MW26300008.

Choe, E., & Min, D. B. (2007). Chemistry of deep-fat frying oils. *Journal of Food Science, 72*(5), R77-R86. Retrieved from <Go to ISI>://WOS:000247780200005. doi:10.1111/j.1750-3841.2007.00352.x

Chow, S. L., & Hollander, D. (1979a). Dual, Concentration-Dependent Absorption Mechanism of Linoleic-Acid by Rat Jejunum Invitro. *Journal of Lipid Research, 20*(3), 349-356. Retrieved from <Go to ISI>://WOS:A1979GP24200005.

Chow, S. L., & Hollander, D. (1979b). Linoleic-Acid Absorption in the Unanesthetized Rat - Mechanism of Transport and Influence of Luminal Factors on Absorption. *Lipids, 14*(4), 378-385. Retrieved from <Go to ISI>://WOS:A1979GS84500009.

Costantine, M. M., Cleary, K., Hebert, M. F., Ahmed, M. S., Brown, L. M., Ren, Z. X., . . . C, E. K. S. N. I. (2016). Safety and pharmacokinetics of pravastatin used for the prevention of preeclampsia in high-risk pregnant women: a pilot randomized controlled trial. *American Journal of Obstetrics and Gynecology, 214*(6). Retrieved from <Go to ISI>://WOS:000377222800014.

Cuesta, C., Sanchezmuniz, F. J., Garridopolonio, C., Lopezvarela, S., & Arroyo, R. (1993). Thermooxidative and Hydrolytic Changes in Sunflower Oil Used in Fryings with a Fast Turnover of Fresh Oil. *Journal of the American Oil Chemists Society, 70*(11), 1069-1073. Retrieved from <Go to ISI>://WOS:A1993MF29500003. doi:Doi 10.1007/Bf02632144

Dam, H., Nielsen, G. K., Prange, I., & Sondergaard, E. (1958). Influence of linoleic and linolenic acids on symptoms of vitamin E deficiency in chicks. *Nature, 182*(4638), 802-803. Retrieved from https://www.ncbi.nlm.nih.gov/pubmed/13590117. doi:10.1038/182802a0

Dam, H., & Sondergaard, E. (1962). The encephalomalacia producing effect of arachidonic and linoleic acids. *Z Ernahrungswiss, 2*, 217-222. Retrieved from https://www.ncbi.nlm.nih.gov/pubmed/13883271. doi:10.1007/BF02020813

Damasio, H., Grabowski, T., Frank, R., Galaburda, A. M., & Damasio, A. R. (1994). The return of Phineas Gage: clues about the brain from the skull of a famous patient. *Science, 264*(5162), 1102-

1105. Retrieved from https://www.ncbi.nlm.nih.gov/pubmed/8178168. doi:10.1126/science.8178168

Delavar, M. A., Lye, M. S., Khor, G. L., Hassan, S. T., & Hanachi, P. (2009). Dietary patterns and the metabolic syndrome in middle aged women, Babol, Iran. *Asia Pac J Clin Nutr, 18*(2), 285-292. Retrieved from https://www.ncbi.nlm.nih.gov/pubmed/19713190.

DeMar, J. C., Jr., Ma, K., Bell, J. M., & Rapoport, S. I. (2004). Half-lives of docosahexaenoic acid in rat brain phospholipids are prolonged by 15 weeks of nutritional deprivation of n-3 polyunsaturated fatty acids. *J Neurochem, 91*(5), 1125-1137. Retrieved from https://www.ncbi.nlm.nih.gov/pubmed/15569256. doi:10.1111/j.1471-4159.2004.02789.x

Demar, J. C., Jr., Ma, K., Chang, L., Bell, J. M., & Rapoport, S. I. (2005). alpha-Linolenic acid does not contribute appreciably to docosahexaenoic acid within brain phospholipids of adult rats fed a diet enriched in docosahexaenoic acid. *J Neurochem, 94*(4), 1063-1076. Retrieved from https://www.ncbi.nlm.nih.gov/pubmed/16092947. doi:10.1111/j.1471-4159.2005.03258.x

DeMar, J. C., Lee, H. J., Ma, K. Z., Chang, L., Bell, J. M., Rapoport, S. I., & Bazinet, R. P. (2006). Brain elongation of linoleic acid is a negligible source of the arachidonate in brain phospholipids of adult rats. *Biochimica Et Biophysica Acta-Molecular and Cell Biology of Lipids, 1761*(9), 1050-1059. Retrieved from <Go to ISI>://WOS:000241273700008. doi:10.1016/j.bbalip.2006.06.006

DeYoung, C. G., Hirsh, J. B., Shane, M. S., Papademetris, X., Rajeevan, N., & Gray, J. R. (2010). Testing predictions from personality neuroscience. Brain structure and the big five. *Psychol Sci, 21*(6), 820-828. Retrieved from https://www.ncbi.nlm.nih.gov/pubmed/20435951. doi:10.1177/0956797610370159

Dias, F. F. G., Augusto-Obara, T. R., Hennebelle, M., Chantieng, S., Ozturk, G., Taha, A. Y., . . . Leite Nobrega de Moura Bell, J. M. (2020). Effects of industrial heat treatments on bovine milk oxylipins and conventional markers of lipid oxidation. *Prostaglandins Leukot Essent Fatty Acids, 152*, 102040. Retrieved from https://www.ncbi.nlm.nih.gov/pubmed/31809946. doi:10.1016/j.plefa.2019.102040

Dietschy, J. M., & Wilson, J. D. (1968). Cholesterol Synthesis in Squirrel Monkey - Relative Rates of Synthesis in Various Tissues and Mechanisms of Control. *Journal of Clinical Investigation, 47*(1), 166-&. Retrieved from <Go to ISI>://WOS:A1968A456100016. doi:Doi 10.1172/Jci105706

Domenichiello, A. F., Kitson, A. P., Chen, C. T., Trepanier, M. O., Stavro, P. M., & Bazinet, R. P. (2016). The effect of linoleic acid on the whole body synthesis rates of polyunsaturated fatty acids from alpha-linolenic acid and linoleic acid in free-living rats. *Journal of Nutritional Biochemistry, 30*, 167-176. Retrieved from <Go to ISI>://WOS:000374347300018. doi:10.1016/j.jnutbio.2015.11.016

Dutton, H. J. (1981). History of the Development of Soy Oil for Edible Uses. *Journal of the American Oil Chemists Society, 58*(3), 234-236. Retrieved from <Go to ISI>://WOS:A1981LJ47400035. doi:Doi 10.1007/Bf02582347

Ekici, F., Gurol, G., & Ates, N. (2014). Effects of linoleic acid on generalized convulsive and nonconvulsive epileptic seizures. *Turk J Med Sci, 44*(4), 535-539. Retrieved from https://www.ncbi.nlm.nih.gov/pubmed/25551918. doi:10.3906/sag-1305-13

Emami, S., Zhang, Z., & Taha, A. Y. (2020). Quantitation of Oxylipins in Fish and Algae Oil Supplements Using Optimized Hydrolysis Procedures and Ultra-High Performance Liquid Chromatography Coupled to Tandem Mass-Spectrometry. *J Agric Food Chem, 68*(35), 9329-9344. Retrieved from https://www.ncbi.nlm.nih.gov/pubmed/32687334. doi:10.1021/acs.jafc.0c02461

Engels, F., Willems, H., & Nijkamp, F. P. (1986). Cyclooxygenase-catalyzed formation of 9-hydroxylinoleic acid by guinea pig alveolar macrophages under non-stimulated conditions. *FEBS Lett, 209*(2), 249-253. Retrieved from https://www.ncbi.nlm.nih.gov/pubmed/3098580. doi:10.1016/0014-5793(86)81121-8

Fang, X., Kaduce, T. L., & Spector, A. A. (1999). 13-(S)-hydroxyoctadecadienoic acid (13-HODE) incorporation and conversion to novel products by endothelial cells. *J Lipid Res*, *40*(4), 699-707. Retrieved from https://www.ncbi.nlm.nih.gov/pubmed/10191294.

Feltenmark, S., Gautam, N., Brunnstrom, A., Griffiths, W., Backman, L., Edenius, C., . . . Claesson, H. E. (2008). Eoxins are proinflammatory arachidonic acid metabolites produced via the 15-lipoxygenase-1 pathway in human eosinophils and mast cells. *Proc Natl Acad Sci U S A*, *105*(2), 680-685. Retrieved from https://www.ncbi.nlm.nih.gov/pubmed/18184802. doi:10.1073/pnas.0710127105

Ferdouse, A., Leng, S., Winter, T., & Aukema, H. M. (2019). The Brain Oxylipin Profile Is Resistant to Modulation by Dietary n-6 and n-3 Polyunsaturated Fatty Acids in Male and Female Rats. *Lipids*, *54*(1), 67-80. Retrieved from <Go to ISI>://WOS:000458961300008. doi:10.1002/lipd.12122

Fife, W. K., Liu, S., & Zeldin, M. (1993). Selective Transesterification Catalyzed by a Synthetic, Linear, Oligomeric 4-(Dialkylamino) Pyridine. *Abstracts of Papers of the American Chemical Society*, *206*, 334-Orgn. Retrieved from <Go to ISI>://WOS:A1993LP32200508.

Flickinger, B., Sun, S., & Empie, M. (2011). N-6/N-3 ratio in the diet of Americans using NHANES 1999-2006 datasets. *Faseb Journal*, *25*. Retrieved from <Go to ISI>://WOS:000310708405071.

Flores-Alvarez Mdel, C., Molina-Hernandez, E. F., Hernandez-Raya, J. C., & Sosa-Morales, M. E. (2012). The effect of food type (fish nuggets or French fries) on oil blend degradation during repeated frying. *J Food Sci*, *77*(11), C1136-1143. Retrieved from http://www.ncbi.nlm.nih.gov/pubmed/23107039. doi:10.1111/j.1750-3841.2012.02930.x

Folch, J., Lees, M., & Sloane Stanley, G. H. (1957). A simple method for the isolation and purification of total lipides from animal tissues. *J Biol Chem*, *226*(1), 497-509. Retrieved from https://www.ncbi.nlm.nih.gov/pubmed/13428781.

Franklin, L. M., Chapman, D. M., King, E. S., Mau, M., Huang, G., & Mitchell, A. E. (2017). Chemical and Sensory Characterization of Oxidative Changes in Roasted Almonds Undergoing Accelerated Shelf Life. *J Agric Food Chem*, *65*(12), 2549-2563. Retrieved from https://www.ncbi.nlm.nih.gov/pubmed/28285524. doi:10.1021/acs.jafc.6b05357

Galliard, T. (1973). Lipids of potato tubers. I. Lipid and fatty acid composition of tubers from different varieties of potato. *J Sci Food Agric*, *24*(5), 617-622. Retrieved from http://www.ncbi.nlm.nih.gov/pubmed/4720550.

Gan, J., Robinson, R. C., Wang, J., Krishnakumar, N., Manning, C. J., Lor, Y., . . . German, J. B. (2019). Peptidomic profiling of human milk with LC–MS/MS reveals pH-specific proteolysis of milk proteins. *Food Chemistry*, *274*, 766-774. Retrieved from http://www.sciencedirect.com/science/article/pii/S0308814618316224 https://ac.els-cdn.com/S0308814618316224/1-s2.0-S0308814618316224-main.pdf?_tid=a03a3697-bb5a-488b-ae11-fe44983c8605&acdnat=1538373557_852f7356857ba92061875eb7bb03d73d. doi:10.1016/j.foodchem.2018.09.051

Gan, J., Siegel, J. B., & German, J. B. (2019). Molecular annotation of food – towards personalized diet and precision health. *Trends in Food Science & Technology*, *91*, 675-680. Retrieved from http://www.sciencedirect.com/science/article/pii/S0924224419301840. doi:10.1016/j.tifs.2019.07.016

Gan, J., Zheng, J., Krishnakumar, N., Goonatilleke, E., Lebrilla, C. B., Barile, D., & German, J. B. (2019). Selective proteolysis of α-lactalbumin by endogenous enzymes of human milk at acidic pH. *Molecular Nutrition & Food Research*, *63*(18), 1900259. Retrieved from https://onlinelibrary.wiley.com/doi/abs/10.1002/mnfr.201900259. doi:10.1002/mnfr.201900259

Gan, J. A., Zhang, Z. C., Kurudimov, K., German, J. B., & Taha, A. Y. (2020). Distribution of Free and Esterified Oxylipins in Cream, Cell, and Skim Fractions of Human Milk. *Lipids*. Retrieved from <Go to ISI>://WOS:000552892400001. doi:10.1002/lipd.12268

Gan, S. N., & Hamid, Z. A. (1997). Partial conversion of epoxide groups to diols in epoxidized natural rubber. *Polymer*, *38*(8), 1953-1956. Retrieved from <Go to ISI>://WOS:A1997WP71700020. doi:Doi 10.1016/S0032-3861(96)00710-0

Gilroy, D. W., Edin, M. L., De Maeyer, R. P., Bystrom, J., Newson, J., Lih, F. B., . . . Bishop-Bailey, D. (2016). CYP450-derived oxylipins mediate inflammatory resolution. *Proc Natl Acad Sci U S A, 113*(23), E3240-3249. Retrieved from https://www.ncbi.nlm.nih.gov/pubmed/27226306. doi:10.1073/pnas.1521453113

Glavind, J., & Sylven, C. (1970). Intestinal absorption and lymphatic transport of methyl linoleate hydroperoxide and hydroxyoctadecadienoate in the rat. *Acta Chem Scand, 24*(10), 3723-3728. Retrieved from https://www.ncbi.nlm.nih.gov/pubmed/5501733.

Gleissman, H., Yang, R., Martinod, K., Lindskog, M., Serhan, C. N., Johnsen, J. I., & Kogner, P. (2010). Docosahexaenoic acid metabolome in neural tumors: identification of cytotoxic intermediates. *Faseb Journal, 24*(3), 906-915. Retrieved from https://www.ncbi.nlm.nih.gov/pubmed/19890019. doi:10.1096/fj.09-137919

Gosset, V., Harmel, N., Gobel, C., Francis, F., Haubruge, E., Wathelet, J. P., . . . Fauconnier, M. L. (2009). Attacks by a piercing-sucking insect (Myzus persicae Sultzer) or a chewing insect (Leptinotarsa decemlineata Say) on potato plants (Solanum tuberosum L.) induce differential changes in volatile compound release and oxylipin synthesis. *Journal of Experimental Botany, 60*(4), 1231-1240. Retrieved from <Go to ISI>://WOS:000264390600017.

Grapov, D., Adams, S. H., Pedersen, T. L., Garvey, W. T., & Newman, J. W. (2012). Type 2 Diabetes Associated Changes in the Plasma Non-Esterified Fatty Acids, Oxylipins and Endocannabinoids. *Plos One, 7*(11). Retrieved from <Go to ISI>://WOS:000312269500039. doi:ARTN e48852
10.1371/journal.pone.0048852

Grapov, D., Fiehn, O., Campbell, C., Chandler, C. J., Burnett, D. J., Souza, E. C., . . . Adams, S. H. (2020). Impact of a weight loss and fitness intervention on exercise-associated plasma oxylipin patterns in obese, insulin-resistant, sedentary women. *Physiol Rep, 8*(17), e14547. Retrieved from https://www.ncbi.nlm.nih.gov/pubmed/32869956. doi:10.14814/phy2.14547

Graveland, A. (1973). Enzymatic oxidation of linolenic acid in aqueous wheat flour suspensions. *Lipids, 8*(11), 606-611. Retrieved from https://www.ncbi.nlm.nih.gov/pubmed/4201716. doi:10.1007/BF02533142

Halarnkar, P. P., Wixtrom, R. N., Silva, M. H., & Hammock, B. D. (1989). Catabolism of epoxy fatty esters by the purified epoxide hydrolase from mouse and human liver. *Arch Biochem Biophys, 272*(1), 226-236. Retrieved from https://www.ncbi.nlm.nih.gov/pubmed/2735763. doi:10.1016/0003-9861(89)90214-2

Hamberg, M., & Samuelsson, B. (1971). On the metabolism of prostaglandins E 1 and E 2 in man. *J Biol Chem, 246*(22), 6713-6721. Retrieved from https://www.ncbi.nlm.nih.gov/pubmed/5126221.

Hamberg, M., Sanz, A., & Castresana, C. (1999). alpha-oxidation of fatty acids in higher plants. Identification of a pathogen-inducible oxygenase (piox) as an alpha-dioxygenase and biosynthesis of 2-hydroperoxylinolenic acid. *J Biol Chem, 274*(35), 24503-24513. Retrieved from https://www.ncbi.nlm.nih.gov/pubmed/10455113. doi:10.1074/jbc.274.35.24503

Hansen, A. E., Haggard, M. E., Boelsche, A. N., Adam, D. J., & Wiese, H. F. (1958). Essential fatty acids in infant nutrition. III. Clinical manifestations of linoleic acid deficiency. *J Nutr, 66*(4), 565-576. Retrieved from https://www.ncbi.nlm.nih.gov/pubmed/13621281. doi:10.1093/jn/66.4.565

Harding, J. E., Cormack, B. E., Alexander, T., Alsweiler, J. M., & Bloomfield, F. H. (2017). Advances in nutrition of the newborn infant. *The Lancet, 389*(10079), 1660-1668. Retrieved from <Go to ISI>://WOS:000399560000033

https://ac.els-cdn.com/S0140673617305524/1-s2.0-S0140673617305524-main.pdf?_tid=d49963c3-a9b3-4b00-9f3b-8c8efda39650&acdnat=1537933707_71c0714f003af91ab6e493052f56ae13. doi:10.1016/s0140-6736(17)30552-4

Harizi, H., Juzan, M., Pitard, V., Moreau, J. F., & Gualde, N. (2002). Cyclooxygenase-2-issued prostaglandin e(2) enhances the production of endogenous IL-10, which down-regulates dendritic cell functions. *J Immunol, 168*(5), 2255-2263. Retrieved from https://www.ncbi.nlm.nih.gov/pubmed/11859113. doi:10.4049/jimmunol.168.5.2255

Hasegawa, Y., Otoki, Y., McClorry, S., Coates, L. C., Lombardi, R. L., Taha, A. Y., & Slupsky, C. M. (2020). Optimization of a Method for the Simultaneous Extraction of Polar and Non-Polar Oxylipin Metabolites, DNA, RNA, Small RNA, and Protein from a Single Small Tissue Sample. *Methods Protoc, 3*(3). Retrieved from https://www.ncbi.nlm.nih.gov/pubmed/32859006. doi:10.3390/mps3030061

Hashimoto, M., Katakura, M., Tanabe, Y., Al Mamun, A., Inoue, T., Hossain, S., . . . Shido, O. (2015). n-3 fatty acids effectively improve the reference memory-related learning ability associated with increased brain docosahexaenoic acid-derived docosanoids in aged rats. *Biochim Biophys Acta, 1851*(2), 203-209. Retrieved from https://www.ncbi.nlm.nih.gov/pubmed/25450447. doi:10.1016/j.bbalip.2014.10.009

Hennebelle, M., Metherel, A. H., Kitson, A. P., Otoki, Y., Yang, J., Lee, K. S. S., . . . Taha, A. Y. (2019). Brain oxylipin concentrations following hypercapnia/ischemia: effects of brain dissection and dissection time. *J Lipid Res, 60*(3), 671-682. Retrieved from https://www.ncbi.nlm.nih.gov/pubmed/30463986. doi:10.1194/jlr.D084228

Hennebelle, M., Morgan, R. K., Sethi, S., Zhang, Z., Chen, H., Grodzki, A. C., . . . Taha, A. Y. (2019). Linoleic acid-derived metabolites constitute the majority of oxylipins in the rat pup brain and stimulate axonal growth in primary rat cortical neuron-glia co-cultures in a sex-dependent manner. *J Neurochem*. Retrieved from https://www.ncbi.nlm.nih.gov/pubmed/31283837. doi:10.1111/jnc.14818

Hennebelle, M., Morgan, R. K., Sethi, S., Zhang, Z., Chen, H., Grodzki, A. C., . . . Taha, A. Y. (2019). Linoleic acid-derived metabolites constitute the majority of oxylipins in the rat pup brain and stimulate axonal growth in primary rat cortical neuron-glia co-cultures in a sex-dependent manner. *Journal of Neurochemistry, 152*(2), 195-207. Retrieved from https://onlinelibrary.wiley.com/doi/abs/10.1111/jnc.14818. doi:10.1111/jnc.14818

Hennebelle, M., Morgan, R. K., Sethi, S., Zhang, Z., Chen, H., Grodzki, A. C., . . . Taha, A. Y. (2020). Linoleic acid-derived metabolites constitute the majority of oxylipins in the rat pup brain and stimulate axonal growth in primary rat cortical neuron-glia co-cultures in a sex-dependent manner. *J Neurochem, 152*(2), 195-207. Retrieved from https://www.ncbi.nlm.nih.gov/pubmed/31283837. doi:10.1111/jnc.14818

Hennebelle, M., Zhang, Z., Metherel, A. H., Kitson, A. P., Otoki, Y., Richardson, C. E., . . . Taha, A. Y. (2017). Linoleic acid participates in the response to ischemic brain injury through oxidized metabolites that regulate neurotransmission. *Sci Rep, 7*(1), 4342. Retrieved from https://www.ncbi.nlm.nih.gov/pubmed/28659576. doi:10.1038/s41598-017-02914-7

Hilditch, T. P., & Meara, M. L. (1944). Human-milk fat: 1. Component fatty acids. *Biochemical Journal, 38*(1), 29-34. Retrieved from https://www.ncbi.nlm.nih.gov/pubmed/16747743. doi:10.1042/bj0380029

Holman, R. T., & Johnson, S. (1981). Profiles of Poly-Unsaturated Fatty-Acids in Human-Disease. *Journal of the American Oil Chemists Society, 58*(7), A587-A587. Retrieved from <Go to ISI>://WOS:A1981LZ25400134.

Howton, D. R., & Mead, J. F. (1960). Metabolism of essential fatty acids. X. Conversion ox 8, 11, 14-eicosatrienoic acid to arachidonic acid in the rat. *J Biol Chem, 235*, 3385-3386. Retrieved from https://www.ncbi.nlm.nih.gov/pubmed/13716294.

Huang, L. S., Yu, X. D., Keim, S., Li, L., Zhang, L., & Zhang, J. (2014). Maternal prepregnancy obesity and child neurodevelopment in the Collaborative Perinatal Project. *International Journal of Epidemiology, 43*(3), 783-792. Retrieved from <Go to ISI>://WOS:000338127000019.

Hungund, B. L., Zheng, Z., & Barkai, A. I. (1995). Turnover of ethyl-linoleate in rat plasma and its distribution in various organs. *Alcohol Clin Exp Res, 19*(2), 374-377. Retrieved from https://www.ncbi.nlm.nih.gov/pubmed/7625572. doi:10.1111/j.1530-0277.1995.tb01518.x

Ichihara, K., & Fukubayashi, Y. (2010). Preparation of fatty acid methyl esters for gas-liquid chromatography. *J Lipid Res, 51*(3), 635-640. Retrieved from https://www.ncbi.nlm.nih.gov/pubmed/19759389. doi:10.1194/jlr.D001065

Igarashi, M., Chang, L., Ma, K., & Rapoport, S. I. (2013). Kinetics of eicosapentaenoic acid in brain, heart and liver of conscious rats fed a high n-3 PUFA containing diet. *Prostaglandins Leukot Essent Fatty Acids, 89*(6), 403-412. Retrieved from https://www.ncbi.nlm.nih.gov/pubmed/24209500. doi:10.1016/j.plefa.2013.09.004

Igarashi, M., DeMar, J. C., Jr., Ma, K., Chang, L., Bell, J. M., & Rapoport, S. I. (2007). Docosahexaenoic acid synthesis from alpha-linolenic acid by rat brain is unaffected by dietary n-3 PUFA deprivation. *J Lipid Res, 48*(5), 1150-1158. Retrieved from https://www.ncbi.nlm.nih.gov/pubmed/17277380. doi:10.1194/jlr.M600549-JLR200

Igarashi, M., Kim, H. W., Chang, L., Ma, K., & Rapoport, S. I. (2012). Dietary n-6 polyunsaturated fatty acid deprivation increases docosahexaenoic acid metabolism in rat brain. *J Neurochem, 120*(6), 985-997. Retrieved from https://www.ncbi.nlm.nih.gov/pubmed/22117540. doi:10.1111/j.1471-4159.2011.07597.x

Jahren, A. H., & Schubert, B. A. (2010). Corn content of French fry oil from national chain vs. small business restaurants. *Proc Natl Acad Sci U S A, 107*(5), 2099-2101. Retrieved from http://www.ncbi.nlm.nih.gov/pubmed/20133856. doi:10.1073/pnas.0914437107

Jardi, C., Aparicio, E., Bedmar, C., Aranda, N., Abajo, S., March, G., . . . Grp, E. S. (2019). Food Consumption during Pregnancy and Post-Partum. ECLIPSES Study. *Nutrients, 11*(10). Retrieved from <Go to ISI>://WOS:000498227300188. doi:ARTN 2447
10.3390/nu11102447

Jenness, R. (1979). The composition of human milk. *Semin Perinatol, 3*(3), 225-239.

Jiao, J. J. (2020). Cooking Oil Consumption is Positively Associated with Risk of Type 2 Diabetes in a Chinese Nationwide Cohort Study (vol 150, pg 1799, 2020). *Journal of Nutrition, 150*(9), 2490-2490. Retrieved from <Go to ISI>://WOS:000568434200033.

Kalogeropoulos, N., Salta, F. N., Chiou, A., & Andrikopoulos, N. K. (2007). Formation and distribution of oxidized fatty acids during deep- and pan-frying of potatoes. *European Journal of Lipid Science and Technology, 109*(11), 1111-1123. Retrieved from <Go to ISI>://WOS:000251232200010. doi:10.1002/ejlt.200700007

Kamata, Y., Shiraga, H., Tai, A., Kawamoto, Y., & Gohda, E. (2007). Induction of neurite outgrowth in PC12 cells by the medium-chain fatty acid octanoic acid. *Neuroscience, 146*(3), 1073-1081. Retrieved from https://www.ncbi.nlm.nih.gov/pubmed/17434686. doi:10.1016/j.neuroscience.2007.03.001

Kanazawa, K., & Ashida, H. (1998). Dietary hydroperoxides of linoleic acid decompose to aldehydes in stomach before being absorbed into the body. *Biochimica Et Biophysica Acta, 1393*(2-3), 349-361. Retrieved from https://www.ncbi.nlm.nih.gov/pubmed/9748650. doi:10.1016/s0005-2760(98)00089-7

Kang, M., Lee, A., Yoo, H. J., Kim, M., Kim, M., Shin, D. Y., & Lee, J. H. (2017). Association between increased visceral fat area and alterations in plasma fatty acid profile in overweight subjects: a cross-sectional study. *Lipids Health Dis, 16*(1), 248. Retrieved from https://www.ncbi.nlm.nih.gov/pubmed/29258511. doi:10.1186/s12944-017-0642-z

Kanter, J. R., Heasley, L. E., & Brunton, L. L. (1985). Enzymatic Formation of Prostaglandin A1-Glutathione (Pga1-Gsh), the Putative Inhibitor of Cyclic-Amp Export by Avian Red-Cells. *Federation Proceedings, 44*(3), 490-490. Retrieved from <Go to ISI>://WOS:A1985ADF6100498.

Kato, S., Shimizu, N., Hanzawa, Y., Otoki, Y., Ito, J., Kimura, F., . . . Nakagawa, K. (2018). Determination of triacylglycerol oxidation mechanisms in canola oil using liquid chromatography-tandem mass spectrometry. *NPJ Sci Food, 2*, 1. Retrieved from https://www.ncbi.nlm.nih.gov/pubmed/31304251. doi:10.1038/s41538-017-0009-x

Keijbets, M. (2001). The manufacture of pre-fried potato products en Frying: Improving quality. *Woodhead Publishing Ltd., Cambridge, UK*.

Keys, A., Anderson, J. T., & Grande, F. (1957). Prediction of serum-cholesterol responses of man to changes in fats in the diet. *Lancet, 273*(7003), 959-966. Retrieved from https://www.ncbi.nlm.nih.gov/pubmed/13482259. doi:10.1016/s0140-6736(57)91998-0

Kim, H., Kim, H., Lee, E., Kim, Y., Ha, E. H., & Chang, N. (2017). Association between maternal intake of n-6 to n-3 fatty acid ratio during pregnancy and infant neurodevelopment at 6 months of age: results of the MOCEH cohort study. *Nutrition Journal, 16*. Retrieved from <Go to ISI>://WOS:000399461400001. doi:ARTN 23
10.1186/s12937-017-0242-9

Klenk, E., & Mohrhauer, H. (1960). [Studies on the metabolism of polyenoic fatty acids in the rat]. *Hoppe Seylers Z Physiol Chem, 320*, 218-232. Retrieved from https://www.ncbi.nlm.nih.gov/pubmed/13756764. doi:10.1515/bchm2.1960.320.1.218

Kokatnur, M. G., Okui, S., Kummerow, F. A., & Scott, H. M. (1960). Effect of long chain keto acids on encephalomalacia in chicks. *Proc Soc Exp Biol Med, 104*, 170-171. Retrieved from https://www.ncbi.nlm.nih.gov/pubmed/14410615. doi:10.3181/00379727-104-25768

Kozak, W., Aronoff, D. M., Boutaud, O., & Kozak, A. (2003). 11,12-epoxyeicosatrienoic acid attenuates synthesis of prostaglandin E2 in rat monocytes stimulated with lipopolysaccharide. *Exp Biol Med (Maywood), 228*(7), 786-794. Retrieved from https://www.ncbi.nlm.nih.gov/pubmed/12876297. doi:10.1177/15353702-0322807-03

Krakowiak, P., Walker, C. K., Bremer, A. A., Baker, A. S., Ozonoff, S., Hansen, R. L., & Hertz-Picciotto, I. (2012). Maternal metabolic conditions and risk for autism and other neurodevelopmental disorders. *Pediatrics, 129*(5), e1121-1128. Retrieved from https://www.ncbi.nlm.nih.gov/pubmed/22492772. doi:10.1542/peds.2011-2583

Kurochkin, I., Khrameeva, E., Tkachev, A., Stepanova, V., Vanyushkina, A., Stekolshchikova, E., . . . Khaitovich, P. (2019). Metabolome signature of autism in the human prefrontal cortex. *Commun Biol, 2*, 234. Retrieved from https://www.ncbi.nlm.nih.gov/pubmed/31263778. doi:10.1038/s42003-019-0485-4

Lahvic, J. L., Ammerman, M., Li, P., Blair, M. C., Stillman, E. R., Fast, E. M., . . . Zon, L. I. (2018). Specific oxylipins enhance vertebrate hematopoiesis via the receptor GPR132. *Proc Natl Acad Sci U S A, 115*(37), 9252-9257. Retrieved from https://www.ncbi.nlm.nih.gov/pubmed/30139917. doi:10.1073/pnas.1806077115

Lammert, C. R., & Lukens, J. R. (2019). Modeling Autism-Related Disorders in Mice with Maternal Immune Activation (MIA). *Methods Mol Biol, 1960*, 227-236. Retrieved from https://www.ncbi.nlm.nih.gov/pubmed/30798536. doi:10.1007/978-1-4939-9167-9_20

Laufer, B. I., Hwang, H., Jianu, J. M., Mordaunt, C. E., Korf, I. F., Hertz-Picciotto, I., & LaSalle, J. M. (2021). Low-pass whole genome bisulfite sequencing of neonatal dried blood spots identifies a role for RUNX1 in Down syndrome DNA methylation profiles. *Human Molecular Genetics, 29*(21), 3465-3476. Retrieved from https://www.ncbi.nlm.nih.gov/pubmed/33001180. doi:10.1093/hmg/ddaa218

Lee, H. B., & Blaufox, M. D. (1985). Blood volume in the rat. *J Nucl Med, 26*(1), 72-76. Retrieved from https://www.ncbi.nlm.nih.gov/pubmed/3965655.

Lee, S. C., & Levine, L. (1975). Prostaglandin Metabolism .2. Identification of 2 15-Hydroxyprostaglandin Dehydrogenase Types. *Journal of Biological Chemistry, 250*(2), 548-552. Retrieved from <Go to ISI>://WOS:A1975V425300025.

Li, H., Handsaker, B., Wysoker, A., Fennell, T., Ruan, J., Homer, N., . . . Genome Project Data Processing, S. (2009). The Sequence Alignment/Map format and SAMtools. *Bioinformatics, 25*(16), 2078-2079. Retrieved from https://www.ncbi.nlm.nih.gov/pubmed/19505943. doi:10.1093/bioinformatics/btp352

Li, Q., Bozek, K., Xu, C., Guo, Y. A., Sun, J., Paabo, S., . . . Khaitovich, P. (2017). Changes in Lipidome Composition during Brain Development in Humans, Chimpanzees, and Macaque Monkeys. *Molecular Biology and Evolution, 34*(5), 1155-1166. Retrieved from <Go to ISI>://WOS:000399373300010.

Li, X., Li, J., Wang, Y., Cao, P., & Liu, Y. (2017). Effects of frying oils' fatty acids profile on the formation of polar lipids components and their retention in French fries over deep-frying process. *Food Chem, 237*, 98-105. Retrieved from http://www.ncbi.nlm.nih.gov/pubmed/28764095. doi:10.1016/j.foodchem.2017.05.100

Lima-Garcia, J. F., Dutra, R. C., da Silva, K. A. B. S., Motta, E. M., Campos, M. M., & Calixto, J. B. (2011). The precursor of resolvin D series and aspirin-triggered resolvin D1 display anti-hyperalgesic properties in adjuvant-induced arthritis in rats. *British Journal of Pharmacology, 164*(2), 278-293. Retrieved from <Go to ISI>://WOS:000294128500010. doi:10.1111/j.1476-5381.2011.01345.x

Lindhauer, M. G., Haase, N. U., & Putz, B. (2003). *POTATOES AND RELATED CROPS | Processing Potato Tubers*. Encyclopedia of Food Sciences and Nutrition (Second Edition): ACADEMIC PRESS.

Lindquist, S., & Hernell, O. (2010). Lipid digestion and absorption in early life: an update. *Current Opinion in Clinical Nutrition and Metabolic Care, 13*(3), 314-320. Retrieved from <Go to ISI>://WOS:000277281500016. doi:10.1097/MCO.0b013e328337bbf0

Liu, M., Chen, P., Vericel, E., Lelli, M., Beguin, L., Lagarde, M., & Guichardant, M. (2013). Characterization and biological effects of di-hydroxylated compounds deriving from the lipoxygenation of ALA. *J Lipid Res, 54*(8), 2083-2094. Retrieved from https://www.ncbi.nlm.nih.gov/pubmed/23740966. doi:10.1194/jlr.M035139

Liu, W., Yin, H., Akazawa, Y. O., Yoshida, Y., Niki, E., & Porter, N. A. (2010). Ex vivo oxidation in tissue and plasma assays of hydroxyoctadecadienoates: Z,E/E,E stereoisomer ratios. *Chem Res Toxicol, 23*(5), 986-995. Retrieved from https://www.ncbi.nlm.nih.gov/pubmed/20423158. doi:10.1021/tx1000943

Lombardo, M. V., Moon, H. M., Su, J., Palmer, T. D., Courchesne, E., & Pramparo, T. (2018). Maternal immune activation dysregulation of the fetal brain transcriptome and relevance to the pathophysiology of autism spectrum disorder. *Mol Psychiatry, 23*(4), 1001-1013. Retrieved from https://www.ncbi.nlm.nih.gov/pubmed/28322282. doi:10.1038/mp.2017.15

Long, N. C., Morimoto, A., Nakamori, T., Yamashiro, O., & Murakami, N. (1991). Intraperitoneal injections of prostaglandin E2 attenuate hyperthermia induced by restraint or interleukin-1 in rats. *J Physiol, 444*, 363-373. Retrieved from https://www.ncbi.nlm.nih.gov/pubmed/1822555. doi:10.1113/jphysiol.1991.sp018883

Lundstrom, S. L., Levanen, B., Nording, M., Klepczynska-Nystrom, A., Skold, M., Haeggstrom, J. Z., . . . Wheelock, C. E. (2011). Asthmatics Exhibit Altered Oxylipin Profiles Compared to Healthy Individuals after Subway Air Exposure. *Plos One, 6*(8). Retrieved from <Go to ISI>://WOS:000294676900023. doi:ARTN e23864
10.1371/journal.pone.0023864

Luo, K. K., Chapman, D. M., Lerno, L. A., Huang, G., & Mitchell, A. E. (2021). Influence of post-harvest moisture on roasted almond shelf life and consumer acceptance. *J Sci Food Agric, 101*(1), 139-150. Retrieved from https://www.ncbi.nlm.nih.gov/pubmed/32614076. doi:10.1002/jsfa.10624

Lynes, M. D., Leiria, L. O., Lundh, M., Bartelt, A., Shamsi, F., Huang, T. L., . . . Tseng, Y. H. (2017). Corrigendum: The cold-induced lipokine 12,13-diHOME promotes fatty acid transport into brown adipose tissue. *Nat Med, 23*(11), 1384. Retrieved from https://www.ncbi.nlm.nih.gov/pubmed/29117173. doi:10.1038/nm1117-1384b

Ma, M., Ren, Q., Yang, J., Zhang, K., Xiong, Z., Ishima, T., . . . Hashimoto, K. (2019). Key role of soluble epoxide hydrolase in the neurodevelopmental disorders of offspring after maternal immune activation. *Proc Natl Acad Sci U S A, 116*(14), 7083-7088. Retrieved from https://www.ncbi.nlm.nih.gov/pubmed/30890645. doi:10.1073/pnas.1819234116

Marmesat, S., Velasco, J., & Dobarganes, M. C. (2008). Quantitative determination of epoxy acids, keto acids and hydroxy acids formed in fats and oils at frying temperatures. *J Chromatogr A, 1211*(1-2), 129-134. Retrieved from http://www.ncbi.nlm.nih.gov/pubmed/18849035. doi:10.1016/j.chroma.2008.09.077

Maszewska, M., Florowska, A., Dluzewska, E., Wroniak, M., Marciniak-Lukasiak, K., & Zbikowska, A. (2018). Oxidative Stability of Selected Edible Oils. *Molecules, 23*(7). Retrieved from <Go to ISI>://WOS:000445301800249. doi:ARTN 1746
10.3390/molecules23071746
McNamara, R. K., & Carlson, S. E. (2006). Role of omega-3 fatty acids in brain development and function: Potential implications for the pathogenesis and prevention of psychopathology. *Prostaglandins Leukotrienes and Essential Fatty Acids, 75*(4-5), 329-349. Retrieved from <Go to ISI>://WOS:000241423400012.
Mead, J. F., & Howton, D. R. (1957). Metabolism of essential fatty acids. VII. Conversion of gamma-linolenic acid to arachidonic acid. *J Biol Chem, 229*(2), 575-582. Retrieved from https://www.ncbi.nlm.nih.gov/pubmed/13502321.
Mead, J. F., Steinberg, G., & Howton, D. R. (1953). Metabolism of essential fatty acids; incorporation of acetate into arachidonic acid. *J Biol Chem, 205*(2), 683-689. Retrieved from https://www.ncbi.nlm.nih.gov/pubmed/13129246.
Meier, S., Mjos, S. A., Joensen, H., & Grahl-Nielsen, O. (2006). Validation of a one-step extraction/methylation method for determination of fatty acids and cholesterol in marine tissues. *Journal of Chromatography A, 1104*(1-2), 291-298. Retrieved from <Go to ISI>://WOS:000235100300037. doi:10.1016/j.chroma.2005.11.045
Metherel, A. H., Lacombe, R. J. S., Chouinard-Watkins, R., & Bazinet, R. P. (2019). Docosahexaenoic acid is both a product of and a precursor to tetracosahexaenoic acid in the rat. *J Lipid Res, 60*(2), 412-420. Retrieved from https://www.ncbi.nlm.nih.gov/pubmed/30573561. doi:10.1194/jlr.M090373
Metherel, A. H., Lacombe, R. J. S., Chouinard-Watkins, R., Hopperton, K. E., & Bazinet, R. P. (2018a). Complete assessment of whole-body n-3 and n-6 PUFA synthesis-secretion kinetics and DHA turnover in a rodent model. *Journal of Lipid Research, 59*(2), 357-367. Retrieved from <Go to ISI>://WOS:000424977400016. doi:10.1194/jlr.M081380
Metherel, A. H., Lacombe, R. J. S., Chouinard-Watkins, R., Hopperton, K. E., & Bazinet, R. P. (2018b). Complete assessment of whole-body n-3 and n-6 PUFA synthesis-secretion kinetics and DHA turnover in a rodent model. *J Lipid Res, 59*(2), 357-367. Retrieved from https://www.ncbi.nlm.nih.gov/pubmed/29229739. doi:10.1194/jlr.M081380
Modi, H. R., Taha, A. Y., Kim, H. W., Chang, L., Rapoport, S. I., & Cheon, Y. (2013). Chronic clozapine reduces rat brain arachidonic acid metabolism by reducing plasma arachidonic acid availability. *J Neurochem, 124*(3), 376-387. Retrieved from https://www.ncbi.nlm.nih.gov/pubmed/23121637. doi:10.1111/jnc.12078
Moghaddam, M. F., Grant, D. F., Cheek, J. M., Greene, J. F., Williamson, K. C., & Hammock, B. D. (1997). Bioactivation of leukotoxins to their toxic diols by epoxide hydrolase. *Nat Med, 3*(5), 562-566. Retrieved from https://www.ncbi.nlm.nih.gov/pubmed/9142128. doi:10.1038/nm0597-562
Moghaddam, M. F., Motoba, K., Borhan, B., Pinot, F., & Hammock, B. D. (1996). Novel metabolic pathways for linoleic and arachidonic acid metabolism. *Biochimica Et Biophysica Acta-General Subjects, 1290*(3), 327-339. Retrieved from <Go to ISI>://WOS:A1996VD34900017.
Molendi-Coste, O., Legry, V., & Leclercq, I. A. (2011). Why and How Meet n-3 PUFA Dietary Recommendations? *Gastroenterol Res Pract, 2011*, 364040. Retrieved from https://www.ncbi.nlm.nih.gov/pubmed/21197079. doi:10.1155/2011/364040
Monteiro, C. A., Cannon, G., Moubarac, J. C., Levy, R. B., Louzada, M. L. C., & Jaime, P. C. (2018). The UN Decade of Nutrition, the NOVA food classification and the trouble with ultra-processing. *Public Health Nutrition, 21*(1), 5-17. Retrieved from https://www.ncbi.nlm.nih.gov/pubmed/28322183. doi:10.1017/S1368980017000234
Montine, T. J., Markesbery, W. R., Morrow, J. D., & Roberts, L. J., 2nd. (1998). Cerebrospinal fluid F2-isoprostane levels are increased in Alzheimer's disease. *Ann Neurol, 44*(3), 410-413. Retrieved from https://www.ncbi.nlm.nih.gov/pubmed/9749613. doi:10.1002/ana.410440322

Moreira, R. G., Sun, X. Z., & Chen, Y. H. (1997). Factors affecting oil uptake in tortilla chips in deep-fat frying. *Journal of Food Engineering, 31*(4), 485-498. Retrieved from <Go to ISI>://WOS:A1997WY53800007. doi:Doi 10.1016/S0260-8774(96)00088-X

Morin, C., Sirois, M., Echave, V., Rizcallah, E., & Rousseau, E. (2009). Relaxing effects of 17(18)-EpETE on arterial and airway smooth muscles in human lung. *Am J Physiol Lung Cell Mol Physiol, 296*(1), L130-139. Retrieved from https://www.ncbi.nlm.nih.gov/pubmed/18978038. doi:10.1152/ajplung.90436.2008

Moushira Zaki , J. H., Amr M.M. Ibrahim and Eman R. Youness. (2020). Circulating Plasma Free Fatty Acids, Insulin Resistance and Metabolic Markers in Obese Women. *Biomedical & Pharmacology Journal, 13*(4), 1595-1600.

Mowbray, S. L., Elfstrom, L. T., Ahlgren, K. M., Andersson, C. E., & Widersten, M. (2006). X-ray structure of potato epoxide hydrolase sheds light on substrate specificity in plant enzymes. *Protein Sci, 15*(7), 1628-1637. Retrieved from https://www.ncbi.nlm.nih.gov/pubmed/16751602. doi:10.1110/ps.051792106

Mukherjee, P. K., Marcheselli, V. L., Serhan, C. N., & Bazan, N. G. (2004). Neuroprotectin D1: a docosahexaenoic acid-derived docosatriene protects human retinal pigment epithelial cells from oxidative stress. *Proc Natl Acad Sci U S A, 101*(22), 8491-8496. Retrieved from https://www.ncbi.nlm.nih.gov/pubmed/15152078. doi:10.1073/pnas.0402531101

Muraki, I., Rimm, E. B., Willett, W. C., Manson, J. E., Hu, F. B., & Sun, Q. (2016). Potato Consumption and Risk of Type 2 Diabetes: Results From Three Prospective Cohort Studies. *Diabetes Care, 39*(3), 376-384. Retrieved from http://www.ncbi.nlm.nih.gov/pubmed/26681722. doi:10.2337/dc15-0547

Murphy, E. J., Barcelo-Coblijn, G., Binas, B., & Glatz, J. F. (2004). Heart fatty acid uptake is decreased in heart fatty acid-binding protein gene-ablated mice. *J Biol Chem, 279*(33), 34481-34488. Retrieved from https://www.ncbi.nlm.nih.gov/pubmed/15194696. doi:10.1074/jbc.M314263200

Ngobese, N. Z., Workneh, T. S., & Siwela, M. (2017). Effect of low-temperature long-time and high-temperature short-time blanching and frying treatments on the French fry quality of six Irish potato cultivars. *J Food Sci Technol, 54*(2), 507-517. Retrieved from http://www.ncbi.nlm.nih.gov/pubmed/28242950. doi:10.1007/s13197-017-2495-x

Node, K., Huo, Y. Q., Ruan, X. L., Yang, B. C., Spiecker, M., Ley, K., . . . Liao, J. K. (1999). Anti-inflammatory properties of cytochrome P450 epoxygenase-derived eicosanoids. *Science, 285*(5431), 1276-1279. Retrieved from <Go to ISI>://WOS:000082130200046. doi:DOI 10.1126/science.285.5431.1276

Nonaka, M., Sayre, R. N., & Weaver, M. L. (1977). Oil Content of French Fries as Affected by Blanch Temperatures, Fry Temperatures and Melting-Point of Frying Oils. *American Potato Journal, 54*(4), 151-159. Retrieved from <Go to ISI>://WOS:A1977DE02400004. doi:Doi 10.1007/Bf02852871

Noschka, E., Moore, J. N., Peroni, J. F., Lewis, S. J., Morrow, J. D., & Robertson, T. P. (2009). Thromboxane and isoprostanes as inflammatory and vasoactive mediators in black walnut heartwood extract induced equine laminitis. *Vet Immunol Immunopathol, 129*(3-4), 200-210. Retrieved from https://www.ncbi.nlm.nih.gov/pubmed/19111354. doi:10.1016/j.vetimm.2008.11.005

Obinata, H., Hattori, T., Nakane, S., Tatei, K., & Izumi, T. (2005). Identification of 9-hydroxyoctadecadienoic acid and other oxidized free fatty acids as ligands of the G protein-coupled receptor G2A. *J Biol Chem, 280*(49), 40676-40683. Retrieved from https://www.ncbi.nlm.nih.gov/pubmed/16236715. doi:10.1074/jbc.M507787200

Oguro, A., Inoue, T., Kudoh, S. N., & Imaoka, S. (2018). 14,15-epoxyeicosatrienoic acid produced by cytochrome P450s enhances neurite outgrowth of PC12 and rat hippocampal neuronal cells. *Pharmacology Research & Perspectives, 6*(5). Retrieved from <Go to ISI>://WOS:000447428900006. doi:ARTN e00428
10.1002/prp2.428

Oliw, E. H. (1993). Bis-Allylic Hydroxylation of Linoleic-Acid and Arachidonic-Acid by Human Hepatic Monooxygenases. *Biochimica Et Biophysica Acta, 1166*(2-3), 258-263. Retrieved from <Go to ISI>://WOS:A1993KN69900018. doi:Doi 10.1016/0005-2760(93)90106-J

Orlando, B. J., Lucido, M. J., & Malkowski, M. G. (2015). The structure of ibuprofen bound to cyclooxygenase-2. *J Struct Biol, 189*(1), 62-66. Retrieved from https://www.ncbi.nlm.nih.gov/pubmed/25463020. doi:10.1016/j.jsb.2014.11.005

Ostermann, A. I., Greupner, T., Kutzner, L., Hartung, N. M., Hahn, A., Schuchardt, J. P., & Schebb, N. H. (2018). Intra-individual variance of the human plasma oxylipin pattern: low inter-day variability in fasting blood samples versus high variability during the day. *Analytical Methods, 10*(40), 4935-4944. Retrieved from <Go to ISI>://WOS:000448338900010. doi:10.1039/c8ay01753k

Ostermann, A. I., Koch, E., Rund, K. M., Kutzner, L., Mainka, M., & Schebb, N. H. (2020). Targeting esterified oxylipins by LC-MS - Effect of sample preparation on oxylipin pattern. *Prostaglandins Other Lipid Mediat, 146*, 106384. Retrieved from https://www.ncbi.nlm.nih.gov/pubmed/31698140. doi:10.1016/j.prostaglandins.2019.106384

Otoki, Y., Metherel, A. H., Pedersen, T., Yang, J., Hammock, B. D., Bazinet, R. P., . . . Taha, A. Y. (2020). Acute Hypercapnia/Ischemia Alters the Esterification of Arachidonic Acid and Docosahexaenoic Acid Epoxide Metabolites in Rat Brain Neutral Lipids. *Lipids, 55*(1), 7-22. Retrieved from https://www.ncbi.nlm.nih.gov/pubmed/31691988. doi:10.1002/lipd.12197

Pagliai, G., Dinu, M., Madarena, M. P., Bonaccio, M., Iacoviello, L., & Sofi, F. (2021). Consumption of ultra-processed foods and health status: a systematic review and meta-analysis. *British Journal of Nutrition, 125*(3), 308-318. Retrieved from <Go to ISI>://WOS:000608451700007.

Penumetcha, M., Khan, N., & Parthasarathy, S. (2000). Dietary oxidized fatty acids: an atherogenic risk? *J Lipid Res, 41*(9), 1473-1480. Retrieved from http://www.ncbi.nlm.nih.gov/pubmed/10974055.

Pitino, M. A., Alashmali, S. M., Hopperton, K. E., Unger, S., Pouliot, Y., Doyen, A., . . . Bazinet, R. P. (2019). Oxylipin concentration, but not fatty acid composition, is altered in human donor milk pasteurised using both thermal and non-thermal techniques. *Br J Nutr, 122*(1), 47-55. Retrieved from https://www.ncbi.nlm.nih.gov/pubmed/31006410. doi:10.1017/S0007114519000916

Pitino, M. A., Alashmali, S. M., Hopperton, K. E., Unger, S., Pouliot, Y., Doyen, A., . . . Bazinet, R. P. (2019). Oxylipin concentration, but not fatty acid composition, is altered in human donor milk pasteurised using both thermal and non-thermal techniques. *British Journal of Nutrition*, 1-9. Retrieved from https://www.cambridge.org/core/article/oxylipin-concentration-but-not-fatty-acid-composition-is-altered-in-human-donor-milk-pasteurised-using-both-thermal-and-nonthermal-techniques/A7E383E1907249ECC1229A31AE9B126D

https://www.cambridge.org/core/services/aop-cambridge-core/content/view/A7E383E1907249ECC1229A31AE9B126D/S0007114519000916a.pdf/div-class-title-oxylipin-concentration-but-not-fatty-acid-composition-is-altered-in-human-donor-milk-pasteurised-using-both-thermal-and-non-thermal-techniques-div.pdf. doi:10.1017/S0007114519000916

Planaguma, A., Pfeffer, M. A., Rubin, G., Croze, R., Uddin, M., Serhan, C. N., & Levy, B. D. (2010). Lovastatin decreases acute mucosal inflammation via 15-epi-lipoxin A4. *Mucosal Immunol, 3*(3), 270-279. Retrieved from https://www.ncbi.nlm.nih.gov/pubmed/20130564. doi:10.1038/mi.2009.141

Popp, R., Bauersachs, J., Hecker, M., Fleming, I., & Busse, R. (1996). A transferable, beta-naphthoflavone-inducible, hyperpolarizing factor is synthesized by native and cultured porcine coronary endothelial cells. *Journal of Physiology-London, 497*(3), 699-709. Retrieved from <Go to ISI>://WOS:A1996WA98000011. doi:DOI 10.1113/jphysiol.1996.sp021801

Pu, Y., Yang, J., Chang, L., Qu, Y., Wang, S., Zhang, K., . . . Hashimoto, K. (2020). Maternal glyphosate exposure causes autism-like behaviors in offspring through increased expression of soluble epoxide hydrolase. *Proc Natl Acad Sci U S A, 117*(21), 11753-11759. Retrieved from https://www.ncbi.nlm.nih.gov/pubmed/32398374. doi:10.1073/pnas.1922287117

Pugh, S. J., Hutcheon, J. A., Richardson, G. A., Brooks, M. M., Himes, K. P., Day, N. L., & Bodnar, L. M. (2016). Child academic achievement in association with pre-pregnancy obesity and gestational weight gain. *Journal of Epidemiology and Community Health, 70*(6), 534-540. Retrieved from <Go to ISI>://WOS:000376596100003.

Quehenberger, O., Dahlberg-Wright, S., Jiang, J., Armando, A. M., & Dennis, E. A. (2018). Quantitative determination of esterified eicosanoids and related oxygenated metabolites after base hydrolysis. *J Lipid Res, 59*(12), 2436-2445. Retrieved from https://www.ncbi.nlm.nih.gov/pubmed/30323111. doi:10.1194/jlr.D089516

Raatz, S. K., Conrad, Z., & Jahns, L. (2018). Trends in linoleic acid intake in the United States adult population: NHANES 1999-2014. *Prostaglandins Leukot Essent Fatty Acids, 133*, 23-28. Retrieved from https://www.ncbi.nlm.nih.gov/pubmed/29789129. doi:10.1016/j.plefa.2018.04.006

Raghavamenon, A., Garelnabi, M., Babu, S., Aldrich, A., Litvinov, D., & Parthasarathy, S. (2009). Alpha-tocopherol is ineffective in preventing the decomposition of preformed lipid peroxides and may promote the accumulation of toxic aldehydes: a potential explanation for the failure of antioxidants to affect human atherosclerosis. *Antioxid Redox Signal, 11*(6), 1237-1248. Retrieved from https://www.ncbi.nlm.nih.gov/pubmed/19186999. doi:10.1089/ARS.2008.2248

Rahman, M. H., Hossain, M. M., Rahman, S. M., Hashem, M. A., & Oh, D. H. (2014). Effect of Repeated Freeze-Thaw Cycles on Beef Quality and Safety. *Korean J Food Sci Anim Resour, 34*(4), 482-495. Retrieved from https://www.ncbi.nlm.nih.gov/pubmed/26761286. doi:10.5851/kosfa.2014.34.4.482

Rainer, J., Gatto, L., & Weichenberger, C. X. (2019). ensembldb: an R package to create and use Ensembl-based annotation resources. *Bioinformatics, 35*(17), 3151-3153. Retrieved from https://www.ncbi.nlm.nih.gov/pubmed/30689724. doi:10.1093/bioinformatics/btz031

Ramon, S., Baker, S. F., Sahler, J. M., Kim, N., Feldsott, E. A., Serhan, C. N., . . . Phipps, R. P. (2014). The specialized proresolving mediator 17-HDHA enhances the antibody-mediated immune response against influenza virus: a new class of adjuvant? *J Immunol, 193*(12), 6031-6040. Retrieved from https://www.ncbi.nlm.nih.gov/pubmed/25392529. doi:10.4049/jimmunol.1302795

Ramsden, C. E. (2013). Use of dietary linoleic acid for secondary prevention of coronary heart disease and death: evaluation of recovered data from the Sydney Diet Heart Study and updated meta-analysis (vol 346, e8707, 2013). *Bmj-British Medical Journal, 346*. Retrieved from <Go to ISI>://WOS:000315087700007.

Ramsden, C. E., Domenichiello, A. F., Yuan, Z. X., Sapio, M. R., Keyes, G. S., Mishra, S. K., . . . Iadarola, M. J. (2017). A systems approach for discovering linoleic acid derivatives that potentially mediate pain and itch. *Sci Signal, 10*(493). Retrieved from https://www.ncbi.nlm.nih.gov/pubmed/28831021. doi:10.1126/scisignal.aal5241

Ramsden, C. E., Faurot, K. R., Zamora, D., Suchindran, C. M., MacIntosh, B. A., Gaylord, S., . . . Mann, D. J. (2013). Targeted alteration of dietary n-3 and n-6 fatty acids for the treatment of chronic headaches: a randomized trial. *Pain, 154*(11), 2441-2451. Retrieved from https://www.ncbi.nlm.nih.gov/pubmed/23886520. doi:10.1016/j.pain.2013.07.028

Ramsden, C. E., Hennebelle, M., Schuster, S., Keyes, G. S., Johnson, C. D., Kirpich, I. A., . . . Taha, A. Y. (2018a). Effects of diets enriched in linoleic acid and its peroxidation products on brain fatty acids, oxylipins, and aldehydes in mice. *Biochim Biophys Acta Mol Cell Biol Lipids, 1863*(10), 1206-1213. Retrieved from https://www.ncbi.nlm.nih.gov/pubmed/30053599. doi:10.1016/j.bbalip.2018.07.007

Ramsden, C. E., Hennebelle, M., Schuster, S., Keyes, G. S., Johnson, C. D., Kirpich, I. A., . . . Taha, A. Y. (2018b). Effects of diets enriched in linoleic acid and its peroxidation products on brain fatty acids, oxylipins, and aldehydes in mice. *Biochim Biophys Acta, 1863*(10), 1206-1213. Retrieved from http://www.ncbi.nlm.nih.gov/pubmed/30053599. doi:10.1016/j.bbalip.2018.07.007

Ramsden, C. E., Makrides, M., Yuan, Z. X., Horowitz, M. S., Zamora, D., Yelland, L. N., . . . Gibson, R. A. (2020). Plasma oxylipins and unesterified precursor fatty acids are altered by DHA supplementation in pregnancy: Can they help predict risk of preterm birth? *Prostaglandins Leukot Essent Fatty Acids, 153*, 102041. Retrieved from https://www.ncbi.nlm.nih.gov/pubmed/31931275. doi:10.1016/j.plefa.2019.102041

Ramsden, C. E., Ringel, A., Feldstein, A. E., Taha, A. Y., MacIntosh, B. A., Hibbeln, J. R., . . . Mann, J. D. (2012). Lowering dietary linoleic acid reduces bioactive oxidized linoleic acid metabolites in humans. *Prostaglandins Leukot Essent Fatty Acids, 87*(4-5), 135-141. Retrieved from http://www.ncbi.nlm.nih.gov/pubmed/22959954

https://www.ncbi.nlm.nih.gov/pmc/articles/PMC3467319/pdf/nihms-404053.pdf. doi:10.1016/j.plefa.2012.08.004

S0952-3278(12)00146-9 [pii]

Ramsden, C. E., Ringel, A., Majchrzak-Hong, S. F., Yang, J., Blanchard, H., Zamora, D., . . . Taha, A. Y. (2016). Dietary linoleic acid-induced alterations in pro- and anti-nociceptive lipid autacoids: Implications for idiopathic pain syndromes? *Mol Pain, 12*. Retrieved from https://www.ncbi.nlm.nih.gov/pubmed/27030719. doi:10.1177/1744806916636386

Ramsden, C. E., Zamora, D., Majchrzak-Hong, S., Faurot, K. R., Broste, S. K., Frantz, R. P., . . . Hibbeln, J. R. (2016). Re-evaluation of the traditional diet-heart hypothesis: analysis of recovered data from Minnesota Coronary Experiment (1968-73). *Bmj-British Medical Journal, 353*. Retrieved from <Go to ISI>://WOS:000374375200001.

Rapoport, S. I., Chang, M. C., & Spector, A. A. (2001). Delivery and turnover of plasma-derived essential PUFAs in mammalian brain. *J Lipid Res, 42*(5), 678-685. Retrieved from https://www.ncbi.nlm.nih.gov/pubmed/11352974.

Rapoport, S. I., & Taha, A. (2014). Imaging Brain DHA Metabolism in Vivo, in Animals, and Humans. *Omega-3 Fatty Acids in Brain and Neurological Health*, 265-275. Retrieved from <Go to ISI>://WOS:000341710100023. doi:10.1016/B978-0-12-410527-0.00022-3

Raygada, M., Cho, E., & Hilakivi-Clarke, L. (1998). High maternal intake of polyunsaturated fatty acids during pregnancy in mice alters offsprings' aggressive behavior, immobility in the swim test, locomotor activity and brain protein kinase C activity. *J Nutr, 128*(12), 2505-2511. Retrieved from https://www.ncbi.nlm.nih.gov/pubmed/9868200. doi:10.1093/jn/128.12.2505

Raz, A. (1972). Metabolities formed after intravenous administration of free or albumin-bound prostaglandin E 2 in the rat. *FEBS Lett, 27*(2), 245-247. Retrieved from https://www.ncbi.nlm.nih.gov/pubmed/4664223. doi:10.1016/0014-5793(72)80631-8

Reinaud, O., Delaforge, M., Boucher, J. L., Rocchiccioli, F., & Mansuy, D. (1989). Oxidative metabolism of linoleic acid by human leukocytes. *Biochem Biophys Res Commun, 161*(2), 883-891. Retrieved from https://www.ncbi.nlm.nih.gov/pubmed/2735926. doi:10.1016/0006-291x(89)92682-x

Reynolds, L. K., Ho, H. P., & Taper, L. J. (1984). Effect of caloric restriction during pregnancy on maternal and fetal body composition in the obese Sprague-Dawley rat. *J Nutr, 114*(12), 2247-2255. Retrieved from https://www.ncbi.nlm.nih.gov/pubmed/6502268. doi:10.1093/jn/114.12.2247

Rhee, K. S., Ziprin, Y. A., Ordonez, G., & Bohac, C. E. (1988). Fatty acid profiles and lipid oxidation in beef steer muscles from different anatomical locations. *Meat Sci, 23*(4), 293-301. Retrieved from https://www.ncbi.nlm.nih.gov/pubmed/22055744. doi:10.1016/0309-1740(88)90013-7

Richardson, C. E., Hennebelle, M., Otoki, Y., Zamora, D., Yang, J., Hammock, B. D., & Taha, A. Y. (2017). Lipidomic Analysis of Oxidized Fatty Acids in Plant and Algae Oils. *J Agric Food Chem, 65*(9), 1941-1951. Retrieved from https://www.ncbi.nlm.nih.gov/pubmed/28157307. doi:10.1021/acs.jafc.6b05559

Rico-Campa, A., Martinez-Gonzalez, M. A., Alvarez-Alvarez, I., Mendonca, R. D., de la Fuente-Arrillaga, C., Gomez-Donoso, C., & Bes-Rastrollo, M. (2019). Association between consumption of ultra-processed foods and all cause mortality: SUN prospective cohort study. *Bmj-British Medical Journal, 365*. Retrieved from <Go to ISI>://WOS:000470151000004. doi:ARTN l1949

10.1136/bmj.l1949
Ringertz, B., Palmblad, J., Radmark, O., & Malmsten, C. (1982). Leukotriene-induced neutrophil aggregation in vitro. *FEBS Lett*, *147*(2), 180-182. Retrieved from https://www.ncbi.nlm.nih.gov/pubmed/6293869. doi:10.1016/0014-5793(82)81037-5
Riu, D. S., Sunarno, I., Lukas, E., Wewengkang, E. T., & Amalia, R. (2020). The effect of pravastatin on endothelin-1 levels and pregnancy outcomes in women who have a high risk for preeclampsia: A randomized control trial. *Enferm Clin*, *30 Suppl 2*, 499-505. Retrieved from https://www.ncbi.nlm.nih.gov/pubmed/32204222. doi:10.1016/j.enfcli.2019.07.147
Robinson, D. T., Palac, H. L., Baillif, V., Van Goethem, E., Dubourdeau, M., Van Horn, L., & Martin, C. R. (2017). Long chain fatty acids and related pro-inflammatory, specialized pro-resolving lipid mediators and their intermediates in preterm human milk during the first month of lactation. *Prostaglandins Leukotrienes and Essential Fatty Acids*, *121*, 1-6. Retrieved from <Go to ISI>://WOS:000405763500001. doi:10.1016/j.plefa.2017.05.003
Robinson, P. J., & Rapoport, S. I. (1989). A method for examining turnover and synthesis of palmitate-containing brain lipids in vivo. *Clin Exp Pharmacol Physiol*, *16*(9), 701-714. Retrieved from https://www.ncbi.nlm.nih.gov/pubmed/2805434. doi:10.1111/j.1440-1681.1989.tb01624.x
Rocha, J. S., Bonkowski, M. S., Masternak, M. M., Franca, L. R., & Bartke, A. (2012). Effects of adult onset mild calorie restriction on weight of reproductive organs, plasma parameters and gene expression in male mice. *Anim Reprod*, *9*(1), 40-51. Retrieved from https://www.ncbi.nlm.nih.gov/pubmed/23667390.
Rodriguez-Alcala, L. M., Ares, I., Fontecha, J., Martinez-Larranaga, M. R., Anadon, A., & Martinez, M. A. (2017). Absorption Kinetics of the Main Conjugated Linoleic Acid Isomers in Commercial-Rich Oil after Oral Administration in Rats. *Journal of Agricultural and Food Chemistry*, *65*(35), 7680-7686. Retrieved from <Go to ISI>://WOS:000410255400010. doi:10.1021/acs.jafc.7b02143
Rosahl, S. (1996). Lipoxygenases in plants--their role in development and stress response. *Z Naturforsch C*, *51*(3-4), 123-138. Retrieved from http://www.ncbi.nlm.nih.gov/pubmed/8639225.
Ruidavets, J. B., Bongard, V., Dallongeville, J., Arveiler, D., Ducimetiere, P., Perret, B., . . . Ferrieres, J. (2007). High consumptions of grain, fish, dairy products and combinations of these are associated with a low prevalence of metabolic syndrome. *Journal of Epidemiology and Community Health*, *61*(9), 810-817. Retrieved from <Go to ISI>://WOS:000248743600012.
Salentinig, S., Phan, S., Hawley, A., & Boyd, B. J. (2015). Self-assembly structure formation during the digestion of human breast milk. *Angewandte Chemie International Edition*, *54*(5), 1600-1603. Retrieved from <Go to ISI>://WOS:000348713900037
http://onlinelibrary.wiley.com/store/10.1002/anie.201408320/asset/1600_ftp.pdf?v=1&t=ik4p8181&s=a5fa8b05ecc17ffa42599f34cd6058379b19c615. doi:10.1002/anie.201408320
Samuelsson, B. (1964). Prostaglandins and Related Factors. 27. Synthesis of Tritium-Labeled Prostaglandin E1 and Studies on Its Distribution and Excretion in the Rat. *J Biol Chem*, *239*, 4091-4096. Retrieved from https://www.ncbi.nlm.nih.gov/pubmed/14247653.
Samuelsson, B. (1982). The Leukotrienes - a New Group of Mediators in Immediate Hypersensitivity Reactions and Inflammation. *European Journal of Respiratory Diseases*, *63*, 53-74. Retrieved from <Go to ISI>://WOS:A1982PX37400019.
Sanders, T. A., & Rana, S. K. (1987). Comparison of the metabolism of linoleic and linolenic acids in the fetal rat. *Ann Nutr Metab*, *31*(6), 349-353. Retrieved from https://www.ncbi.nlm.nih.gov/pubmed/2892461. doi:10.1159/000177293
Santoro, N., Caprio, S., Giannini, C., Kim, G., Kursawe, R., Pierpont, B., . . . Feldstein, A. E. (2014a). Oxidized Fatty Acids: A Potential Pathogenic Link Between Fatty Liver and Type 2 Diabetes in Obese Adolescents? *Antioxidants & Redox Signaling*, *20*(2), 383-389. Retrieved from <Go to ISI>://WOS:000329349800014. doi:10.1089/ars.2013.5466
Santoro, N., Caprio, S., Giannini, C., Kim, G., Kursawe, R., Pierpont, B., . . . Feldstein, A. E. (2014b). Oxidized fatty acids: A potential pathogenic link between fatty liver and type 2 diabetes in obese

adolescents? *Antioxid Redox Signal, 20*(2), 383-389. Retrieved from https://www.ncbi.nlm.nih.gov/pubmed/23815500. doi:10.1089/ars.2013.5466

Sarkar, P., Narayanan, J., & Harder, D. R. (2011). Differential effect of amyloid beta on the cytochrome P450 epoxygenase activity in rat brain. *Neuroscience, 194*, 241-249. Retrieved from https://www.ncbi.nlm.nih.gov/pubmed/21843605. doi:10.1016/j.neuroscience.2011.07.058

Saubeau, G., Goulitquer, S., Barloy, D., Potin, P., Andrivon, D., & Val, F. (2013). Differential induction of oxylipin pathway in potato and tobacco cells by bacterial and oomycete elicitors. *Plant Cell Rep, 32*(5), 579-589. Retrieved from http://www.ncbi.nlm.nih.gov/pubmed/23479199. doi:10.1007/s00299-012-1377-y

Schuster, S., Johnson, C. D., Hennebelle, M., Holtmann, T., Taha, A. Y., Kirpich, I. A., . . . Feldstein, A. E. (2018a). Oxidized linoleic acid metabolites induce liver mitochondrial dysfunction, apoptosis and NLRP3 activation in mice. *J Lipid Res*. Retrieved from http://www.ncbi.nlm.nih.gov/pubmed/30084831. doi:10.1194/jlr.M083741

Schuster, S., Johnson, C. D., Hennebelle, M., Holtmann, T., Taha, A. Y., Kirpich, I. A., . . . Feldstein, A. E. (2018b). Oxidized linoleic acid metabolites induce liver mitochondrial dysfunction, apoptosis, and NLRP3 activation in mice. *J Lipid Res, 59*(9), 1597-1609. Retrieved from https://www.ncbi.nlm.nih.gov/pubmed/30084831. doi:10.1194/jlr.M083741

Schwab, M., Bauer, R., & Zwiener, U. (1997). The distribution of normal brain water content in Wistar rats and its increase due to ischemia. *Brain Res, 749*(1), 82-87. Retrieved from https://www.ncbi.nlm.nih.gov/pubmed/9070630. doi:10.1016/s0006-8993(96)01165-1

Serbanescu, I., Ryan, M. A., Shukla, R., Cortez, M. A., Snead, O. C., 3rd, & Cunnane, S. C. (2004). Lovastatin exacerbates atypical absence seizures with only minimal effects on brain sterols. *J Lipid Res, 45*(11), 2038-2043. Retrieved from https://www.ncbi.nlm.nih.gov/pubmed/15314096. doi:10.1194/jlr.M400097-JLR200

Serhan, C. N., Clish, C. B., Brannon, J., Colgan, S. P., Chiang, N., & Gronert, K. (2000). Novel functional sets of lipid-derived mediators with antiinflammatory actions generated from omega-3 fatty acids via cyclooxygenase 2-nonsteroidal antiinflammatory drugs and transcellular processing. *J Exp Med, 192*(8), 1197-1204. Retrieved from https://www.ncbi.nlm.nih.gov/pubmed/11034610. doi:10.1084/jem.192.8.1197

Serhan, C. N., Hong, S., Gronert, K., Colgan, S. P., Devchand, P. R., Mirick, G., & Moussignac, R. L. (2002). Resolvins: a family of bioactive products of omega-3 fatty acid transformation circuits initiated by aspirin treatment that counter proinflammation signals. *J Exp Med, 196*(8), 1025-1037. Retrieved from https://www.ncbi.nlm.nih.gov/pubmed/12391014. doi:10.1084/jem.20020760

Shearer, G. C., & Newman, J. W. (2008). Lipoprotein lipase releases esterified oxylipins from very low-density lipoproteins. *Prostaglandins Leukotrienes and Essential Fatty Acids, 79*(6), 215-222. Retrieved from <Go to ISI>://WOS:000261994800005. doi:10.1016/j.plefa.2008.09.023

Shen, Q., Zhang, Z., Emami, S., Chen, J., Leite Nobrega de Moura Bell, J. M., & Taha, A. Y. (2021). Triacylglycerols are preferentially oxidized over free fatty acids in heated soybean oil. *NPJ Sci Food, 5*(1), 7. Retrieved from https://www.ncbi.nlm.nih.gov/pubmed/33795687. doi:10.1038/s41538-021-00086-3

Shrestha, H. K., Beg, M. A., Burnette, R. R., & Ginther, O. J. (2012). Plasma Clearance and Half-Life of Prostaglandin F2alpha: A Comparison Between Mares and Heifers. *Biology of Reproduction, 87*(1). Retrieved from <Go to ISI>://WOS:000306548400017. doi:ARTN 18
10.1095/biolreprod.112.100776

Siegfried, M. R., Aoki, N., Lefer, A. M., Elisseou, E. M., & Zipkin, R. E. (1990). Direct cardiovascular actions of two metabolites of linoleic acid. *Life Sci, 46*(6), 427-433. Retrieved from https://www.ncbi.nlm.nih.gov/pubmed/2304379. doi:10.1016/0024-3205(90)90086-7

Simopoulos, A. P. (1999). Evolutionary aspects of omega-3 fatty acids in the food supply. *Prostaglandins Leukot Essent Fatty Acids, 60*(5-6), 421-429. Retrieved from https://www.ncbi.nlm.nih.gov/pubmed/10471132. doi:10.1016/s0952-3278(99)80023-4

Singh, H., & Gallier, S. (2017). Nature's complex emulsion: the fat globules of milk. *Food Hydrocolloids, 68*, 81-89. Retrieved from <Go to ISI>://WOS:000398868000009
https://www.sciencedirect.com/science/article/pii/S0268005X16305410?via%3Dihub. doi:10.1016/j.foodhyd.2016.10.011
Smilowitz, J. T., Gho, D. S., Mirmiran, M., German, J. B., & Underwood, M. A. (2014). Rapid measurement of human milk macronutrients in the neonatal intensive care unit: accuracy and precision of Fourier transform mid-infrared spectroscopy. *Journal of Human Lactation, 30*(2), 180-189. Retrieved from <Go to ISI>://WOS:000340422500010
http://jhl.sagepub.com/content/30/2/180.long. doi:10.1177/0890334413517941
Soler, J., Saura, P., Garcia-Lopez, D., Masgrau, L., Lluch, J. M., & Gonzalez-Lafont, A. (2016). How Can Linoleic Acid Be the Preferential Substrate of the Enzyme 15-Lipoxygenase-1? A QM/MM Approach. *Journal of Physical Chemistry B, 120*(8), 1950-1960. Retrieved from <Go to ISI>://WOS:000371562700060.
Stanley, J. C., Elsom, R. L., Calder, P. C., Griffin, B. A., Harris, W. S., Jebb, S. A., . . . Sanders, T. A. (2007). UK Food Standards Agency Workshop Report: the effects of the dietary n-6:n-3 fatty acid ratio on cardiovascular health. *Br J Nutr, 98*(6), 1305-1310. Retrieved from https://www.ncbi.nlm.nih.gov/pubmed/18039412. doi:10.1017/S000711450784284X
Steenweg-de Graaff, J., Tiemeier, H., Ghassabian, A., Rijlaarsdam, J., Jaddoe, V. W., Verhulst, F. C., & Roza, S. J. (2016). Maternal Fatty Acid Status During Pregnancy and Child Autistic Traits: The Generation R Study. *Am J Epidemiol, 183*(9), 792-799. Retrieved from https://www.ncbi.nlm.nih.gov/pubmed/27052119. doi:10.1093/aje/kwv263
Stefanovski, D., Shih, P. A. B., Hammock, B. D., Watanabe, R. M., & Youn, J. H. (2020). Assessment of soluble epoxide hydrolase activity in vivo: A metabolomic approach. *Prostaglandins & Other Lipid Mediators, 148*. Retrieved from <Go to ISI>://WOS:000534430200004. doi:ARTN 106410
10.1016/j.prostaglandins.2020.106410
Steinberg, G., Slaton, W. H., Jr., Howton, D. R., & Mead, J. F. (1956). Metabolism of essential fatty acids. IV. Incorporation of linoleate into arachidonic acid. *J Biol Chem, 220*(1), 257-264. Retrieved from https://www.ncbi.nlm.nih.gov/pubmed/13319343.
Storey, M. L., & Anderson, P. A. (2013). Contributions of white vegetables to nutrient intake: NHANES 2009-2010. *Adv Nutr, 4*(3), 335S-344S. Retrieved from http://www.ncbi.nlm.nih.gov/pubmed/23674802. doi:10.3945/an.112.003541
Strassburg, K., Esser, D., Vreeken, R. J., Hankemeier, T., Muller, M., van Duynhoven, J., . . . Jacobs, D. M. (2014). Postprandial fatty acid specific changes in circulating oxylipins in lean and obese men after high-fat challenge tests. *Mol Nutr Food Res, 58*(3), 591-600. Retrieved from https://www.ncbi.nlm.nih.gov/pubmed/24127338. doi:10.1002/mnfr.201300321
Suganuma, H., McPhee, A. J., Collins, C. T., Liu, G., Leemaqz, S., Andersen, C. C., . . . Gibson, R. A. (2019). Intravenous fat induces changes in PUFA and their bioactive metabolites: Comparison between Japanese and Australian preterm infants. *Prostaglandins Leukot Essent Fatty Acids*, 102026. Retrieved from https://www.ncbi.nlm.nih.gov/pubmed/31753522. doi:10.1016/j.plefa.2019.102026
Sugiyama, S., Hayakawa, M., Nagai, S., Ajioka, M., & Ozawa, T. (1987). Leukotoxin, 9, 10-epoxy-12-octadecenoate, causes cardiac failure in dogs. *Life Sci, 40*(3), 225-231. Retrieved from https://www.ncbi.nlm.nih.gov/pubmed/3796222. doi:10.1016/0024-3205(87)90336-5
Summers, L., Clingerman, K. J., & Yang, X. (2012). Validation of a body condition scoring system in rhesus macaques (Macaca mulatta): assessment of body composition by using dual-energy X-ray absorptiometry. *J Am Assoc Lab Anim Sci, 51*(1), 88-93. Retrieved from https://www.ncbi.nlm.nih.gov/pubmed/22330874.
Sura, P., Sura, R., EnayetAllah, A. E., & Grant, D. F. (2008). Distribution and expression of soluble epoxide hydrolase in human brain. *Journal of Histochemistry & Cytochemistry, 56*(6), 551-559. Retrieved from <Go to ISI>://WOS:000255890300003. doi:10.1369/jhc.2008.950659

Swardfager, W., Yu, D., Scola, G., Cogo-Moreira, H., Chan, P., Zou, Y., . . . Black, S. E. (2017). Peripheral lipid oxidative stress markers are related to vascular risk factors and subcortical small vessel disease. *Neurobiol Aging, 59*, 91-97. Retrieved from https://www.ncbi.nlm.nih.gov/pubmed/28756941. doi:10.1016/j.neurobiolaging.2017.06.029

Taha, A. Y. (2020). Linoleic acid-good or bad for the brain? *NPJ Sci Food, 4*, 1. Retrieved from https://www.ncbi.nlm.nih.gov/pubmed/31909187. doi:10.1038/s41538-019-0061-9

Taha, A. Y., Blanchard, H. C., Cheon, Y., Ramadan, E., Chen, M., Chang, L., & Rapoport, S. I. (2017). Dietary Linoleic Acid Lowering Reduces Lipopolysaccharide-Induced Increase in Brain Arachidonic Acid Metabolism. *Mol Neurobiol, 54*(6), 4303-4315. Retrieved from https://www.ncbi.nlm.nih.gov/pubmed/27339880. doi:10.1007/s12035-016-9968-1

Taha, A. Y., Chang, L., & Chen, M. (2016). Threshold changes in rat brain docosahexaenoic acid incorporation and concentration following graded reductions in dietary alpha-linolenic acid. *Prostaglandins Leukot Essent Fatty Acids, 105*, 26-34. Retrieved from https://www.ncbi.nlm.nih.gov/pubmed/26869088. doi:10.1016/j.plefa.2015.12.002

Taha, A. Y., Hennebelle, M., Yang, J., Zamora, D., Rapoport, S. I., Hammock, B. D., & Ramsden, C. E. (2018a). Regulation of rat plasma and cerebral cortex oxylipin concentrations with increasing levels of dietary linoleic acid. *Prostaglandins Leukot Essent Fatty Acids, 138*, 71-80. Retrieved from https://www.ncbi.nlm.nih.gov/pubmed/27282298. doi:10.1016/j.plefa.2016.05.004

Taha, A. Y., Hennebelle, M., Yang, J., Zamora, D., Rapoport, S. I., Hammock, B. D., & Ramsden, C. E. (2018b). Regulation of rat plasma and cerebral cortex oxylipin concentrations with increasing levels of dietary linoleic acid. *Prostaglandins Leukotrienes and Essential Fatty Acids, 138*, 71-80. Retrieved from <Go to ISI>://WOS:000451102400011. doi:10.1016/j.plefa.2016.05.004

Takayama, K., Yuhki, K., Ono, K., Fujino, T., Hara, A., Yamada, T., . . . Ushikubi, F. (2005). Thromboxane A2 and prostaglandin F2alpha mediate inflammatory tachycardia. *Nat Med, 11*(5), 562-566. Retrieved from https://www.ncbi.nlm.nih.gov/pubmed/15834430. doi:10.1038/nm1231

Teixeira, B. F., Dias, F. F. G., Vieira, T., Leite Nobrega de Moura Bell, J. M., & Taha, A. Y. (2021). Method optimization of oxylipin hydrolysis in nonprocessed bovine milk indicates that the majority of oxylipins are esterified. *Journal of Food Science, 86*(5), 1791-1801. Retrieved from https://www.ncbi.nlm.nih.gov/pubmed/33864645. doi:10.1111/1750-3841.15697

Tijet, N., Helvig, C., Pinot, F., Le Bouquin, R., Lesot, A., Durst, F., . . . Benveniste, I. (1998). Functional expression in yeast and characterization of a clofibrate-inducible plant cytochrome P-450 (CYP94A1) involved in cutin monomers synthesis. *Biochemical Journal, 332 (Pt 2)*, 583-589. Retrieved from https://www.ncbi.nlm.nih.gov/pubmed/9601090. doi:10.1042/bj3320583

Trepanier, M. O., Kwong, K. M., Domenichiello, A. F., Chen, C. T., Bazinet, R. P., & Burnham, W. M. (2015). Intravenous infusion of docosahexaenoic acid increases serum concentrations in a dose-dependent manner and increases seizure latency in the maximal PTZ model. *Epilepsy & Behavior, 50*, 71-76. Retrieved from <Go to ISI>://WOS:000361186300015. doi:10.1016/j.yebeh.2015.05.034

Tulk, H. M., & Robinson, L. E. (2009). Modifying the n-6/n-3 polyunsaturated fatty acid ratio of a high-saturated fat challenge does not acutely attenuate postprandial changes in inflammatory markers in men with metabolic syndrome. *Metabolism, 58*(12), 1709-1716. Retrieved from https://www.ncbi.nlm.nih.gov/pubmed/19625064. doi:10.1016/j.metabol.2009.05.031

Turley, S. D., Burns, D. K., Rosenfeld, C. R., & Dietschy, J. M. (1996). Brain does not utilize low density lipoprotein-cholesterol during fetal and neonatal development in the sheep. *J Lipid Res, 37*(9), 1953-1961. Retrieved from https://www.ncbi.nlm.nih.gov/pubmed/8895061.

Ulu, A., Harris, T. R., Morisseau, C., Miyabe, C., Inoue, H., Schuster, G., . . . Hammock, B. D. (2013). Anti-inflammatory effects of omega-3 polyunsaturated fatty acids and soluble epoxide hydrolase inhibitors in angiotensin-II-dependent hypertension. *J Cardiovasc Pharmacol, 62*(3), 285-297. Retrieved from https://www.ncbi.nlm.nih.gov/pubmed/23676336. doi:10.1097/FJC.0b013e318298e460

USDA. (2016). Potatoes.

Vahratian, A. (2009). Prevalence of overweight and obesity among women of childbearing age: results from the 2002 National Survey of Family Growth. *Matern Child Health J, 13*(2), 268-273. Retrieved from https://www.ncbi.nlm.nih.gov/pubmed/18415671. doi:10.1007/s10995-008-0340-6

van Leyen, K., Kim, H. Y., Lee, S. R., Jin, G., Arai, K., & Lo, E. H. (2006). Baicalein and 12/15-lipoxygenase in the ischemic brain. *Stroke, 37*(12), 3014-3018. Retrieved from https://www.ncbi.nlm.nih.gov/pubmed/17053180. doi:10.1161/01.STR.0000249004.25444.a5

Velasco, J., Marmesat, S., Bordeaux, O., Marquez-Ruiz, G., & Dobarganes, C. (2004). Formation and evolution of monoepoxy fatty acids in thermoxidized olive and sunflower oils and quantitation in used frying oils from restaurants and fried-food outlets. *Journal of Agricultural and Food Chemistry, 52*(14), 4438-4443. Retrieved from <Go to ISI>://WOS:000222540800015. doi:10.1021/jf030753f

Veronese, N., Stubbs, B., Noale, M., Solmi, M., Vaona, A., Demurtas, J., . . . Fontana, L. (2017a). Fried potato consumption is associated with elevated mortality: an 8-y longitudinal cohort study. *American Journal of Clinical Nutrition, 106*(1), 162-167. Retrieved from <Go to ISI>://WOS:000404593900022. doi:10.3945/ajcn.117.154872

Veronese, N., Stubbs, B., Noale, M., Solmi, M., Vaona, A., Demurtas, J., . . . Fontana, L. (2017b). Fried potato consumption is associated with elevated mortality: an 8-y longitudinal cohort study. *Am J Clin Nutr, 106*(1), 162-167. Retrieved from http://www.ncbi.nlm.nih.gov/pubmed/28592612. doi:10.3945/ajcn.117.154872

Wei, W., Yang, J., Yang, D., Wang, X., Yang, Z., Jin, Q., . . . Wang, X. (2019). Phospholipid Composition and Fat Globule Structure I: Comparison of Human Milk Fat from Different Gestational Ages, Lactation Stages, and Infant Formulas. *J Agric Food Chem, 67*(50), 13922-13928. Retrieved from https://www.ncbi.nlm.nih.gov/pubmed/31746600. doi:10.1021/acs.jafc.9b04247

Weiss, G. A., Troxler, H., Klinke, G., Rogler, D., Braegger, C., & Hersberger, M. (2013). High levels of anti-inflammatory and pro-resolving lipid mediators lipoxins and resolvins and declining docosahexaenoic acid levels in human milk during the first month of lactation. *Lipids in Health and Disease, 12*, 89. Retrieved from <Go to ISI>://WOS:000321134000001
https://lipidworld.biomedcentral.com/track/pdf/10.1186/1476-511X-12-89. doi:10.1186/1476-511x-12-89

Wesson, L. G., & Burr, G. O. (1931). The metabolic rate and respiratory quotients of rats on a fat-deficient diet. *Journal of Biological Chemistry, 91*(2), 525-539. Retrieved from <Go to ISI>://WOS:000187545700009.

Whelan, J. (2008). The health implications of changing linoleic acid intakes. *Prostaglandins Leukotrienes and Essential Fatty Acids, 79*(3-5), 165-167. Retrieved from <Go to ISI>://WOS:000261995200022. doi:10.1016/j.plefa.2008.09.013

Wilson, R., Lyall, K., Smyth, L., Fernie, C. E., & Riemersma, R. A. (2002). Dietary hydroxy fatty acids are absorbed in humans: Implications for the measurement of 'oxidative stress' in vivo. *Free Radical Biology and Medicine, 32*(2), 162-168. Retrieved from <Go to ISI>://WOS:000173416100008. doi:Doi 10.1016/S0891-5849(01)00780-8

Wu, H., Karayiannis, T. G., & Tassou, S. A. (2013). A two-dimensional frying model for the investigation and optimisation of continuous industrial frying systems. *Applied Thermal Engineering, 51*(1-2), 926-936. Retrieved from <Go to ISI>://WOS:000316036300095. doi:10.1016/j.applthermaleng.2012.10.002

Wu, J., Gouveia-Figueira, S., Domellof, M., Zivkovic, A. M., & Nording, M. L. (2016). Oxylipins, endocannabinoids, and related compounds in human milk: Levels and effects of storage conditions. *Prostaglandins Other Lipid Mediat, 122*, 28-36. Retrieved from https://www.ncbi.nlm.nih.gov/pubmed/26656029. doi:10.1016/j.prostaglandins.2015.11.002

Wu, J. F., Gouveia-Figueira, S., Domellof, M., Zivkovic, A. M., & Nording, M. L. (2016). Oxylipins, endocannabinoids, and related compounds in human milk: levels and effects of storage

conditions. *Prostaglandins & Other Lipid Mediators, 122*, 28-36. Retrieved from <Go to ISI>://WOS:000372762300004
https://ac.els-cdn.com/S1098882315300174/1-s2.0-S1098882315300174-main.pdf?_tid=7768cad1-548e-4dd7-9be5-d9af922716a4&acdnat=1537633421_33f1a8c96f419eea844582b2a40dd494. doi:10.1016/j.prostaglandins.2015.11.002
Yu, G., Wang, L. G., & He, Q. Y. (2015). ChIPseeker: an R/Bioconductor package for ChIP peak annotation, comparison and visualization. *Bioinformatics, 31*(14), 2382-2383. Retrieved from https://www.ncbi.nlm.nih.gov/pubmed/25765347. doi:10.1093/bioinformatics/btv145
Yuan, T., Qi, C., Dai, X., Xia, Y., Sun, C., Sun, J., . . . Wang, X. (2019). Triacylglycerol Composition of Breast Milk during Different Lactation Stages. *J Agric Food Chem, 67*(8), 2272-2278. Retrieved from https://www.ncbi.nlm.nih.gov/pubmed/30706708. doi:10.1021/acs.jafc.8b06554
Yuan, Z. X., Rapoport, S. I., Soldin, S. J., Remaley, A. T., Taha, A. Y., Kellom, M., . . . Ramsden, C. E. (2013). Identification and profiling of targeted oxidized linoleic acid metabolites in rat plasma by quadrupole time-of-flight mass spectrometry. *Biomed Chromatogr, 27*(4), 422-432. Retrieved from https://www.ncbi.nlm.nih.gov/pubmed/23037960. doi:10.1002/bmc.2809
Yuhas, R., Pramuk, K., & Lien, E. L. (2006). Human milk fatty acid composition from nine countries varies most in DHA. *Lipids, 41*(9), 851-858. Retrieved from <Go to ISI>://WOS:000242101500005.
Zarek, J., & Koren, G. (2014). The fetal safety of statins: a systematic review and meta-analysis. *J Obstet Gynaecol Can, 36*(6), 506-509. Retrieved from https://www.ncbi.nlm.nih.gov/pubmed/24927189. doi:10.1016/S1701-2163(15)30565-X
Zeldin, D. C., Kobayashi, J., Falck, J. R., Winder, B. S., Hammock, B. D., Snapper, J. R., & Capdevila, J. H. (1993). Regiofacial and Enantiofacial Selectivity of Epoxyeicosatrienoic Acid Hydration by Cytosolic Epoxide Hydrolase. *Journal of Biological Chemistry, 268*(9), 6402-6407. Retrieved from <Go to ISI>://WOS:A1993KT36800049.
Zhang, P., Xing, X., Hu, C., Yu, H., Dong, Q., Chang, G., . . . Zhang, D. (2016). 15-Lipoxygenase-1 Is Involved in the Effects of Atorvastatin on Endothelial Dysfunction. *Mediators Inflamm, 2016*, 6769032. Retrieved from https://www.ncbi.nlm.nih.gov/pubmed/27594770. doi:10.1155/2016/6769032
Zhang, Z., Emami, S., Hennebelle, M., Morgan, R. K., Lerno, L. A., Slupsky, C. M., . . . Taha, A. Y. (2021). Linoleic acid-derived 13-hydroxyoctadecadienoic acid is absorbed and incorporated into rat tissues. *Biochim Biophys Acta Mol Cell Biol Lipids, 1866*(3), 158870. Retrieved from https://www.ncbi.nlm.nih.gov/pubmed/33340768. doi:10.1016/j.bbalip.2020.158870
Zhang, Z., Jackson, S. L., Martinez, E., Gillespie, C., & Yang, Q. (2020). Association between ultraprocessed food intake and cardiovascular health in US adults: a cross-sectional analysis of the NHANES 2011-2016. *American Journal of Clinical Nutrition*. Retrieved from https://www.ncbi.nlm.nih.gov/pubmed/33021623. doi:10.1093/ajcn/nqaa276
Zhang, Z. C., Richardson, C. E., Hennebelle, M., & Taha, A. Y. (2017). Validation of a One-Step Method for Extracting Fatty Acids from Salmon, Chicken and Beef Samples. *Journal of Food Science, 82*(10), 2291-2297. Retrieved from <Go to ISI>://WOS:000412742700009. doi:10.1111/1750-3841.13850
Zhuang, P., Mao, L., Wu, F., Wang, J., Jiao, J. J., & Zhang, Y. (2020). Cooking Oil Consumption Is Positively Associated with Risk of Type 2 Diabetes in a Chinese Nationwide Cohort Study. *Journal of Nutrition, 150*(7), 1799-1807. Retrieved from <Go to ISI>://WOS:000568433300017.